

T  
D1-90  
YAH

# AERODYNAMIC INTERFERENCE IN TALL BUILDINGS

**A THESIS**

submitted in fulfilment of the  
requirements for the award of the degree  
of  
DOCTOR OF PHILOSOPHY  
in  
CIVIL ENGINEERING



By

**MAHMOOD YAHYAI**



DEPARTMENT OF CIVIL ENGINEERING  
UNIVERSITY OF ROORKEE  
ROORKEE-247 667 (INDIA)

DECEMBER, 1990

**DEDICATED**  
**TO**  
**MY PARENTS**

## CANDIDATE'S DECLARATION

I hereby certify that the work which is being presented in the thesis entitled **AERODYNAMIC INTERFERENCE IN TALL BUILDINGS** in fulfilment of the requirement for the award of the Degree of Doctor of Philosophy submitted in the Department of Civil Engineering University of Roorkee, Roorkee of the University is an authentic record of my own work carried out during a period from August 1987 to November 1990 under the supervision of Dr. Prem Krishna, Dr. P.K. Pande and Dr. Krishen Kumar, Professors of Civil Engineering Department.

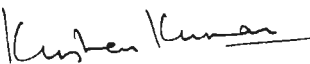
The matter embodied in this thesis has not been submitted by me for the award of any other Degree.




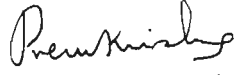
(MAHMOOD YAHYAI)  
Candidate's Signature

Date: 29.12.1990

This is to certify that the above statement made by the candidate is correct to the best of our knowledge.

  
(Krishen Kumar)  
Professor  
Civil Engg. Deptt.  
University of  
Roorkee, Roorkee


  
( P.K. Pande )  
Professor  
Civil Engg. Deptt.  
University of  
Roorkee, Roorkee

  
( Prem Krishna )  
Professor  
Civil Engg. Deptt.  
University of  
Roorkee, Roorkee

### Signatures of Supervisors

The Ph.D. Viva-Voce examination of Mr Mahmood Yahyai, Research Scholar has been held on aug. 7, 1991 The thesis is recommended for award of the Ph.D. Degree.

  
Signature of Supervisors

  
Signature of External Examiner(s)

## ABSTRACT

With the increase in population and land cost in large cities, the construction of tall buildings is becoming increasingly a necessity. Use of higher strength materials, improved capabilities in analysis and design as also in construction technology have lead to the construction of tall slender buildings of lighter density, thus making their aerodynamic stability an important concern.

A tall building which is interfered by another in its vicinity will behave differently under wind action as compared to when it is in isolation, due to the modified wind flow around it.

In this thesis the response of a typical tall rectangular building having 6:1:1.2 aspect ratio has been studied both experimentally as well as using theoretical approaches. An aeroelastic model of this building was designed and fabricated and its along-wind as well as across-wind responses have been measured. The building model has been tested in a 2 m x 2 m boundary layer wind tunnel for two orientations of the model, i.e., shorter and longer side facing the wind.

Extensive measurements were made to determine the wake boundary behind the building model as well as to observe the change in turbulence intensity on the upstream and downstream sides of the model.

For the determination of the extent of interference, initially, two rigid models of the same size and height were placed in a simulated open terrain in the wind tunnel and forces as well as moments were measured for the buildings arranged in tandem and offset positions in plan.

Next an aeroelastic model of the building was tested in the wind tunnel with a rigid interfering model placed at a number of locations upstream as well as downstream of the aeroelastic building model. Testing was carried



out in a simulated flow expected over a built-up approach terrain. Responses of the aerolastic model were recorded in the two principal directions, i.e., along-wind and across-wind by a set of strain gauge transducers developed to measure the displacements at the top of the model. It was observed that due to the presence of an interfering building, the mean response of the building generally reduced on account of shielding, while the dynamic response of the building usually increased. The effect of interference is more pronounced when an interfering building is located on the upstream side than if it is situated on the downstream side.

For theoretical analysis, Davenport's approach [29] was adopted to estimate the along-wind response of the isolated building. The results computed by using this method agree closely with those predicted from experimental observations. The across-wind response of the building has been computed using force spectra obtained by Saunders [108] for rectangular [1:1.5 and 1:2 aspect ratio in plan ] and square buildings as well as Kareem [64] for square buildings. According to the study made in this thesis, Saunders force spectra for square building may be used for estimation of across-wind response of buildings with 1:1.2 aspect ratio in plan. Kareem's spectra yield results not far from those of Saunders.

## ACKNOWLEDGEMENT

I express my gratitude to Dr. Prem Krishna, Dr. P.K. Pande and Dr. Krishen Kumar, Professors of Civil Engineering Department for their guidance, constant encouragement and kind treatment allthrough the research carried out.

The encouragement received from Dr. A. K. Ahuja is thankfully acknowledged.

I am obliged to the staff of Boundary Layer Wind Tunnel for their assistance during the experimental work.

My affectionate appreciation is reserved for my wife and daughter for their sense of devotion and the hardship they shared throughout the study.

The author is thankful to his colleagues and friends for their best wishes.

## CONTENTS

Abstract
Acknowledgement
List of Tables
List of Figures
List of Photographs
Notations

CHAPTER		Page No.
1.0	INTRODUCTION	1
2.0	WIND CHARACTERISTICS	5
2.1	Wind Characteristics	5
2.1.1	Nature of Wind	5
2.1.2	Types of Winds	5
2.2	Winds in Atmospheric Boundary Layer	7
2.2.1	Mean Wind Velocity	8
2.2.2	The Longitudinal Velocity Spectrum	9
2.3	Flow Around a Bluff Body	10
2.4	Static Wind Load	11
2.4.1	Aerodynamic Coefficients	11
2.5	Parameters Describing a Tall Building at its Response	12
2.6	Response of Tall Buildings	13
2.6.1	Along-wind Response	14
2.6.2	Across-wind Response	14
2.6.3	Torsional Response	15
2.7	Acceleration Criteria and Building Stiffness	16
2.8	Motion Perception in Tall Buildings	17

2.9	Reduction of Wind Excited Motion	18
2.10	Interference Effects	19
3.0	REVIEW OF LITERATURE	22
3.1	Preliminary Remarks	22
3.2	Background Information	22
3.3	Isolated Buildings	24
3.3.1	Along-wind Response	24
3.3.2	Across-wind Response	25
3.3.3	Torsional Response	28
3.3.4	Full-Scale Measurements	30
3.4	Interference Effects in Tall Buildings	31
3.5	Closure	36
4.0	EXPERIMENTAL PROGRAMME	37
4.1	Preliminary Remarks	37
4.2	Modelling Criteria for the Atmospheric Boundary Layer	37
4.3	Modeling of the Atmospheric Boundary Layer	40
4.4	Geometric Modelling	44
4.5	Aeroelastic Modelling of Tall Buildings	44
4.6	Design of Aeroelastic Model	47
4.7	Fabrication of Models	48
4.8	Reliability of the Stick Aeroelastic Model	50
4.9	The Wind Tunnel	50
4.10	Instrumentation and Measurements	52
4.10.1	Design and Fabrication of Strain Gauge Transducers	52
4.10.2	Measurements on Aeroelastic Model	53
4.10.3	Measurements on Rigid Model	54

	4.10.4 Measurements of Wind Parameters	55
	4.11 Procedures and Data Reduction	55
	4.12 Calibration	58
5.0	ISOLATED RECTANGULAR BUILDINGS	60
	5.1 Preliminary Remarks	60
	5.2 Analytical Approaches	61
	5.2.1 Along-Wind Response	61
	5.2.1.1 Mean Response	61
	5.2.1.2 Fluctuating Response	62
	5.2.1.3 Response Analysis	65
	5.2.2 Across-wind Response	66
	5.3 Experimental Approach	68
	5.4 Comparison of Experimental and Theoretical Results	70
6.0	INTERFERENCE EFFECTS ON TALL RECTANGULAR BUILDINGS	72
	6.1 Preliminary Remarks	72
	6.2 Flow Characteristics Around the Building Model	73
	6.2.1 Wake Boundary	73
	6.2.2 Mean Velocity and Turbulence Intensity	74
	6.3 Rigid Model Study	75
	6.4 Aeroelastic Model Study	77
	6.4.1 Short Afterbody Case	77
	6.4.2 Long Afterbody Case	79
	6.5 Contours of the Peak Buffeting Factors	82
	6.6 Displacement Response	82
	6.7 Critical Interference Zone	83

7.0	CONCLUSIONS AND RECOMMENDATIONS FOR FURTHER RESEARCH	84
7.1	Preliminary Remarks	84
7.2	Conclusions	84
7.2.1	Flow Field	84
7.2.2	Isolated Buildings	85
7.2.3	Interference Study	86
7.3	Recommendation for Future Research	88
	REFERENCES AND OTHER RELATED PUBLICATIONS	89
	APPENDIX - A	176
	APPENDIX - B	183

## LIST OF TABLES

Table No.	Description	Page No.
6.1	Turbulence Intensity Measurements Around Model	99
6.2	Buffeting Factors for Mean Forces and Moments	100
6.3	Buffeting Factors for Short Afterbody Model	101

## LIST OF FIGURES

Fig. No.	Description	Page No.
2.1	Flow Around a Rectangular Block	102
2.2	Drag Coefficient $C_D$ as a Function of the Ratio of Plan Dimensions $d$ and $b$	103
4.1	Mean Velocity Profiles	104
4.2	Turbulence Intensity Profiles	105
4.3	Scaling of Spectra by Variance and Peak Frequency	106
4.4	Schematic Diagram of Aeroelastic Model	107
4.5	Aeroelastic Sway Response Obtained with Multi-degree of Freedom and Conventional Stick Models of a Tall Building of Square Cross-section	108
4.6	Static Pressure Variation Along the Test Section	109
4.7	Schematic Diagram of Boundary Layer Wind Tunnel at University of Roorkee	110
4.8	Scheme of Instrumentation for Measurements on Aeroelastic Model	111
4.9	Response at the Top of the Building Model (Long Afterbody) at Reduced Velocity 4	112
4.10	Response at the Top of the Building Model (Long Afterbody) at Reduced Velocity 6	113
4.11	Response at the Top of the Building Model (Long Afterbody) at Reduced Velocity 8	114
4.12	Response at the Top of the Building Model (Long Afterbody) at Reduced Velocity 10	115
4.13	Effect of Sampling Time on Displacement Amplitude Computed from the Records	116
4.14	Probability Density of Fluctuation in Displacement Response of the Building Model	117
4.15	Arrangement for Static Calibration of the S.G. Transducers	118
5.1	Relationship Between Response and Force Spectra for Lightly Damped System	119



5.2	Theoretical Along-Wind Displacement for Long Afterbody Case	120
5.3	Theoretical Along-Wind Displacement for Short Afterbody Case	121
5.4	Theoretical Values of Along - Wind Acceleration	122
5.5	Theoretical Across - Wind Displacement of Long Afterbody Building	123
5.6	Theoretical Across - Wind Displacement Short Afterbody Building	124
5.7	Computed Across - Wind Acceleration Using Different Spectra	125
5.8	Computed Across-Wind Acceleration Using Different Spectra	126
5.9	Variation of rms Along-Wind Response of Aeroelastic Model (Long Afterbody)	127
5.10	Variation of rms Along-Wind Response of Aeroelastic Model (Short Afterbody)	128
5.11	Variation of rms Across-Wind Response of Aeroelastic Model (Long Afterbody)	129
5.12	Variation of rms Across-Wind Response of Aeroelastic Model (Short Afterbody)	130
5.13	Along-Wind Displacement (Long Afterbody)	131
5.14	Along-Wind Displacement (Short Afterbody)	132
5.15	Comparison of Across-Wind Response of Long Afterbody Building	133
5.16	Comparison of Across-Wind Response of Short Afterbody Building	134
6.1	Mean Wake Boundary Behind Building Model	135
6.2	Position of Hot Wire Anemometer in Turbulence Intensity Measurements	136
6.3	Turbulence Intensity Measurements in Some Typical Interference Case	137
6.4	Maximum Buffering Factors for Mean Along-Wind Displacement	138
6.5	Maximum Buffeting Factors for Along-Wind Peak Fluctuating Component of Displacement	139

6.6	Maximum Buffeting Factors for Across-Wind Peak Fluctuating Component of Displacement	140
6.7	Maximum Buffeting Factors for Along-Wind Mean Response (Interfering Building Downstream)	141
6.8	Maximum Buffeting Factors for Along-Wind Peak Response (Interfering Building Downstream)	142
6.9	Maximum Buffeting Factors for Across- Wind Peak Response (Interfering Building Downstream)	143
6.10	Buffeting Factor Contours (Mean Response) at $U_r = 4$	144
6.11	Buffeting Factor Contours (Mean Response) at $U_r = 6$	144
6.12	Buffeting Factor Contours (Mean Response) at $U_r = 8$	145
6.13	Buffeting Factor Contours (Mean Response) at $U_r = 10$	145
6.14	Buffeting Factor Contours (Peak Response) at $U_r = 4$	146
6.15	Buffeting Factor Contours (Peak Response) at $U_r = 6$	147
6.16	Buffeting Factor Contours (Peak Response) at $U_r = 8$	148
6.17	Buffeting Factor Contours (Peak Response) at $U_r = 10$	149
6.18	Response of Aeroelastic Model, A	150
6.19	Response of Aeroelastic Model, A	151
6.20	Response of Aeroelastic Model, A	152
6.21	Response of Aeroelastic Model, A	153
6.22	Response of Aeroelastic Model, A	154
6.23	Response of Aeroelastic Model, A	155
6.24	Response of Aeroelastic Model, A	156
6.25	Response of Aeroelastic Model, A	157
6.26	Response of Aeroelastic Model, A	158
6.27	Response of Aeroelastic Model, A	159
6.28	Response of Aeroelastic Model, A	160
6.29	Response of Aeroelastic Model, A	161
6.30	Response of Aeroelastic Model, A	162
6.31	Response of Aeroelastic Model, A	163

6.32	Response of Aeroelastic Model, A	164
6.33	Response of Aeroelastic Model, A	165
6.34	Response of Aeroelastic Model, A	166
6.35	Response of Aeroelastic Model, A	167
6.36	Response of Aeroelastic Model, A	168
6.37	Response of Aeroelastic Model, A	169
6.38	Response of Aeroelastic Model, A	170
6.39	Response of Aeroelastic Model, A	171
6.40	Response of Aeroelastic Model, A	172
6.41	Response of Aeroelastic Model, A	173
6.42	Response of Aeroelastic Model, A	174
6.43	Critical Interference Zone for the Building model	175

## LIST OF PHOTOGRAPHS

Photo No.	Description	Page no.
1.	Aeroelastic Model in the Wind Tunnel	185
2.	Details of Extended Portion of the Model Below Wind Tunnel Floor	185
3.	Interference Study (Rigid Model Case)	186
4.	Interference Study (Aeroelastic Model case)	186

## NOTATIONS

A	Projected area of the building
B	Breadth of the building
$C_D$	Drag coefficient
$C_L$	Lift coefficient
$C_M$	Moment coefficient
$C_p$	Pressure coefficient
$C_T$	Drag coefficient of terrain
D	Depth of the building
E	Modulus of elasticity
$E_c$	Eckert number
$f_i$	Number of times the record touches or crosses a horizontal line.
$\bar{F}$	Generalized mean wind load
$F_e$	Froude number
$F_x, F_y$	Mean forces in x- and y-directions
g	Peak factor
G	Gust factor
H	Height of the building
$ H(N) ^2$	Mechanical admittance
$ J_H(N) ^2$	Horizontal joint acceptance
$ J_Z(N) ^2$	Vertical joint acceptance
K	Generalized stiffness
M	Generalized mass
$M_x, M_y$	Aerodynamic moments
$n_m$	Frequency at peak
$N_x$	Fundamental frequency in x- direction

$N_y$	Fundamental frequency in y- direction
$N_z$	Fundamental frequency in z- direction
$\bar{p}(z)$	Mean pressure at height z
$P_0$	Pressure in the undisturbed flow
$P_r$	Prandtl number
$ r $	Arm of the torque
$r_g$	Building radius of gyration
Re	Reynolds number
Ro	Rosby number
$S_p(N)$	Pressure spectrum at frequency N
St	Strouhal number
$S_U(N)$	Power spectral density at frequency N
$S_Y(N)$	Response spectrum at frequency N
T	Averaging time
$t_R$	Reference time
$T_R$	Reference temperature
$T_{rms}$	rms torsion
$T_{max}$	Maximun torsion
$u'$	Fluctuating longitudinal velocity
$u_*$	Surface shear velocity
$\bar{U}$	Mean longitudinal velocity
$\overline{U'^2}$	Mean square value of fluctuating longitudinal velocity
$U_R$	Reference velocity
$\bar{U}(Z), \bar{U}_{10}$	Mean speed at height Z and 10 M
$v'$	Fluctuating lateral velocity
$\bar{v}$	Mean lateral velocity
$w'$	Fluctuating vertical velocity

$\bar{w}$	Mean vertical velocity
$\bar{Y}$	Mean displacement response
$Z_G$	Gradient height
$Z_r, Z_0$	Reference and roughness height
$\alpha$	Power law coefficient
$E$	Strain
$\eta$	Loss factor
$\lambda_L$	Length scale
$\lambda_F$	Stiffness scale
$\lambda_M$	Mass scale
$\lambda_a$	Acceleration scale
$\lambda_U$	Velocity scale
$\lambda_{\rho_b}$	Density scale
$\lambda_{\xi}$	Damping scale
$\Delta E$	Energy dissipated in one cycle of vibration
$\Delta T_R$	Reference excess temperature
$\bar{\mu}(z)$	First mode shape at height z
$\nu$	Kinetic viscosity
$\xi$	Critical damping ratio
$\rho$	Air density
$\rho_b$	Bulk density of building
$\sigma^2$	Variance of the velocity
$\sigma_x, \sigma_y$	rms displacement of the building in x and y directions
$\sigma_{x2}, \sigma_{y2}$	rms acceleration of the building in x and y directions
$\tau_0$	Shear stress at surface
$\omega_n$	First mode natural frequency

## CHAPTER 1

### INTRODUCTION

Heavy masonry structures of yester years had substantial inherent strength to resist wind forces. These forces were thus not considered seriously. It is only when more slender structures began to be built as a result of the development of other construction materials, and failures occurred in slender trussed bridges, that wind loading attained a degree of importance. During the 1880s, several bridge collapses were witnessed [82]. The main cause of these disasters was their mainly poor lateral resistance against wind loads. Of major consequence was the failure of the Tay Bridge in Scotland in 1879 [82], in which 75 people lost their lives. This collapse was investigated by a board of enquiry, which pointed out that the major weakness of the bridge was its low resistance to the wind forces.

It was not until the collapse of Tacoma Narrow Bridge in 1940 that full scientific attention was given to wind engineering. The crash, which was caused by the phenomenon of dynamic instability, started a new era of research. Through the centuries, due to its conservatism, the building art has been extremely slow to react to changes. However, the energetic attitude of twentieth-century Civil Engineers, which stems from the dynamic character of the industrial society of today, has been the moving force behind the wind engineering advancements in the past 50 years.

Unlike bridges, there have been no reported catastrophic collapses of completed buildings due to wind action, but a few have collapsed during erection [34]. At least two tall buildings have suffered permanent deformation. Firstly the Meyer-Kiser building in Miami in 1926, and then the 82 m Great Plains Life Building in Lubbock, Texas suffered a one foot permanent deflection in a tornado, when the wind velocity peaks were



estimated at 290 km/h. However, there are sufficient number of allusions to walls cracking, window breakage and occupant discomfort to suggest that there are significant problems to the designer of contemporary tall buildings [34]. For example, the Gulf and Western Building in New York city had to be evacuated during a storm of particular intensity, which occurred in 1973. The building sway, according to press, terrified the occupants of the building [82]. In general, the popping of windowpanes and damage to partitions and other non-structural elements are often unavoidable in certain windy locations.

The sensitivity of residents to the perception of acceleration in tall buildings with rectangular cross-sections is a paramount design criterion so as to ensure necessary living comfort. Many of the tall buildings have been found to become unserviceable due to accelerations during wind storms [61]. It is therefore necessary to design tall buildings for aerodynamic action of the wind. Building design codes of most of the countries contain such provisions. The interference studies are thus more relevant to meet the criteria of 'minimum human comfort' and save buildings from becoming 'troublesome' to its occupants and many a times even becoming 'uninhabitable'.

In the past three decades the nature of along-wind response due to fluctuations in the wind velocity has been reasonably well developed. The characteristics of across-wind response are still not well understood and require further detailed investigation.

Interaction effects from a nearby building in an urban situation can produce strong changes in the dynamic response of a tall building. The interactions of neighbouring tall buildings, commonly known as interference effects, may result from mutual interference between the fluid flow and the building. Interference is known in many cases to cause complication of

dynamic motion putting occupants to discomfort. Both upstream and downstream buildings may get affected. In addition, if a new building has any adverse effect on the existing buildings, the owner of the new building may be held responsible, adding a new dimension to the field of professional liability. "The first lawsuit of this type was filed against the Port Authority of New York and New Jersey, the owners of the World Trade Centre for adverse wind effects on a nearby building" [73].

Attention is increasingly being paid to wind tunnel studies of the aerodynamic forces and the aeroelastic characteristics of neighbouring tall buildings. Wind loading codes have been developed on the basis of wind tunnel tests of isolated models in different wind environments, which adequately cover response of the majority of tall buildings. However, little information is available on the aerodynamic forces acting on two tall buildings where significant interaction may occur. It is for this reason the study reported in this thesis was undertaken.

An open circuit boundary layer wind tunnel of 2 x 2 m cross-section has been used in the present study. In the first phase rigid and aeroelastic models have been tested to study the behaviour of isolated rectangular buildings under the action of wind. The responses of these models have also been theoretically predicted and compared with the experimentally obtained responses. The analysis has been carried out by using Davenport's method for the along-wind response and the force spectra of Saunders and Kareem for the across-wind response. The latter analysis is truly a semi-analytical approach.

In the second phase, a series of tests were conducted systematically on an aeroelastic model to investigate the interference effects between two rectangular tall buildings placed in a turbulent boundary layer. The building response has been determined by measuring the displacements at the top of the

model in the two principal directions- along and across the wind. The results for the interference case have been expressed/presented as a multiple of the isolated model responses, termed as buffeting factors. These non-dimensional buffeting factors therefore represent the interference phenomenon in a straight forward manner.

Lastly, an attempt has been made to demarcate a zone of high interference covering upstream as well as the downstream regions around the interfered building. This zone has been termed as the critical interference zone, beyond which the interference effect is insignificant and hence not so important in the design.

Following this Chapter which introduces the problem and the study made, Chapter 2 describes the types of winds and their characteristics, the aerodynamic response of a tall building and the modified response of the building due to the interference effect of a nearby building. Chapter 3 reviews the background literature, firstly describing the behaviour of isolated buildings and subsequently covering a detailed review of the interference studies. In Chapter 4 the modelling laws for design and fabrication of aeroelastic models and techniques used for the collection and reduction of experimental data are explained. Chapter 5 gives the responses of an isolated tall rectangular building as observed in this study and also as obtained analytically. The experimental and analytical results have then been compared. In Chapter 6 the interaction of two tall buildings and their adverse or beneficial effect on each other has been studied. The important conclusions and suggestions for further studies are summarized in Chapter 7. Appendix-A discusses structural and aerodynamic damping.

Appendix-B depict the flow diagram of the computer programmes developed for theoretical analysis of along-wind and across-wind responses of rectangular buildings.

## CHAPTER 2

### WIND RESPONSE OF TALL BUILDINGS

#### 2.1 Wind Characteristics

##### 2.1.1 Nature of wind

Wind is a meteorological factor, which by definition is the motion of air with respect to the surface of the earth. The earth is enveloped by gases which cannot transmit shear forces. Therefore to keep the external forces in equilibrium, it is easily set in motion. These forces include gravitational forces, forces resulting from rotation of the earth, centrifugal forces due to the curvature of the path of the motion and the variations of air density and volume caused by heating and moisture [69]. A pressure field in the atmosphere is produced due to these forces. If the gradient of this has a horizontal component, the air masses begin to travel in that direction. Air movement produces the Coriolis force which deflects the wind direction to the right in the northern hemisphere and to the left in the southern hemisphere until air masses are directed along an isobar. These air masses continue to move in the direction of this isobar at a constant speed at a specific height above the earth surface. This type of wind is known as gradient wind.

##### 2.1.2 Types of Winds

The following are some types of winds:

Monsoons are winds which develop as a result of different heating of the air over the ocean and land, especially over the southern coast of Asia. There are two types of monsoon winds; The winter monsoon blows from the land to the ocean, the summer monsoon from the colder ocean towards the land which is heated more intensely. Summer monsoons carry moisture and rain from the ocean surface but their speed is usually not disastrous.

Fohn winds develop when the air passing over mountain crest gets heated up while descending on leeward side. On windward side air loses its water vapour content and condenses in the form of rain and snow at certain height. Wind of this type usually does not attain disastrous speeds.

Bara winds are similar to Fohn winds but with a difference that while descending they do not get warmed up because of a steep slope and may travel at speeds of 50 m/s or more.

Thunderstorms develop when a warm moist air gets suddenly cooled at high altitude and as a result of this heavy rain-fall exerts viscous drag forces on the air through which it falls and gives rise to winds when the rain spreads over the ground. These winds develop suddenly and are characterized by violent irregular gusts.

Hurricanes are known as typhoons in Far East and as cyclones in Australia and the region of the Indian Ocean. Their energy is largely derived from the latent heat released by the condensation of water vapour. Diameter of a hurricane is of several hundred kilometers and extends to a height of 10 km and more. These generally develop between 5 and 20 latitude circles in late summer and early autumn. The central zone of hurricane is known as the eye. The strongest winds occur near the eye, up to a distance of about 200 km from the storm centre [5]. Hurricane winds may reach speeds of about 90 m/s.

Tornadoes are the most destructive of all winds. They develop over the land during warm, moist, unsettled weather. A tornado is in the form of a vortex with a funnel shape which travels on the earth at speeds of 10-30 m/s for about 15 kilometers. The diameter of the tornado vortex is nearly 300 m and its tangential speed is estimated to be as high as 100 m/s. This type of wind is predominantly directed towards north-east. The difference in pressures between centre of tornado vortex to its periphery is as high as  $10^4$

Pascals. Although tornadoes strike a narrow region for a short period of time, their effects are disastrous.

## 2.2 Winds in Atmospheric Boundary Layer

In the case of fluid flow past a stationary solid wall, the influence of viscosity at high Reynold's numbers is confined to a very thin layer in the immediate neighbourhood of the solid wall. The fluid at the wall adheres to it, while the frictional forces retard the motion of the fluid in this thin layer. In, this layer, known as the "boundary layer" the fluid velocity increases from zero at the wall (no slip condition) to its full value which corresponds to external frictionless flow. The boundary layer can be either laminar or turbulent.

In the case of atmosphere also, a turbulent boundary layer forms because of the retarding action of the earth's surface. The height of this boundary layer varies from approximately 300 m for a flat ground to about 500 m for a rough terrain. the flow in the atmospheric boundary layer being turbulent, one has to talk of the instantaneous value of the various flow parameters which can be expressed as the sum of a mean and a fluctuating component. thus the instantaneous velocity components  $u, v,$  and  $w$  along three mutually perpendicular directions,  $x, y$  and  $z$  can be written as

$$u = \bar{u} + u'$$

$$v = \bar{v} + v'$$

$$\text{and } w = \bar{w} + w'$$

where  $\bar{u}, \bar{v}$  and  $\bar{w}$  are the mean and  $u', v'$  and  $w'$  the fluctuating components respectively of the velocity. The main component is given by the expression

$$\bar{u}_i = \frac{1}{T} \int_0^T u_i dt$$

Where  $T$  is the averaging time and should be chosen large enough to get a proper value of the mean.

The velocity profile in the atmospheric boundary layer is thus governed by the terrain conditions. The velocity at the edge of the boundary layer is called the "gradient velocity".

### 2.2.1 Mean wind velocity

The mean wind speed is used to determine the static wind effect on a structure. Since the mean wind speed depends on the averaging time  $T$ , an appropriate value of  $T$  must be chosen. Davenport [32] recommends an averaging time  $T$  of 5-30 minutes, preferably 10-15 minutes. The mean wind profile in strong winds in the lowest 150 m atmosphere follows a logarithmic law [90] which may be written as,

$$\frac{\bar{U}(Z)}{\bar{U}(Z_r)} = \frac{\ln(Z/Z_0)}{\ln(Z_r/Z_0)}$$

where  $\bar{U}$ =mean speed,  $Z$ =height above ground,  $Z_r$ =reference height and  $Z_0$ =roughness length. The logarithmic law is based upon the both theory and experiment. An alternative formulation of the dependence of mean wind speeds upon height above ground is the well known power law,

$$\frac{\bar{U}(Z)}{\bar{U}(Z_r)} = \left(\frac{Z}{Z_r}\right)^\alpha$$

Where  $\alpha$  is an exponent depending upon the roughness of terrain. The use of power law has a number of advantages as follows

1. Simplicity
2. The local mean velocity  $\bar{U}(Z)$  is fairly insensitive to the gradient height  $Z_G$  (which is difficult to measure), but more sensitive to power law exponent  $\alpha$  (normally a more accurate measurement);

3. The use of gradient mean velocity  $\bar{U}_G$ , which is dependent on meteorological pressure system and not on roughness, supplies a simple base measurement. By the use of exponent and gradient height, the  $\bar{U}_G$  allows transference of wind information from measurement locations, such as airport, to nearby areas.

Ekman [36] has shown that due to spiral effect a rotation in the wind vector is produced that increases with the height. This feature is not incorporated in the power law. Scruton [111] has measured a 30° change in wind direction over the first 300 m. Owen [89] suggested a smaller value than this, nearer 2° to 3° per 100 m.

However, many researchers like Davenport [21,22,23], and Jensen [59] presented a large amount of evidence to support the use of the "power law" to represent the mean velocity profile of strong winds, and it has also been used in this thesis.

### 2.2.2 *The longitudinal velocity spectrum*

The energy available in the turbulence fluctuations of the wind which have frequencies similar to the natural frequency of a building is of fundamental importance to the dynamic response of the building.

The energy available can be assessed by a measurement of the velocity spectral density of each component of turbulence. In particular, when resonance in the streamwise direction is being considered, one measure of energy available is the longitudinal velocity spectrum. The longitudinal velocity spectrum then defines the frequency composition of the variance of the fluctuating velocity component. Davenport [22,30] has analyzed a considerable amount of strong wind data and evolved the following empirical formula.



$$\frac{NS_U(N)}{U'^2} = \frac{2/3 X^2}{(1+X)^2 4/3}$$

where

$$X = \frac{NL(Z)}{U'^2}$$

$S_U(N)$  is the power spectral density,  $N$  is the frequency,  $\overline{U'^2}$  is the variance, and  $L(Z)$  is the length scale proportional to the integral scale and  $\bar{U}(Z)$  is the mean velocity.

Harris [49] has suggested a modified form, which can be expressed as

$$\frac{NS_U(N)}{U'^2} = \frac{0.6 X}{(2+X^2)^{5/6}}$$

### 2.3 Flow Around a Bluff Body

When a rectangular body is immersed in an air flow, streamlines change their path as shown in Fig.2.1. At point C the flow velocity becomes zero - this is referred to as the, 'Stagnation' point. Flow separation occurs at corners A and B of the windward face, where negative pressure gradients are strong. Near separation zones strong shear stresses impart to the fluid particles rotational motions that generate discrete vortices in the separation layers. Through mechanisms that are not well understood, vortices are shed into the wake of the body, which are more or less well organized depending upon the Reynold's number of the flow. Well organized sequence of alternating vortices are referred to as Von Karman (or Benard) vortex streets. Flow visualizations of vortex streets are available in the literature for both laboratory and geophysical flows. The latter in the form of satellite pictures of cloud formations in the wake of islands with quasi-cylindrical shapes (Ref.116, pp.137,140 and 141). The region between

separation points and the wake is referred to as the shear layer.

The frequency,  $n$ , at which vortices are then shed in the wake of a rectangular body is found experimentally to satisfy the relation  $S = nd / \bar{u}$  where  $S$ ,  $d$  and  $\bar{u}$  are Strouhal number, across-wind dimension and mean velocity respectively. The Strouhal number generally depends upon the aspect ratio (plan), the characteristics of the oncoming flow, and the details of the exterior surface (roughness, texture, ribs). For a sharp-edged rectangular body of aspect ratio 1:2, Strouhal number is between 0.14 and 0.18 depending upon the wind direction.

#### 2.4 Static Wind Load

A steady air flow striking a tall building imparts a portion of its kinetic energy in the form of a force which is constant in time and space. The magnitude of this force is given as:

$$\bar{F} = 1/2 \rho C_D \bar{U}^2 A$$

where  $\rho$ ,  $C_D$ ,  $\bar{U}$  and  $A$  are air density, drag coefficient, mean speed and projection of the building area in the wind direction. The total static pressure force is then given as

$$\bar{F} = 1/2 C_D \rho \int_A (\bar{U}_Z)^2 dA$$

but 
$$\bar{U}_Z = \bar{U}_{10} (Z/10)^\alpha$$

therefore 
$$\bar{F} = 1/2 C_D \rho B (\bar{U}_{10})^2 \int_0^h (Z/10)^{2\alpha} dh$$

##### 2.4.1 Aerodynamic coefficients

Every point on the surface of a body experiences pressures due to the wind load. It is usually preferred to express these pressures in a

non-dimensional form with respect to a reference point where the flow is undisturbed. These coefficients are defined as follows:

$$C_p = \frac{p-p_0}{q}$$

$$C_D = \frac{F_x}{qA}$$

$$C_L = \frac{F_y}{qA}$$

$$C_M = \frac{M}{qAZ}$$

where

$$q = 1/2 \rho \bar{U}^2$$

$\bar{U}$  = Mean wind velocity at reference height

$p_0$  = Pressure in the undisturbed flow far upwind of the body

$F_x$  = Drag force

$F_y$  = Lift force

$M$  = Aerodynamic moment

$A$  = Exposed area

$Z$  = Some conveniently chosen dimension

The drag of a rectangular cylinder depends upon the ratio between height and width of its cross-section. If the ratio  $d/b$  Fig (2.2) is larger than 0.5 or so, flow reattachment occurs and the drag coefficient drops [116,74].

## 2.5 Parameters Describing a Tall Building and its Response

One of the rational ways of defining a tall building is by the ratio of its height to the least lateral dimension. A value of about 6 and above for

this ratio has come to be accepted for defining a tall building. This definition, however, need not necessarily contradict the conventional definition in terms of the number of storeys or the absolute height.

A representative tall building of rectangular cross-section have the following design parameters [140].

1. Height,  $h$  of 150-300m
2. Breadth,  $b$  approximately equal to the depth  $d$
3. Time period of the fundamental mode,  $T$  of 5 seconds
4. Internal damping,  $\xi$  of the fundamental sway mode, equivalent to 1% of critical
5. Bulk density,  $\rho_b$  of  $1600 \text{ N/m}^3$  and an air density of  $12.5 \text{ N/m}^3$
6. Amplitude,  $Y(H)$  taken equal to a standard deviation value of 0.031 m which is equal to a sine wave amplitude of 0.493 m, and corresponds to a standard deviation of acceleration of 0.5% gravity for a period of 5 seconds [96].
7. Mean velocity at the top of building,  $\bar{U}(H)$  of 30 m/s. Novak and Davenport [88] recommended the use of mean velocity for galloping calculations due to the time required for full development of the galloping phenomena; and 30 m/s could be a reasonable mean velocity for a return period of 6 years.

## 2.6 Response of Tall Buildings

The response of tall buildings has been observed to occur in three modes of action. For rectangular buildings with one face near perpendicular to the mean flow, the motion has been measured in the along-wind and across-wind directions, as well as in the torsional mode. Each mode of vibration will now be briefly reviewed.

### 2.6.1 *Along-wind response*

Building response in streamwise direction consists of a mean component corresponding to mean wind, and a fluctuating component corresponding to "gusts" or frequency components of the turbulent wind. Davenport [29] has emphasized that the fluctuating component of the along-wind response of the building can be divided into two parts; non-resonant response and response due to resonance. the ratio of this "background" response to resonant response depends on the relation between the geometric plus dynamic properties of the building and those of the turbulent natural wind. So in different situations either of these dynamic phenomena may dominate.

### 2.6.2 *Across-wind response*

Buildings are very sensitive to across-wind motion, if they are rectangular in shape and the mean wind direction is near perpendicular to one face. the sensitivity amplifies as the wind speed increases.

In John Hancock building, when the mean wind speed at the top of the building was estimated at 46 km/h, the standard deviation of the across-wind component was about three times the streamwise value. For a less than 40 percent increase in wind velocity the ratio of standard deviations had risen until the across-wind motion was nine times the along-wind response [33]. No attempts have been made to develop a technique based on the "gust factor approach" for dynamic response in across-wind direction of rectangular buildings. The complex nonlinear relationship between the approach flow and across-wind response has inhibited prediction of across-wind response with sufficient degree of reliability. However, across-wind response is due to the complex interaction of the following three factors [84].

1. Unsteady approach flow
2. Wake excitation, and

3. Aerodynamic forces associated with movement of the structure.

There are techniques which can easily treat all three phenomena separately. Unfortunately, there is a complex feedback interaction among these three factors which renders the application of the available techniques inaccurate. However, if one of these three mechanisms is very dominant, it is possible to predict the response within a reasonable degree of accuracy [107], [91] and [92].

### 2.6.3 Torsional response

The rotational motion of tall buildings has received comparatively lesser attention. Torsional motion in a building results from a possible aerodynamic and/or inertial coupling in various degrees of freedom. If the wind force does not coincide with the centre of elastic and mass at each floor level, an eccentric loading pattern can be expected which is responsible for exciting the torsional mode of vibration. An amplification of response is possible by dynamic inertial coupling, if the vertical elastic axis of the building, and the centre of gravity are not in alignment. If the torsional and translational periods of vibration are nearly the same, "Wandering of energy" or "beating" phenomenon evidenced in other dynamic systems could conceivably add to the resonant response of tall buildings. Reed [96] studied a 153 m moment resisting frame building which showed the ratios of the torsional, transverse and streamwise accelerations to be 2.7:1.8:1. This occurred at a wind speed of 72 km/h at the top of the building and the motion was sufficient to cause much objection from the occupants.

## 2.7 Acceleration Criteria and Building Stiffness

Robertson and Chen [101] reported that 90% of the population could perceive accelerations of about 1% of the gravity. As a result of a thorough investigation of two office buildings Reed [96], [48] has recommended that the return period for storms causing a standard deviation of acceleration at the top of a building equal to 0.5% of gravity, be not less than 6 years, the acceleration standard deviation being averaged over 20 minutes. If the acceleration level is any higher than this, there will be loss in tenancy.

Consider a building where the period of fundamental frequency is 5 seconds. (A collation of data from full scale buildings by Yokoo and Akiyona [140] suggests that this is typical of 50-70 storey buildings.) If Reed's 0.5% standard deviation of acceleration is converted to displacement for a 5 second period, it corresponds to a displacement standard deviation of 0.31 m. This assumes that the building motion can be taken as an amplitude-modulated sine wave in the fundamental mode. Following Reed's criterion, if the motion can be considered as approximately Gaussian and the motion is averaged over 20 minutes interval over the peak of a 6 year-return storm, then the time that the amplitude of the motion spends within one standard deviation will be about 13-14 minutes.

For this storm, a 150 m building cannot exceed a deflection of  $1/4800$  of height for more than 14 minutes to satisfy Reed's criterion. If a 300 m building has the same stiffness to mass ratio as the 150 m building (not normally so), the deflection criterion would fall to  $1/9600$ . The basic flaw in the traditional recommendation for deflection limits of around  $1/500$  can be seen.

It must be emphasised that these calculations and the 0.5% value are not conservative [107]. Reed's recommendation is on the basis that this acceleration and return period is extrapolated back to one year. If the

building then oscillates to this level during that year, it is likely that 2% of the tenants in the top third of the building will vacate the premises due to concern about the movement. With this large error in traditional design estimate, a major reason why more problems have not occurred in established buildings is that buildings are much stiffer than the calculations on the bare frame. In Empire State building the cladding increased the design stiffness by a factor of three [95]. The damping in older buildings is also high due to the heavier materials used, which further reduces the building response.

In summary then, this section highlights that the assessment of the level of motion in a modern tall building design is essential.

## 2.8 Motion Perception in Tall Buildings

Reed [96] emphasized that motion can be perceived by any of the following

1. perception of motion
2. noise due to cracking and groaning
3. lifts 'slapping' against shafts
4. visual observation of 'fixtures' moving
5. viewing out of the building (building sensitive to torsion), and
6. psychological inducements such as the noise of the wind whistling.

Occupant education of the likelihood of occasional motion of the building, improves the tolerance levels of the occupants, but Reed notes that it would be expected that the level of complaints will vary between offices and apartment buildings. He found the standard deviation of acceleration of the top floors to be nearly proportional to the cube of the mean wind velocity, which emphasize a strong need for reliable meteorological



statistics and accurate wind tunnel measurements.

From his study of 117 occupants in two office buildings, he suggests that the number of storm events per year where motion is perceived is a better measure of human dislike of building motion rather than the total time spent in perceiving motion. This study does not include apartment buildings.

Chen and Robertson [17] have provided a relationship for the geometric mean of the perception threshold as function of motion characteristics, physical parameters and expectancy level. Yamada [139] developed a series of curves between period of oscillations and the acceleration levels and classified human comfort zones on these curves.

In conclusion Reed emphasised that, " the problem of human discomfort is a very real, potential problem which should be considered in the design of every tall building."

## 2.9 Reduction of Wind Excited Motion

The wind induced motion of a tall building can be controlled either by reduction at the source or by reducing the response [61]. An appropriate choice of building shape and architectural modifications can result in the reduction of motion by altering the flow pattern around a building. Open passages in the building would allow the air to bleed into the wake and separated regions thereby increasing the base pressure and consequently reducing aerodynamic pressure.

Buildings with tapered and non-uniform cross-sections along the height would have less potential of creating a coherent wake. New modified structural systems have been developed [67, 68], [38] to reduce the drift due to wind, which includes steel framed tapered tubes, tube in tube, and bundled tube structural systems. Use of post-tensioned cables and tendons, and application of external cables for very tall buildings are possible

solutions to reduce lateral displacements against wind loading [133] and [102]. The problems due to self-excited oscillations of guy cables should however be considered while designing such a system.

Addition of structural damping or dissipative devices, such as passive energy absorbers and active feedback control systems to the basic structural system of a building result in the reduction of motion. A fairly detailed discussion on structural damping is given in Appendix-A.

### 2.10 Interference Effects

The characteristics of the aerodynamic forces on a structure will be different when it is located near another structure of comparable height. The change in aerodynamic forces are due to "interference effects". The first dramatic alarm was rung in 1965 with the collapse of three cooling towers in an array of eight at Ferrybridge Power Plant in England. The cause was determined [100] to be increased loading on the towers due to the presence of adjacent towers. Since then there is a growing awareness that the wind forces, to which tall buildings are subjected in urban environments, may be of a more complex nature than usually acknowledged. This complexity arises from interaction of turbulence and shear in mean flow with a variety of buildings with different shapes and heights. Additional complexity arises due to the presence of one building in the wake of another or wakes of a number of other buildings undergoing complicated wake interactions. These interference effects may be adverse or beneficial, and, can be identified as changes in the local pressure fluctuations or in the overall static as well as dynamic loading.

There is scattered evidence that the power spectral density of the wind pressure recorded in tall structures in urban areas presents, for fixed orientations of the incident wind, spikes and valleys at characteristic

frequencies. The spectra of the wind velocity used in design are smoothed functions, obtained by averaging many such records. Clearly the resulting error grows when the size of the obstacles i.e. surface roughness or neighbouring structures, become more. The characteristics of oncoming flow and wake flow on one hand, together with shape, dimensions and dynamic properties of upstream as well as downstream building on the other, can be viewed as the basic interaction parameters.

When a building is located in the wake of another building at its vicinity, it experiences the effect of shielding. This shielding effect generally reduces the static wind loads. In such a case, the proximity effect is beneficial. However, the flow modifications due to the interaction of the two buildings, or, a group of buildings close-by in certain cases, develop well correlated flow fluctuations which increase the strength of the wake fluctuations. The above conditions cause adverse effects on the response of tall buildings located close to one another. In many cases interference effects enhance dynamic response of a building resulting in discomfort to the occupants in the higher floors. If the adverse effect is severe it breaks glass panels, moves or breaks some of the fixtures in the building and may cause development of cracks in the claddings.

Till today no analytical approach or even mathematical model based on experimental results is available to predict the amount of interference effects between two or more buildings. The reason behind this as mentioned earlier also is the complexity of interaction between modified flow and characteristics of the building under study. Hence the only reliable technique for identifying beneficial or adverse effects of nearby buildings is wind tunnel testing.

A proposed structure may be modelled with the surrounding buildings in a wind tunnel suitably designed to model the natural wind. A

long-test-section boundary layer wind tunnel like the one at the University of Roorkee is suitable for such tests.

A thorough review of the last few years research works is followed in the next chapter.

## CHAPTER 3

### REVIEW OF LITERATURE

#### 3.1 Preliminary Remarks

This chapter presents a review of relevant literature to bring out the background of the study undertaken in this thesis. The research contributions which have a more direct relevance are treated in greater detail. First, a brief review of the historical background. Then the background studies on aerodynamic response of a single building in three principle modes of vibration; namely along-wind, across-wind and torsional motion. This is followed by a more detailed review of the work on tall buildings subjected to interaction effects from neighbouring building(s).

#### 3.2 Background Information

In 1687 Newton developed an expression for the wind pressure on a two dimensional flat plate [9]. Alexandre Eiffel in France (1910-1914) reported that by dividing pressures by square of velocity, pressure coefficients independent of the size of similar shape can be obtained. On the basis of his measurements, he found the principle of geometric similarity and the "independence of Reynolds number for sharp edged bodies."

With the failure of the Tay Bridge in 1879, the need for a thorough understanding of wind load on civil engineering structures was felt. Till the collapse of Tacoma Narrows Bridge in 1940 the wind loads were represented by equivalent static loads. It was emphasized that this failure is possibly due to the dynamic effects of wind even at moderate velocities. Interference effects have been recognized and emphasized after the collapse of three cooling towers out of the eight at the Ferrybridge Power Plant on 1st Nov. 1965.

The first significant (or reported) studies of wind loading on tall buildings were carried out around 1930, coinciding with the Skyscraper boom in the U.S.A. Many of the problems arising from static design were identified by a series of aeronautical wind tunnel measurements. The statistical nature of the phenomena was recognized and dynamic responses of the taller buildings were measured.

After 1930's the properties of materials used in tall buildings changed substantially. Lighter material were used with an average building density of about  $1600 \text{ N/M}^3$  which is half of the value in old buildings. Because of these light materials the buildings become more flexible and hence more sensitive to wind. Also the use of more integrated structural systems and use of welded connections have reduced damping of the buildings. All of these trends have increased the susceptibility of tall buildings to wind action [34].

The susceptibility of such buildings to wind forces is likely to be more pronounced if they are affected by the presence of other building(s). The increase in turbulence due to an interfering building generally amplifies these susceptibilities and affects the building serviceability. Till today there is no report of any completed building failure due to the interaction effects, but as also mentioned in Chapter 1, very recently the first lawsuit was registered by Metropolitan Life Insurance Co. against the Port Authority of New York and New Jersey. The World Trade Centre was claimed to have caused "unusual, increased and unnatural wind pressures" on the Plaintiff's building in its neighbourhood [73]. Interference effects on tall buildings thus added a new dimension in litigation and professional liability.

In the next section the background of isolated building response is reviewed followed by review of literature on the interface effects.

### 3.3 Isolated Buildings

#### 3.3.1 *Along-wind Response*

The effect of atmospheric turbulence on response of an elastic structure immersed in turbulent flow, was first published by Liepmann [77] in 1952. Using this concept Davenport [23] proposed models representing the turbulent wind flow near the ground. He further developed "Gust Loading Approach" for analytical prediction of along-wind response of tall buildings [29]. A procedure for estimating along-wind response of tall buildings based essentially on Davenport approach has been included in the Canadian Structural Design Manual [13]. Subsequently, Vickery [132] developed a similar procedure as that of Davenport [29] that allows, however, for more flexibility with respect to the choice of certain meteorological parameters. Vellozi and Cohen [130] in 1968 published a procedure for the along-wind response of tall buildings in which a reduction factor was introduced for the fluctuating pressures on the leeward face of a building as it is understood that there is no perfect correlation between fluctuating pressures on windward and leeward faces of a building. However, it has been shown [96], [112] that owing to the manner in which this factor is applied, the procedure given by Vellozi and Cohen underestimates the resonant amplification effect. According to the results of modern meteorological research, the energy of turbulent fluctuations that cause resonant oscillations in tall buildings decreases significantly at higher elevations [116]. Simiu [114] in his last revision has suggested various refinements of the approaches due to Davenport [29] and Vellozi and Cohen [132], including the above mentioned decrease of turbulence with height. Solari [117] has also developed a closed form solution for estimation of along-wind response of tall buildings as well as point like structures. His method seems to be more practical for routine use. Both the methods given by Solari [117] and Simiu [114] account for the

dependence of turbulent fluctuations on height, and on the basis of which rapid manual calculations of the along-wind response can be performed. Simiu's procedure [114] has been incorporated in the Appendix to the American National Standards ANS(I), A58.1 [3].

All the procedures mentioned above are based on following assumptions:

1. Terrain is approximately horizontal and that its roughness is reasonably uniform over a sufficiently large fetch, and,
2. Mean wind is normal to the building face. This is considered to be the worst orientation as explained by Ruscheweyh [104].

Any situation other than these make the analytical approaches inapplicable and hence wind tunnel testing becomes even more necessary.

### 3.3.2 *Across-wind Response*

Saunders [107] has provided a series of curves for the across-wind forcing function of tall buildings in different approach flows. He measured the across-wind displacement spectra of constant rectangular cross-section building models in a wind tunnel. The across-wind force spectra were calculated from measured displacement spectra through division by the mechanical admittance function. The reliability of this technique depends primarily on how accurately the dynamic properties of the aeroelastic model have been established. Saunders concluded that the across-wind motion of rectangular building models is essentially due to the energy available in the high frequency side-band of the mechanism of vortex shedding. That is, the across-wind motion is predominantly due to wake excitations. His research work has been a major contribution towards the definition of across-wind loading functions. Vickery [131] conducted model experiments on Prismatic bodies and developed an empirical curve for the peak across-wind accelerations of buildings.



Kareem [61] made simultaneous pressure measurements at various levels throughout the height of a square building model. The cross correlation between pressures at various levels had been subsequently monitored by him and an expression for the integral wind loading function on the building model has been developed through statistical integration.

Ellis [37] developed a technique based on the experimental measurements of dynamic strains and accelerations at various points on a model with a specially calibrated transducer. The output of the dynamic strains and accelerations was used to evaluate the unsteady aerodynamic forces. The transducer core flexibility and mass distribution was carefully designed to keep the displacements small enough so as not to significantly affect the aerodynamic admittance function. This approach does not require modelling of the full-scale mass, stiffness and damping parameter and only the geometric shape has to be modelled.

Kareem in his further contribution to across-wind response of buildings [63, 64] has developed a mathematical model for reduction of the across-wind response of isolated square cross-section buildings to typical atmospheric boundary layers, over different terrains. Closed-form expressions for the auto-and co-spectra of the across-wind force fluctuations are formulated, based on wind tunnel measurements. A statistical integration scheme is used to develop mode-generalized across-wind spectrum for three approach flow conditions. He has also given a simplified expression based on random vibration analysis to compute the model response. The approach is being used in this thesis to predict the across-wind response of the rectangular building model studies (plan dimensions 1:1.2) and then to compare with those measured in the wind tunnel.

Expressions based on first principles for estimating the across-wind response of tall buildings do not currently exist. However, empirical

information obtained from wind tunnel measurements is available concerning the across-wind response of tall buildings not subjected to interference effects. Kwok [72] has shown that different expressions for across-wind response of tall buildings are applicable depending upon whether or not the rms value of the across-wind oscillations at the tip of the building,  $\sigma_x$  exceeds a critical value  $\sigma_{xcr}$ . If  $\sigma_x > \sigma_{xcr}$ , aeroelastic (lock-in) effects become significant and contribute to a considerable and dangerous increase of the across-wind response. Wind tunnel experiments by Kwok [72] and Rosati [103] suggest that it is conservative from structural design viewpoint to assume approximately the following values:

$$\sigma_{xcr}/b \approx 0.015 \text{ (open terrain, } Z_0 \approx 0.07 \text{ m)}$$

$$\sigma_{xcr}/b \approx 0.025 \text{ (suburban terrain, } Z_0 \approx 1 \text{ m)}$$

$$\sigma_{xcr}/b \approx 0.045 \text{ (city centre, } Z_0 \approx 2.5 \text{ m)}$$

where  $b$  = horizontal across-wind dimension of building. For  $\sigma_x < \sigma_{xcr}$  the across-wind response corresponding to the case where the mean wind is normal to a building face can be estimated by using expressions given by, Simiu [115]

$$\sigma_x(h) = \frac{\pi^{1/2}}{2\xi^{1/2}} \frac{1}{(2\pi n)^2 M} \frac{1}{2} \xi \bar{u}^2(h) b h \bar{y}$$

$$\sigma_{x2}(h) = (2\pi n)^2 \sigma_x$$

where  $\sigma_x(h)$  = rms of across-wind oscillations at top of structure

$\rho_b$  = air density

$n$  = fundamental frequency of vibration of structure

$\xi$  = damping ratio

$\bar{u}(h)$  = mean wind speed at elevation  $h$ , a non dimensional constant.

Values of  $\tilde{\gamma}$  are based on measurements reported in references [63], [72], [103] and [98] and implicit in [132].

For buildings with a uniformly distributed mass, a square shape in plan and a fundamental mode shape that may be approximated by a straight line the generalized mass,  $M$  can be expressed as follows:

$$M = 1/3 \rho_b b^2 h$$

### 3.3.3 Torsional Response

In the 1926 Florida hurricane, two buildings of Miami - the 15-Storey Realty Building, and the 17-Storey Meyer-Kiser Building got severe distortions due to the combined effects of across-wind loads and torsional moments [116]. The two transverse end frames of the Meyer-Kiser Building experienced horizontal deflections of about 0.60 m and 0.20 m respectively. MacDonald [79], while investigating the effect of a Tornado that hit Lubbock on the Plains Life Building noted that the cracks in the cladding showed considerable torsional strain, inferring substantial torque on the building.

Vickery [129] has reported that he measured a significant fluctuating torque in a model study, which appeared to be due to Vortex Shedding. This was confirmed by Kao [60] who measured sharp peaks in the pressure co-spectra at the Strouhal frequency, suggesting a possible torsional moment induced by Vortex Shedding.

A first attempt for estimating analytically the torsional moments induced on buildings by the fluctuating wind loads was reported by Patrickson and Friedman [92]. More recently, Foutch and Safak have presented potentially useful methods for estimating the along-wind,

across-wind and torsional response of rectangular buildings [40, 41]. However, owing to the absence of sufficient information on aerodynamic loads, the methods are not presently usable for design purposes.

Reinhold and Sparks [98] have studied the influence of wind direction on the response of a square building. According to their results, torsional moments are largest when the wind direction is normal to the building face. When the angle  $\alpha$  between the mean wind direction and the normal to the building face increases from  $0^\circ$  to  $45^\circ$  the torsional moments decrease by 25%.

Systematic wind tunnel studies conducted at the University of Western Ontario were subsequently reported in [118], [45], [58]. These studies have led to the following empirical relation for estimating the peak base torque  $T_{\max}[U(h)]$  induced by the winds with speed  $U(h)$  at the top of the building:

$$T_{\max}[U(h)] = \psi \{ \bar{T}[U(h)] + g_T T_{\text{rms}}[U(h)] \}$$

where  $\psi$  is a reduction coefficient ( $0.75 < \psi \leq 1$  in most cases) and  $g_T \approx 3.8$  is a torsional peak factor. Mean and rms base torque are given by expressions:

$$\bar{T}[U(h)] \approx 0.038 \rho L^4 h n_T^2 U_r^2$$

$$T_{\text{rms}}[U(h)] \approx 0.00167 \frac{1}{\sqrt{\xi_T}} \rho L^4 h n_T^2 U_r^2 \cdot 68$$

and

$$U_r = \frac{U(h)}{n_T L}$$

$$L = \frac{\int |r| ds}{\sqrt{A}}$$

where  $\rho$  is the air density,  $h$  is the height of the building,  $n_T$  and  $\xi_T$  are the natural frequency and damping ratio in the torsional mode of vibration,  $ds$  is the elemental length of the building perimeter,  $|r|$  is the torque arm of the element  $ds$  (i.e. the distance between the elastic centre and the normal to the building boundary at the centre of element  $ds$ ), and  $A$  is the cross-sectional area of the building.

### 3.3.4 Full-scale Measurements

In 1930, measurements were made of the horizontal deflections at the top of the Empire State Building in New York [95]. The total height of the building including the tower is 448 m, with a natural frequency of 0.12 Hz in the first mode of vibration. The deflection of the building was measured at the top by means of a long-suspension pendulum which deflected by 163 mm and vibrated with a double amplitude of 180 mm at a wind speed of 35 m/s. The acceleration corresponding to these values lies near 0.5%  $g$  [42].

Korchinskiy [70] measured the response of Moscow State University, a 190 m tall building with 0.55 Hz natural frequency to be 0.14 mm at 36th storey in along-wind direction.

Davenport [33] measured the response of 370 m tall John Hancock Centre in Chicago. The first bending frequencies in two perpendicular planes are 0.15 Hz and 0.21 Hz respectively. The RMS of the dynamic deflection determined at the top of the building in along-wind direction was 1.05 mm at mean wind speed of  $\bar{U}_{10} = 18$  m/s. Davenport [31] has summarized the history of full-scale measurements and outlined many of the difficulties encountered, particularly in pressure measurements.

Newberry [87] determined horizontal and vertical scale of gusts, as experienced by the building. These are much larger than that of the undisturbed wind due to the cushioning effects on the front of the building.

The cushioning effect can be explained by the vorticity stretching and tilting effects as the mean flow distorts in the "presence of a bluff body".

Because full-scale measurements not only provide information for better understanding of the basic flow around structures but also help to correlate measurements with existing wind tunnel experiments, hence after 1970's there have been a number of full-scale measurements made by different investigators. Among these researchers the work done by Isyumov and Davenport [56], Melbourne [83, 85], Makino [81], Takeuchi [122], Yoshikawa [141] and Reed [96] are appreciable for their contribution in this field.

### 3.4 Interference Effects in Tall Buildings

The first study of interaction effects in relation to tall buildings seems to be due to Harris [51], who found by means of a wind tunnel study in 1934, that two blocks planned to be built in the vicinity of the Empire State Building in New York city, would practically double the torsional wind loading on the latter. Several authors, such as Chien [18], Hamilton [47], Blessmann [11] and Leutheusser [78], observed that in two prismatic building models located close to each other, suctions may attain values much higher than those observed on isolated models.

Other studies related to pressure and wind velocity between buildings are due to Kelnhofer [66], Ishizaki and Sung [55] and Wiren [135].

Thomas and Isyumov [124] have reported the results of a wind tunnel model study which examined the mean and peak surface pressures on a rectangular tall building in the presence of another identical building. They concluded that in a relatively smooth terrain the maximum peak surface suctions could increase up to about 20 per cent due to the addition of a nearby building. They observed that very close proximity generally offers some shelter (shielding) from the action of the wind and also it is likely

that a nearby building causes a redistribution of high suctions resulting in reduction in some area and increase in others.

Blessmann and Riera [11, 12] studied the interaction effects between two square prisms for 15 relative positions with 24 different orientations. They conducted these tests in uniform flow and also in a turbulent shear flow and [12] respectively. These authors have calculated force and torsional moment coefficients for each face as well as for the entire building from pressure readings on a rigid model, and, reported a 30% increase in the maximum resultant force coefficient caused by buffeting with respect to the isolated building in both the flow conditions. The maximum torsional moment coefficient was estimated to be threefold due to the presence of upwind structure. A maximum of 5.4% blockage for the shear flow studies was reported which resulted in about 3% overestimation of the pressure coefficients. Peterka and Cermak [93] investigated the adverse wind loads on central tower in Renaissance Centre Complex proposed for Detroit. The centre circular structure has 210 m height, 39 m diameter and 7.3 m circular elevator shaft attached from outside to the tower and surrounded by four octagonal structures each 150 m high with two 11.4 m diameter circular elevator shafts. They observed that the presence of adjacent buildings and the building surface roughness, both have important influences on the pressure distribution on the central circular building of the Renaissance Centre Complex. While the roughness variation had approximately the same influence on mean pressures as the adjacent buildings, its influence on the peak pressures was significantly larger.

The interaction effects on aerodynamic forces were studied by Reinhold [97, 99]. He recommended that any interference study should be carried out in a turbulent flow that closely simulates the flow at the site of the full scale structures. He observed that the presence of an upstream object did

afford a significant degree of shielding when the two objects were in line. However, significant fluctuating forces and moments were developed even in those cases. The strongest mean moments occurred when the two prisms were offset normal to the velocity direction. The fluctuating moments indicated strong possibility of torsional excitation of the square prism.

Ruscheweyh [104] investigated interference effects from an upstream building of similar size and different shape on a downstream building. The investigation showed that the turbulence of the approach flow has only little influence on the intensity of the interference effects. This is in contradiction to other reportings. While the dynamic interference effect showed increase by a factor of about two in bending vibration, he confirmed a threefold enhancement in torsional vibration reported by Blessmann [11, 12] due to proximity effects.

The first systematic set of tests were performed by Melbourne and Sharp [86] to investigate the effect of a building positioned upwind of an aeroelastic square across-sectional model with aspect ratio of 6. They found that the rms cross-wind response was increased by a maximum of 75% in the suburban environment, while in the urban environment the increase was a lesser value of 25%. In the along-wind direction the respective increase were 25% and 15%. Saunders and Melbourne [109,110] highlighted the interferences of a medium-size building using buffeting factors which was defined as a measure of the wind loads produced by the presence of the upstream structure(s) compared to the loads without the upstream structure(s). their results showed that the presence of an upstream building of the same size could increase the dynamic loads by a factor of 1.65. A 220 m tall square building upstream of the 150 m high building increased the factor to 1.90. In case of twin 220 m buildings upstream of an aeroelastic model for 5 width airspace between models further enhanced this factor to



2.15 at a reduced velocity of 4. The critical locations for upstream building were reported to occur from  $4b$  to  $8b$  on streamwise direction and  $1b-3b$  at transverse direction where  $b$  was the width of the building. For twin models on upstream, the highest buffeting factors developed generally between  $4b$  to  $16b$ . Saunders and Melbourne [109] suggested that buffeting factors for both along-wind and across-wind are significant up to a distance of  $750\text{ m}$  for a same size building on upstream side and about  $1\text{ km}$  for a twin taller structures in full-scale which corresponds to nearly  $20b$  for the first case and  $30b$  for latter.

Sykes [121] studied the interaction effects between two buildings of rectangular planform in an atmospheric shear flow. He also observed that except some cases, the mean longitudinal displacements experienced shielding effect whereas fluctuating along-wind displacements were generally enhanced by interference effects. He has shown that the fluctuating lateral displacements reduce at reduced velocity around 10, at which the isolated dynamic model experienced peak response amplitudes, but enhanced at lower reduced velocity of around 6 by presence of the wake from upwind model. He claims that the relative change in response amplitude, i.e. buffeting factor was independent of the applied damping. He also concluded that the largest response occurs when the face of the model is normal to the mean wind direction.

Recent work by Bailey and Kwok [8,73], who have investigated the interference effects of both an upstream and a downstream building of the same size, have provided more information about the interference excitation mechanisms. A summary of the conclusions given in these papers is as follows:

1. Interference effect is significant for upstream interfering building for a large range of reduced velocity. A maximum buffeting factor of

up to 3.2 in both along-wind and across-wind directions were reported when the interfering building was a circular cylinder.

2. In most of the cases, maximum response of the principal building occurred in the uniformly fluctuating high-velocity flow near the edge of the incident wake rather than in the highly turbulent low-velocity flow within the wake region.
3. Although downstream interfering building has very little effect on the response of an upstream building for most relative locations, it produces consistently the larger buffeting factors. A buffeting factor of 4.36 was reported in this case.
4. The magnitude of increase in wind loads due to interference is strongly dependent on the approach terrain. A change of terrain from open to suburban caused 30% reduction in wind loads.

Taniike and Inaoka [123] has studied the increased response and its possible aeroelastic mechanism of a high-rise rectangular building under the interference excitation of three types of upwind buildings with different breadths. They observed that in a low turbulent flow over open terrain, while the along-wind response has a tendency to increase with the size of upstream building, the across-wind response of the downstream building under an interfering building of smaller breadth may increase up to 20 times as large as that of the isolated building due to occurrence of resonance at reduced velocity range of 5 to 6.

Kareem [61, 65] has also investigated the adverse or beneficial effects due to a single or a pair of upstream prisms of the same size on a downstream building. His general conclusions are almost like those reported by Saunders and Melbourne, Sykes and Bailey and Kwok.

Very recently Sakamoto and Haniu [105] have investigated the aerodynamic forces on two square prisms placed vertically in a turbulent

boundary layer. The mean and fluctuating drag force as well as fluctuating lift and the vortex shedding frequency were investigated experimentally for three types of arrangements, namely tandem, side-by-side and staggered. They have classified the fluid forces and Strouhal number into different regions. Their contribution is mainly on elaboration of the interference mechanism and development of different regions for aerodynamic forces on two square models placed nearby.

### 3.5 Closure

The above studies include some investigations experienced in the local pressure fluctuations, static and dynamic force coefficients, aeroelastic response of prismatic building models and a variety of proprietary tests of particular topographical features and geometric layouts of surrounding structures. These investigations have provided information for the development of a data base to provide guidance in at least qualitatively estimating the level of interference for a selected group of building geometries and their respective layout configuration.

Only a few wind tunnel studies to determine the extent of interference effects between two buildings (of the same size) have been reported. As pointed out earlier, some discrepancies exist amongst the values of the maximum increase in wind loads reported and also in the critical interference locations. These anomalies present difficulties in making use of these results in design application. Hence more experimental work - both qualitative and quantitative - are required to accurately determine the changes in wind loads and to demarcate the critical interference zones. This exercise would be required firstly for two tall building models of same size and subsequently for buildings of different sizes, heights and shapes. Lastly, similar studies may also be required for a group of more than two buildings.

## CHAPTER 4

### EXPERIMENTAL PROGRAMME

#### 4.1 Preliminary Remarks

An investigation can be either mathematical or experimental. In the former, a mathematical model of the process under study is formulated. In most of the complex situations, the mathematical model is based on some simplifying assumptions and the accuracy of the results obtained depends upon the extent to which these assumptions hold. The experiments, on the other hand, can either be field measurements on prototypes or laboratory measurements on models. The advantage of experiments on models over full scale measurements derives chiefly from the possibility of modelling well the properties of the basic material, the boundary conditions of the model and the air flow characteristics; and being able to conduct the experiments under controlled conditions. The deviation of model laws is based on the physical similitude of two processes, i.e. on the fact that the process satisfy the physical similarity requirements. Two processes are similar to one another if their corresponding physical quantities are in a constant ratio.

#### 4.2 Modelling Criteria for the Atmospheric Boundary Layer

Plate in 1971 [94] has derived a set of non-dimensional equations of motion and energy conservation by using some reference quantities. These reference quantities are

- (i) a reference length for the vertical extent of the flow field,  $L_R$
- (ii) a reference velocity,  $U_R$
- (iii) a reference time,  $t_R$
- (iv) a reference temperature,  $T_R$

(v) a reference excess temperature,  $\Delta T_R$

The equations of motion and of energy of the atmosphere are:

$$\frac{1}{St} \frac{\partial \vec{U}}{\partial t} + (\vec{U} \Delta) \vec{U} = -\Delta p + \frac{1}{Re} \Delta^2 \vec{U} - \frac{1}{Ro} \vec{K} \vec{U} + \frac{1}{Fr^2} \frac{\Delta T}{T} \vec{K} \quad 4.1$$

and

$$\frac{1}{St} \frac{\partial \Delta T}{\partial T} + (\vec{U} \Delta) \Delta T = \frac{1}{Pr \cdot Re} \Delta^2 \Delta T + \frac{EC}{Re} \phi \quad 4.2$$

Here  $\vec{U}$  is the dimensionless velocity vector ( $U = \text{Velocity}/U_R$ ),  $p$  the pressure which is made non-dimensional by  $\rho U_R^2$  and  $\Delta T$  is made dimensionless by  $\Delta T_R$ . The latter is the dimensionless deviation from a suitable mean temperature with scale factor  $T_R$ . The vector  $\vec{K}$  is the unit vector pointing vertically upward from the earth surface, and  $\phi$  is the dimensionless energy dissipation per unit volume or mass. Apart from the boundary conditions, the flow field is governed by the following dimensionless numbers contained in the above expressions:

(a) the Rossby number,

$$Ro = U_R / L_R f \quad 4.3$$

with  $f = \text{Coriolis parameter}$

$$= z \times (\text{rotation rate of earth}) \times$$

(sine of latitude)

(b) the Reynolds number,

$$Re = U_R L_R / \nu \quad 4.4$$

with  $\nu = \text{kinetic viscosity of air}$ :

(c) the Strouhal number:

$$St = U_R / L_R \cdot t_R \quad 4.5$$

(d) the Froude number:

$$Fr = U_R / \sqrt{g' / L_R} \quad 4.6$$

$$g' = \frac{\Delta T_R}{T_R} g$$

(e) the Eckert number:

$$Ec = \rho U_R^2 / C_p \Delta T_R \quad 4.7$$

(f) the Prandtl number,

$$Pr = \rho \nu C_p / k \quad 4.8$$

with  $k$ =thermal conductivity of air:

The foregoing requirements must be supplemented by the stipulation that the surface boundary conditions and the approach flow characteristics be similar for the atmosphere and the model. A detailed discussion of the similarity requirements for the atmospheric boundary layer is also given by Cermak [14, 15].

If all the foregoing requirements were met simultaneously, all scales of the motion; namely micro-scale ( $10^{-3}$ -  $10^1$  m), small scale ( $10^1$ -  $10^4$  m), and meso-scale ( $10^4$ -  $10^5$  m) could be simulated within the same flow field for a given set of boundary conditions. In such a case the exact simulation of the atmosphere is achieved. However, all of these requirements cannot be satisfied simultaneously by existing laboratory facilities, so that partial or approximate simulation must be used.

The main effect of the Rossby number is that it describes the strength of the Coriolis effect which manifests itself in a rotation of the velocity vector with height. Little is known about how this affects strong winds but it is usually assumed that the veering of the wind does not affect the forces on tall structures. Further, in most of the cases of practical importance it

assumption that large scale unsteadiness of the atmospheric flow takes place so gradually (in a time period of the order of hours) that its effect can be neglected. With air as fluid, the Prandtl number is the same in model and prototype. Also the Eckert number which denotes the ratio of kinetic to excess internal energy, does not seem to be of dynamic significance [94].

The Froude number enters into modelling either if the atmospheric flow is thermally stratified, or if the disturbance of the atmospheric flow whose effect is to be studied introduces buoyancy effects. In principle, it is possible to obtain Froude number similarity, even though it may require for stratified flow, the use of a wind tunnel whose floor and/or roof can be heated or cooled. Reynolds number similarity can usually not be obtained, because velocities, densities, and kinematic viscosities are of the same order in model and prototype, while geometric scales vary from 1:50 to 1:5000 [94]. Fortunately, it is possible to circumvent the effect of Reynolds number in many cases. For example when the structures, as in the present study are of a block form with sharp edges, a relaxation of the Reynolds number requirement for similarity is possible. The equality of Reynolds number is replaced by a minimum Reynolds number for the scaled down model, which ensures invariance of the flow pattern or the drag coefficient with Reynolds number for a representative structure. Accordingly of the aforesaid dimensionless numbers, only the Strouhal number is considered to be significant in the present study.

#### 4.3 Modelling of the Atmospheric Boundary Layers

##### a) Modelling of Mean Velocity Profile

The requirement of zero pressure gradient in the boundary layer cannot be achieved in the wind tunnel since the wind tunnel boundary layer obtains its energy input from the external flow above the boundary layer, which

ultimately is driven by a pressure gradient alone. However, Plate [94] and others have shown that the lower part of the atmospheric boundary layer presents an exact analog of the lower part of the wind tunnel boundary layer. It is therefore possible to represent the atmospheric boundary layer by a wind tunnel boundary layer. As it has been explained in section 2.2.1, the most convenient way of representing the total depth of boundary layer is by the power law. The exponent of this law in the atmosphere and the wind tunnel must be the same to simulate the mean wind speed. Equality of the exponents does not necessarily imply that the ratio of the  $Z_0$  values is matched ( $Z_0$  is the roughness height); in fact, for each  $Z_0$  there exists only one exponent factor  $\alpha$ . In the wind tunnel, any required exponent  $\alpha$  can be obtained by a suitable arrangement of roughness elements and externally impressed disturbances—such as by grids or fences at the inlet of the test section.

The mean velocity profiles used in this thesis are presented in Fig. 4.1. Two wind profiles having exponent factors approximately 0.30 and 0.10 to represent a built-up environment (urban) and open area respectively were developed in the wind tunnel with the help of vortex generators and roughness blocks (photo 3 and 4).

The variation of the mean velocity (at the test section) along the width of the tunnel was determined by measuring the mean velocity while traversing the hot-wire at  $2/3$  model height. For the central 0.40 m width the variation in the mean velocity was found to be within 4% of the mean flow at the mid-section where the model was placed. The width of 0.40 m is about 4 times the breadth of the building models used.

#### b) Modelling of Turbulence Parameters

Turbulence parameters which are important in engineering problems include turbulence intensities, scales and turbulence spectra. Experience



with simulating atmospheric boundary layers has shown that similarity for turbulence parameters can in fact be obtained.

The longitudinal intensity profiles as a function of height are presented for both boundary layers in Fig. 4.2. The values of intensities at model height are 10.5% and 4% corresponding to power law coefficients of 0.30 and 0.10 respectively.

### c) Modelling of Atmospheric Spectra

The input of turbulent energy into the atmosphere is associated with eddies ranging from those generated by nearby sources of small scale to eddies generated by global processes. The spectral gap of Van der Hoven separates the atmospheric spectrum into two parts, with modelling of the high frequency part well within the scope of wind tunnel capabilities and ideally modelled if the scale of the wind tunnel experiment is about 1:1000 [15]. The low frequency part of the spectrum is dynamically of no significance.

From the theory of Kolmogorov the high frequency portion of the longitudinal spectrum of turbulent velocity fluctuations, on the average takes the form:

$$\frac{nS_u(z, n)}{u_*^2} = 0.26 \left( \frac{nz}{\bar{u}(z)} \right)^{-2/3} \quad 4.9$$

where  $u_*$  is the surface shear or friction velocity  $u_* = \sqrt{\tau_0/\rho}$ ,  $\tau_0$  is shear stress at the surface. Davenport [23] and Harris [H.8] have expressed the longitudinal spectrum of wind in terms of fixed length and velocity scales. Davenport [23] suggested the following empirical representation of the spectrum:

$$\frac{nS_u(n)}{u_*^2} = \frac{4x^2}{[1+x^2]^{4/3}} \quad 4.10$$

where  $x = Ln / \bar{u}(10)$ ,  $L$  (equals to 1200 m) is a scale of turbulence. The principal difference between these two equations lies in the scaling of the frequency or the local wave length. In equation 4.9 scaling is in proportion to the height whereas in equation 4.10 it is a fixed length scale.

The longitudinal velocity spectrum at model height in the wind tunnel is presented in Fig. 4.3. The measurements were made using a DANTEC constant Temperature Hot Wire Anemometer system with an Oscilloscope (used as a frequency analyzer) which held two filters of 1 Hz to 100 KHz and 10 Hz to 1 MHz frequencies used as High Pass and Low Pass filters respectively. The spectrum is compared with those reported by Davenport, Harris and Schnabel and Plate. The results show a good agreement with those of full scale measurements. In Fig. 4.3,  $n_m$ ,  $S(n)$  and  $\sigma^2$  are frequency at peak, energy density (spectral density) at frequency  $n$  and variance of the velocity fluctuations.

With the shape of the spectrum the same in the model and prototype, it may be inferred that

$$\frac{u_M S(0)}{\overline{u'^2}} = \text{constant} \quad 4.11$$

and since  $S(0) \approx \overline{u'^2}$ ,  $L / \bar{u}$ , it follows

$$\frac{n_M L}{\bar{u}} = \text{constant} \quad 4.12$$

or

$$\lambda_L = \frac{L_m}{L_p} = \frac{n_{M_p}}{n_{M_m}} \frac{\bar{u}_m}{\bar{u}_p} \quad 4.13$$

Exact scaling is then accomplished by keeping  $\overline{u'^2}$  constant in the model and the prototype, and by having  $n_M$  scaled properly. The first condition is

met by establishing the correct turbulence intensity profile. It follows from eq. 4.13 that the characteristic frequency  $n_M = \bar{u}/L_R$  is scaled if, for constant  $\bar{u}$ ,  $(n_M)_{\text{model}} / (n_M)_{\text{prototype}} = 1/\lambda$  ( $L_R$  is reference or characteristic length). This condition can indeed be satisfied as shown in Fig. 4.3. It seems that if mean velocity profiles are matched in model and prototype, the scaling frequencies are also matched [94].

#### 4.4 Geometric Modelling

The geometric scale is selected to maintain equality of the ratio of overall building dimensions to the inherent lengths of the generated model of the natural wind. The most important lengths of the flow for aeroelastic simulations of tall buildings are the boundary layer depth, the scale of the turbulence and boundary roughness. Under the ideal simulation of a boundary layer all three should lead to the same linearly geometric scaling. In general, this does not hold true exactly, however, the length scaling is limited by the size of the wind tunnel facilities and should be chosen with due regard to wind tunnel blockage. Corrections are generally required if the blockage exceeds about 5% of the wind tunnel cross section.

Considering the above requirements and difficulties of modelling a particular flow field, a geometric length scale  $\lambda_L = 1/250$  was selected. The blockage for the building models were 1.5% and 1.8%.

#### 4.5 Aeroelastic Modelling of Tall Buildings

Having selected the geometric scale for the building model, the additional modelling requirements are to be met in relation to the similarity of the dynamic behaviour of the model and full scale. These additional modelling criteria require equality of the following ratios in model and in prototype [57]:

$$\text{Mass : } \frac{\rho_b}{\rho} = \frac{\text{inertia forces of building}}{\text{inertia forces of flow}} \quad 4.14$$

$$\text{Stiffness : } \frac{E}{\rho u^2} = \frac{\text{elastic forces}}{\text{inertia forces of flow}} \quad 4.15$$

$$\text{Damping: } \xi = \frac{\text{dissipative structural forces}}{\text{inertia forces of flow}} \quad 4.16$$

where  $\rho_b, \rho, E, u$  and  $\xi$  are the bulk building density, air density, the modulus of elasticity or equivalent, wind speed and the damping expressed as a proportion of critical damping respectively.

Sharp edged structures have fixed points of separation. The flow around such bodies, therefore can be considered to be more or less independent of Reynolds number. The studies related to curved bodies however, should be considered with caution.

Froude number scaling, in general is not important for tall buildings and free standing structures where the stiffness depends predominantly on elastic forces. Froude number is important for structures whose stiffness is dependent on gravitational forces, such as suspension bridges and hanging roofs.

Air density for the model and the prototype being the same the similarity of inertia requires that the bulk building density be maintained constant in both the model as well as the prototype. In situations where there are significant differences in the model and prototype air densities due to significant changes in elevation or temperature, the bulk density of the structure must be carefully modelled. Strict modelling of the elastic properties is not necessary for buildings and a sufficient requirement is to

achieve similarity of dynamic behaviour in modes of vibration for which wind action is important [57]. Most aeroelastic studies are based on a discrete representation of the building and the modelling of inertia and elastic effects requires similarity of the mass and stiffness of the model and prototype buildings.

The mass scaling parameter  $\lambda_M$  is determined by equation 4.14 ( for translation ),

$$\lambda_M = \frac{L_m^3 \rho_{b_m}}{L_p^3 \rho_{b_p}} = \lambda_L^3 \lambda_{\rho_b} \quad 4.17$$

In the absence of Froude number scaling requirements, the velocity scale is required to achieve a minimum body Reynolds number. For a consistent scaling of all relevant modes of vibration, the velocity scale becomes,

$$\lambda_U = \frac{u_m}{u_p} = \lambda_L / \lambda_T \quad 4.18$$

Where T is the time or period of vibration.

Having chosen the velocity scale for the simulation, the stiffness scaling becomes,

$$\lambda_K = \frac{\lambda_F}{\lambda_L}$$

but

$$\lambda_F = \lambda_M \lambda_a = \lambda_M \lambda_L / \lambda_T^2$$

therefore

$$\lambda_K = \frac{\lambda_M \lambda_L}{\lambda_L \lambda_T^2}$$

or 
$$\lambda_K = \frac{\lambda_M \lambda_U}{\lambda_L \lambda_T}$$

hence 
$$\lambda_K = \lambda_L \lambda_U^2 \lambda_{\rho_b}$$
 4.19

In most wind tunnel situations  $\lambda_{\rho} \approx 1$

The degree of aeroelastic similarity achieved depends on the intended function of the model and the limitations on the size of the model, available model materials, economic considerations and fabrication techniques used.

#### 4.6 Design of Aeroelastic Model

A typical tall rectangular building having the following dimensions and characteristics was selected for study:

Height	:	150 m
Cross section	:	25 m x 30 m
Bulk building density	:	1700 N/M <sup>3</sup> ( $\approx 170 \text{ kg/m}^3$ )
Time period of vibration	:	4 sec and 4.5 sec (in two principal directions respectively)
Damping ratio	:	1 % (in both directions)
(in first mode)		

A summary of the scaling parameters used and their corresponding design values are given below

PARAMETER	SCALING REQUIREMENT	DESIGN VALUE
Length	$\lambda_L = \frac{L_m}{L_p}$	1/250

Bulk Building Density	$\lambda_{\rho_b} = \frac{\rho_{b_m}}{\rho_{b_p}}$	1
Mass	$\lambda_M = \lambda_L^3 \lambda_{\rho_b}$	$6.4 \times 10^{-8}$
Velocity	$\lambda_U = \frac{u_m}{u_p}$	2/9
Time Period	$\lambda_T = \frac{\lambda_L}{\lambda_U}$	9/500
Stiffness	$\lambda_K = \lambda_L \lambda_U \lambda_{\rho_b}$	$19.7 \times 10^{-5}$
Damping	$\lambda_{\xi} = \frac{\xi_m}{\xi_p}$	1

For the above scale values the total weight of the model worked out to be 12.24 Newtons.

#### 4.7 Fabrication of Models

##### a) Rigid Models

A set of rigid models were fabricated in the laboratory using 5 mm thick plywood.

##### b) Aeroelastic Model

An aeroelastic model whose principle is similar to that given by Isyumov [57] and others [107], [61] was adopted for fabrication. the conventional "stick" aeroelastic model, as called by Isyumov, is a rigid model of the building, spring mounted near the base to provide a simulation

of one or two orthogonal fundamental sway modes of vibration. The schematic representation of this model is shown in Fig. 4.4 and photographs of the same in Photo No. 1 and 2. The mounting hardware consists of the following:

- i) a set of gimbals consisting of two metallic rings of 50 mm thickness pivoted at  $90^\circ$  &  $180^\circ$  orientation in a brass frame
- ii) a rigid aluminium tube extending below the model through inner ring of gimbals and
- iii) two sets of specially designed and fabricated helical springs to restrain the building model.

A stiffened box made from 6 mm thick perspex sheets was used to accommodate and hold the springs and transducers.

The stiffness as well as the natural frequency of the building model could simultaneously be changed if desired. This was achieved by changing the position of the metallic rings holding the springs on aluminium tube on one side and spring holders in the slots of perspex box on the other side of the springs in both the directions. This arrangement is shown in Fig. 4.6.

The body of the building model was made from 3 mm thick Plywood to minimize the weight and was stiffened with two aluminium plates of 2 mm thickness to ensure the rigidity of the model. The rigidity of the model and perspex box was tested later on.

An electro-magnet damping device was also fabricated to increase damping in two directions. However, after a free vibration test of the model without electro-magnet damper it was noticed that damping ratio of the model itself is higher than the desired value (about 2.5%) and hence the electro-magnet damping device was not used in the whole experimental work. The correction due to the higher than needed damping was applied in the analyses.

The total mass of the vibratory part of the model (including two



accelerometers at the top) was maintained at the design value.

#### 4.8 Reliability of the Stick Aeroelastic Model

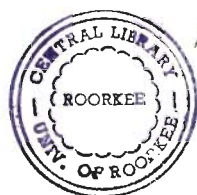
The basic assumption in this type of the model is that the two orthogonal fundamental sway modes of vibration are linear. The wind induced response is primarily in these two principal directions for most tall buildings of compact cross section [57]. Of the higher modes of vibration, only the fundamental torsional mode requires consideration in certain situations. If this is the case, a stick aeroelastic model cannot be used.

A comparison of the dynamic drag and lift responses of a tall building obtained with a stick model and seven lumped mass simulations is given by Isyumov [57] and presented in Fig. 4.5. The agreement between the estimates of the rms drag response is seen to be good. This supports the comments about the predominance of the fundamental modes of vibration and shows the reliability of the use of stick models if torsion is not dominating. The indicated structural damping of about 1% is a nominal value and the differences in lift response around the vortex shedding peak are mainly attributed to slight differences in actual damping values.

The principal advantage of the stick aeroelastic model is its simplicity, economy and speed of fabrication. It is possible to readily change the mass, stiffness, damping and even the geometric properties to provide information on the sensitivity of the wind induced response to changes in the building configuration.

#### 4.9 The Wind Tunnel

All the experiments carried out for this thesis were conducted in an open circuit wind tunnel located in Civil Engineering Department at University of Roorkee, which was the largest boundary layer wind tunnel



245698

among the existing tunnels in the country. This wind tunnel has a working section of 2 m x 2 m (average) and 15 m long. The tunnel section at the entrance is 2.00 m x 1.85 and increase to 2.10m x 2.15m at the end of the test section, there by providing a flare to the side walls. The ceiling is adjustable such that alongwith the sidewall flare gives a zero pressure gradient. By suitably adjusting the ceiling a zero pressure gradient has been obtained at a distance of about 6 m from the upstream end (Fig. 4.6). A schematic diagram of the wind tunnel is shown in Fig. 4.7. near the downstream edge of the test section, a natural boundary layer approximately 0.20 m [4] thick develops due to the long length of the tunnel, even without provision of any grid or floor roughening divices. However, presence of a barrier wall, vortex generators and friction blocks helps in obtaining a much thicker boundary layer. A boundary layer of the order of 1.0 m was obtained for the models used in this study. The salient features of the open circuit boundary layer wind tunnel are as follows:

Total length of wind tunnel	: 38.0 m
Length of test section	: 15.0 m
Length of diffuser	: 16.0 m
Test section cross section	
at upstream end	: 2.00 x 1.85 m
at downstream end	: 2.10 x 2.15 m
Contraction ratio of effuser	: 9.5 : 1
Effuser profile	: Elliptical
Maximum wind speed	: 20 m/s at ≈1.0 height
Boundary layer thickness	: Nearly 1.0 m
Capacity of fan	: 75 m <sup>3</sup> /sec
Power of motor	: 125 H.P.
Speed of motor	: 1440 rpm

## 4.10 Instrumentation and Measurements

### 4.10.1 Design and Fabrication of Strain Gauge Transducers

For measuring mean and fluctuating components of along-wind as well as fluctuating across-wind responses of the model, a set of cantilever type strain gauge displacement transducers were developed and fabricated in the laboratory. Considering the limitations of fabrication techniques, it was attempted to make a reliable as well as a simple and economic transducer. Three alternatives for location of the transducers were tried-near the gimbals to measure movements, close to the springs to observe forces, and at the end of the aluminium tube to measure displacements. The latter alternative was adopted because of its simplicity in fabrication.

The transducer was based on the concept of bending moment created due to the force applied at the free end of a cantilever elastic strip acting as a leaf spring. The strain corresponding to the bending moment at the fixed end could then be related to the deflection at the free end. A relationship between strain and deflection was obtained from linear stress-bending relation as follows:

$$E = \frac{1.5 t_h \Delta}{L^2}$$

where  $E$ ,  $\Delta$ ,  $t_h$  and  $L$  are strain measured in one gauge, deflection, thickness and length of the leaf spring respectively. The leaf spring chosen had the following dimensions with a modulus of elasticity equal to  $10.0 \times 10^4$  N/mm<sup>2</sup>.

$L = 50$  mm; breadth = 10mm and  $t_h = 0.35$  mm

Two transducers were made to measure displacements in two principal directions (along-wind and across-wind). Each transducer consisted of a brass leaf spring rigidly pasted and screwed to a solid brass rod of about 7 mm diameter. At the extreme end of the leaf spring (near the rod), two

strain gauges are pasted to sense strains developed at the end of leaf spring due to the force near its free end.

The strain gauges used were of type BKSAR-5 of Rohit and Co (India) Roorkee with resistance of  $120.8 \pm 0.2$  Ohms and gauge factor of 2.00. The strain gauges were pasted according to the instructions given by the manufacturer and the adhesive was also provided by them. The gauges were moisture-proofed by Rohit and Co.

#### 4.10.2 Measurements on Aeroelastic Model

Since it was not possible to place the aeroelastic models on the turn table, a cut was made in the wind tunnel floor at a distance of about 1.6 m from centre of the turn table. The difference in the boundary layer thickness between these two sections was found to be negligible. Two parameters viz displacement and acceleration were measured near the top on the aeroelastic model in along-wind as well as across-wind directions by a set of strain gauge transducers and accelerometers respectively. The strain gauge transducers had the details as explained above. The accelerometers were designed and supplied by M/S New Engineering Enterprises, Roorkee. The outputs of strain gauge transducers and accelerometers were amplified and then recorded by using two sets of universal amplifiers and strip chart recorders. The arrangement of the instruments are shown in Fig. 4.8. The specifications of amplifiers and chart recorder are as follows:

##### a) Universal amplifier Model (U040 with no display)

- \*) Maximum sensitivity : 1 micro vatt/mm
- \*) Transducer excitation : 2 V at 5KHz
- \*) Attenuation range : x1, 2, 5, 20, 50, 100, 200, 500  
& 1000
- \*) Gain control : For smooth control of  
system gain

- \* ) Frequency response : DC to 100 Hz (with 40 mm/channel recorder) DC to 200 HZ (with CRO)
  - \* ) Transducer impedance : min-100 ohms  
Max-1500 ohms
  - \* ) Output impedance : Less than 50 ohms
- b) Recorder
- \* Number of channels : 2
  - \* Chart width : 50 mm (each)
  - \* Chart speed (mm/sec) : 1, 2, 5, 10, 25, 50, 125, 250

#### 4.10.3 Measurements on Rigid Model

The rigid model was fixed in the middle of turn table and mounted firmly on a 3-component load cell Model DSA-100 from M/S N.E.W, Japan having following specifications:

- \* Applicable bridge resistance : 60 ohms to 2000 ohms
- \* Voltage impressed : DC 3, 6, 9, 12 V  $\pm 0.2\%$  50MA
- \* Range of equilibrium adjustment
  - i) Coarse adjustment :  $\pm 5\text{mV/V}$
  - ii) Fine adjustment :  $\pm 100\text{ mV max}$
- \* Amplification factor : Max. 17,000
- \* Sensitivity : 0, 1, 2, 5, 10, 20, 50
- \* Non linearity : 0.005% FS
- \* Response characteristics : 2 KHz/-3dB
- \* Calibration strain :  $\pm 50, 100, 200, 500, 1000, 2000,$   
 $5000 \times 10^{-6}$  strain

- \* Filter frequency range  
attenuation characteristics : 0.3, 1, 3, 10, 30, 100, 300 Hz,  
Pass -12 dB/Octave
- \* Needed power supply : AC 100 V  $\pm$ 10%, 50/60 Hz, 20VA

The resultant forces and moments were integrated for 10 seconds using a digital integrator.

#### 4.10.4 Measurements of Wind Parameters

Mean velocity and turbulence intensity were measured both at the middle of turn table as well as at the aeroelastic test section. A constant temperature anemometer obtained from DANTEC of Denmark was obtained for measurements of mean and fluctuating components of velocity. The output of main unit 55M01 was linearized on a 55M25 linearizer and read on a 56N22 mean value unit and a 56N25 rms unit (all from M/S Dantec).

The probe used for measuring all the above mentioned parameters was a 55P11 strain probe having 5 $\mu$  thick platinum coated tungsten wire. The resistance of the probe including the leads was 4.0 ohms.

The hot-wire anemometer was calibrated against a static alcohol manometer with specific gravity of 0.82 and inclined at approximately 15<sup>o</sup> to the horizontal.

#### 4.11 Procedures and Data Reduction

The velocity profile measurements in the wind tunnel were made in shear flow with five elliptical vortex generators at the entrance of the test section and having 1 m height. The velocity probe would be moved vertically by mounting it to an attachment on a vertical threaded rod supported on a frame fixed inside the tunnel. The threaded rod can be rotated by an electric motor mounted on the frame which would be controlled from outside

the tunnel.

The intensity of turbulence was calculated by dividing the fluctuating velocity component obtained from the rms unit by the value indicated on the mean unit.

The spectrum of the horizontal component of velocity  $S_u(n)$  represents a spectral decomposition of energy at various frequencies. Variance of the velocity fluctuation was used to normalise the velocity spectrum and is defined as  $S_u(n)/\sigma^2$ .

The area under the normalized spectra is equal to unity. The velocity spectrum can also be represented as a reduced normalised spectrum as  $nS_u(n)/\sigma^2$ .

Acceleration near the top of the model were also measured in both the directions for some of the cases to cross-check the fluctuating components of displacement measured from strain gauge transducers. The peak displacements were calculated from acceleration records as follows:

$$\text{displacement} = \text{acceleration} / (2\pi\omega_n)^2$$

where  $\omega_n$  is the first mode natural frequency in cycles per second. However, since the mean along-wind response could not be obtained from these accelerometers, they were not used in later stages.

Typical records of the variation of displacement amplitude with time for both along-wind and across-wind and different reduced velocity are shown in Figs. 4.9 through 4.12. From analysis of these records the mean, peak and rms values of fluctuating components of along-wind and across-wind responses of building model could be obtained. One of the important considerations in this type of analysis is to choose a suitable sampling time. In order to assess the effect of sampling time on the values obtained, the record was analyzed using various lengths of sampling time ranging from 1 to 10 seconds. The results obtained are shown in Fig. 4.13. As is obvious, the values

become constant after about 5 seconds, indicating that a length of record of 5 seconds should be adequate. However, the length of record was generally taken about 45 seconds to have sufficient number of repeated peaks.

The probability density measurements of displacements for both along-wind and across-wind response of the aeroelastic model are plotted in Fig. 4.14 and compared with the normalised Gaussian distribution. The results appear reasonably close to Gaussian distribution.

The fluctuating components are generally presented in the form of peak values since it was a very time consuming job to calculate rms values from the records for all cases studied. However, for some cases the rms values were obtained from the records in two ways. Firstly, every horizontal line on the record was chosen to represent one value of  $y_1$  which could be known from the calibration. The number of times the record touched or crossed each line was noted and mean and rms values of fluctuating components were obtained from the formulae

$$\bar{y} = \frac{\Sigma(f_i y_1)}{\Sigma f_i}$$

$$\sigma = \sqrt{\frac{\Sigma f_i (y_1 - \bar{y})^2}{\Sigma f_i}}$$

where

$f_i$  = number of times the record touches or crosses a horizontal line

$\bar{y}$  = mean value of fluctuating displacement/acceleration

$\sigma$  = rms value of fluctuating displacement/acceleration

Secondly, a very close fixed interval of time (0.04 seconds) was taken on the horizontal line and  $y_1$  ordinates were drawn perpendicular to the



horizontal line till they met the record. These ordinates were obtained from the expressions,

$$\bar{y} = \frac{\sum y_i}{n}$$

and

$$\sigma = \sqrt{\frac{\sum (y_i - \bar{y})^2}{n}}$$

where n = total number of ordinates

#### 4.12 Calibration

A direct calibration of strain gauge transducer verses the static displacement of the building model near the top (15mm below the top) was obtained in both the principal directions. Deflections were obtained on a dial gauge placed on one face of the model by gradually applying loads through a pulley system on the opposite face as shown in Fig. 4.15. The model stiffness was also calculated theoretically for both streamwise and transverse directions. The difference between measured and computed values was within 2%. The pen deflection on chart recorder corresponding to the applied load for one mm deflection at a particular gain of amplifier was taken as the calibration constant for each direction.

Free vibration tests were also carried out against known loads by snapping the thread and recording the resulting vibrations on the chart recorder for both directions of the rectangular building. The first peak showed very close agreement (within 5%) with the calibration constant.

The overall accuracy of experimental measurements can be ideally obtained by considering each component of the measurement system. However, there are a number of additional factors influencing the level of accuracy. It is very difficult to estimate the level by any bias errors in the

consideration of experimental procedures. Therefore, repeatability of each measurement, has been considered as an assessment criteria for consistency. This seems to be a more realistic and easily understood measure of the quality of measurements. Hence repeatability was adopted in this study to check the accuracy of the measurements which showed a reasonably good repetition in all the measurements made.

## CHAPTER 5

### ISOLATED RECTANGULAR BUILDINGS

#### 5.1 Preliminary Remarks

The design of tall buildings for wind loads is based on estimation of the overall wind effects (which must be taken into account in the design of the structure) and the local wind effects (which govern the design of cladding). The overall wind effects on tall rectangular buildings are of concern in this study. In general, the aerodynamic information needed to estimate such effects cannot be determined from the first principles, and must be obtained from wind tunnel tests. However, for a number of common situations the aerodynamic information is already available and procedures for estimating structural response which incorporate that information may be employed. In case a building is subjected to strong interference effects caused by the presence of neighbouring structure(s), and/or has geometric shape which is structurally or aerodynamically unusual, the above mentioned procedures cannot be used.

The total aerodynamic forces experienced by a building subjected to wind loads can be resolved into a drag (along-wind) force acting in the direction of the mean wind speed and a lift (across-wind) force acting normal to that direction. If the point of application of the resultant wind force, elastic centre, and the mass centre of the structure do not coincide, the building is subjected to torsional moments also. This is true even for a symmetric building immersed in a symmetric mean flow, since the instantaneous flow will in general be asymmetric on account of randomness of the flow fluctuations [116]. However, in case of rectangular buildings the wind induced response is principally in the along-wind and across-wind directions and the torsional response has been found to be of secondary order [57].

## 5.2 Analytical Approaches

### 5.2.1 Along-wind Response:

Davenport's gust loading factors [29] which lead to one of the most reliable approaches for predicting along-wind response of slender structures have been used to estimate the motion of the rectangular building chosen for study in the streamwise direction.

The approach in this formulation is based on certain statistical concepts of random vibration and have been described in [23, 24, and 28].

The total along-wind response of the building is divided into mean and fluctuating (dynamic) components. The dynamic along-wind response due to turbulence for tall slender structures has been further subdivided into non-resonant and resonant components as shown in Fig. 5.1. Davenport [29] assumed that the first mode of vibration of most of the tall cantilever structures is a straight line pivoted at the base. He further assumed that the amplitude of fluctuations about the mean is approximately the same throughout the height of the structure.

#### 5.2.1.1 Mean Response:

The mean velocity variation with height is assumed to follow a power law profile as:

$$\frac{\bar{U}(Z)}{\bar{U}(H)} = \left(\frac{Z}{H}\right)^\alpha \quad 5.1$$

in which  $\bar{U}(Z)$  is the mean velocity at height  $Z$ ,  $\bar{U}(H)$  is the mean velocity at the top of the building of height  $H$  and  $\alpha$  is the power law coefficient. Correspondingly, since pressure is proportional

to square of the velocity, the pressure at height  $Z$  can be written as

$$\bar{p}(Z) \approx \bar{p}_H \left( \frac{Z}{H} \right)^{2\alpha} \quad 5.2$$

where  $\bar{p}_H$  is the pressure at the top of the building. Assuming that the building deflects linearly under the wind load, a generalized mean wind load  $\bar{F}$  can be defined by the equation

$$\bar{F} = \int_0^H \bar{p}(Z) \bar{\mu}(Z) dZ B \quad 5.3$$

where  $\bar{\mu}(Z)$  is the linear mode shape. Assuming,  $\bar{\mu} \approx \sqrt{3} (Z/H)$ ,

$$\bar{F} = \sqrt{3} \left[ \frac{B}{H(1+2\alpha)} \right] \bar{p}_H \int_0^H Z^{1+2\alpha} dZ \quad 5.4$$

$$\text{or } \bar{F} = \frac{\sqrt{3}}{2} \frac{A}{(1+\alpha)} \bar{p}_H \quad 5.5$$

where  $A$  is the projected area of the building normal to the mean wind flow and  $B$  is the width of the building. The mean response,  $\bar{Y}$  of the first mode at the building height can be obtained as

$$\bar{Y} = \frac{\bar{F}}{K} = \frac{1}{K} \left[ \frac{\sqrt{3}}{2(1+\alpha)} \right] A \bar{p}_H \quad 5.6$$

in which  $K$  is the generalized stiffness in the first mode of vibration.

#### 5.2.1.2 Fluctuating Response:

According to Davenport [26], the generalized fluctuating drag forces acting on the structure can be written in terms of the pressure spectrum

$S_p(N)$  as follows:

$$NS_p(N) = 4 \frac{\bar{p}_H^2}{\bar{U}_H} |J_Z(N)|^2 |J_H(N)|^2 \frac{NS_U(N)}{2} \quad 5.7$$

in which  $|J_Z(N)|^2$  and  $|J_H(N)|^2$  are the vertical and horizontal joint acceptances and  $S_U(N)$  is the power spectral density of velocity at frequency  $N$  and is given by Davenport [22] as

$$\frac{NS_U(N)}{\bar{U}(10)} = \frac{4 C_T X^2}{[1 + X^2]^{4/3}} \quad 5.8$$

in which  $C_T$  = drag coefficient of the terrain,

≈ 0.005 for open country and 0.05 for large cities

$X$  =  $1200 N/\bar{U}_H$  and

$\bar{U}(10)$  = mean velocity taken at a height equal to 10 m.

If the mechanical admittance is  $|H(N)|^2$ , the spectrum of response in the first mode

$$NS_Y(N) = \frac{4}{K} \frac{\bar{p}_H^2 A}{\bar{U}_H} |H(N)|^2 |J_Z(N)|^2 |J_H(N)|^2 NS_U(N) \quad 5.9$$

the above expression can be expressed as a ratio to the mean displacement  $\bar{Y}$  from equation 5.5

$$\frac{NS_Y(N)}{\bar{Y}} = \frac{16}{3} (1+\alpha) |H(N)|^2 |J_Z(N)|^2 |J_H(N)|^2 \frac{NS_U(N)}{\bar{U}} \quad 5.10$$

The vertical and horizontal joint acceptances have been obtained experimentally by Davenport [25] and approximated in the following formulae

$$|J_Z(N)|^2 = \frac{1}{(1+\alpha)^2} \frac{1}{(1+\frac{C}{3})} \quad 5.11$$

$$|J_H(N)|^2 = \frac{1}{\left[1 + \frac{C_1}{3}\right]} \quad 5.12$$

in which  $C \approx 8 \frac{HN}{\bar{U}_H}$  and  $C_1 \approx 20 \frac{HN}{\bar{U}_H} \frac{B}{H}$

where B is the horizontal dimension of building normal to mean wind direction, H is the height of the building and the dimensionless frequency  $HN/\bar{U}$  is denoted as  $\beta$  (used subsequently).

The normalized variance of response,  $\sigma^2(Y)/\bar{Y}^2$  has been expressed as follows

$$\frac{\sigma^2(Y)}{\bar{Y}^2} = \int_{-\infty}^{\infty} \frac{NS_Y(N)}{\bar{Y}^2} d \ln(N) \quad 5.13$$

The area under the spectral curve in Fig.5.1 (showing spectrum  $[NS_Y(N)]/\bar{Y}^2$  vs  $\ln(N)$ ) consists of two parts ; a peak of area, A1 at the natural frequency and a low frequency "hump" of area A2. The area under the peak is approximately equal to [26, 27],

$$A_1 = \frac{\pi}{4\xi} \frac{N_0 S_P(N_0)}{\bar{p}^2} \cdot \frac{16}{3} (1+\alpha)^2 \quad 5.14$$

where  $N_0$  is the structural first natural frequency and  $\xi$  is the critical damping ratio. Substituting equations 5.7 and 5.8 in the above equation, the area A1 will be finally

$$A_1 = \frac{\pi}{4\xi} \frac{1}{1+8/3 \beta_0} \frac{1}{1+10\beta_0 B/H} \frac{4(1200 N_0/\bar{U})^2}{[1+(1200 N_0/\bar{U})^2]^{4/3}} \frac{16}{3} \frac{K}{A} (9/H)^{2\alpha}$$

...5.15

in which  $\beta_0 = HN_0/\bar{U}_H$

The non-resonant response which is represented by area under the hump is approximately

$$A_2 = \int_{-\infty}^{\infty} \frac{NS_P(N)}{p^2} d \ln(N) \quad 5.16$$

Substituting equation 5.7 in the above equation

$$A_2 = 32 \frac{K}{A} (g/H)^{2\alpha} \left\{ \frac{1}{[1+(450/H)^2]^{1/3}} - 1 \right\} \quad 5.17$$

According to Davenport [28], the average largest response during a period T is given by

$$Y_{\max} = \bar{Y} + g\sigma_y \quad 5.18$$

where peak factor

$$g = \sqrt{2 \ln(vT)} + \frac{0.57}{\sqrt{2 \ln(vT)}} \quad 5.19$$

and  $\sigma_y$  = rms of response ;

$v$  = the number of times the mean value is crossed per unit time. For a lightly damped structure,  $v \approx N_0$ , the natural frequency of the structure.

The expression for maximum deflection can also be written as

$$Y_{\max} = G \bar{Y} \quad 5.20$$

in which G is the gust factor and can be defined as

$$G = 1 + g \frac{\sigma_y}{\bar{Y}} \quad 5.21$$

$$\text{or } G = 1 + g \sqrt{A_1 + A_2} \quad 5.22$$

### 5.2.1.3 Response Analysis:

Based on the above formulation a computer programme was written to compute



the mean, peak, rms and maximum displacements at the top of the building in the first mode of vibration for a range of reduced velocity. The flow diagram of the programme is given in Appendix-B1.

Using the above programme the building chosen for this study was analyzed with both short and long face normal to the wind direction. From the literature [54] the drag coefficient for windward and leeward faces of the building was taken as 0.80 and 0.25 respectively ( $C_D=1.05$ ); the air density was assumed as  $12.08 \text{ N/m}^3$ , sampling time (T) as 600 sec and gradient height ( $Z_G$ ) corresponding to power law coefficient of 0.30 as 450 m.

The variation of maximum along-wind response of the building in two orientations ( $0^\circ$  and  $90^\circ$ ) are plotted in Figs 5.2 and 5.3 in which the vertical axis represents nondimensional amplitude of response  $Y/B$  and the horizontal axis defines reduced velocity  $\bar{U}_H/NB$ . The response can be expressed as

$$\frac{Y}{B} \propto \left[ \frac{\bar{U}_H}{NB} \right]^k \quad 5.23$$

where  $\bar{U}_H$  is the mean wind velocity at building height,  $H$ ,  $N$  is the natural frequency of vibration in across-wind direction, and  $k$  is the slope of the line passing through plotted points. The slope  $k$  defines the rate at which the response of the building varies with the reduced velocity. In other words it is indicative of the sensitivity of the response to the reduced velocity. The value of  $k$  for both the orientations is 2.5. It is worth noting that although the slope of the lines for both the orientations are the same, the response of the longer side facing the wind is obviously larger. Along-wind acceleration response is also shown in Fig. 5.4.

### 5.2.2 Across-wind response

As mentioned earlier in Chapter 2, section 2.6.2, no generalized

response spectrum has been developed for theoretical prediction of the across-wind response of tall rectangular buildings. However, an experiment based analysis may be employed by using the available force spectra obtained from wind tunnel measurements.

The force spectra measured by Saunders [107,108] and Kareem [64] are used for the analysis of the building model adopted in this study. The former gives the force spectra for building models of dimensions 6:1:1, 6:1:1.5 and 6:1:2 for 0 and 90 orientations to wind direction and two different terrain conditions ( $\alpha = 0.21, 0.37$ ), while the latter gives the measured force spectra for a 6:1:1 building model for three terrain categories, namely, open country, suburban, and urban ( $\alpha = 0.12, 0.24$  and  $0.34$ ). These measurements have been made on models designed on the assumption that the first mode shape is linear.

For the purpose of predicting across-wind response of the building model, a computer programme has been developed. The programme needs the force spectrum as input data. Accordingly the force spectra measured by Saunders as well as Kareem were digitized. Since these spectra were available for values of  $\alpha$  different from that used in the present investigation ( $\alpha = 0.30$ ), the force spectrum values for  $\alpha = 0.30$  were obtained by interpolation from these digitized values. With this as input, the across-wind response of the tall rectangular building chosen for this study was computed. The flow diagram of this programme is given in Appendix-B2.

Using the force spectra for a square building given by Saunders [107, 108] and Kareem [64], the building model used in this study was analyzed for a terrain having power law coefficient  $\alpha$  equal to 0.30.

Fig. 5.5 and 5.6 show the across-wind response of the building for  $0^\circ$  and  $90^\circ$  wind directions and for both sets of spectra. As can be seen, displacements based on Saunders spectra are lower than displacements

obtained by Kareem 's spectra at low reduced velocities and higher at high reduced velocities. This is because of the difference in the nature of spectra measured by them. The band-width of the force spectra measured by Saunders is slightly narrower than the ones measured by Kareem.

The variation of across-wind acceleration response of the building as a percentage of the acceleration due to gravity 'g' with reduced velocity is plotted in Figs. 5.7 and 5.8. The slope of the line, k, varies from 3.6 to 4.8, the higher value being obtained in case of the Saunders spectra. Also shown in the figures are the computed across-wind acceleration response of a square cross-section building obtained by Kareem [61] using a power law coefficients of 0.34. The building dimensions and characteristics for his study were,  $H=180$  m ;  $B=31$  m ;  $n$  (natural frequency )  $=0.2$  Hz ; building density  $=192$  kg/m<sup>3</sup> and  $\xi =0.01$ . It can be observed , that inspite of the differences in the characteristics of the building used in the present study and that used by Kareem [61], the trend of the response is very much similar.

### 5.3 Experimental Approach

The aeroelastic model of the building was placed in the boundary layer wind tunnel in a simulated urban terrain, whose power law coefficient was adjusted to 0.30. Along-wind and across-wind displacements and accelerations of the building model near the top were measured for two cases; the long afterbody (shorter face normal to the wind direction) and short afterbody (longer side facing the wind). The tests were carried out in a range of reduced velocity between 4 to 10 which covers the design wind speed for most tall buildings. The corresponding full scale velocity was between 22 m/s to 75 m/s at the top of the prototype. Mean along-wind displacements were measured by gradual increase of the wind speed from zero to the maximum design velocity (corresponding to a reduced velocity of 10) by using the

strain gauge transducers. The chart recorder was run at a low speed and the shift in the pen of the recorder at each velocity was marked and then measured. The rms along-wind and across-wind responses of the aeroelastic model were calculated from the records by procedures explained in section 4.10 .

Fig.5.9 through 5.12 show the rms displacement of along-wind and across-wind responses of the aeroelastic model for the different configurations-short and long afterbody . The slope 'k' in the relationship given by equation 5.23 was 2.2 and 2.5 for along-wind and 3.9 and 4.5 for across-wind responses. For a comparison of the trend of variation in the value of k, the results obtained by Kareem [61] for a square building model (4:1:1) are also plotted in Figs. 5.9 to 5.12. Kareem reported values of k to be 2.32 and 2.79 for along - wind and across-wind respectively. The model tested had a frequency = 15 Hz, and, damping of 0.025 and 0.05 in along and across-wind directions respectively. It is seen that the results conform to a trend similar to that obtained in the present investigations.

For both along-wind and across-wind directions it was found that the response of the building with its longer side facing the wind was more than the case when the shorter side was kept perpendicular to the wind direction. This is clear from comparison of the response curves for each direction.

Similar behaviour has been reported by Saunders for the across-wind response of two buildings with aspect ratios of 1:1.5 and 1:2 in plan. The maximum standard deviations (rms) of the across-wind displacements were measured as 4.2% of model width (b) for short afterbody and 2.6 % of b for long afterbody cases. These values show that the levels of motion in absolute terms were not large for the model. Low model responses have also been reported by Saunders [108] and has explained them on the basis of that

the main reason for the insensitivity of the force spectrum to the level of motion of the model is possibly that the levels of motion are quite small compared to the intensities and scales of turbulence and hence have an insignificant effect on the aerodynamic input. Saunders found similar effects for his rectangular models. Vickery has also reported these effects in his experiments on cylinders at small amplitudes [127]. It can be concluded that within the experimental limits, the negative aerodynamic damping is of such small level that its effects together with 'galloping' do not have a significant effect on the response of tall rectangular buildings.

#### 5.4 Comparison of Experimental and Theoretical Results

Results of theoretical analyses in Figs. 5.2, 5.3, 5.5 and 5.6 have been compared with those predicted on the basis experiments on the model in Figs. 5.13 and 5.14, for both along-wind and across-wind responses. The experimentally predicted along-wind displacements of the building lie within 10% of the corresponding values obtained from Davenport's approach and hence show fairly good agreement. Peak along-wind factor obtained experimentally was 3.40 against the theoretical value of 3.34.

Across-wind response of the building was computed using Saunders 6:1:1, 6:1;1.5 and 6:1:2 and Kareem's 6:1:1 building spectra for 2.5% damping. The rms acceleration response of the building thus obtained is compared with the response predicted from the experimental results in Figs. 5.15 and 5.16. As is clear from these figures, the measured values are closer to the Saunders spectrum for square buildings. There exists only a small difference between predicted and experimental values over the entire range of the reduced velocities. It can therefore be inferred that Saunders spectrum for square buildings can also be used for tall rectangular buildings of aspect ratios in plan up to 1:1.2 for both the long as well as the short

after- body orientations.

Acceleration at the top of the building (which is an amplitude related parameter) allows direct comparison of the levels of motion that occur in the experiments with typical values of motion of the full-scale buildings. In Figs. 5.15 and 5.16 the standard deviations (rms) of accelerations of the top of the model are expressed as a percentage of gravity,  $g$ . These accelerations range from 0.30% to 32% of gravity.

As discussed in Chapter 2, Reed's recommendation [96] for maximum acceptable acceleration of a building is 0.5% averaged over 20 minutes for a 6 year return period. Although the averaging period for the present study will correspond to a value less than 20 minutes, one can see that in the present study a 0.5% acceleration will correspond to a prototype velocity of nearly 95 km/h. The typical 6 year return velocities are expected to be around this value only. Thus building tested in these investigations apparently conforms to the criterion laid down by Reed. Further it is also seen that the tests cover a sufficiently wide range of levels of motion ranging from values smaller than the Reed's criterion for human comfort to very large values which would correspond to very severe dynamic loading such as extremely severe winds or earthquake shocks.

## CHAPTER 6

### INTERFERENCE EFFECTS ON TALL RECTANGULAR BUILDINGS

#### 6.1 Preliminary Remarks

Dynamic response of an isolated rectangular building has been studied and discussed in the preceding chapter. Aerodynamic interference between two neighbouring buildings has been found to greatly change the response of each of them due to the flow modifications. The interaction of the characteristics of flow and the building complicates the response prediction. The behaviour of a structure subjected to interference changes with alterations in the related parameters. These parameters include turbulence and shear in mean flow, building size and height, and the relative position of buildings. Because of the variety of architectural shapes and sizes of the buildings existing in the vicinity of each other and the limited number of experimental data available on interference effects, it is difficult to estimate the effect of a nearby structure on the aerodynamic response of a building. This is possibly the reason why interference effects do not as yet figure in the codes of practice. However, interference is unavoidable and there is need therefore to give this matter due attention.

Two wind models have been used in the study. These have been discussed in Chapter 4. The profiles of longitudinal velocity and turbulence intensity of these are given in Figs. 4.1 and 4.2. The power law coefficient,  $\alpha$ , for the mean velocity profiles has values of 0.10 and 0.30 for the two cases.

The experimental programme consists of rigid and aeroelastic model studies to investigate the interaction phenomenon. Initially flow characteristics, i.e., the mean wake boundary and the turbulence intensity, all around the building model were established. Rigid model study was

conducted to identify the extent to which a building could be moved away such that its effect of interference on the other building became insignificant. This was followed by a detailed systematic study on an aeroelastic model to determine changes due to interference, in the aerodynamic response of a building placed in boundary layer turbulent flow corresponding to a built up approach terrain (power law index  $\alpha = 0.30$ ).

## 6.2 Flow Characteristics Around the Building Model

### 6.2.1 Wake boundary

In order to obtain the outlines of the wake boundary, and, thus the zone wherein interference is likely to be significant, either in the direction of the flow or in the transverse direction, a series of mean velocity measurements were made in the wake of the building model, placed in the wind tunnel.

A rigid model was used for this purpose and the mean wind velocity distribution across the wind tunnel, within the wake of the model, was measured at different sections along the length of the tunnel. A Pitot static tube was used for these measurements at one third the height of the model and moved in the transverse direction with the help of a remote control electric device. The Pitot tube was also traversed along the length of the tunnel upto a distance of 14 times the larger plan dimension of the model. At each section the mean velocity was taken at locations 0, 1, 2, 3, 4 and 5 times the width of the building model. These distances are centre to centre of the model. The wind velocity throughout the test, measured at one third model height was kept constant at 5.7 m/s. Fig. 6.1 shows the mean wake boundary of the rectangular model. The flow separates at the outer edges of the model and, thin shear layers lie just beyond the wake boundary forming a distinct and narrow zone within which the wake boundary can fluctuate and



influence the flow responsible for the interference phenomenon. The wake boundary widens up to  $3b$  on either side of the centre line of the tunnel, at a distance of  $3.5d$  from the model. This  $6b$  wide wake extends to a distance of about  $10d$  on the downstream side of the model and thereafter converges to a width of  $4b$  at a distance of  $14d$ .

### 6.2.2 Mean velocity and turbulence intensity

Turbulence intensity of flow is one of the governing parameters in interference studies. As such the variations of the mean velocity and turbulence intensities of flow in the free stream at three locations upstream and four locations downstream of the model have been studied. Measurements were made using a hot-wire anemometer up to  $0.6$  m height (model height) in the tunnel, at  $0.05$  m intervals in a simulated urban terrain ( $\alpha=0.30$ ). At first, turbulence intensity was measured in the free stream at the mid, one-eighth and quarter points of the tunnel cross-section. The turbulence intensity values at all the three locations were nearly same at any particular height, the difference being only  $1\% - 4\%$  at the one-eighth location and  $1\% - 6\%$  at the one-quarter location over the entire height of the model. The aeroelastic model was then placed in the tunnel and the mean and fluctuating velocity components were observed both upstream and downstream of the model over its full height. Table 6.1 gives the intensity of the turbulence at different locations on both upstream and downstream of the model. Several observations were also taken at various offsets to the centre line of the tunnel as shown in Fig. 6.2. The measured values are given in Table 6.1. It is noteworthy that, whereas for some locations the change with respect to the free-stream turbulence is not significant, at others there is more than a two-fold increase. The maximum percentage increase in turbulence intensity as compared to the corresponding

free stream value is 19% on upstream and 255% on the downstream side of the model. While the largest increase of 255% in turbulence was observed in the wake just behind the model a 20% increase was measured at a distance of 1.8 m downstream (about 15 times the model along - wind dimension). At 1.8 m distance on upstream side of the model the increase in turbulence intensity was only 10%.

An interfering building model was next introduced and placed at different locations to study its influence on the turbulence intensity profiles. Three cases were studied (case-II, III and IV given in Fig. 6.3). The coordinates  $x$ - and  $y$ - in Table 6.1 are the centre to centre spacing between the two building models in the transverse and streamwise directions respectively. The hot-wire probe was kept just in front of the model (approximately 0.15 m clearance). The results obtained are given in Table 6.1 and typical plots are shown in Fig. 6.3. In case of the interfering building lying transversely at an offset of two times the width with respect to the aeroelastic model, there was negligible increase in turbulence. The increase at the location  $y=3.5d$ ,  $x=1.5b$  was maximum being about 33% of the turbulence in free stream flow. In all the above studies the reference turbulence was the free stream mid-section turbulence at 0.1 m height of the model.

### 6.3 Rigid Model Study

In this experiment, a series of tests were conducted in a simulated open country terrain to measure the extent of the interference effects in the streamwise direction. A rigid model of the building with height equal to 600 mm and cross-sectional dimensions 120 mm x 100 mm was rigidly fixed on a three-component load cell on the centre line of the tunnel with its longer side facing the wind. The rigid model is not expected to give any idea about

the fluctuating along-wind force or the across-wind force, hence only the drag force and along-wind base bending moment were measured. Another rigid model of the same geometrical dimensions and orientation was initially located at distances varying from 2 to 24 times depth of the building and in-line with the first mode. In the next series of measurements, the upstream interfering model was moved transversely from the centre line of the tunnel and observations taken at 8 locations covering a longitudinal distance from the other building same as in the first series of tests.

Table 6.2 depicts the values of buffeting factors for the forces and moments on the downstream building model under interaction effects from the upstream model. The buffeting factor is the ratio of the force or moment experienced by the building under the influence of interference, to the corresponding values without interference. Therefore,

$$\text{Buffeting factor, BF} = \frac{\text{force on building with interference}}{\text{force on isolated building}}$$

The use of a BF concept allows convenient use for evaluating loads on buildings.

In the tandem arrangement (without offset), the mean wind force is greatly reduced up to a distance of  $4d$  between the two buildings. Flow observations taken by Sakamoto [105] have revealed that the negative pressures on the rear face are smaller compared to that on the front face. This has been explained by Sakamoto on the basis of the observed behaviour of the shear layers which get separated from the leading edges on the two sides of the upstream model and reattach on the side faces of the downstream model after which they roll up weakly into the region to its rear. When the spacing becomes larger than  $4d$ , the shielding effect decreases monotonically

with increase in spacing, and, is almost non-existent beyond a spacing of 24d.

In the case of the interfering building placed at one width offset to the centre line, the shielding decreased greatly, as compared to the values in the tandem arrangement, for cases of closer spacing (up to 5d). According to Sakamoto, this is due to the fact that the shear layers generated from the upstream building collide with the front surface of the downstream building. A part of this shear layer is greatly accelerated and forms a rapid flow circulation around the side faces of the downstream building model which results in an increase in the negative pressures on these faces. When the interfering model (with offset) moves further than 5d, the shielding decreases and once again at a large distance of 24d no shielding effect was observed.

#### 6.4 Aeroelastic Model Study

In this study the aeroelastic model was used as the principle model instrumented to investigate the effect of interference. The aeroelastic model was first placed with its longer side facing the wind (short afterbody case) and in the next series of tests, it was the shorter side that was placed facing the wind (long afterbody case). Testing was carried out in flow conditions simulating an urban environment.

##### 6.4.1 Short afterbody case

These tests were performed with the aeroelastic model placed on the downstream side of a rigid model of the same size in a tandem arrangement. Both the models had the same orientation to the wind direction. The mean and fluctuating components of along-wind, as well as the fluctuating across-wind displacement responses of the aeroelastic model were recorded.

This experiment was carried out at a reduced velocity of about 6.

Table 6.3 depicts the values of buffeting factors for the aeroelastic displacement responses in both the principle directions near the top of the model. The values of buffeting factors for the static response in the along-wind direction, even though a little different from those of the rigid model study given in Table 6.2, showed a similar trend. The dynamic responses of the aeroelastic model in both along as well as across wind directions exhibited similar variation. The buffeting factors are almost equal and less than 1.0 for small spacings up to  $3d$ . This indicates the occurrence of shielding for these cases, as was also seen for the rigid model. As the longitudinal distance  $y/d$  increased beyond the value of 3 the buffeting factors also increased. At  $y/d$  equal to 5 or 6 these factors attained their maximum value for the across and the along-wind directions. The increase in the across-wind buffeting factors may be due to the synchronization of vortex shedding between the upstream and downstream buildings while the increase in the along-wind buffeting factors are probably due to the shear layers of upstream building rolling up to its wake region and increasing the wake velocity. Even at a distance of  $y/d$  equal to 24, the across-wind response of the aeroelastic model exhibited a larger value than that obtained for an isolated model. This reveals that the affected building is still exposed to the wake of the upstream building.

#### 6.4.2 Long afterbody case

The aeroelastic model was placed in the wind tunnel with its shorter side facing the wind so as to study the interference effects in such a case (long afterbody case). The interfering model was introduced first in the upstream and later in the downstream side of the aeroelastic model in the same terrain condition as in the preceding case. In this experiment the

rigid model was located at 40 different locations on the upstream and at 9 locations on the downstream side, both in-line as well as with an offset to the aeroelastic model. As in the previous cases, the mean and the fluctuating components of responses were observed. The along-wind and across-wind responses were recorded at reduced velocities of 4, 6, 8 and 10 which cover adequately the design wind speeds. The corresponding mean velocities at the model height in the wind tunnel were adjusted to 4.93, 7.40, 9.87 and 12.34 m/s. For convenience in comparison, the peak displacement of the aeroelastic model at the top has been expressed by the buffeting factor.

**Interfering building upstream:** The maximum values of buffeting factors for mean and fluctuating along-wind and the fluctuating across-wind displacements of the downstream aeroelastic model are depicted in Figs. 6.4 through 6.6.

(a) *Mean Response:* A significant shielding effect is observed from Fig. 6.4, in the mean along-wind displacements, when the upstream building is between 1 to 3.5 times of the depth of model. As the distance between the two models is increased this shielding effect decreases and at a distance of  $12d$  this is found to be negligible. The flow mechanisms for tandem arrangement have been already discussed earlier. When the upstream model is at an offset to the downstream model, the shielding effect on the mean response of the latter is found to decrease with consequent increase in the buffeting factor. For an offset distance greater than the width of the model,  $b$ , the buffeting factors become close to unity when the distance between the models is more than  $5d$ . At distances closer than  $5d$ , the buffeting factor reaches a value of unity at much greater offsets.

(b) *Fluctuating Response*: The fluctuating responses are given in Fig. 6.5 and 6.6 for the along-, and, across- wind directions respectively. The fluctuating component of along-wind response of the downstream building is seen to be small when the upstream model is in the "in-line" position and close to the downstream model. The response was larger when the offset spacing was more than  $1.5 b$ . This phenomenon holds good until the downstream building is located well within the wake boundary of the upstream model. Nearer to the wake boundary of the upstream building, the buffeting factors of the downstream model are seen to be maximum. The maximum buffeting factor of peak along-wind response of the downstream model occurs when it is placed at  $6d$  upwind and  $2b$  offset to the upstream building for a reduced velocity of about  $6.0$ . The buffeting factors are substantially large up to a distance of  $12d$  and except for a few beneficial locations, the upstream building model has an adverse effect on the downstream aeroelastic model.

✓ The across-wind response of the downstream building is also amplified by the introduction of an interfering upstream building. The dynamic responses in both the directions are shown in Figs. 6.18 to 6.42.

The across-wind response of the isolated building is seen to increase with velocity (up to  $U_r = 10$ ). As per other studies reported (121, 57), the trend is the same up to  $U_r = 10$ , where after the response is seen to decrease. ✓ For most cases the across-wind response under interference effects reduces to a large extent compared to the isolated model due to vortex disruption caused by the wake deformation and increased turbulence. Furthermore, the buffeting factors are more pronounced near the reduced velocity of  $6$  and decrease as the reduced velocity increases. This trend is present for both the along-wind as well as the across-wind directions. Similar trends in the responses were observed by Kareem [65] and Sykes [121]. As can be seen from the Figs. 6.5 and 6.6 the general trend of the buffeting



factors for the across-wind response of the building is similar to that of the along-wind response. The maximum buffeting factor of peak across-wind response of the downstream model is 2.61 (Fig.6.6) and occurs at a reduced velocity of 6 when the it is  $2.5d$  away and offseted at  $2.5b$  to the upstream building. The peak buffeting factors as well as the responses in the region  $2.5 \leq y/d \leq 6$  are generally larger. This is because the downstream building is in a position where the effect of the separated shear layers from the upstream building are expected to be maximum, in addition to the fact (as explained earlier) that the rolling up of the shear layers separated from the upstream model is synchronized with those from the downstream building.

It is interesting to note that the peak buffeting factors of both along-wind and across-wind dynamic responses of the downstream building undergo the maximum increase along an axis oriented diagonally towards the wake boundary of the upstream building rather than perpendicular to the mean wind direction.

**Interfering building downstream:** The effect of a downstream building on the principal building located upstream is not as significant as in the case when the interfering building is located on the upstream side. This is shown in Fig. 6.7 to 6.9. Such a trend was also observed by Bailey and Kowk [8].

Except for the tandem arrangement, the mean along-wind response of the upstream model is not significantly affected by the presence of the downstream interfering model.

Maximum values of the buffeting factors are found to occur in the along-wind as well as across-wind directions when the two buildings are spaced a distance  $2d$  to  $3d$  without or with an offset.

When the interfering building was placed at  $8d$  downstream of the aeroelastic model, very little interference effect was noticed on the latter.



As in the preceding case, the buffeting factors in this case also have peak values at a reduced velocity of  $U_r=6$ . It is also observed from Figs. 6.8 and 6.9 that the interference effect on the across-wind response of an upstream building is not as prominent as on the along-wind response.

### 6.5 Contours of the peak Buffeting Factors

The pattern of variation in the buffeting factors can best be seen from contours. This depicts best the directional as well as the zonal variation of the interference effects. Figs. 6.10 through 6.17 show the contour diagrams for the buffeting factors of along-wind and across-wind responses for the aeroelastic model over the range of reduced velocities from 4 to 10. As can be seen from these contours the variation of buffeting factors is generally systematic with the change in spacing between the two models. In these figures R and A are representing rigid and aeroelastic models respectively. The contours for the factors corresponding to the fluctuating response of the aeroelastic model are mostly extending diagonally to the mean flow direction. These contours (which are for rectangular buildings) have a pattern similar to that reported by Bailey and Kwok [8,73] for square buildings. However, the values are a little higher than those reported by Bailey. The differences in the values of the buffeting factors are possibly due partly to the differences in the characteristics of the approach flow, especially the longitudinal turbulence intensities.

### 6.6 Displacement Responses

The variation of fluctuating peak displacement of the aeroelastic model with the reduced velocity in both along-wind and across-wind directions for the isolated model as well as for the case of interference between the buildings is plotted in Figs. 6.18 through 6.42 for all the cases studied.

The broken lines indicate the responses of the isolated model while the solid lines represent the responses for the building subjected to interference effect. It is evident from these figures that the across-wind response in all the cases is greater than the along-wind response except at very low velocities below  $U_r=4$ . The results of these figures have been transformed into buffeting factors to have a uniform basis of comparison and have been presented in the preceding sections.

### 6.7 Critical Interference Zone

The interference effect between buildings can seriously increase the wind induced responses and the purpose of a detailed study of this kind is to determine this effect and obtain its zonal distribution around the affected building. The information contained on the interference effects in Fig. 6.4 to 6.9 in the form of buffeting factors showing their distribution can best be condensed in a single figure depicting the worst affected areas. Fig. 6.43 has therefore been derived to give the demarcation of the critical zones for the interference effect. On the upstream side even though the measurements were taken only in the zone beyond  $2d$ , the critical zone has been demarcated from  $1.5d$  to include observations of Bailey and Kwok [8].

## CHAPTER 7

### CONCLUSIONS AND RECOMMENDATIONS FOR FURTHER RESEARCH

#### 7.1 Preliminary Remarks

The preceding chapters of this thesis cover a study of the effects of the wind on tall buildings. Detailed experimentation has been made to determine the wake region around a building. Likewise extensive measurements have been made in a boundary layer wind tunnel to monitor the response of an isolated building, as well as under the situation when another building is placed upstream or downstream of the same. A rigid as well as an aeroelastic model were used for the study. Theoretical analysis is made to compute the along-wind mean as well as fluctuating response of such a building, in addition to its across-wind response.

On the basis of the review of literature made, and the experimental and theoretical studies carried out, the broad conclusions arrived at and the future area of research identified are given below.

#### 7.2 Conclusions

##### 7.2.1 Flow Field

1. Measurements on the building model revealed that the wake boundary extends transversely up to 3 times the width of the building,  $b$ , on either side of the centre line of the building parallel to the flow direction for a distance of about  $10d$  and thereafter reduces gradually to  $2b$ .
2. Extensive measurements around an aeroelastic model showed that there is an increase in turbulence intensity of about 12% in the upstream region extending between 0.15 m to 1.8m from the model compared to the free

stream values. A very large increase of 214% is observed close to the model on the downstream side, that is, at 0.15m behind its face. However, the corresponding increase is 59% at 0.8m, 32% at 1.0m and 20% at 1.8m distance downstream of the model. All the above values are at 0.1 m height of the model. On the downstream side of the model and beyond a distance of about  $3b$  (0.3m on either side of the centre line) the flow is seen to gradually regain its freestream characteristics. For example at 0.5m offset the increase is negligible suggesting that this location is outside the wake.

### 7.2.2 Isolated Buildings

3. Across-wind response of tall rectangular building having aspect ratio 6:1:1.2 is found to dominate over the along-wind response (except at very low wind velocities upto a reduced velocity of at least 10). Further, the across-wind response of the rectangular building having its longer side facing the mean wind, is higher than for the same building oriented with its shorter side facing the wind. Similar trend has been observed by Saunders [108] for larger aspect ratios of 6:1:1.5 and 6:1:2.
4. The non-dimensional across-wind force spectrum reported by Saunders [107] for a tall square building of 6:1:1 aspect ratio has been used for theoretical prediction of the across-wind response for the tall rectangular building adopted in this study. A very close agreement is seen between the results obtained and the response predicted from the experimental measurements. Hence it is concluded that this spectrum can be used for establishing the across-wind response of tall buildings of aspect ratios up to 1:1.2 in plan under similar wind environment.

### 7.2.3 Interference Study

#### Interfering Building Placed Upstream:

5. Mean along-wind forces and displacements of the rectangular building reduce on account of shielding if a building of the same size is placed on the upstream side. This effect is very large up to a distance of about 3.5 times the depth of building,  $d$ , when the interfering building is straight upwind (i.e. without any offset) of the downstream building. The shielding effect reduces monotonically with increase in the spacing between the two buildings. The shielding effect decreases substantially at a distance of about  $12d$  and almost disappears at  $24d$ .
6. The fluctuating along-wind response of a downstream rectangular building (plan size 1:1.2) with another building of the same size in its vicinity on the upstream side may get increased up to 2.5 times. This is due to the increased turbulence created by the flow separation from the upstream building.
7. The across-wind response of the downstream building model increases likewise due to interference effect to a maximum of 2.6 times that of the isolated model. This large increase occurs due to synchronization of the vortices shed from the two buildings.
8. The largest buffeting factors generally occur at a reduced velocity of about 6, which yields the critical value of the Strouhal's number as 0.16.
9. The dynamic interference effects become more pronounced as the downstream building is moved from any particular position within the wake of the upstream building towards the boundary of the wake (as shown in Figs. 6.5 and 6.6) in a direction inclined approximately at  $45^\circ$  to the direction of the oncoming wind. Thereafter, the dynamic effects due to interference gradually diminish.

#### Interfering Building Placed Downstream:

10. Mean along-wind response of the upstream building reduces with the presence of a downstream building in tandem arrangement. However, the reduction is negligible when both the buildings are in offset position.
11. A building placed downstream has generally insignificant effect on the dynamic response of the upstream building. The maximum interference occurs when the downstream building is close to the upstream building.
12. The fluctuating across-wind response of the upstream building is not as significant as the along-wind response, because the downstream building distorts the wake and weakens the vortices shed from the upstream building.
13. The buffeting factors of the upstream building responses in both the principle directions initially increase with the rise in wake turbulence up to a small extent. however, this trend reverses subsequently.
14. On the downstream side of the building, the interference zone for both the mean as well as the fluctuating components is about 24 times the depth of the building,  $d$ . This effect is maximum at distances between  $1.5d$  and  $12d$ , and thereafter it tapers off. Similarly, in the transverse direction the interference zone is about three times the width of building,  $b$  (Fig.6.43 ).
15. On the upstream side, the interference zone is much smaller compared to the downstream side, reducing from  $24d$  to about  $8d$  along the flow and in the transverse direction it is limited to about  $2b$  on either side of the centre line . The largest buffeting factors occur up to a distance of nearly  $4d$ .

### 7.3 Recommendations For Future Research:

On the basis of the research work presented in this dissertation and the related literature, the following area can be explored for further investigations:

1. Determining the force spectra for a wider range of rectangular buildings in the across-wind direction for all terrain categories to enable predictions of the across-wind response of tall rectangular buildings of various aspect ratios.
2. Carrying out studies on interference effects so as to cover a wide range of all the parameters such as height, plan size, shape, a cluster of more than two buildings, with different approach terrain (and hence flow).
3. To demarcate the interference zones for other cases mentioned above and to obtain the responses / buffeting factors for both upstream and downstream buildings.
4. Determination of design forces for common shapes (circular, rectangular, hexagonal, etc.) of tall buildings.
5. Introduction of wind load factors for interference cases in codes of practices for design of buildings.

## REFERENCES AND OTHER RELATED PUBLICATIONS

1. Ahmad, M.B., "Wind Response of Self Supporting Tall Towers", Ph.D. Thesis, Department of Civil Engineering, University of Roorkee, August, 1981.
2. Akins, R.E., Peterka, J.A. and Cermak, J.E., "Mean Force and Moment Coefficients for Buildings in Turbulent Boundary Layers", J. of Wind Engg. and Industrial Aerodyn., Vol.2, No.3, No.1977, pp. 195-209.
3. American National Standard Building Code Requirement for Minimum Design Loads in Buildings and other Structures, A58.1, American Standard Institute, New York, 1982.
4. Asawa, G.L., Pathak, S.K. and Ahuja, A.K., "Industrial Wind Tunnel at University of Roorkee", Asia Pacific Symposium on Wind Engineering, University of Roorkee, India, Dec.1985.
5. ASCE, "Wind Loading and Wind Induced Structural Response", A State-of-the-art Report Prepared by the Committee on Wind Effects of the Committee on Dynamic Effects, Struct. Div., 1987.
6. ASCE, "The Engineering Aesthetics of Tall Buildings", Proceedings of the Session Sponsored by the Structural Division of ASCE in Connection with the ASCE Convention, Denver, Colorado, May, 1985.
7. Bailey, P.A. and Kwok, K.C.S., "Dynamic Interference and Proximity Effects Between Tall Buildings", Proc. 3rd Int. Conf. on Tall Buildings, Hong Kong and Guangzhou, 1984, pp. 305-311.
8. Bailey, P.A. and Kwok, K.C.S., "Interference Excitation of Twin Tall Buildings", J. Wind Engg. and Industrial Aerodyn., Vol.21, 1985, pp.323-338.
9. Biggs, J.M., "Wind Forces on Structures: Introduction and History", Proc. J. Struc. Div., ASCE, Vol.84, No.ST4, July, 1958, p.1707.
10. Biggs, J.M., "Introduction to Structural Dynamics", Mc GrawHill, New York, 1964.
11. Blessmann, J. and Riera, J.D., "Interaction Effects in Neighbouring Tall Buildings", 5th Int. Conf. on Wind Effects on Buildings and Structures, 1975, Colorado State Univ., U.S.A., pp. 381-395.
12. Blessmann, J. and Riera, J.D., "Wind Excitation of Neighbouring Tall Buildings", J. Wind Engg. and Industrial Aerodyn., Vol.18, 1985, pp. 91-103, 105-110.
13. Canadian Structural Design Manual, Supplement No.4 to the National Building Code of Canada, Associate Committee on the National Building Code and National Research Council of Canada, Ottawa, 1975.
14. Cermak, J.E., "Laboratory Simulation of the Atmospheric Boundary Layer", American Institute of Aeronautics and Astronautics J., Vol.9, No.9, Sept.1971, pp. 1746-54.



15. Cermak, J.E., "Application of Fluid Mechanics to Wind Engineering-A Freeman Scholar Lecture", J. Fluids Engg., ASME, Vol.97, March, 1976, pp. 9-38.
16. Cermak, J.E., "Aerodynamics of Buildings", Annual Review of Fluid Mechanics, Vol.8, 1976, pp. 75-106.
17. Chen, P.W. and Robertson, L.E., "Human Perception Threshold of Horizontal Motion", J. Struc. Div., ASCE, Vol.98, No.ST8, Aug.1972, pp. 1681-1696.
18. Chien, N., Feng, Y., Siao, T. and Wang, H., "Wind-Induced Studies of Pressure Distribution on Elementary Buildings Forms, Iowa city, Iowa Institute of Hydraulics Research, 1951.
19. Cooper, K.R. and Wardlaw, R.L., "Aeroelastic Instabilities in Wakes", Proc. 3rd Int. Conf. on Wind Effects on Buildings and Structures, 1971, pp. 647-655.
20. Counhan, J., "An Improved Method of Simulating an Atmospheric Boundary Layer in a Wind Tunnel", Atmospheric Environment Pergamon Press, Vol.3, 1963, pp. 197-214.
21. Davenport, A.G., "Rationale for Determining Design Wind Velocities", Proc. ASCE, J. Struc. Div., May, 1960.
22. Davenport, A.G., "The Spectrum of Horizontal Gustiness Near the Ground in High Winds", Quarterly J. Roy. Met. Soc., Vol.87, 1961.
23. Davenport, A.G., "The Application of Statistical Concepts to the Wind Loading of Structures", Proc. ICE, London, Vol.19, August, 1961.
24. Davenport, A.G., "The Response of Slender Line-like Structures to Gusty Wind", Proc., ICE, London, Vol.23, 1962, pp. 389-408.
25. Davenport, A.G., "The Relationship of Wind Structure to Wind Loading", Wind Effects on Buildings and Structures, Proc. Conf. held at NPL, London, 1963.
26. Davenport, A.G., "Buffeting of Structures by Gusts", Proc. of the 1963 Int. Symp. on the Effects of Wind on Structures, London, 1965.
27. Davenport, A.G., "The Buffeting of Large Superficial Structures by Atmospheric Turbulence", Proc. of the Conf. on Large Radio Antennas, Annals of the New York Academy of Science, Vol.116, June, 1964.
28. Davenport, A.G., "The Distribution of Largest Values of a Random Function with Application to Gust Loading", Proc., ICE, London, Vol.28, 1964, pp. 187-196.
29. Davenport, A.G., "Gust Loading Factors", J. Struc. Div., ASCE, Vol.43, No.ST3, June, 1967, pp. 11-34.
30. Davenport, A.G., "The Dependence of Wind Loads on Meteorological Parameters", Proc. Second Int. Conf. on Wind Effects on Buildings and Structures, Ottawa, Canada, Sept., 1967.

31. Davenport, A.G., "Perspective of Full-scale Measurement of Wind Effects", J. of Industrial Aerodyn., Vol.1, June, pp. 23-54.
32. Davenport, A.G., "Statistical Concepts of Wind Loading", Proc. Conf. on Tower Shaped Structures, Den Haag, 1969.
33. Davenport, A.G., Hogan, M. and Vickery, B.J., "An Analysis of the Wind Induced Building Movement and Column Strain taken at The John Hancock Centre (Chicago)", Laboratory Research Report BLWT-10-70, 1970.
34. Davenport, A.G., "Approaches to Design of Tall Buildings Against Wind Action", Theme Report, Tech. Comm., 7.Vol.1b-7, ASCE-IABSE Conf. on Planning and Design of Tall Buildings, Lehigh Univ., Bethlehem, Penn. USA, August, 1972.
35. Durgin, F.H. and Tong, P., "The Effects of Twist Motion on the Dynamic Multimode Response of a Building", Symp. on Flow-Induced Structural Vibrations, IUTAM-IAHR, Korlsruhe, Germany, Aug., 1972.
36. Ekman, V.M., "On the Influence of the Earth's Rotation on Ocean Currents", Arkiv. Mat. Astr. Fysik, 1905.
37. Ellis, N., "A New Technique for Evaluating the Fluctuating Lift and Drag Force Distributions on Building Structures", 4th Int. Conf. on Wind Effects on Buildings and Structures, Cambridge Univ. Press 1975, England, pp. 527-536.
38. Feld, L.S., "Super Structure for 1350 ft. World Trade Center", Civil Engg., June, 1971, pp. 66-70.
39. Fludge, "Handbook of Engineering Dynamics", Mc Graw-Hill, 1962.
40. Foutch, D.A. and Safak, E., "Torsional Vibrating of Wind Excited Symmetrical Structures", J. Wind Engg. and Ind. Aerodyn. 7, 1981, pp. 191-201.
41. Foutch, D.A. and Safak, E., "Torsional Vibration of Along-wind Excited Structures", J. Engg. Mech., ASCE, 107, 1981, pp. 323-337.
42. Fu-Kuel Chang, "Wind and Movement in Tall Buildings", Trans. Civil Engg., 8, 1967.
43. Goodman, L.E., "A Review of Progress on Analysis of Interfacial Slip Damping", Proc. of a Colloquium on Structural Damping, Atlantic City, M.J.Ed. J.E.Ruzicka, Published by ASME, New York, 1959.
44. Gowda, B.H.L. and Sitheeq, M.M., "Interference Effects on a Tall Prismatic Body in Tandem Arrangement", Proc. 2nd Asia Pacific Conf. on Recent Advances in Wind Engg., Peking, June, 1989, pp. 293-299.
45. Greig, G.L., "Toward an Estimation of Wind-Induced Dynamic Torque on Tall Buildings", Master's Thesis, Deptt. of Engg., Univ. of Western Ontario, London, Ontario.

46. Grootenhuis, P., "Damping Mechanisms in Structures and some Applications of the Latest Techniques", Symp. on the Applications of Experimental and Theoretical Structural Dynamics, Univ. of Outhampton, April, 1972, pp. 1-26.
47. Hamilton, G.F., "Effect of Velocity Distribution on Wind Loads on Walls and Low Buildings", University of Toronto, Ontario, 1962.
48. Hansen, J.R., Reed, J.W. and Vanmarke, E.H., "Human Response to Wind Induced Motion of Buildings", J. Struc. Div., ASCE, Vol.99, No.ST7, July, 1973, pp. 1589-1606.
49. Harris, R.I., "Measurements of Wind at Height up to 598 ft. Above Ground Level", Paper 1, Proc. Symp. of Wind Effects on Buildings and Structures, Loughborough, U.K.
50. Harris, R.I., "The Nature of the Wind", The Modern Design of Wind Sensitive Structures, Construction Industry Research and Information, London, 1971.
51. Harris, C.L., "Influence of Neighbouring Structures on the Wind Pressures on Tall Buildings", Bureau of Standards Journal of Research, Vol. 12, Jan., 1934, (Research Paper RP 637).
52. Hart, G.C. and Vasudevan, R., "Earthquake Design of Buildings:Damping", J. Struc. Div., ASCE, Vol.101, No.ST1, Jan., 1975, pp. 11-30.
53. Hart, G.C., DiJulio, R.M. and Lew, M., "Torsional Response of High Rise Buildings", J. Struc. Div., ASCE, Vol.101, 1975, pp. 397-416.
54. IS:875 (part 3)-1987, "Indian Standard Code of Practice for Design Loads (other than Earthquake) for Buildings and Structures-Part 3 Wind Loads", Bureau of Indian Standards, New Delhi, India.
55. Ishizaki, H. and Sung, I.W., "Influence of Adjacent Buildings to Wind", 3rd Int. Conf. on Wind Effects on Buildings and Structures, Tokyo, Japan, 1971, pp. 221-30.
56. Isyumov, N. and Davenport, A.G., "Comparison of Full-Scale and Wind Tunnel Speed Measurements in the Commerce Court Plaza", J. of Industrial Aerodyn., 1, 1975, pp. 201-212.
57. Isyumov, N., "The Aeroelastic Modelling of Tall Buildings", Proc. Int. Workshop on Wind Tunnel Modelling for Civil Engineering Applications, Cambridge University Press, 1982.
58. Isyumov, N. and Poole, M., "Wind Induced Torque on Square and Rectangular Building Shapes", Proc. 6th Int. Conf. on Wind Engg., 1983, Elsevier, Amsterdam.
59. Jensen, M., "The Model Law for Phenomena in Natural Wind", Ingeniren, Int. Ed., Vol.2, No.2, 1958.
60. Kao, K.H., "Measurements of Pressure/Velocity Correlation on a Rectangular Prism in Turbulent Flow", BLWT-2-70, Jan. Partial

Fulfillment of masters Degree, Faculty of Graduate Studies, Univ. of Western Ontario, 1970.

61. Kareem, A., "A Wind Excited Motion of Buildings", Ph.D. Thesis, Civil Engg. Deptt., Colorado State Univ., Colorado, USA, 1978.
62. Kareem, A., "Wind-Excited Response of Buildings in Higher Modes", J. Struc. Div., ASCE, Vol.107, No.ST4, April, 1981, pp. 701-706.
63. Kareem, A., "Cross-Wind Response of Buildings", J. Struc. Div., ASCE, Vol.108, April, 1982, pp. 869-887.
64. Kareem, A., "Model for Predicting the Across-Wind Response of Buildings", Engg. Struct., Vol.6, April, 1984, pp. 136-141.
65. Kareem, A., "The Effect of Aerodynamic Interference on the Dynamic Response of Prismatic Structures", J. Wind Engg. and Industrial Aerodyn., Vol.25, 1987, pp. 365-372.
66. Kelnhofer, W.J., "Influence of a Neighbouring Building on Flat Roof Wind Loading", Proc. 3rd Int. Conf. on Wind Effects on Buildings and Structures, Tokyo, 1971, pp. 221-230.
67. Khan, F.R., "The John Hancock Center", Civil Engg., Oct.1967, pp. 38-42.
68. Khan, F.R., "New Structural Systems for Tall Buildings and their Scale Effects on Cities", Proc. of the Symp. on Tall Buildings, Vanderbilt Univ., Nov., 1974, pp. 99-128.
69. Kolousek, V., Pirner, M., Fischer, O. and Naprstek, "Wind Effects on Civil Engineering Structures", Studies in Wind Engineering and Industrial Aerodynamics, 2, Elsevier Science Publishing Company Inc., 1984.
70. Kortchinskiy, J.L., "Vibration of Tall Buildings (in Russian), Strojitel'naja Promyšlenost 11, 1952.
71. Koten, H., "The Comparison of Measured and Calculated Amplitudes of Some Buildings and Determination of Damping Effects of the Buildings", Proc. 3rd Int. Conf. on Wind Effects on Buildings and Structures, Tokyo, 1971, pp. 825-840.
72. Kwok, C.S. and Melbourne, W.H., "Wind-Induced Lock-In Excitation on Tall Structures", J. Struc. Div., ASCE, Vol.107, No.ST1, Jan., 1981, pp. 57-72.
73. Kwok, K.C.K., "Interference Effects on Tall Buildings", Proc. 2nd Asia Pacific Conf. on Recent Advances in Wind Engg., June, 1989, Peking, pp. 446-453.
74. Laneville, A., Gartshore, I.S. and Parkinson, G.V., "An Explanation of Some Effects of Turbulence on Bluff Bodies", Proc. Fourth Int. Conf. on Wind Effects on Buildings and Structures, Cambridge Univ. Press, 1976.

75. Lawson, T.A., "Wind Effects on Buildings", Applied Science Publishers Ltd., London, 1980.
76. Lazan, B.J., "Damping of Materials and Members in Structural Mechanics", Pergamon.
77. Liepmann, H.W., "On the Application of Statistical Concepts to the Buffeting Problem", J. Aeronaut. Sci., 19, Dec., 1952, 793-800, 822.
78. Leutheusser, H.J., "Static Wind Loading of Grouped Buildings", Proc. 3rd Int. Conf. on Wind Effects on Buildings and Structures, Tokyo, 1971, pp. 211-219.
79. MacDonald, J.R., "Structural Response of a Twenty Storey Building to the Lubbock Tornado", Texas Tech. Univ., Storm Research Report No.1, Oct., 1970, Lubbock, Texas.
80. Mair, W.A. and Maull, D.J., "Aerodynamic Behaviour of Bodies in the Wakes of Other Bodies", Phil. Trans. of the Roy. Soci., London, England, Vol.A269, 1971, pp. 425-37.
81. Makino, M., Nakahara, M. and Sato, T., "Some Field Test Results of Wind Pressure on a Tall Building", Proc. 3rd Int. Conf. on Wind Effects on Buildings and Structures, Tokyo, 1971, pp. 253-262.
82. Melaragno, M., "Wind in Architectural and Environmental Design", Van Nostrand Reinhold Company, New York, 1982.
83. Melbourne, W.H., "Comparison of Pressure Measurements Made on a Large Isolated Building in Full and Model Scale", Proc. 3rd Int. Conf. on Wind Effects on Buildings and Structures, Tokyo, 1971, pp. 253-262.
84. Melbourne, W.H., "Cross-Wind Response of Structures to Wind Action", Proc. 5th Int. Conf. on Wind Effects on Buildings and Structures, Cambridge Univ. Press 1975, pp. 343-358.
85. Melbourne, W.H., "Probability Distribution of Response of BHP House to Wind Action and Model Comparisons", J. of Industrial Aerody., 1, 1975, pp. 167-176.
86. Melbourne, W.H. and Sharp, D.B., "Effects of Upwind Buildings on the Response of Tall Buildings", Proc. Regional Conf. on Tall Buildings, Hong Kong, Sept., 1976, pp. 174-191.
87. Newberry, C.W., Eaton, K.J. and Mayn, J.R., "Wind Loading on Tall Buildings-Further Results from Royex House", Industrial Aerodyn. Abstract 4, July-August, 1973.
88. Novak, M. and Davenport, A.G., "Aeroelastic Instability of prisms in Turbulent Flow", Proc. ASCE, J. Engg. Mech. Div., Feb. 1970.
89. Owen, P.R., "The Prospect Ahead", Phil. Trans. Roy. Soc., London, Series A, Vol. 269, 1971.
90. Panofsky, H.A. and McCormick, R.A., "Properties of the Spectrum of Atmospheric Turbulence", Quarterly J. Roy. Soc., 80, 1954.

91. Parkinson, G.V., "Mathematical Models of Flow Induced Structural Vibration", Proc. Symp. Flow-Induced Structural Vibration, Karlsruhe Germany, Springer-Verlag, Berlin, 1974, pp. 81-127.
92. Patrickson, C.P. and Friedman, P.A., "A Study of Coupled Lateral and Torsional Response of Tall Buildings to Wind Loadings", Tech. Report UCLA-Engg., 76126, Dec., 1976.
93. Peterka, J.A. and Cermak, J.E., "Adverse Wind Loading Induced by Adjacent Buildings", J. Struc. Div., ASCE, No.ST3, March, 1976, pp. 533-548.
94. Plate, J.E., "Engineering Meteorology", Elsevier Scientific Publishing Company, 1982.
95. Rathbun, J.C., "Wind Forces on a Tall Building", Trans. ASCE, Vol.105, 1940, pp. 1-41.
96. Reed, J.W., "Wind-Induced Motion and Human Discomfort in Tall Buildings", M.I.T. Deptt. of Civil Engg. Research Report R71-42, Structures Publication, No.310, Nov., 1971.
97. Reinhold, T.A., Tielman, H.W. and Maher, F.J., "Interaction of Square Prisms in Two Flow Fields", J. Wind Engg. and Industrial Aerodyn. Vol.2, 1977, pp. 223-241.
98. Reinhold, T.A. and Sparks, P.R., "The Influence of Wind Direction on the Response of a Square-Section Tall Building", Proc. 5th Conf. on Wind Effects on Buildings and Structures, Fort Collins, Colorado, July, 1979, Pergamon Press, 1980.
99. Reinhold, T.A. and Sparks, P.R., "The Influence of an Upstream Structure on Dynamic Response of a Square-Section Tall Building", Proc. 4th Colloq. on Industrial Aerodyn., Aachen, 1980.
100. "Report of the Committee of Enquiry into Collapse of Cooling Towers at Ferrybridge", Central Electric Generating Board, Nov., 1965 (as Edited by Peter Sachs, Pergamon Press).
101. Robertson, L.E. and Chen, P.W., "Application to Design of Research on Wind Effects", Proc. 2nd Int. Conf. Wind Effects on Buildings and Structures, Univ. of Toronto Press, Ottawa, Sept., 1961, Canada.
102. Roorda, J., "Tendon Control in Tall Structures", J. Struc. Div., ASCE, Vol.101, No.ST3, March, 1975, pp. 505-522.
103. Rosati, P.A., "An Experimental; Study of Response of a Square Prism to Wind Load", BLWT II\_68, Faculty of Graduate Studies, Univ. of Western Ontario, Canada, 1968.
104. Ruscheweyh, H., "Dynamic Response of High Rise Buildings Under Wind Action with Interference Effects from Surrounding Buildings of Similar Size", 5th Int. Conf. on Wind Effects on Buildings and Structures, 1979, Colorado State Univ., U.S.A., pp. 725-734.



105. Sakamoto, H. and Haniu, H., "Aerodynamic Forces acting on two Square Prism Placed Vertically in a Turbulent Boundary Layer", J. Wind Engg. and Industrial Aerodyn., Vol.31, 1988, pp. 41-66.
106. Sarrazin, M.A., Roesset, J.M. and Whithman, R.V., "Dynamic Soil-Structure Interaction", J. Struc. Div., ASCE, Vol.89, No.ST7, July, 1972, p. 1525.
107. Saunders, J.W. "Wind Excitation of Tall Buildings", Ph.D. Thesis, Mech. Engg. Deptt., Monash Univ., Australia, 1974.
108. Saunders, J.W. and Melbourne, W.H., "Tall Rectangular Building Response to Cross-Wind Excitation", 4th Int. Conf. on Wind Effects on Buildings and Structures, Cambridge Univ. Press, 1975, pp. 527-536.
109. Saunders, J.W. and Melbourne, W.H., "Buffeting Effects of Upstream Buildings", 5th Int. Conf. on Wind Effects on Buildings and Structures, 1975, Colorado State Univ., U.S.A., pp. 593-607.
110. Saunders, J.W., "Further Measurements of Buffeting Effects of Twin Upstream Buildings", Proc. 7th Australian Conf. Hydraulics and Fluid Mechanics, Brisbane, The Instit. of Engg., Australia, 1980, pp. 83-86.
111. Scruton, C., "Aerodynamics of Structures", Proc. 2nd Int. Conf. on Wind Effects on Buildings and Structures, Univ. of Toronto Press, Ottawa, Canada.
112. Simiu, E., "Gust Factors and Along-wind Pressure Correlations", J. Struc. Div., ASCE, Vol.99, No. ST4, Proc. Paper 9686, April, 1973, pp. 773-783.
113. Simiu, E. and Lozier, D.W., "The Buffeting of Structures by Strong Winds-WindLoad Programme", NTIS Accession No. PB294757/AS, Computer Programme for Estimating Along-Wind Response, National Technical Information Service, Springfield, VA, 1979.
114. Simiu, E., "Revised Procedures for Estimating Along-Wind Response", J. Struc. Div., ASCE, Vol.106, No.ST1, Jan., 1980, pp. 1-10.
115. Simiu, E., "Modern Developments in Wind Engineering Part-IV", Engg. Struct., Vol.5, Oct., 1983, pp. 273-281.
116. Simiu, E. and Scanlan, R.H., "Wind Effects on Structures", Second Edition, John Wiley and Sons, New York, 1986.
117. Solari, G., "Along-Wind Response Estimation: Closed Form Solution", J. Struc. Div., ASCE, Vol.1108, No.ST1, Jan., 1982, pp. 225-244.
118. Surry, D. and Lythe, G., "Mean Torsional Loads on Tall Buildings", Proc. 4th U.S. National Conf. on Wind Engg. Research, V.Hartz Edition, Deptt. of Civil Engg., Univ. of Washington, Scattle. WA, July, 1981.
119. Surry, D. and Mallais, W., "Adverse Local Wind Loads Induced by an Adjacent Building", J. Struc. Div., ASCE, Vol.198, 1982.

120. Sykes, D.M., "Dynamic Response of a Building Model with a Second Model in Proximity", Proc. 4th Colloq. on Industrial Aerodyn., Aachen, 1980, pp. 205-221.
121. Sykes, D.M., "Interference Effects on the Response of a Tall Building Model", J. Wind Engg. and Industrial Aerodyn., Vol.11, 1983, pp. 365-380.
122. Takeuchi, M., Matsui, G., Nagai, R. and Kazama, S., "Actual Fluctuating Wind Pressure on a Tall Building and its Response", Proc. 3rd Int. Conf. on Wind Effects on Buildings and Structures, Tokyo, 1971, pp. 285-294.
123. Tanlike, Y. and Inaoka, H., "Aeroelastic Behaviour of Tall Buildings in Wakes", Proc. 7th Conf. on Recent Advances in Wind Engg., 1987, Aachen, W. Germany, pp. 209-219.
124. Thomas, R., Isymov, N. and Steckner, M., "Aerodynamic Interference Effects on local Surface Pressures, Proc. 4th Conf. on Wind Effects on Buildings and Structures, 1975.
125. Trifunac, M.D., "Comparisons Between Ambient and Forced Vibration Experiments, "Earthquake Engg. and Struc. Dynamics, Vol.1, No.2, 1972, pp. 81-110.
126. Ungar, "The Status of Engineering Knowledge Concerning the Damping of Built-up Structures", J. Sound and Vibration, Vol.26, 1973, pp. 141-154.
127. Vickery, B.J. and Watkins, R.D., "Flow Induced Vibrations of Cylindrical Structures", Proc. 1st Australian Conf. on Hydraulics and Fluid Mechanics, University of Western Australia, Dec., 1963, p. 213.
128. Vickery, B.J., "On the Assessment of Wind Effects on Elastic Structures", CE. Trans. Inst. Eng. Aust., Oct., 1966, pp. 183-192.
129. Vickery, B.J., "Wind Loads on Buildings with Particular Reference to the Dynamic Nature of Wind and its Effects", Ph.D. Thesis, Deptl. of Civil Engg., Univ. of Sydney, Australia, May, 1968.
130. Vickery, B.J., "On the Reliability of Gust Loading Factors", Tech. Meeting Concerning Wind Loads on Buildings and Structures, Natl. Bureau of Standards, Washington, DC., 1970.
131. Vickery, B.J., "Notes on Wind Forces on Tall Buildings", Annex to Australian Standard 1170, Part-2-1983, SAA Loading Code Part-2-Wind Forces, Standard Association of Australia, Sydney, 1973.
132. Vellozi, J. and Cohen, E., "Gust Response Factors", J. Struc. Div., ASCE, Vol.94, No.ST6, June, 1968, pp. 1245-1313.
133. Wargon, A., "Application of Post-tensioning Techniques and Other uses US-Japan Research Seminar on Wind Effects on Structures, Sept., 1974, pp. 111-122.



134. Williams, D., "Method of Damping out Bending Vibrations of Beam-Like Structures by Dry (or Coulomb) Friction", Proc. I. Mech. E., J. Mech. Engg. Scie., June, 1960, Vol.2, No.2, p. 77.
135. Wiren, B.G., "A Wind Tunnel Study of Wind Velocities in Passages Between and Through Buildings", Proc. Fourth Int. Conf. on Wind Effects on Buildings and Structures, London, 1975, pp. 465-475.
136. Wise, A.F.E., "Effects Due to Groups of Buildings", Phil. Trans. Roy. Soc., London, England, Vol.A269, 1971, pp. 469-85.
137. Wyatt, T.A., "A Review of Wind Loading Specifications", The Structural Engineer, Vol.49, No.5, 1971.
138. Yamada, M. and Goto, T., "The Criteria to Motion in Tall Buildings for Wind Loading", Proc. 3rd Int. Conf. on Wind Effects on Buildings and Structures, Tokyo, 1971, pp. 401-408.
139. Yamada, M. and Goto, T., "Human Response to Tall Buildings", Stroudsburg, Pennsylvania,;Dowden, Hutchinson and Ross, 1977, pp. 58-71.
140. Yakoo, Y. and Akiyama, H., "Lateral Vibration and Damping due to Earthquake and Wind Effects", S.D.A. Report, Tokyo Meeting of ASCE-IABSE Joint Committee, TC No.17, 1971, pp. 1-12.
141. Yoshikawa, Y. and Ishizaki, H., "on the Wind Pressure and the Wind Flow Around a Tall Building", IABSE-ASCE-AIA-IFHP-VIA Regional Conf. on Tall Buildings, Bangkok, Jan. 1974, pp. 505-520.

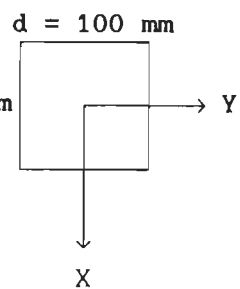
Table 6.1 Turbulence Intensity Measurements Around Model

S.No.	Location of Hot-wire Probe	0.6 m	0.5 m	0.4 m	0.3 m	0.2 m	0.1 m
1	Free Stream-Mid Section	11.20	11.60	13.60	15.40	17.70	21.05
2	Free Stream-0.25 m Offset (one-eighth section)	11.08	11.36	12.76	15.14	17.64	21.00
3	Free Stream-0.50 m Offset (quarter section)	10.79	11.24	13.71	14.60	17.49	21.07
<b>U/S of Aeroelastic Model</b>							
4	0.15 m From Face	12.26	13.21	15.73	17.38	20.67	25.11
5	0.80 m From Face	12.34	12.92	15.73	17.67	20.81	24.03
6	1.80 m From Face	12.27	12.70	15.20	17.07	16.33	23.49
<b>D/S of Aeroelastic Model</b>							
7	0.15 m From Face	16.69	26.23	34.80	35.92	38.19	45.19
8	0.15 m From Face & 0.20 m Offset	11.96	12.28	14.23	16.44	18.91	23.75
9	0.15 m From Face & 0.45 m Offset	11.39	11.63	13.20	15.55	18.21	21.95
10	0.80 m From Face	12.43	14.16	18.77	21.96	25.25	28.74
11	0.80 m From Face & 0.45 m Offset	11.67	12.15	14.11	16.74	19.11	23.61
12	1.00 m From Face	12.99	14.11	17.39	20.73	23.69	27.86
13	1.80 m From Face	12.25	13.09	15.76	17.71	20.58	25.28
14	1.80 m From Face & 0.20 m Offset	11.85	12.82	15.50	17.16	19.77	24.08
<b>Interface Case</b>							
15	y=2.5d ; x=4.5b	12.14	12.08	14.12	15.70	18.56	21.74
16	y=6.0d ; x=2.0b	11.82	13.60	17.39	18.75	22.40	26.64
17	y=3.5d ; x=1.5b	12.10	15.65	19.03	21.68	23.88	28.08

Table 6.2 Buffeting Factors for Mean Forces and Moments

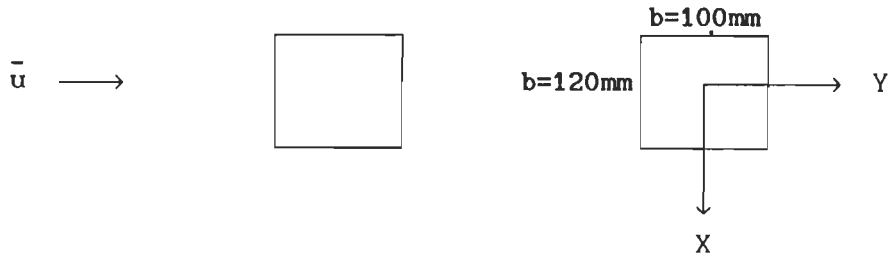
Terrain Coeff.  $\alpha = 0.10$ 

Wind Speed at 1 m = 10 m/s

 $\bar{u} \longrightarrow b = 120 \text{ mm}$ 

Spacing	$F_Y$	$M_X$	Spacing	$F_Y$	$M_X$
0, 2D	0.01	0.02	1B, 2D	0.76	0.71
0, 2.5D	0.02	0.04		0.52	0.50
0, 3D	0.03	0.06	1B, 3D	0.52	0.50
0, 4D	0.02	0.15			
0, 5D	0.30	0.38	1B, 5D	0.43	0.49
0, 6D	0.50	0.51			
0, 7D	0.54	0.59			
0, 8D	0.55	0.62	1B, 8D	0.60	0.66
0, 9D	0.58	0.63			
0, 11D	0.66	0.74	1B, 11D	0.66	0.72
0, 13D	0.71	0.74	1B, 13D	0.71	0.78
0, 21D	0.90	0.89	1B, 21D	0.88	0.91
0, 24D	0.96	0.94	1B, 26D	0.92	0.95

Table 6.3 Buffeting Factors for Short afterBody Model

Terrain Coef.  $\alpha = 0.30$  $U_r = 6$ 

S.No.	Interfering Model Position $x/b, y/d$	B.Fs for along-wind displacements		BFs for across-wind displacements
		Static	Dynamic	
1.	0,2	0.05	0.625	0.845
2.	0,2.5	0.08	0.850	0.914
3.	0,3	0.13	0.867	0.980
4.	0,4	0.19	1.250	1.149
5.	0,5	0.27	1.113	1.540
6.	0,6	0.45	1.372	1.276
7.	0,7	0.50	0.909	1.106
8.	0,8	0.50	1.018	1.151
9.	0,9	0.52	1.092	1.178
10.	0,11	0.70	1.060	1.216
11.	0,13	0.88	1.143	1.209
12.	0,21	0.96	1.071	1.062
13.	0,24	1.03	0.941	1.121

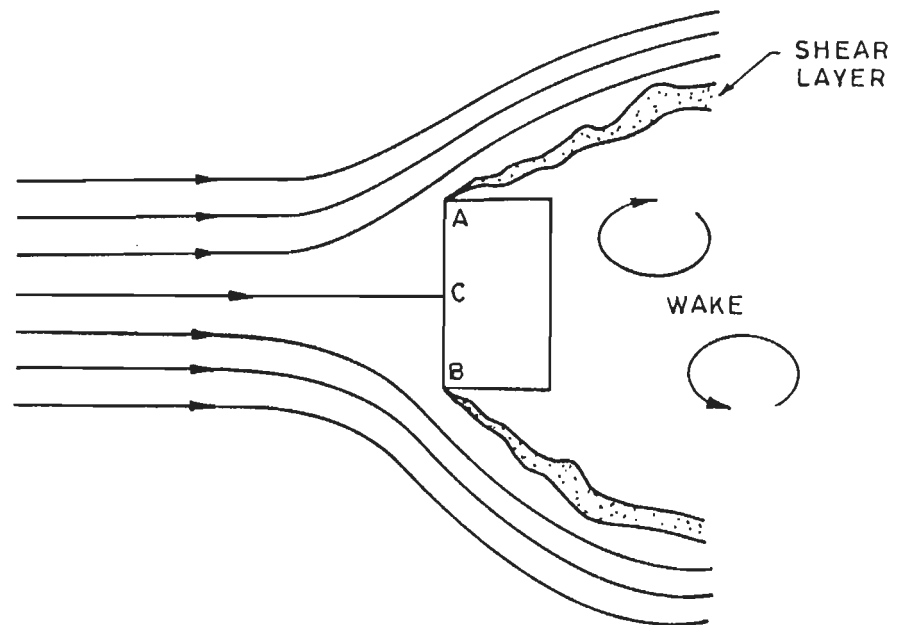


Fig.2.1 Flow Around a Rectangular Block



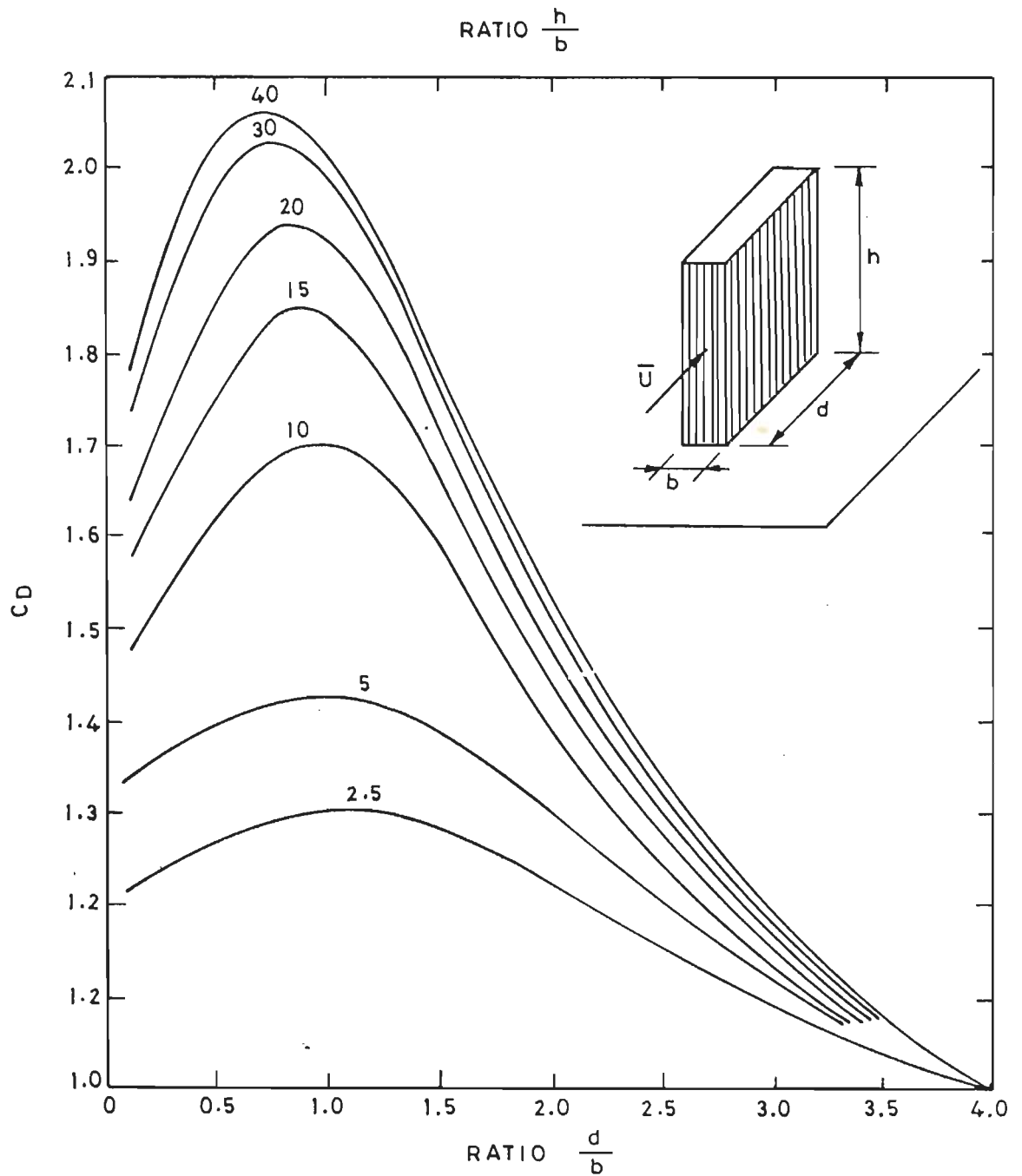


Fig.2.2 Drag Coefficient  $C_D$  as a Function of the Ratio of Plan Dimensions  $d$  and  $b$  (According to [69])

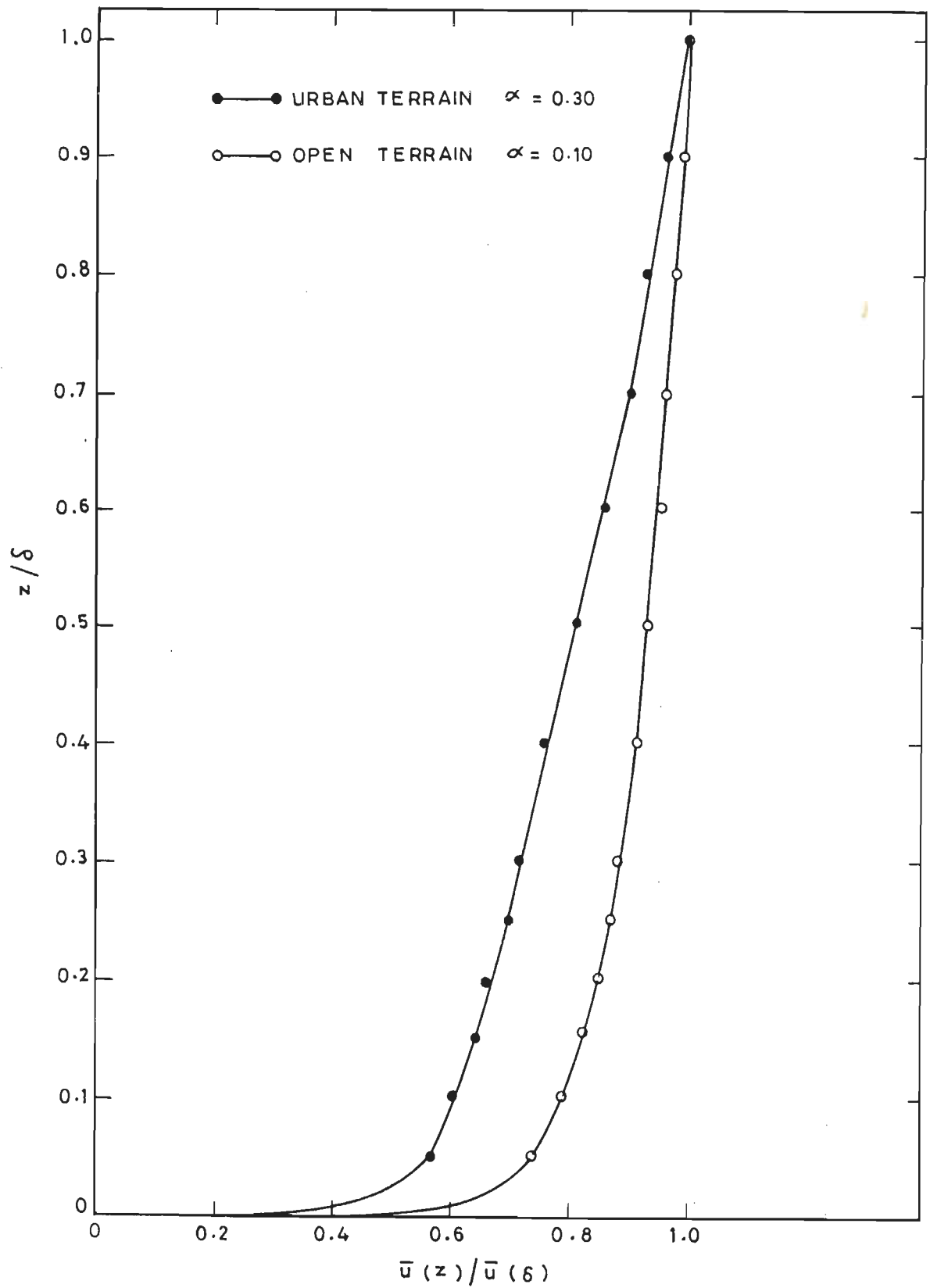


Fig. 4.1 Mean Velocity Profiles

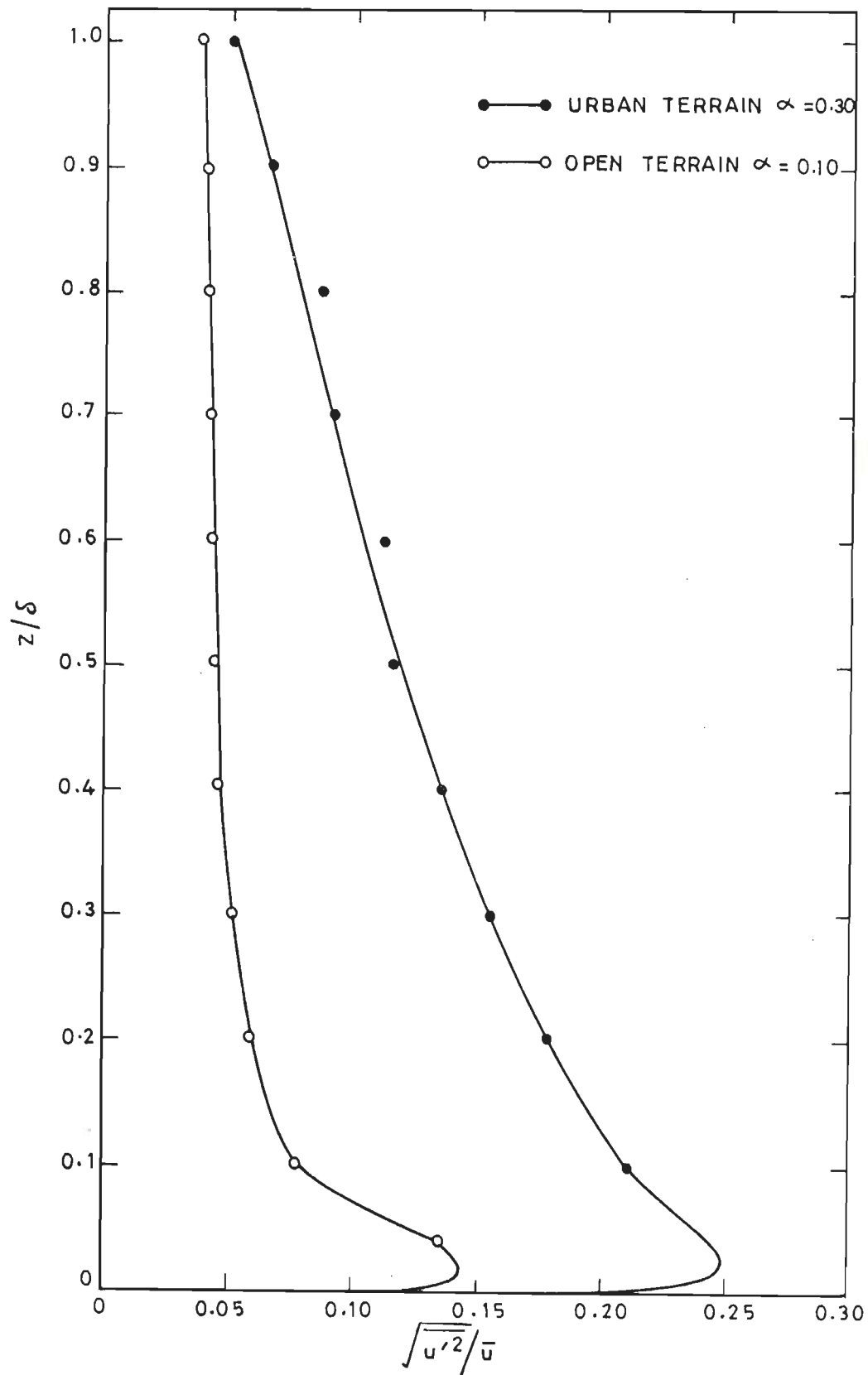


Fig.4.2 Turbulence Intensity Profiles



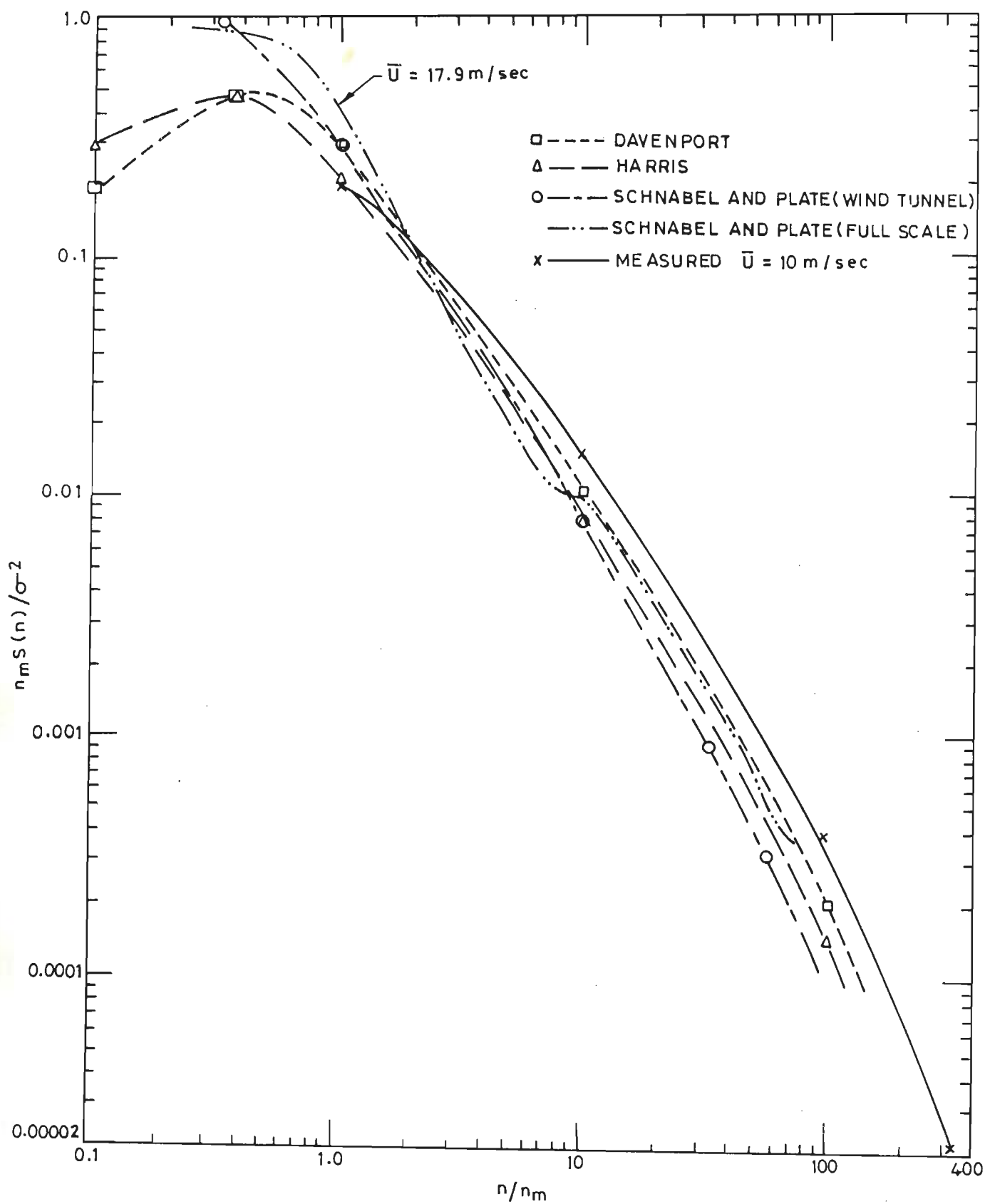


Fig. 4.3 Scaling of Spectra by Variance and Peak Frequency

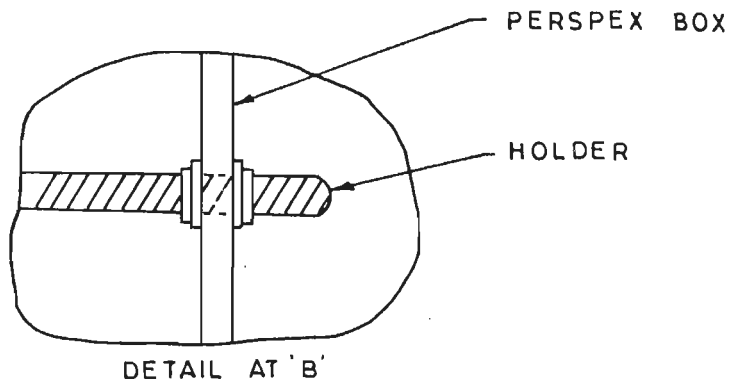
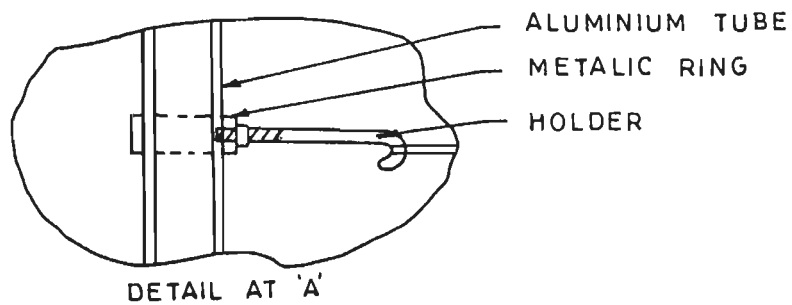
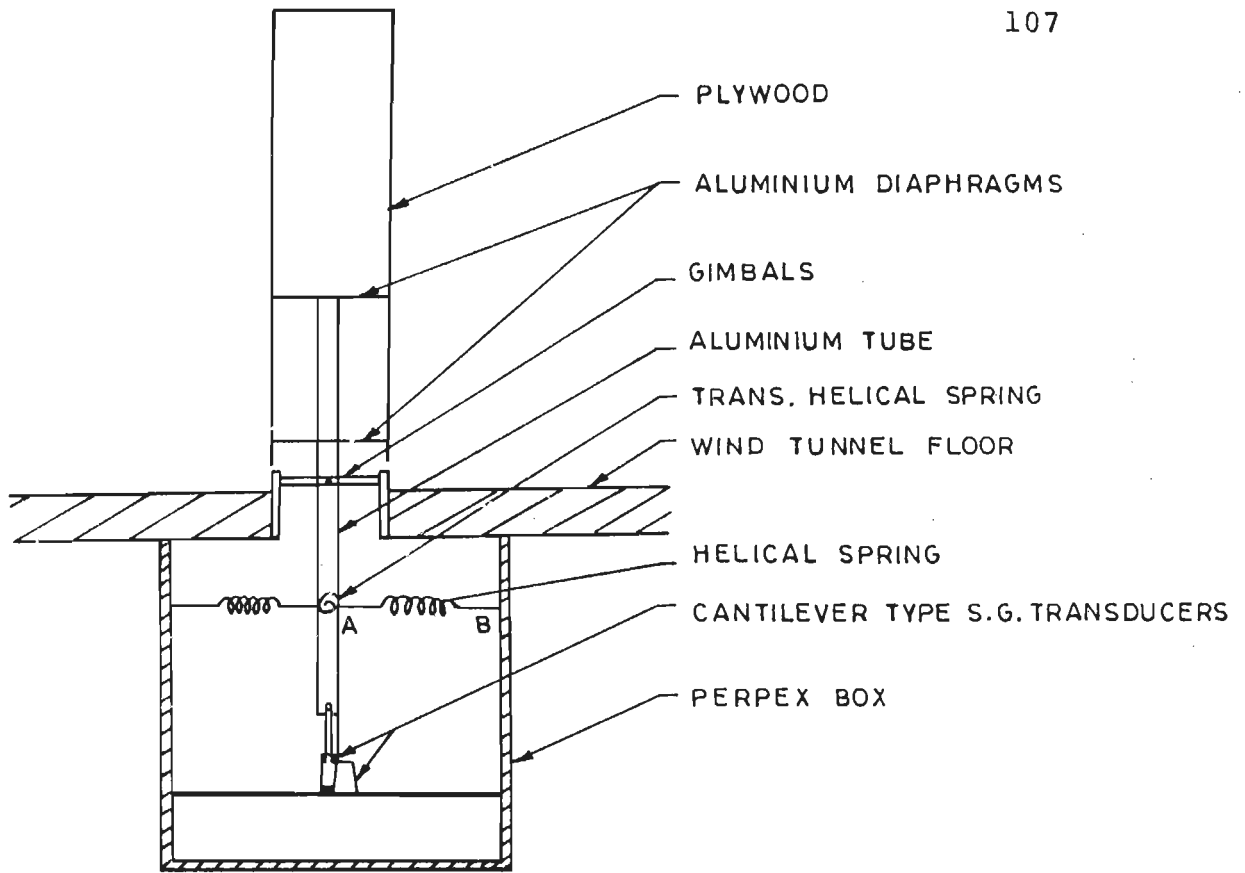


Fig.4.4 Schematic Diagram of Aeroelastic Model

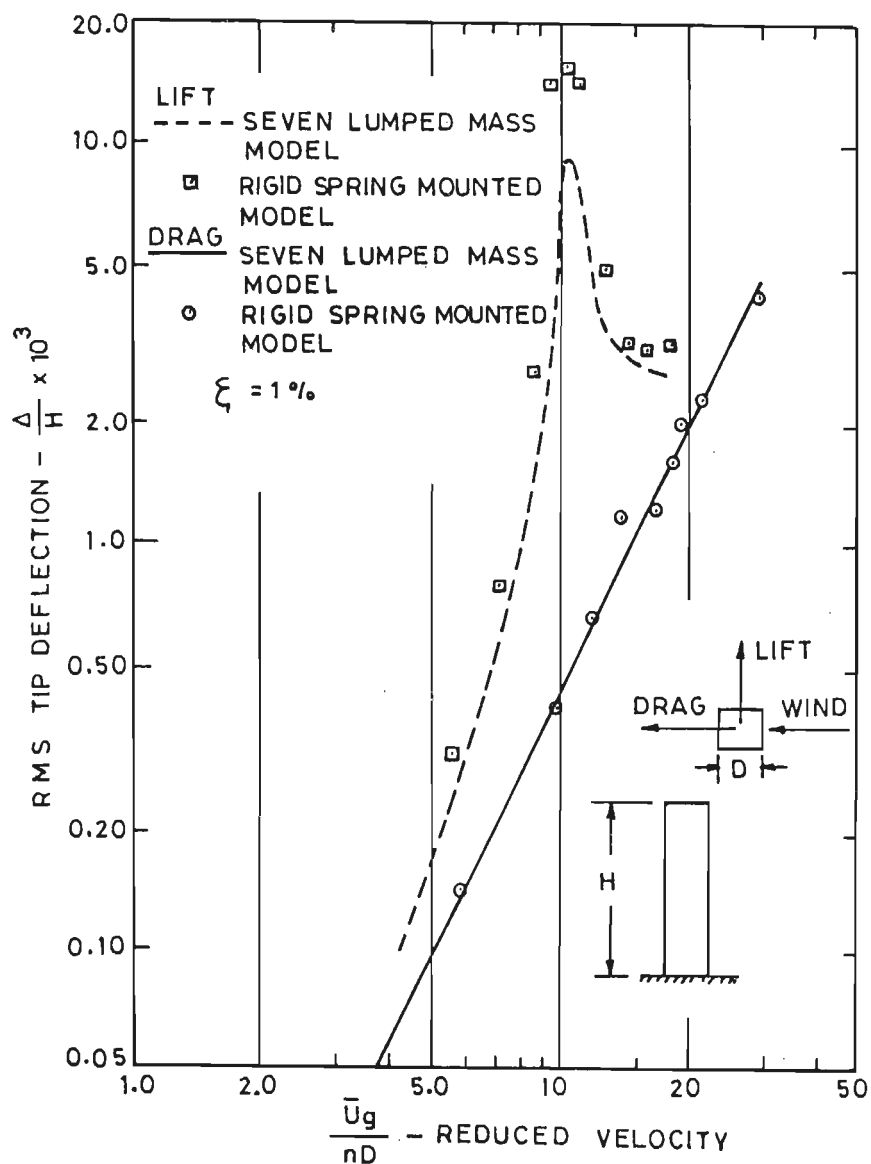


Fig.4.5 Aeroelastic Sway Response Obtained with Multi-degree of Freedom and Conventional Stick Models of a Tall Building of Square Cross-section [57]

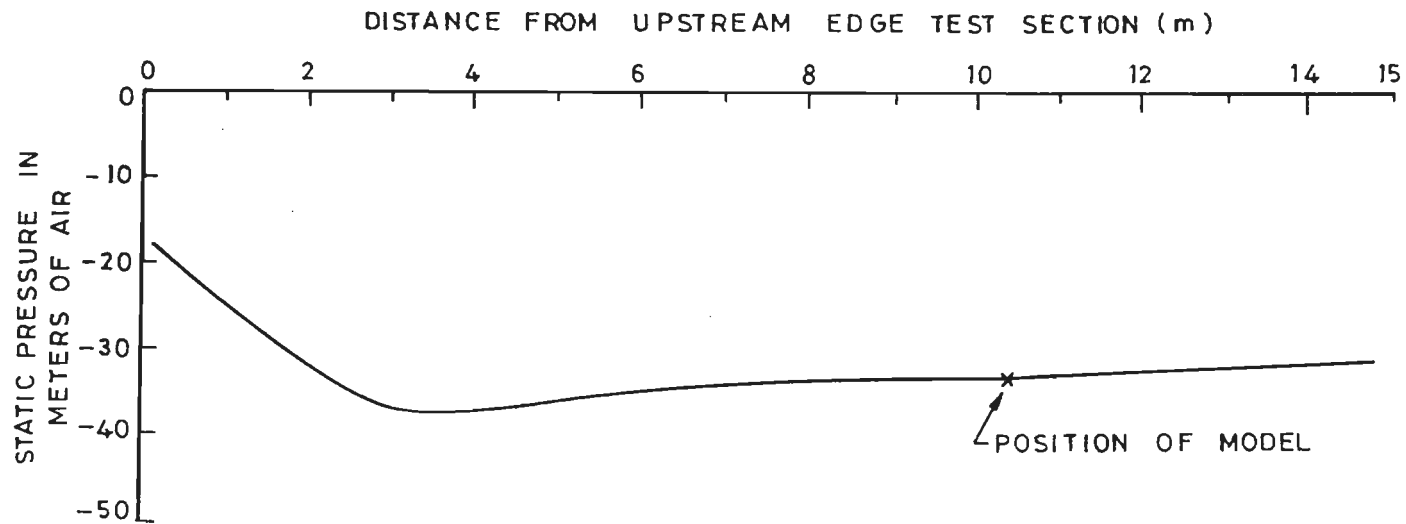


Fig.4.6 Static Pressure Variation Along the Test Section [4]

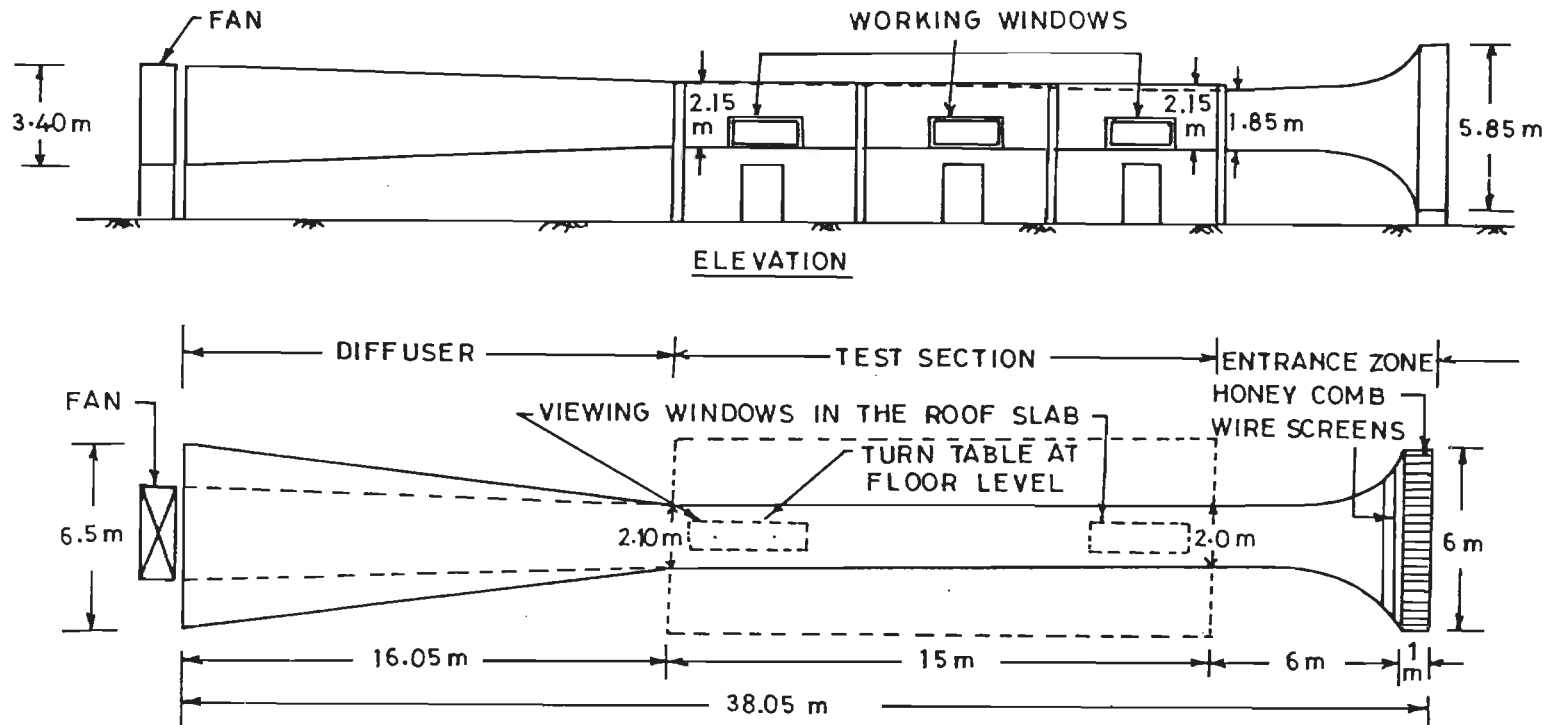


Fig.4.7 Schematic Diagram of Boundary Layer Wind Tunnel at University of Roorkee

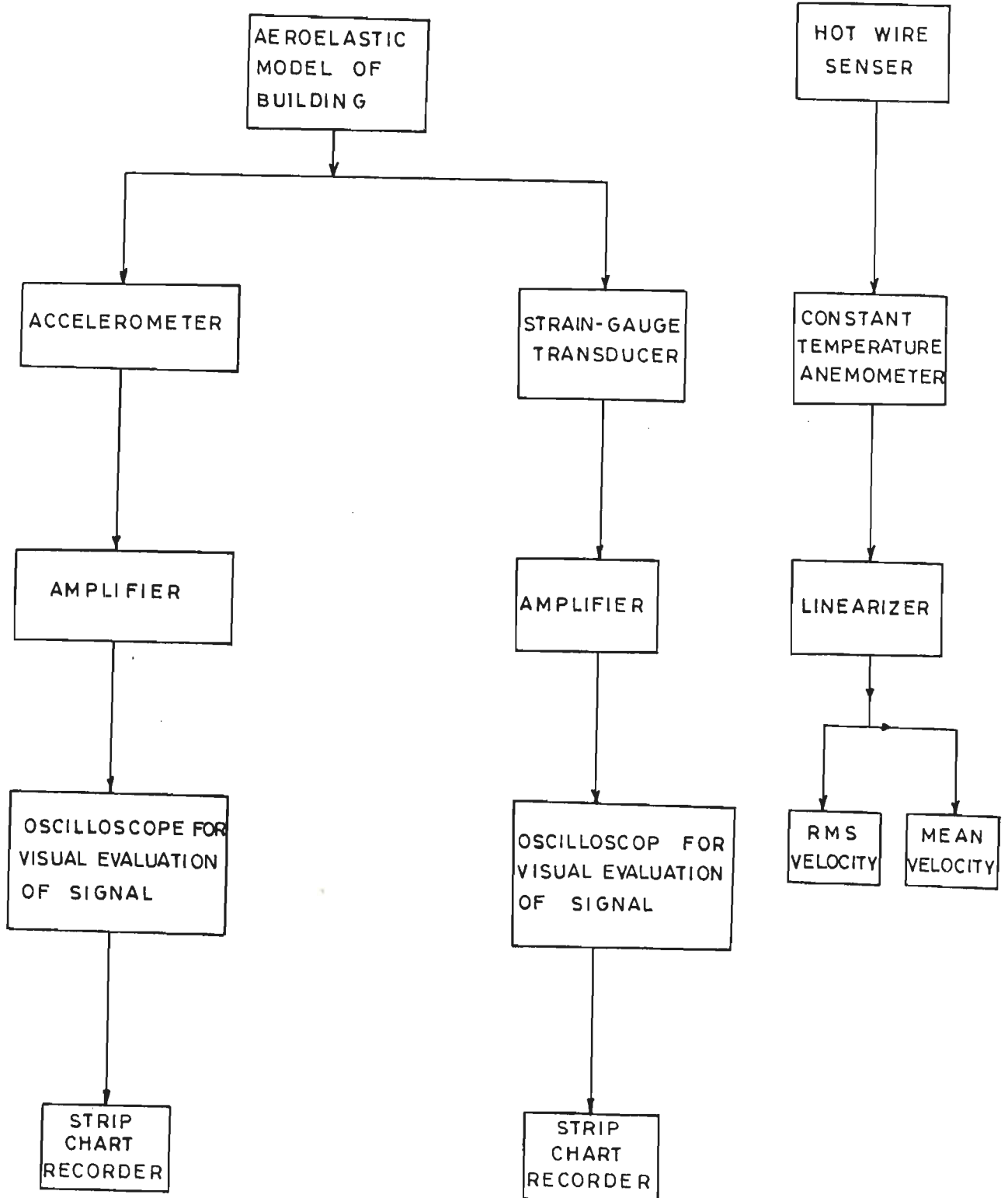


Fig.4.8 Scheme of Instrumentation for Measurements on Aeroelastic Model

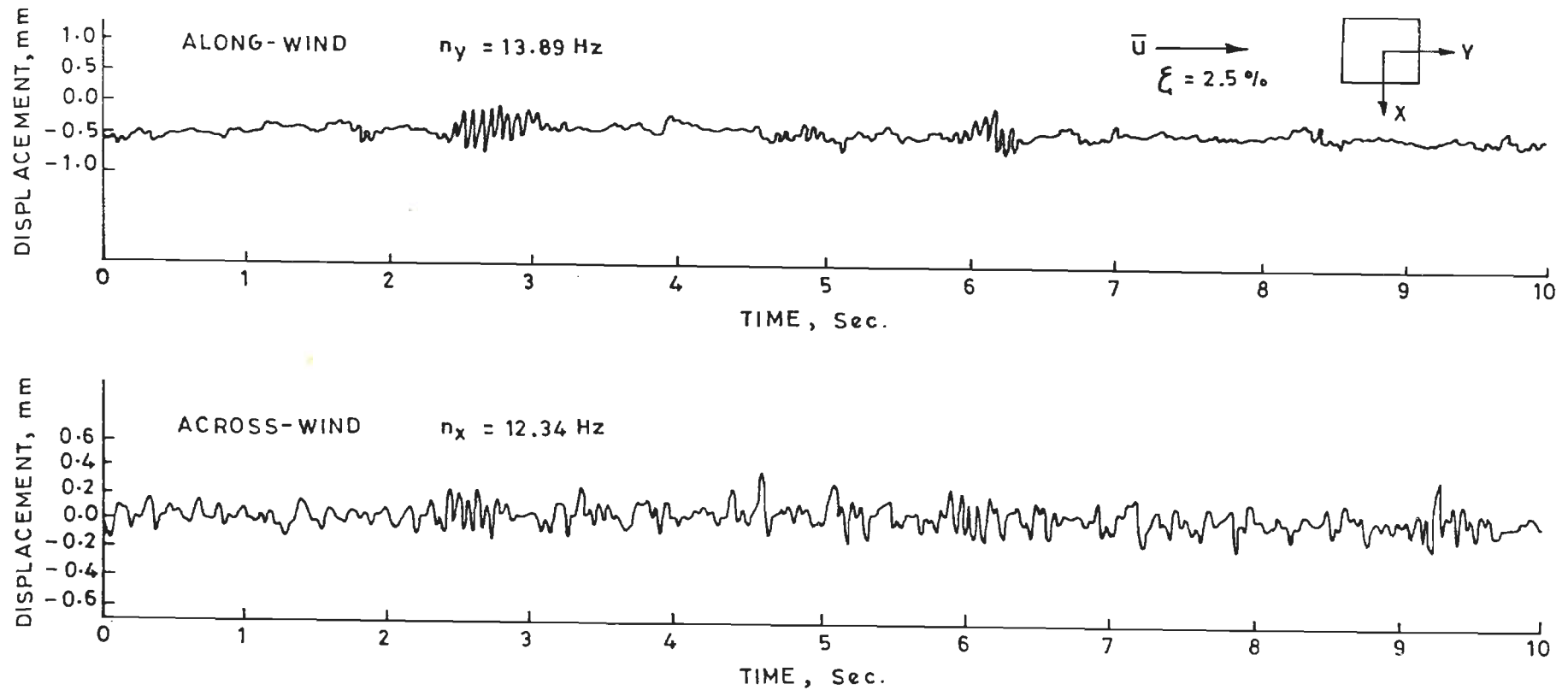


Fig.4.9 Response at the Top of the Building Model  
(Long Afterbody) at Reduced Velocity 4

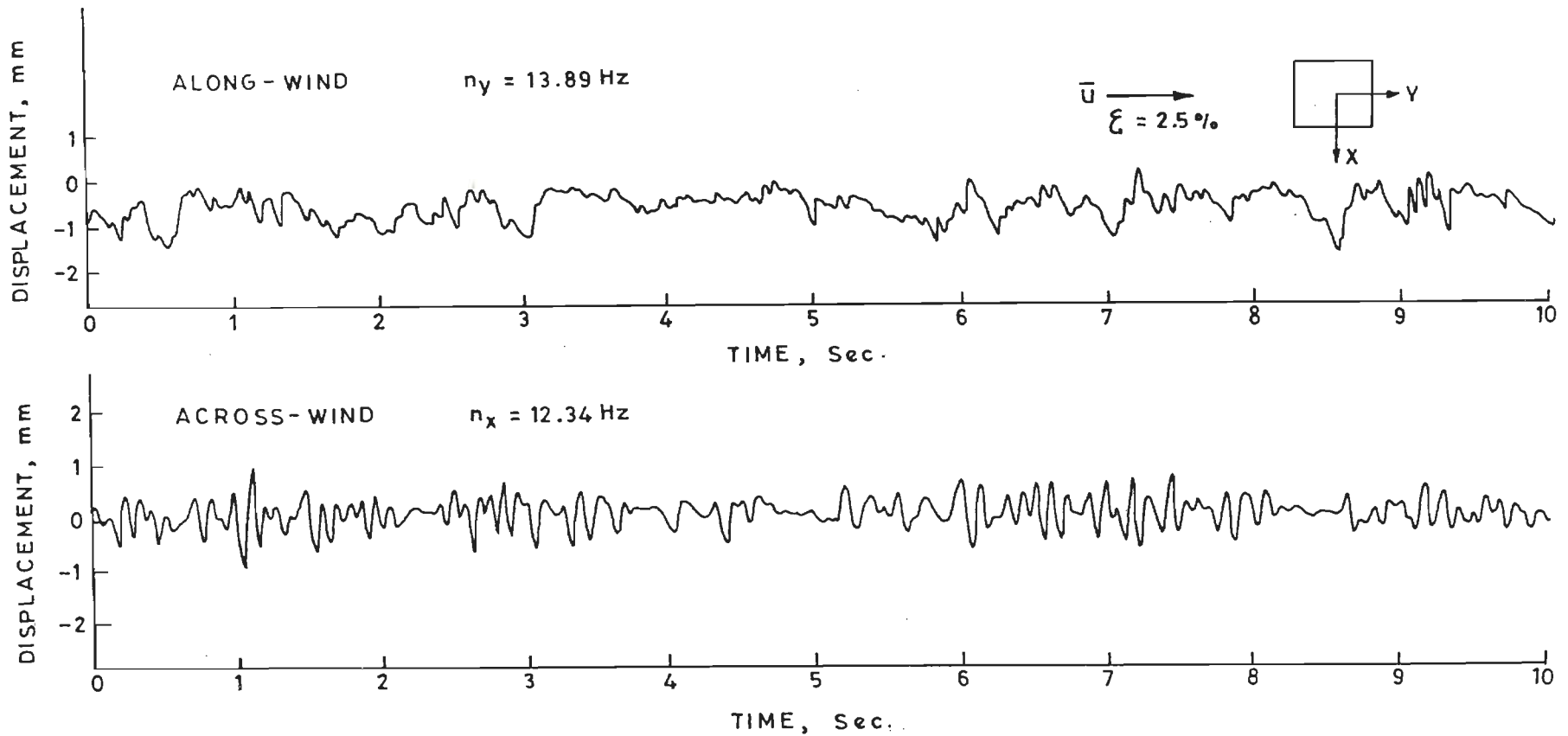


Fig.4.10 Response at the Top of the Building Model  
(Long Afterbody) at Reduced Velocity 6



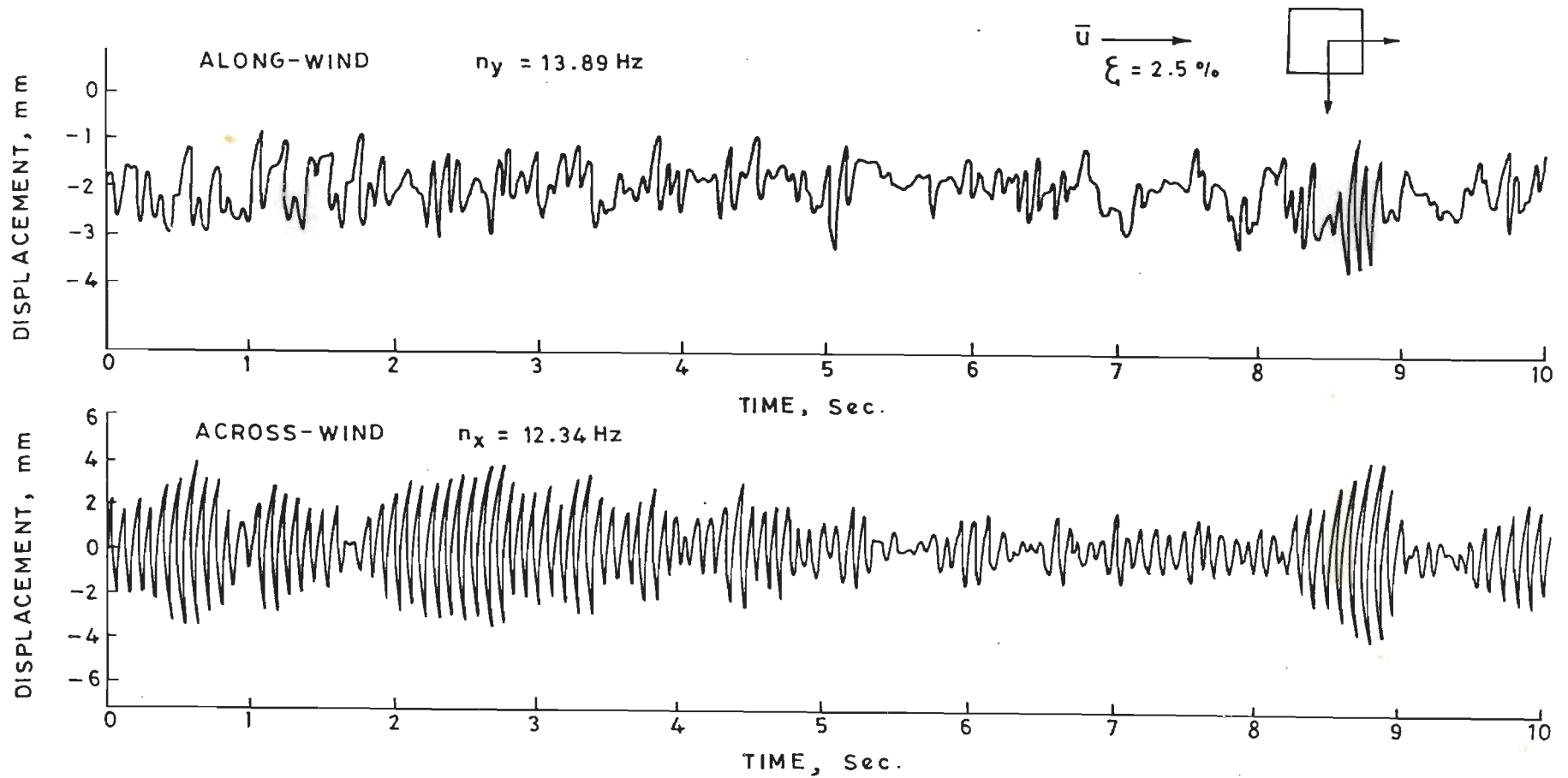


Fig.4.11 Response at the Top of the Building Model (Long Afterbody) at Reduced Velocity 8

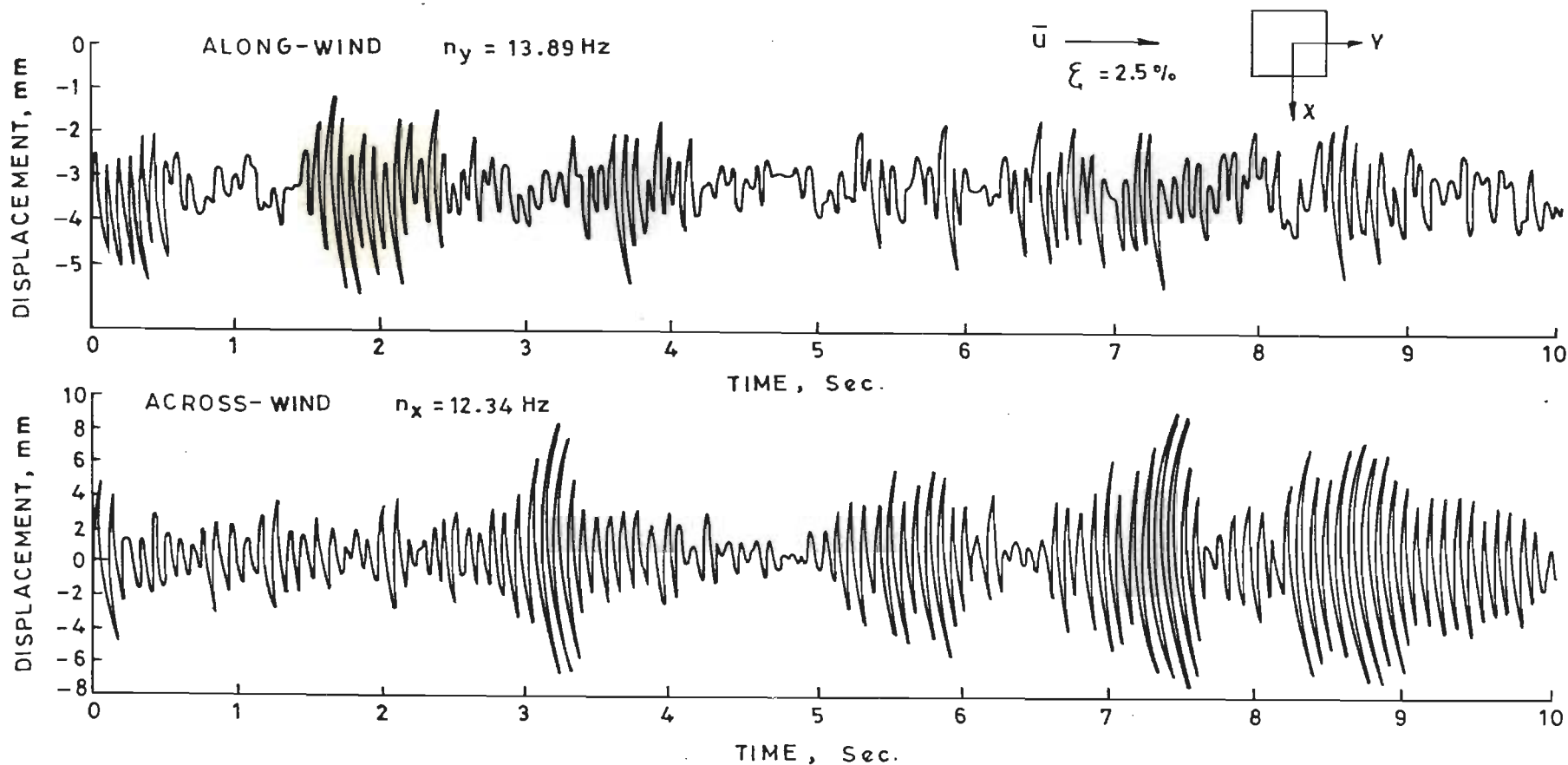


Fig.4-12 Response at the Top of the Building Model (Long Afterbody) at Reduced Velocity 10

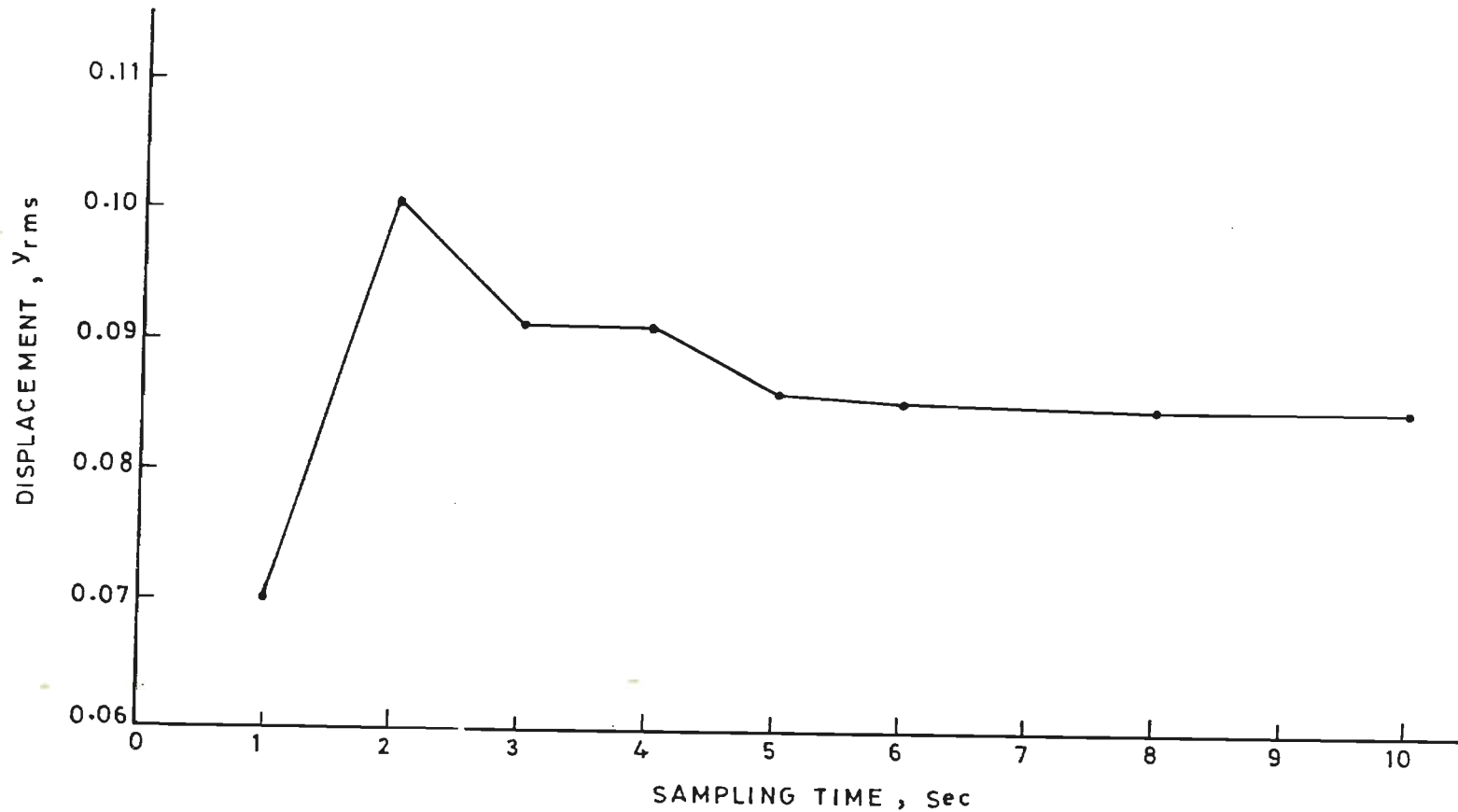


Fig.4.13 Effect of Sampling Time on Displacement Amplitude Computed from the Records

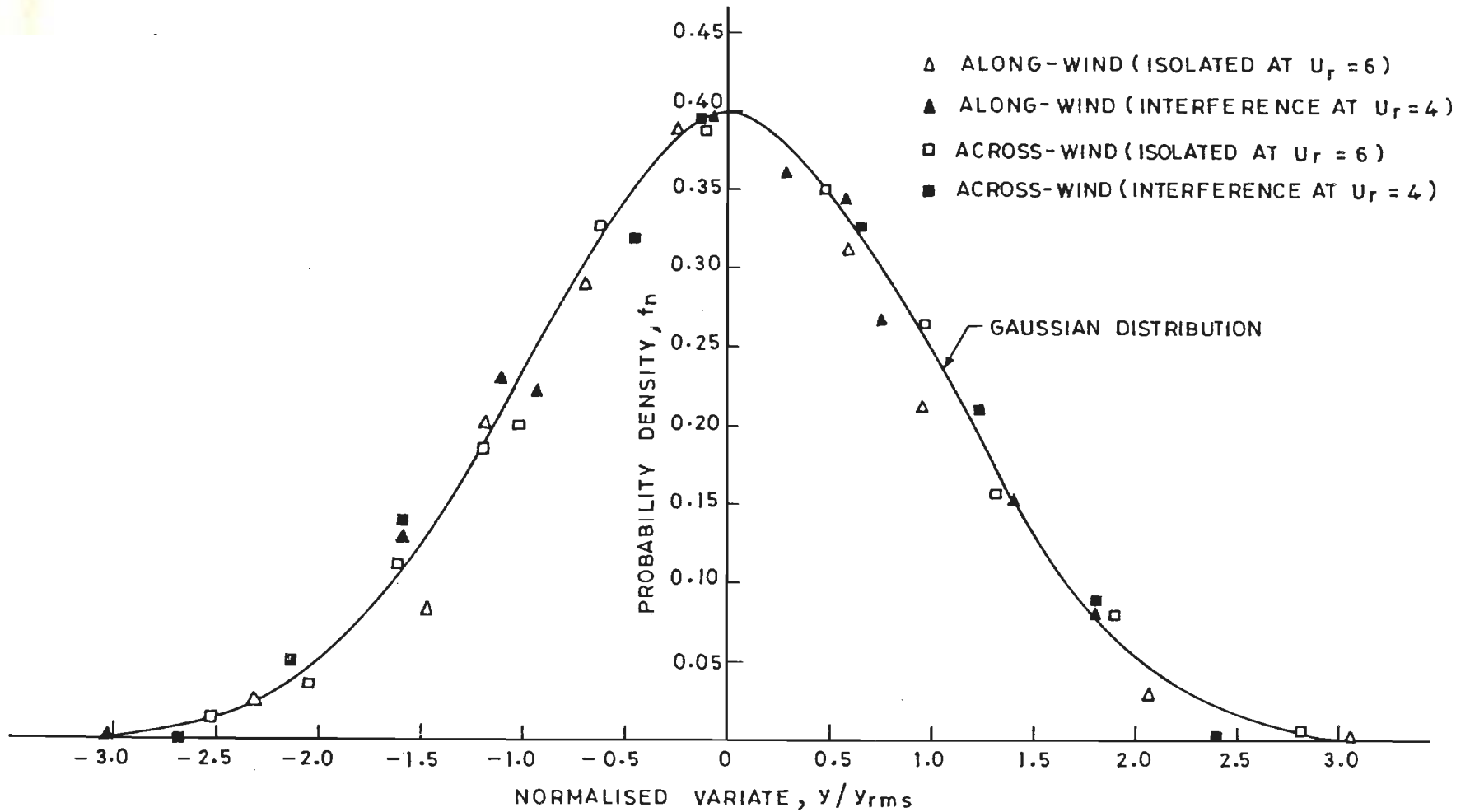


Fig.4.14 Probability Density of Fluctuation in Displacement Response of the Building Model

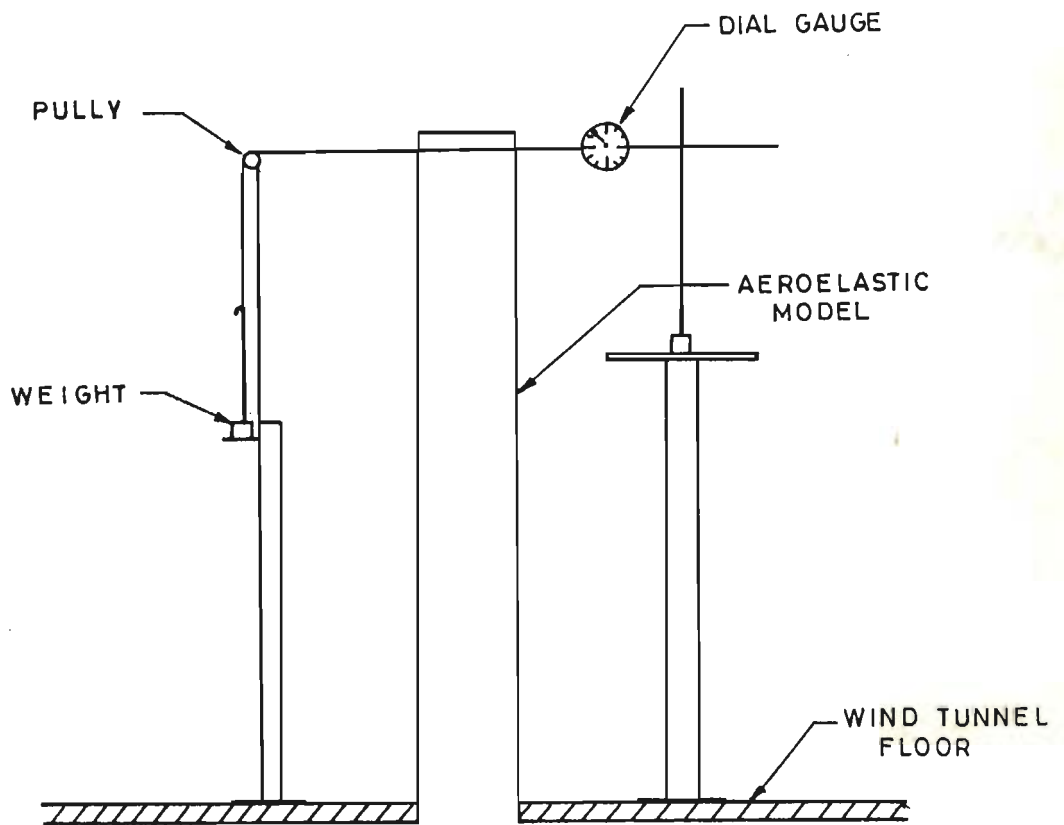


Fig.4.15 Arrangement for Static Calibration of the S.G. Transducers

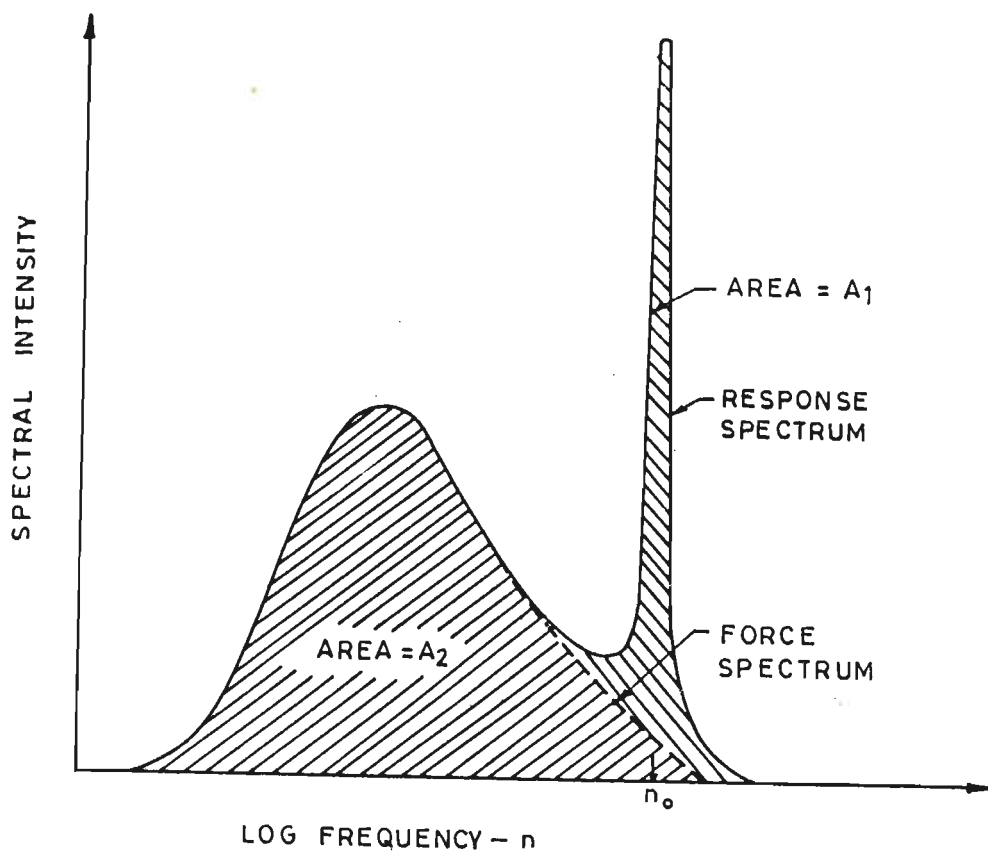


Fig. 5.1 Relationship Between Response and Force Spectra for Lightly Damped System [29]

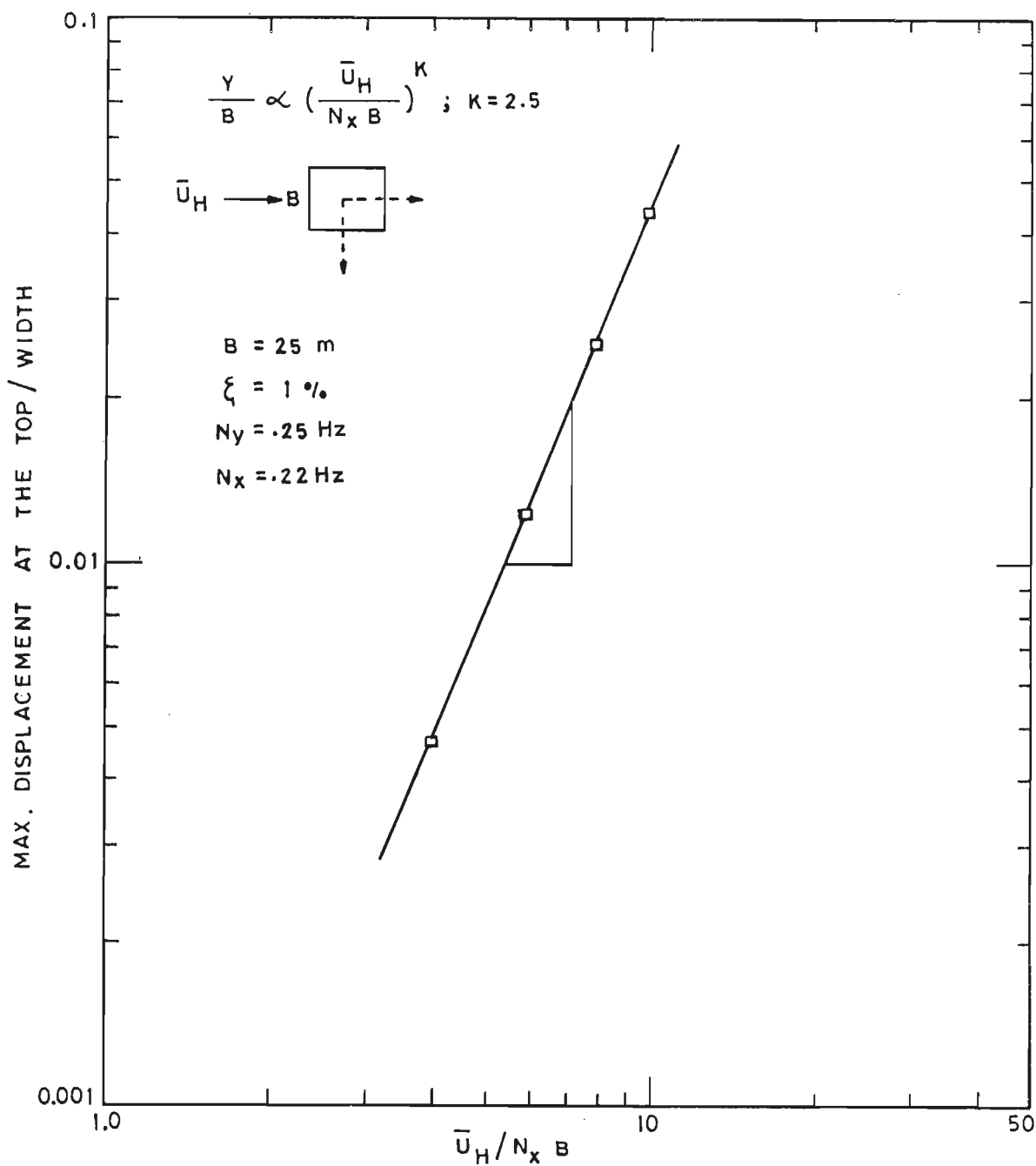


Fig. 5.2 Theoretical Along-Wind Displacement for Long Afterbody Case

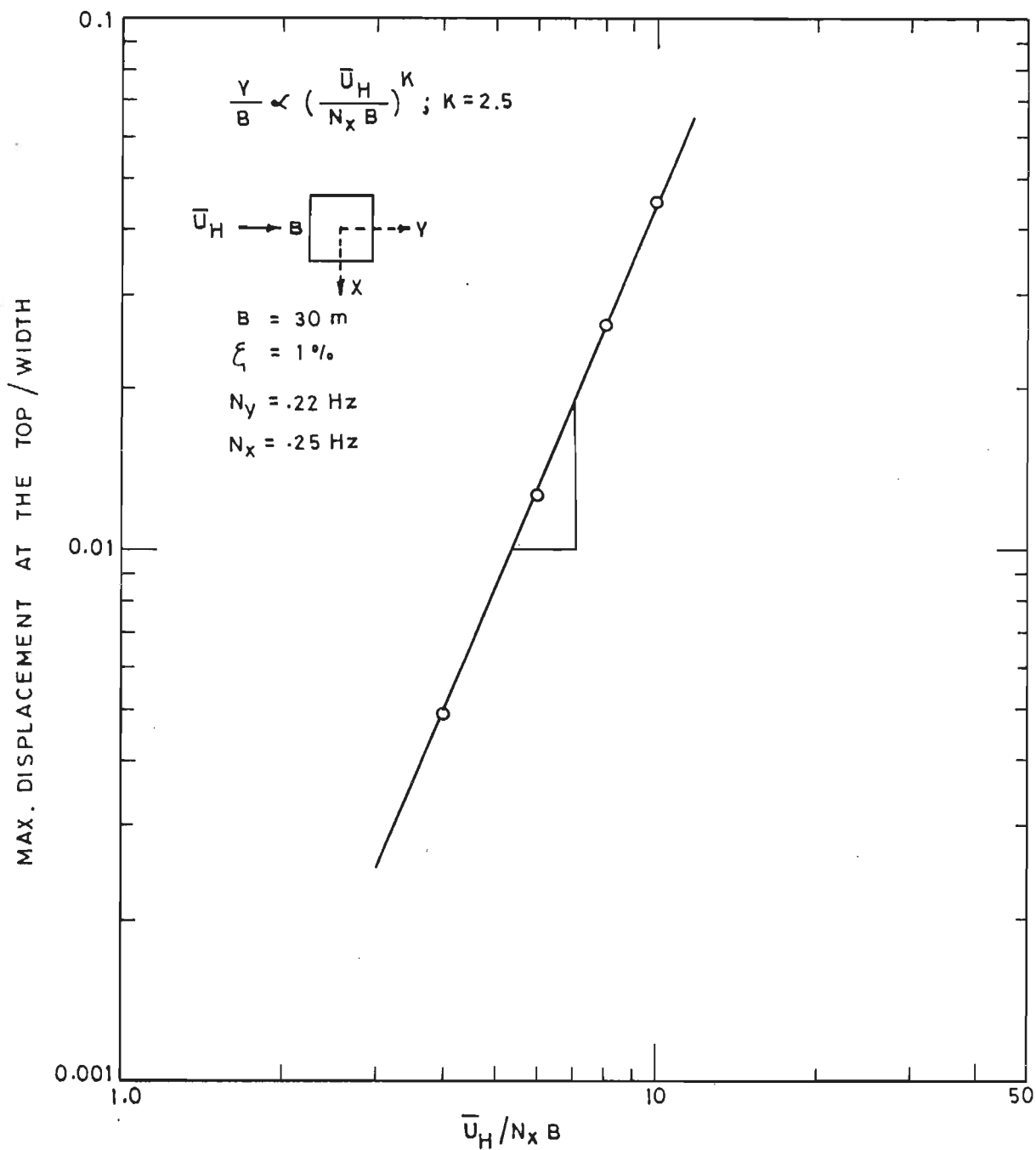


Fig. 5.3 Theoretical Along-Wind Displacement for Short Afterbody Case



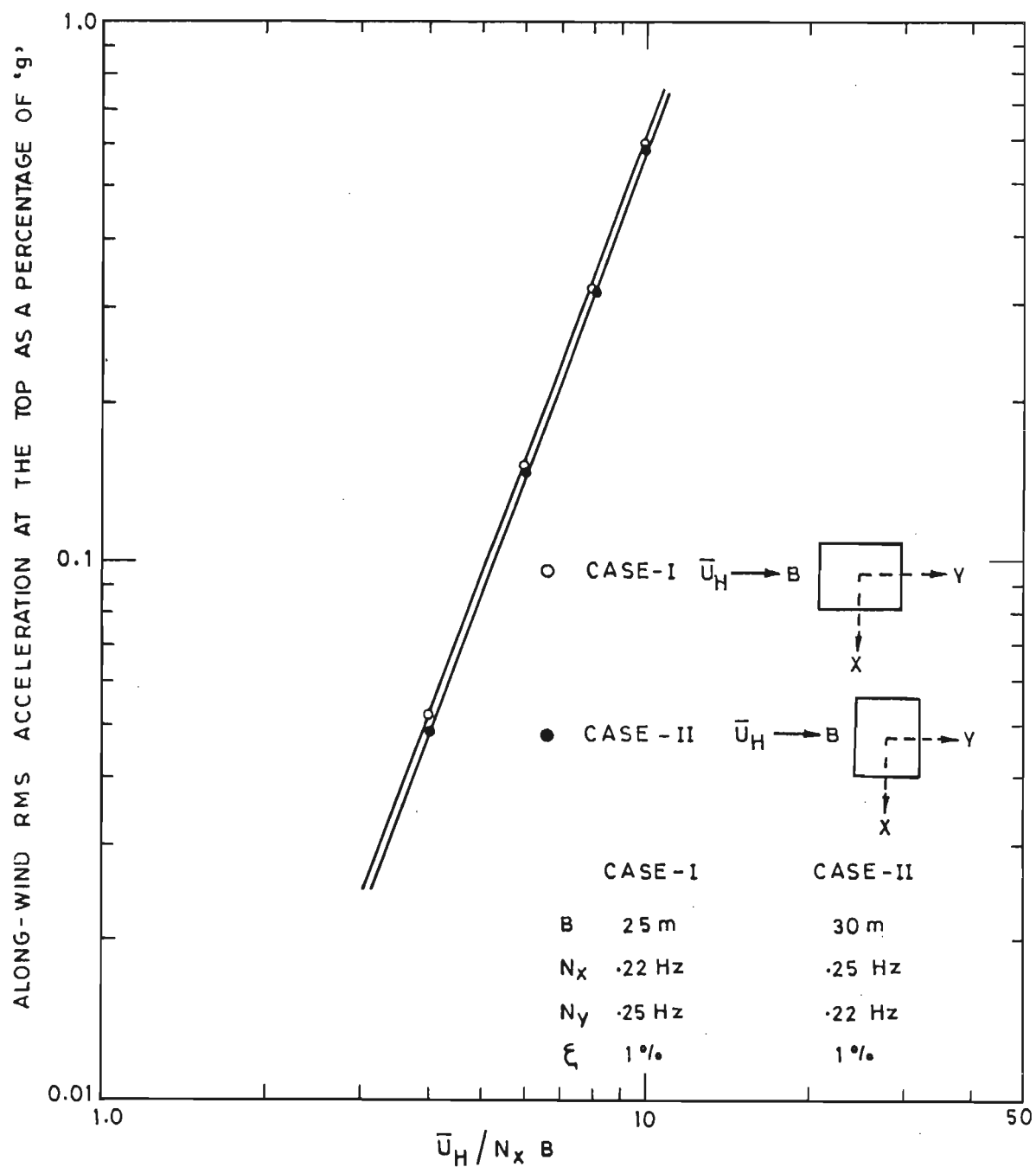


Fig.5.4 Theoretical Value of Along-Wind Acceleration

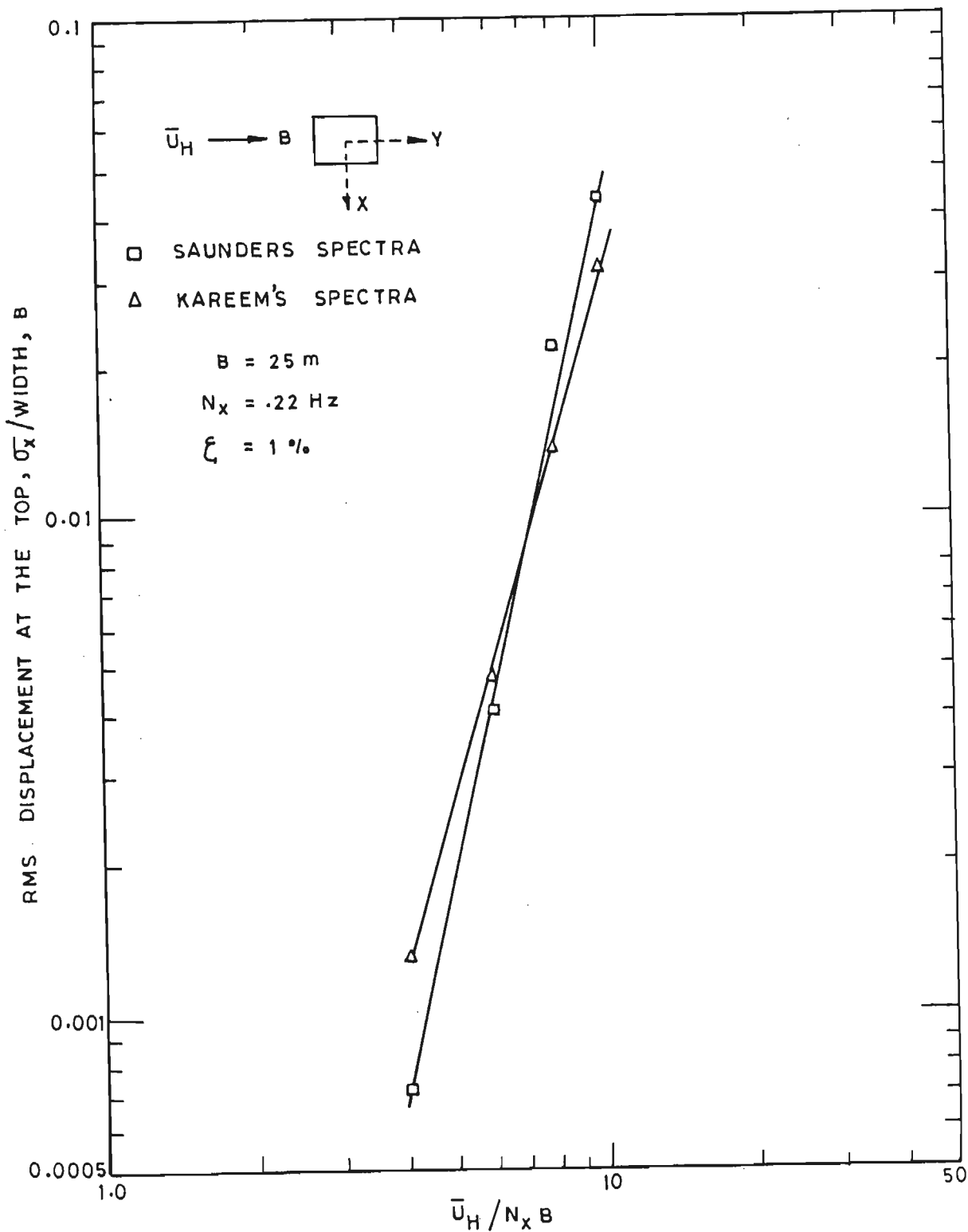


Fig. 5.5 Theoretical Across-Wind Displacement of Long Afterbody Building

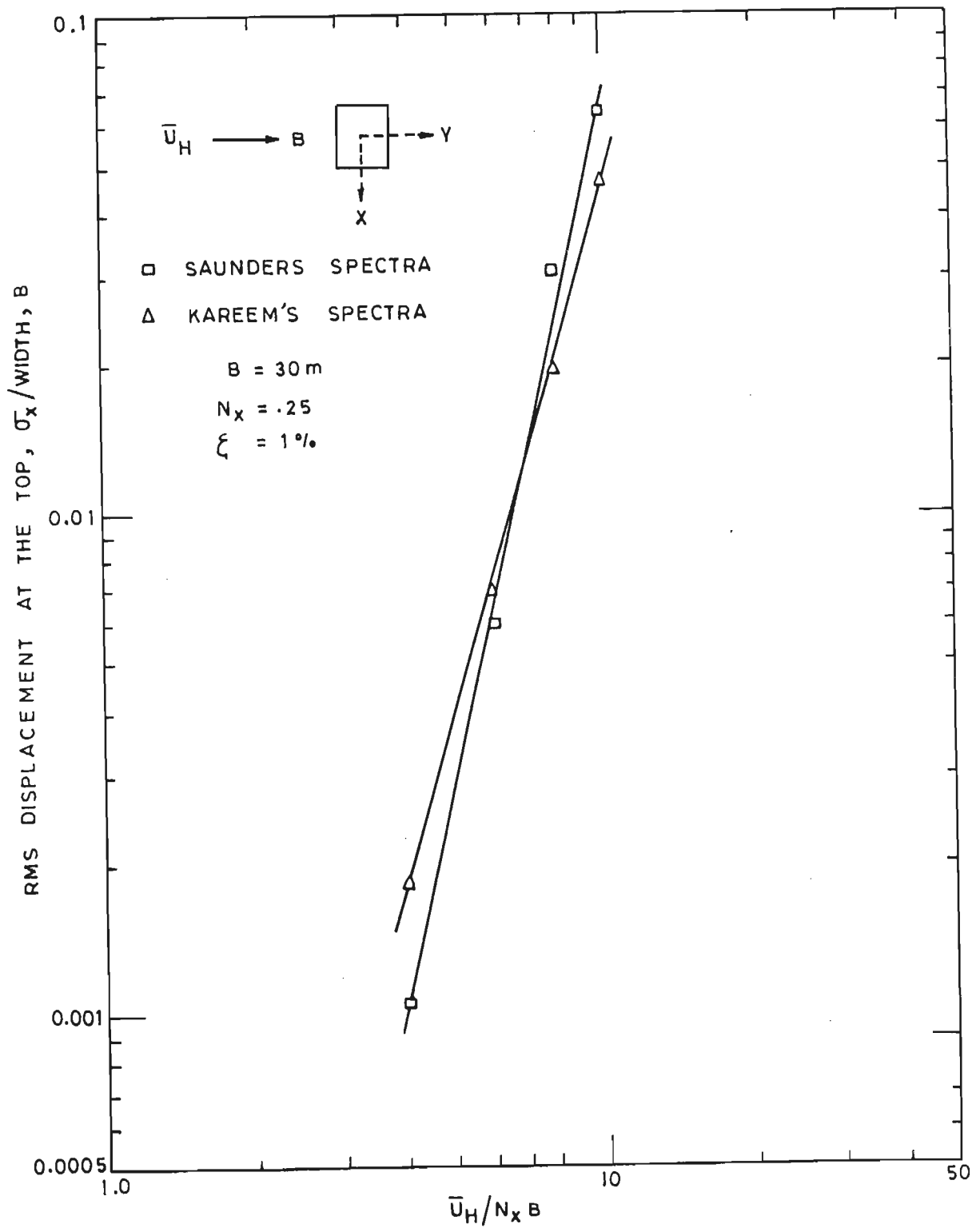


Fig. 5.6 Theoretical Across-Wind Displacement Short Afterbody Building

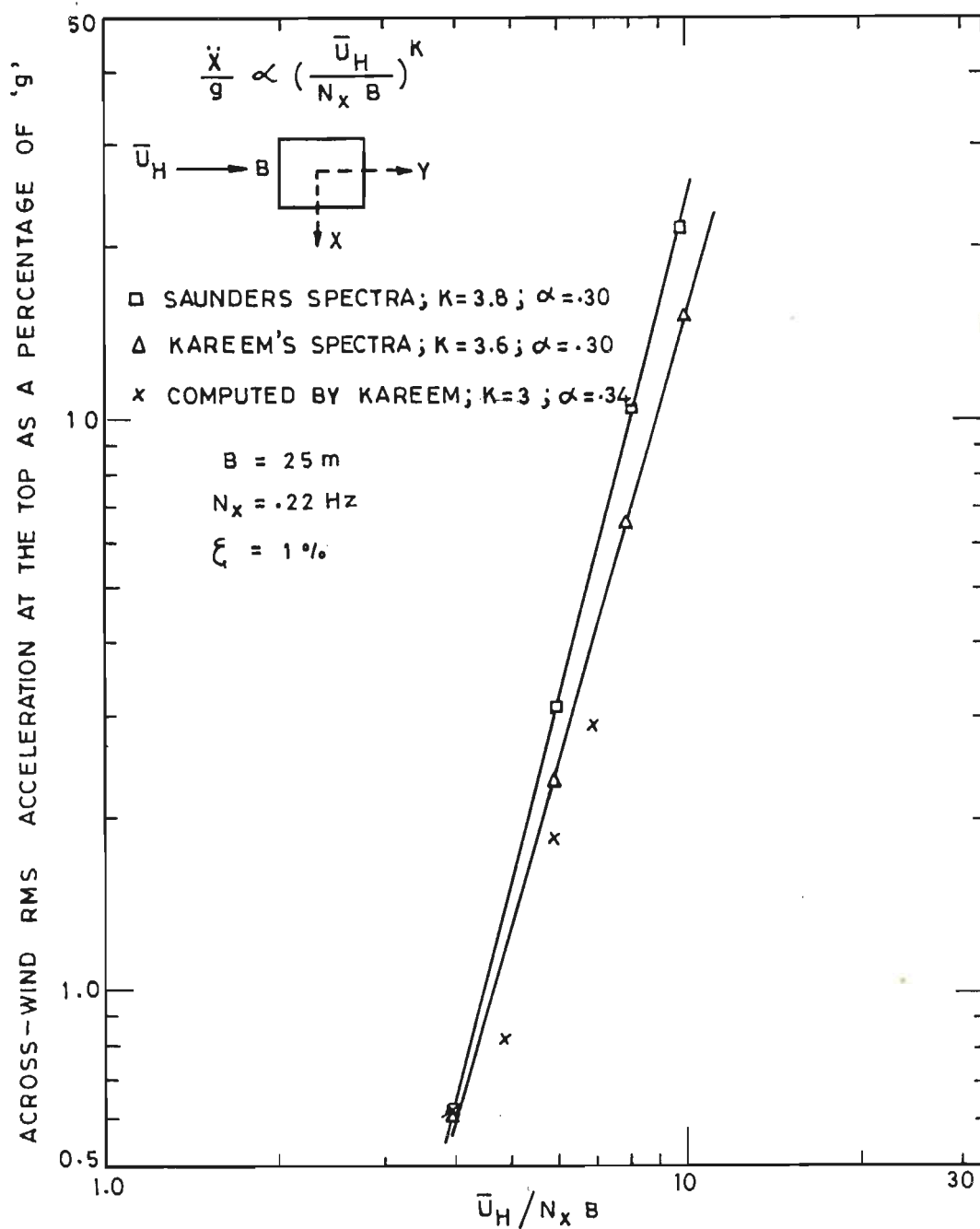


Fig. 5.7 Computed Across-Wind Acceleration Using Different Spectra

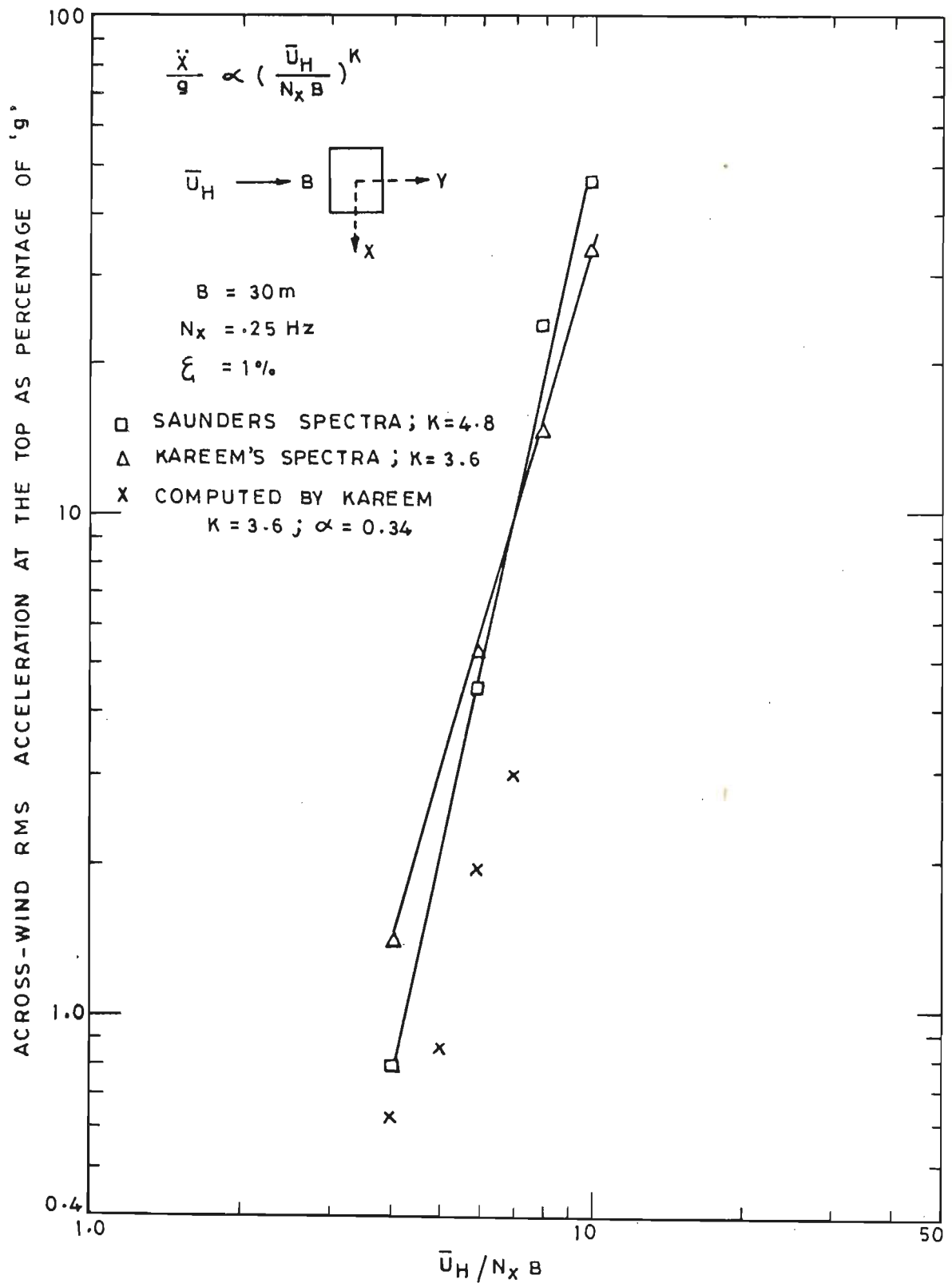


Fig. 5.8 Computed Across-Wind Acceleration Using Different Spectra

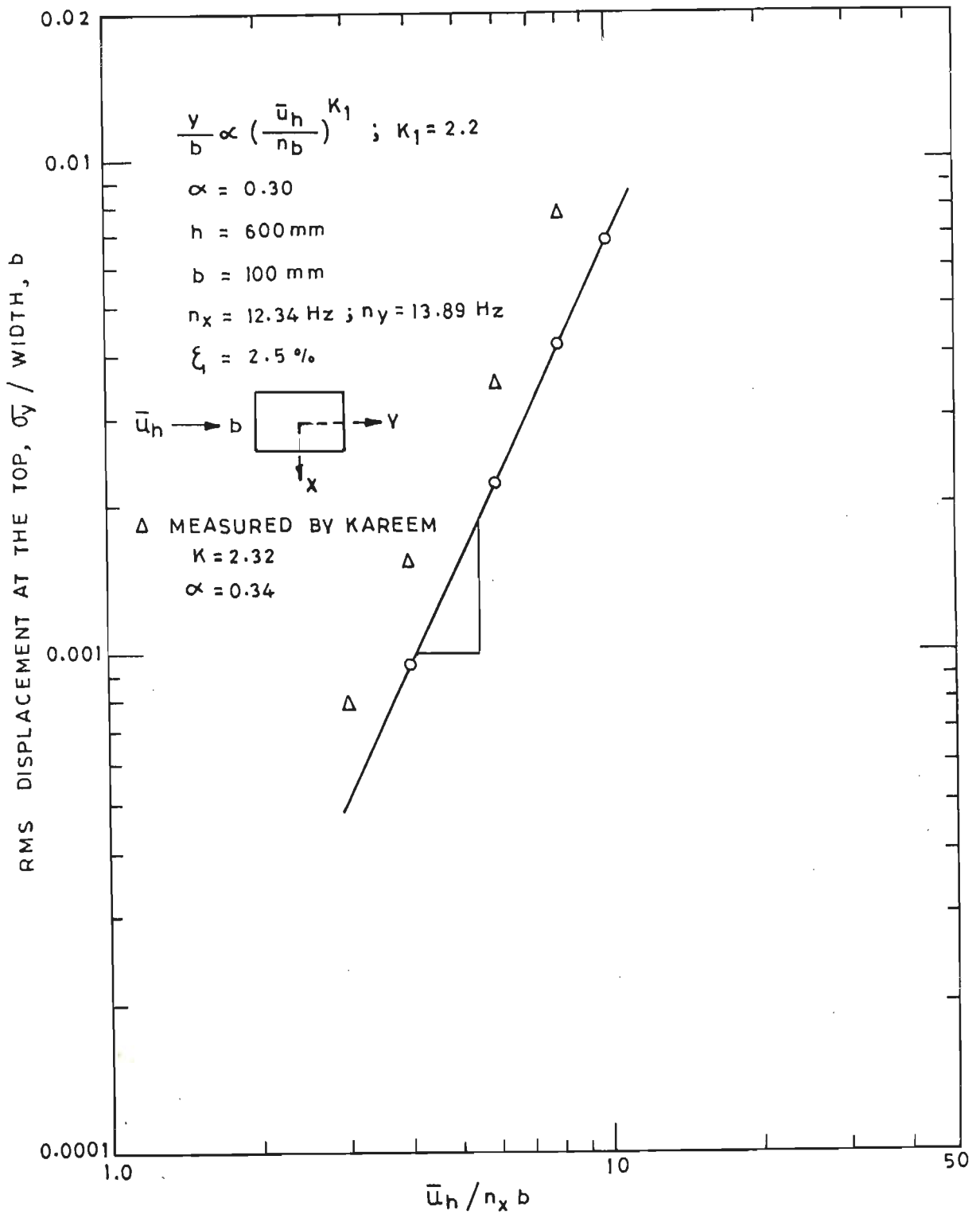


Fig.5.9 Variation of rms Along-Wind Response of Aeroelastic Model (Long Afterbody)

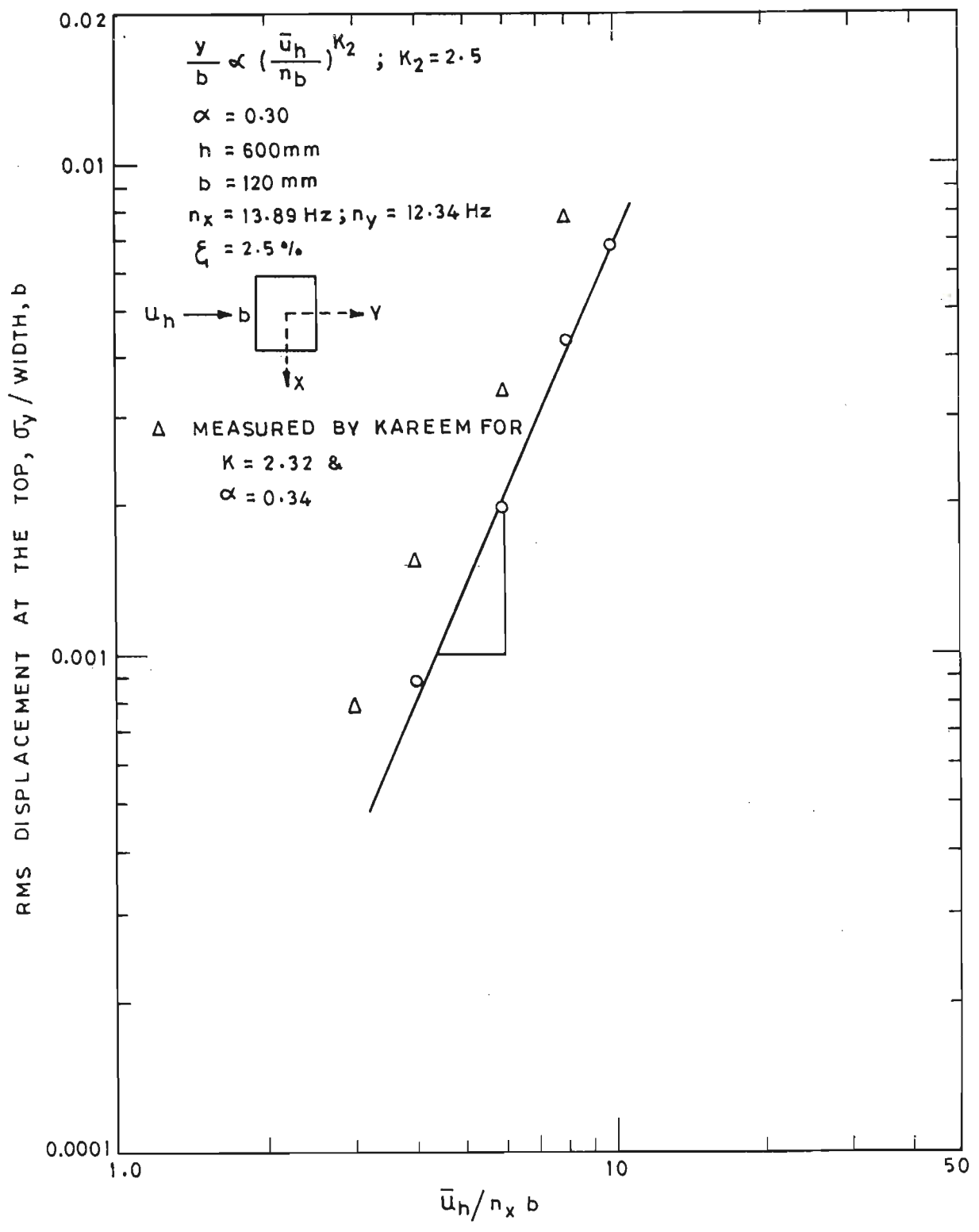


Fig.5.10 Variation of rms Along-Wind Response of Aeroelastic Model (Short Afterbody)

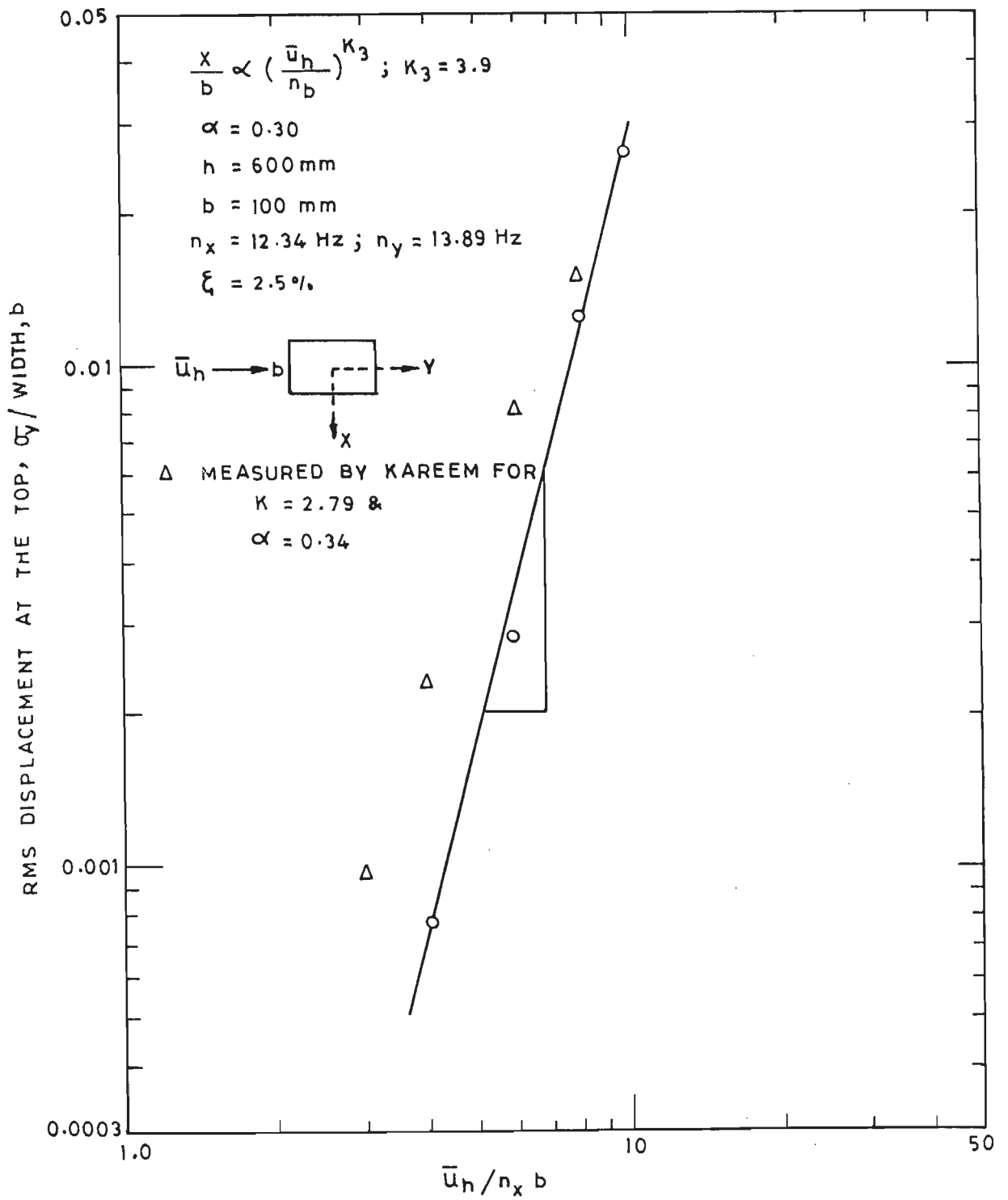


Fig. 5.11 Variation of rms Across-Wind Response of Aeroelastic Model (Long Afterbody)



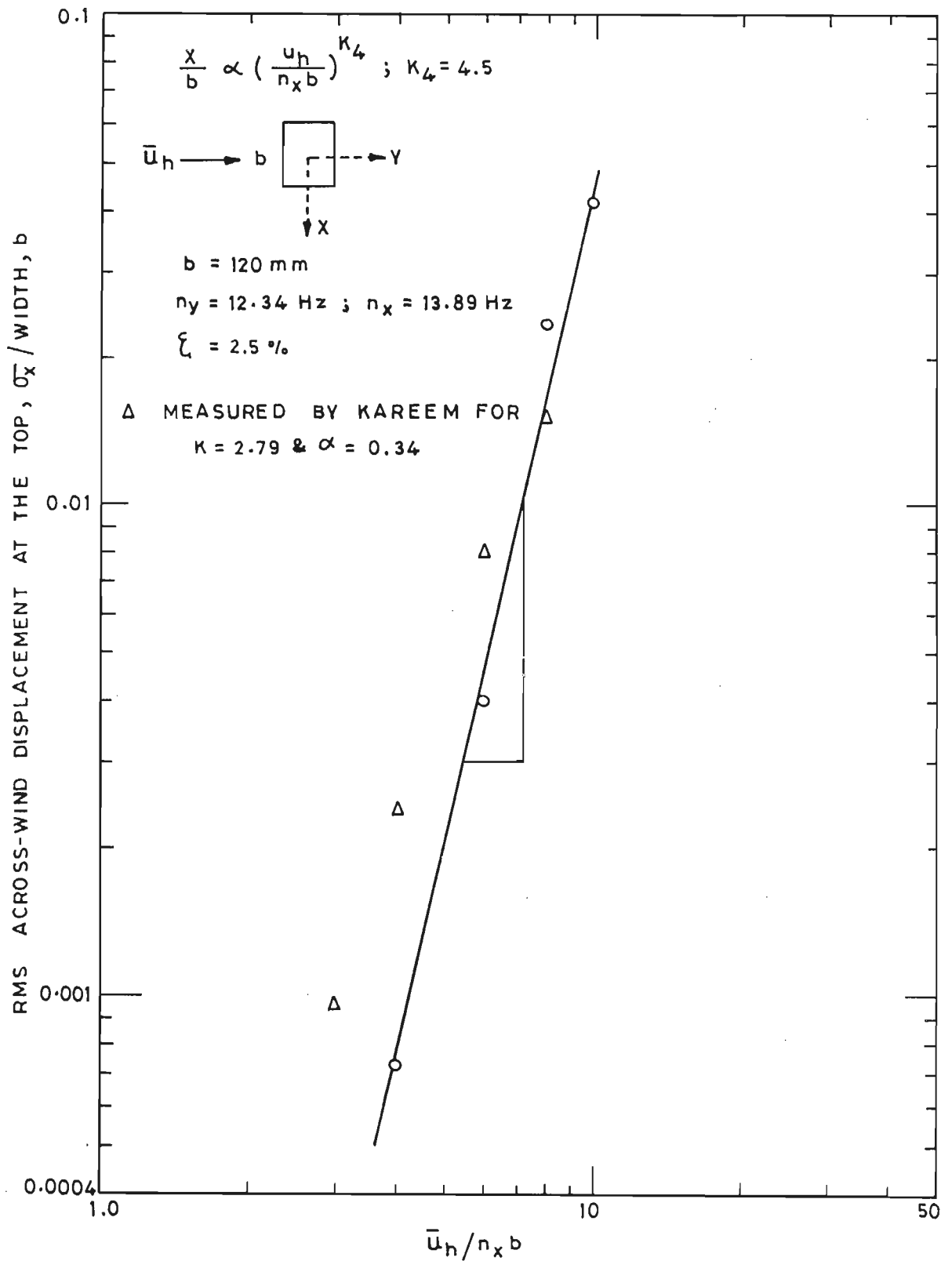


Fig. 5.12 Variation of rms Across-Wind Response of Aeroelastic Model (Short Afterbody)

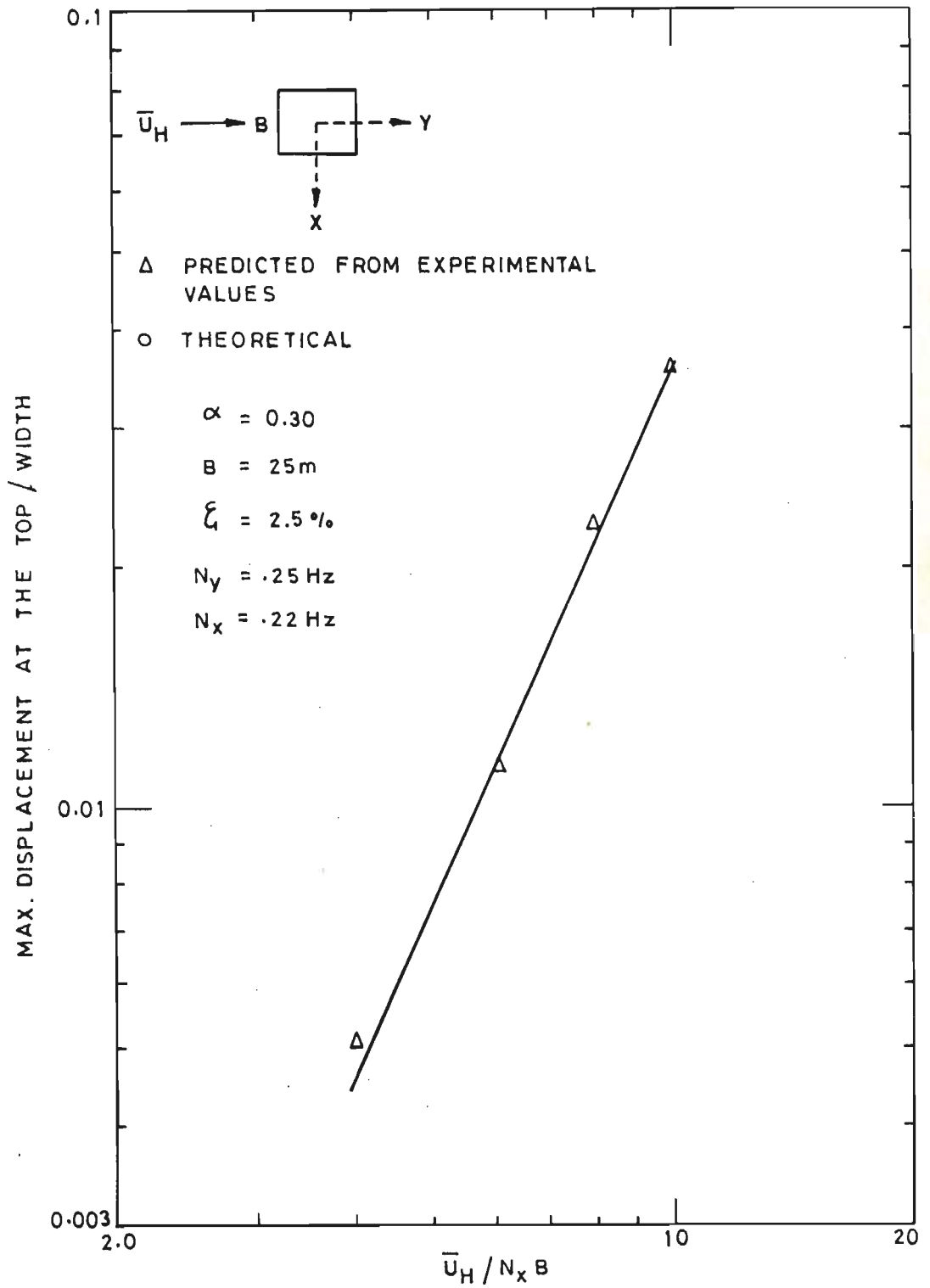


Fig. 5.13 Along-Wind Displacement (Long-Afterbody)

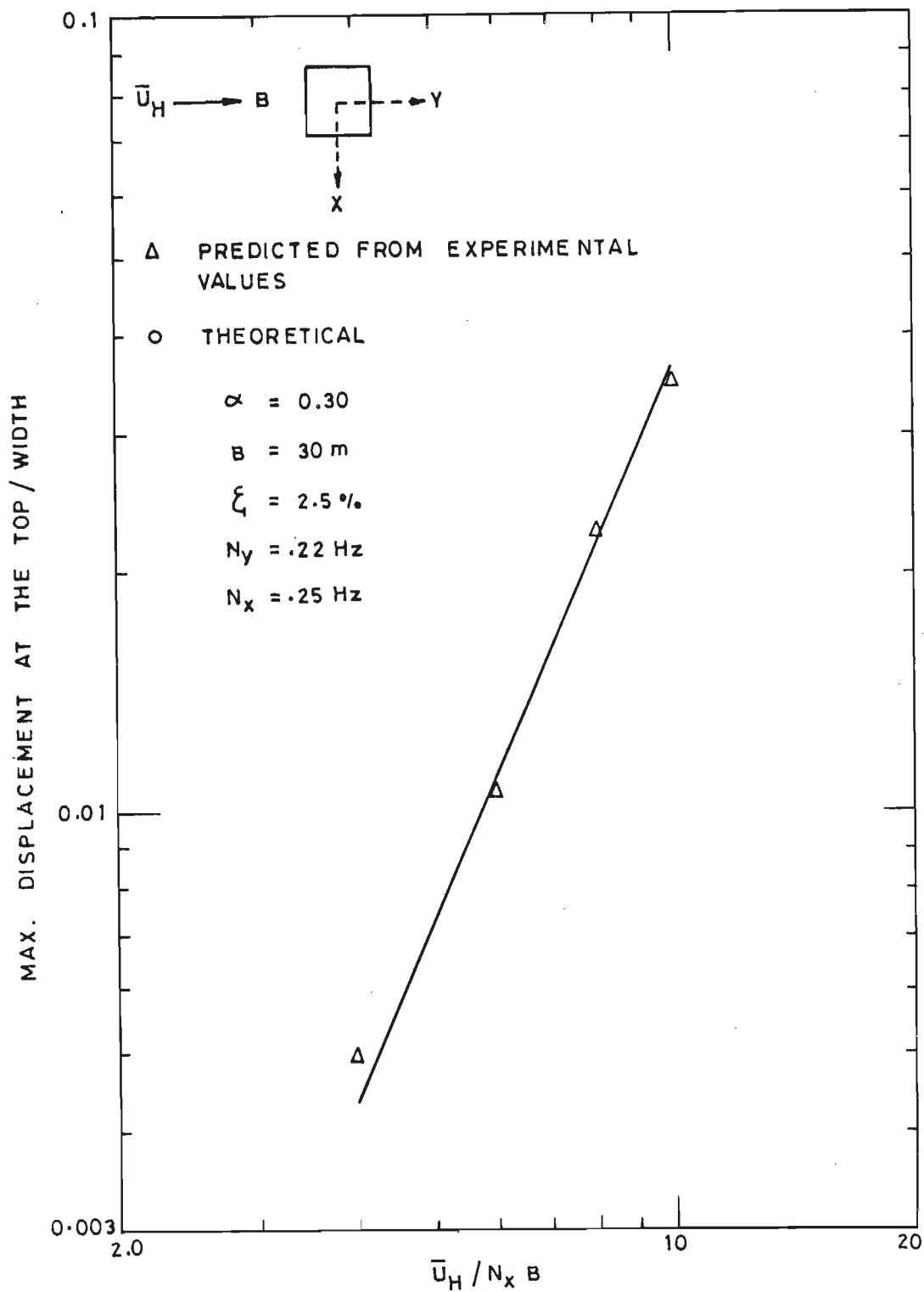


Fig.5.14 Along-Wind Displacement (Short Afterbody)

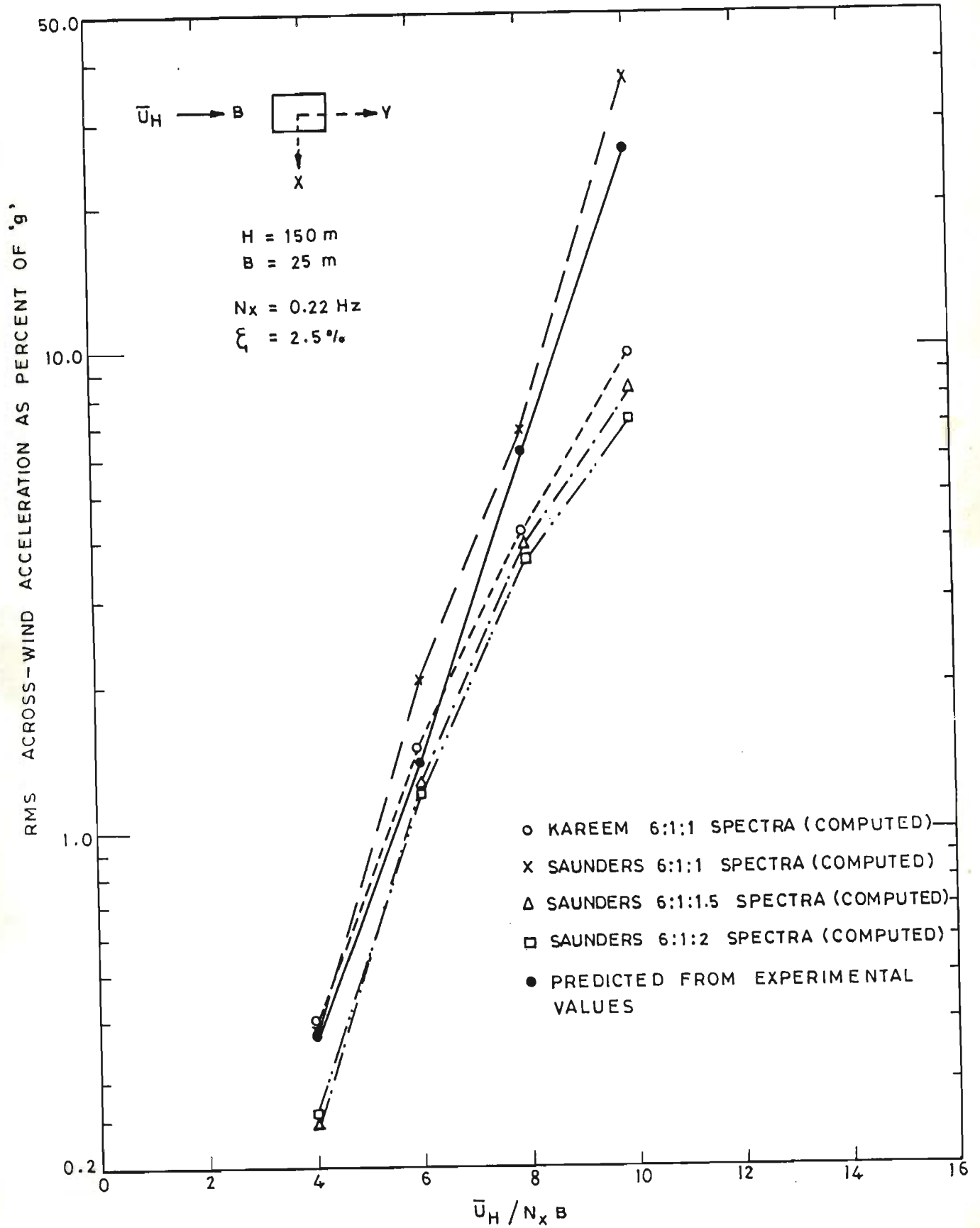


Fig. 5.15 Comparison of Across-Wind Response of Long Afterbody Building

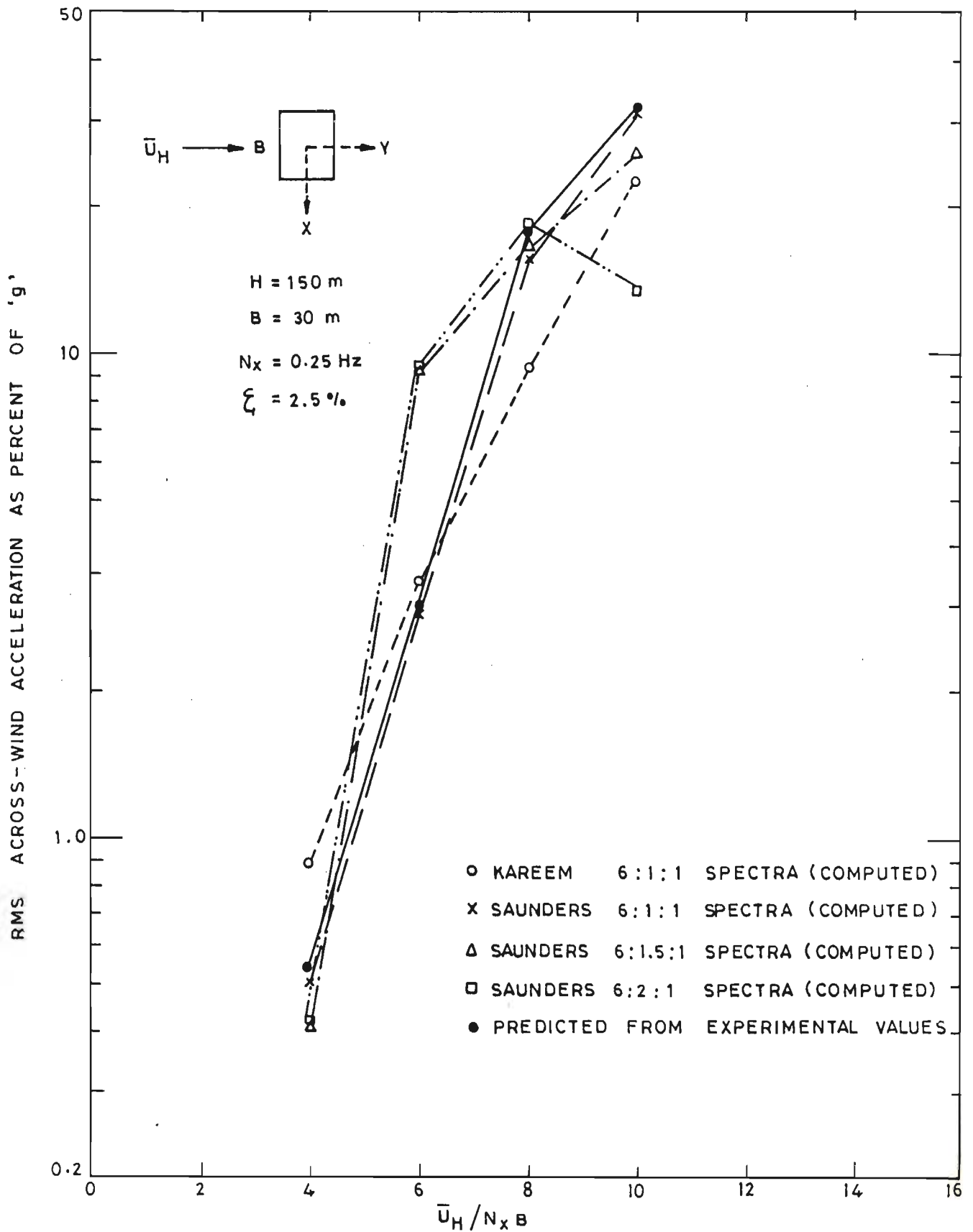


Fig.5.16 Comparison of Across-Wind Response of Short Afterbody Building

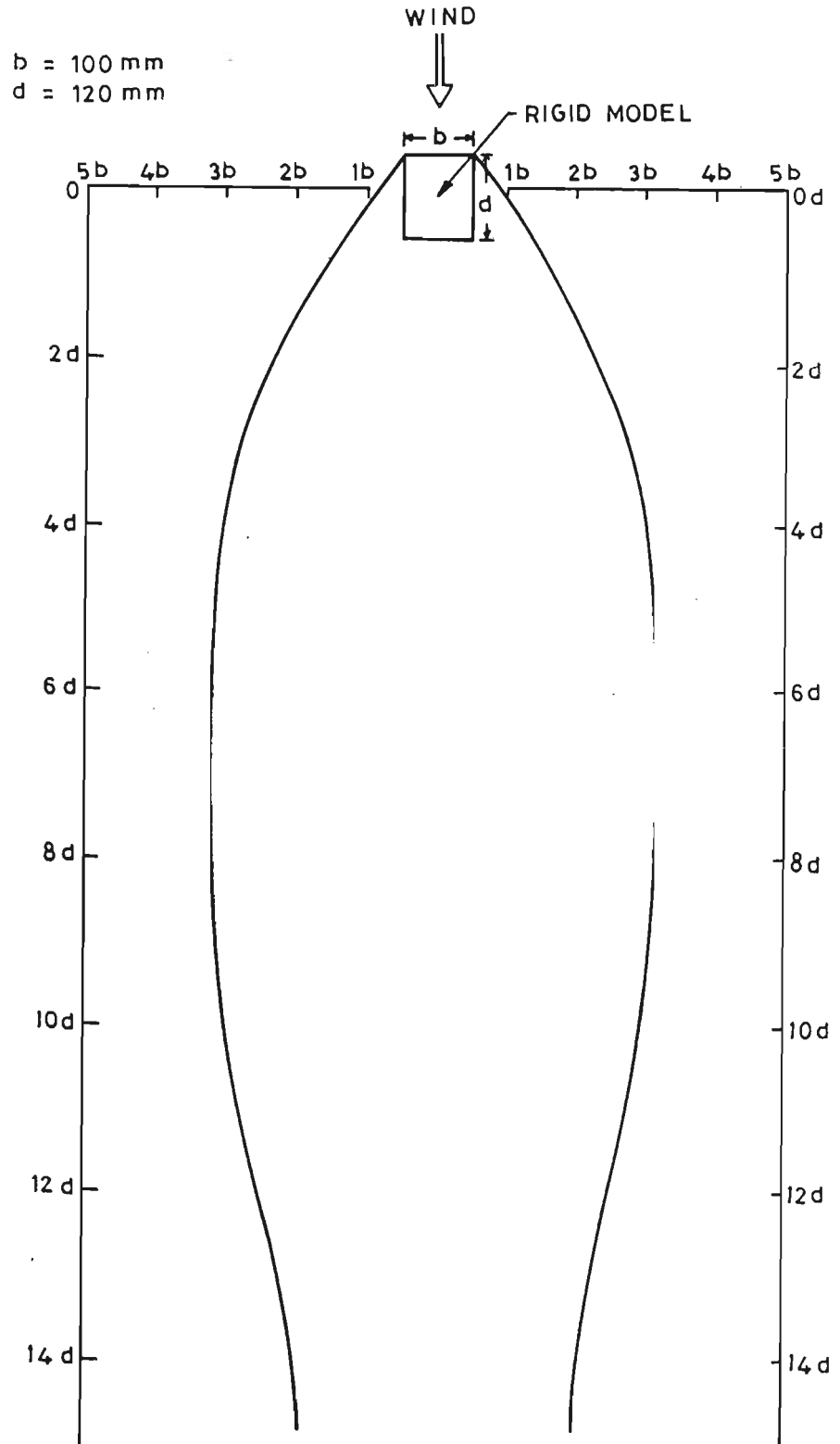
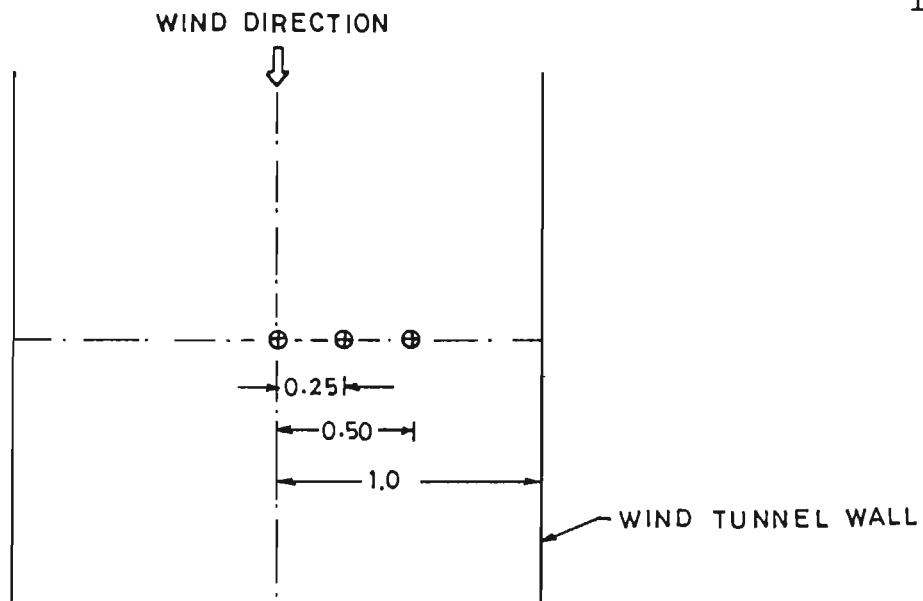
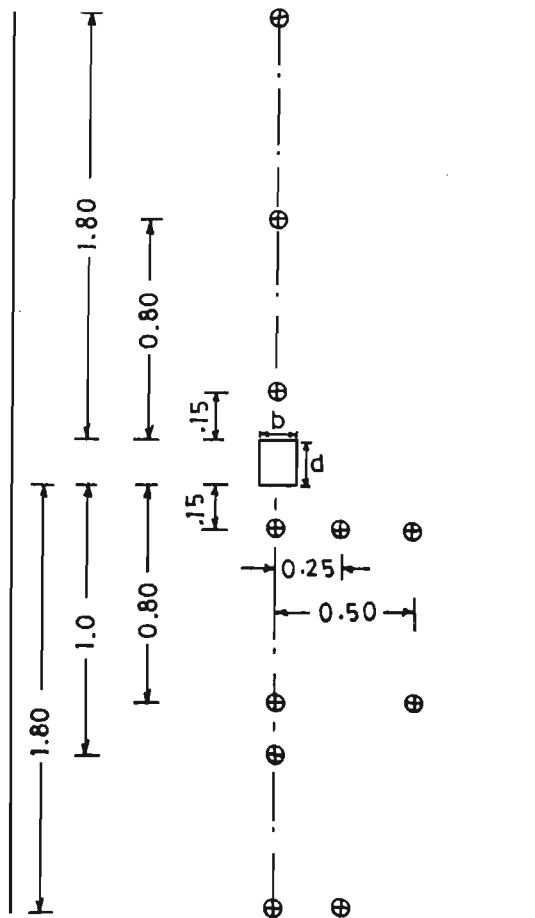


Fig. 6.1 Mean Wake Boundary Behind Building Model



(a) FREE STREAM

⊕ POSITION OF HOT WIRE PROBE IN PLAN



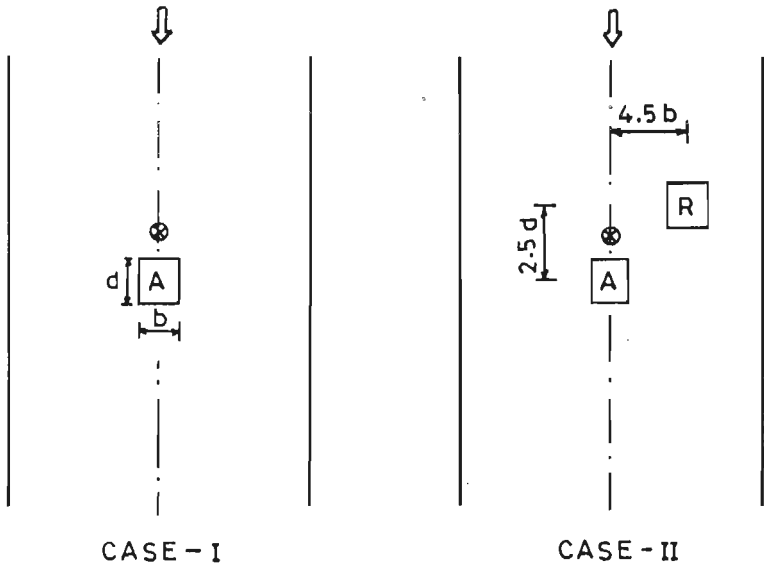
$b = 0.10 \text{ m}$

$d = 0.12 \text{ m}$

(b) WITH THE MODEL

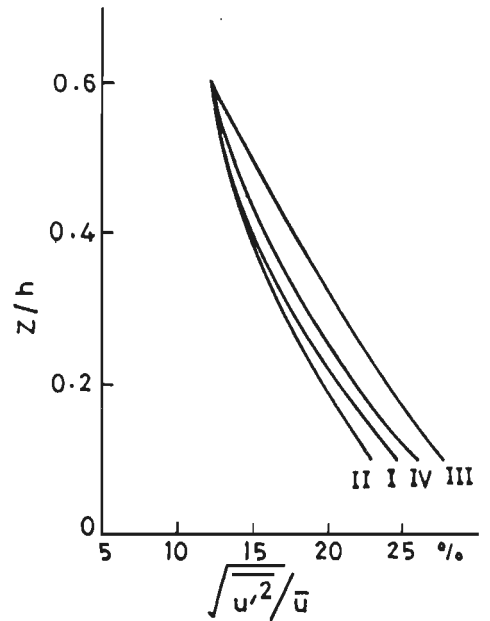
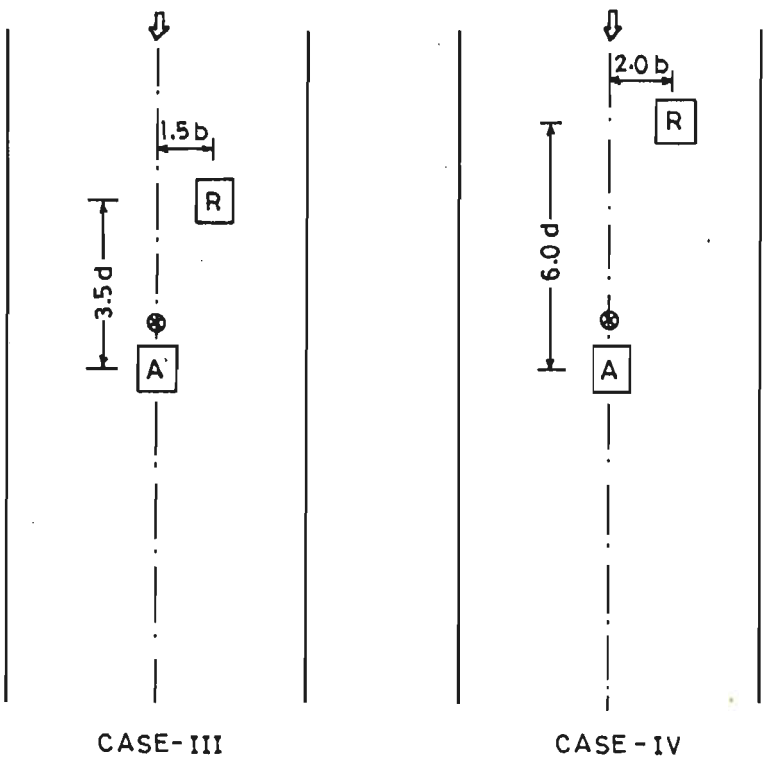
ALL DIMENSIONS IN METER (NOT TO THE SCALE)

Fig.6.2 Position of Hot Wire Anemometer in Turbulence Intensity Measurements



A AEROELASTIC MODEL  
 R RIGID MODEL  
 ⊕ POSITION OF HOT WIRE PROBE IN PLAN

$b = 0.10 \text{ m}$   
 $d = 0.12 \text{ m}$   
 $h = 0.60 \text{ m}$



(DIMENSIONS NOT TO THE SCALE)

Fig. 6.3 Turbulence Intensity Measurements in Some Typical Interference Case



$h = 600 \text{ mm}$   
 $d = 120 \text{ mm}$   
 $b = 100 \text{ mm}$   
 $\alpha = 0.30$

$U_r = 4, 6, 8, 10$

● POSITION OF AEROELASTIC MODEL

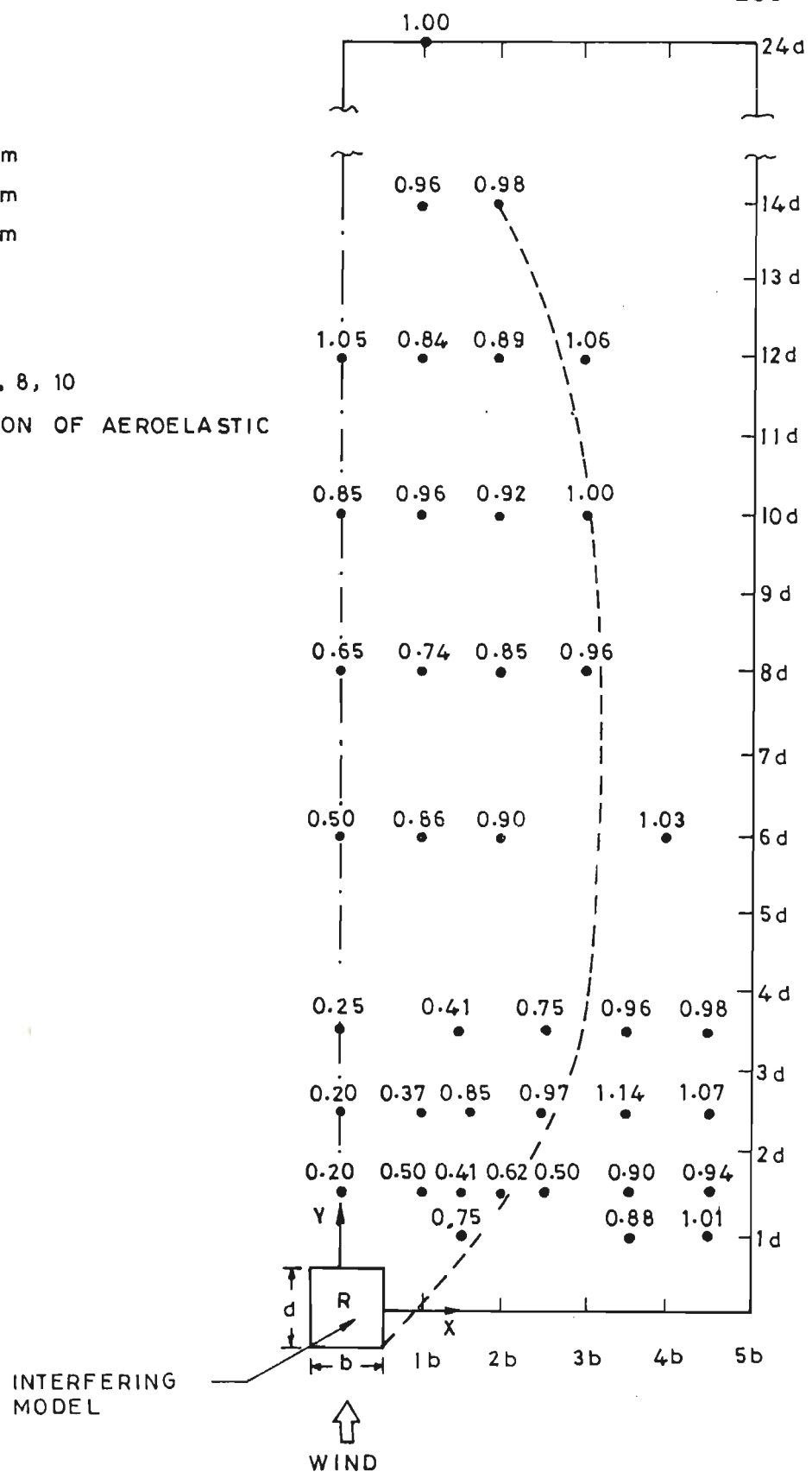


Fig.6.4 Maximum Buffeting Factors for Mean Along-Wind Displacement

$h = 600 \text{ mm}$   
 $d = 120 \text{ mm}$   
 $b = 100 \text{ mm}$   
 $\alpha = 0.30$

$U_r = 4, 6, 8, 10$

● POSITION OF AEROELASTIC MODEL

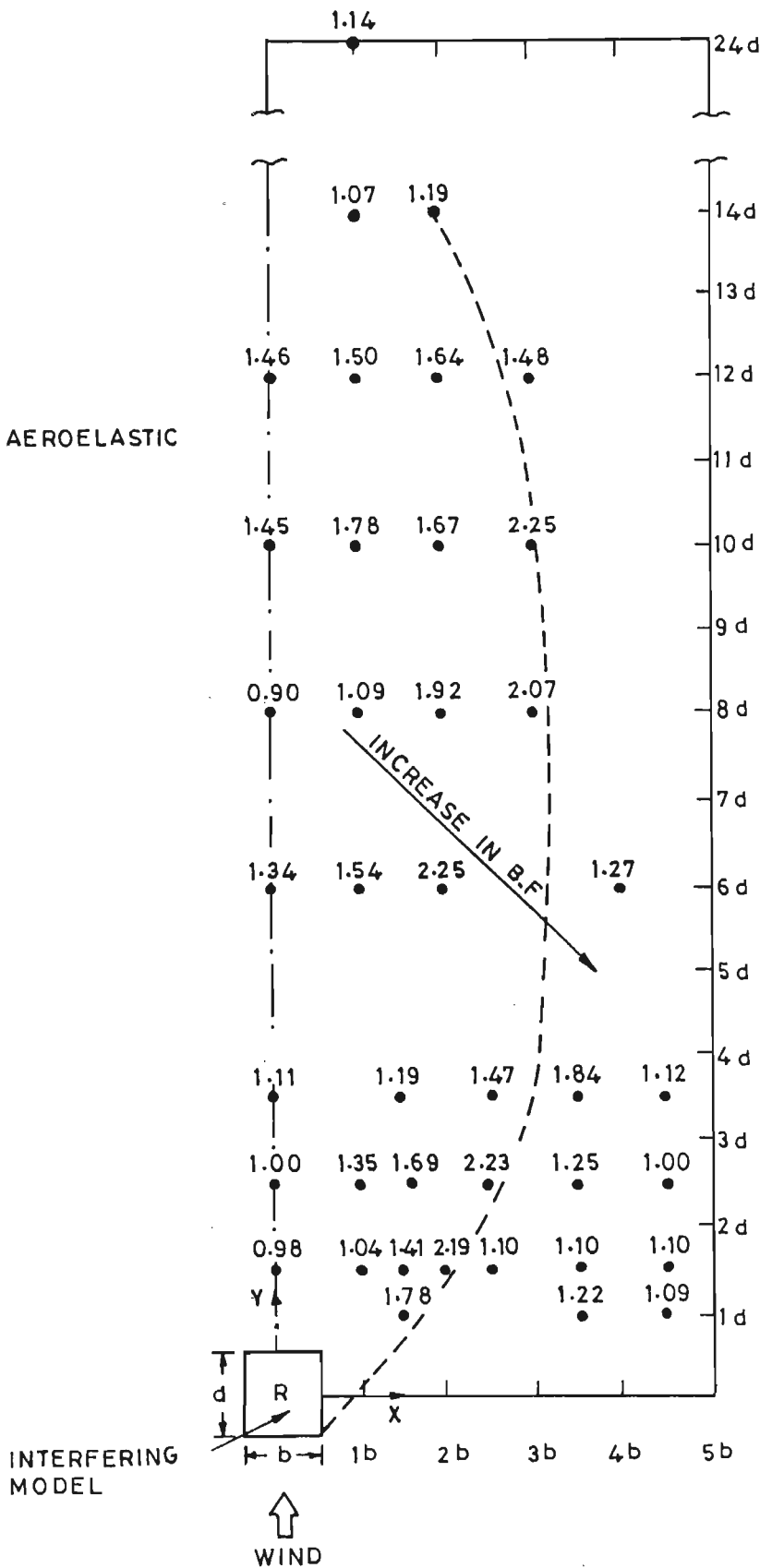


Fig.6.5 Maximum Buffeting Factors for Along-Wind Peak Fluctuating Component of Displacement

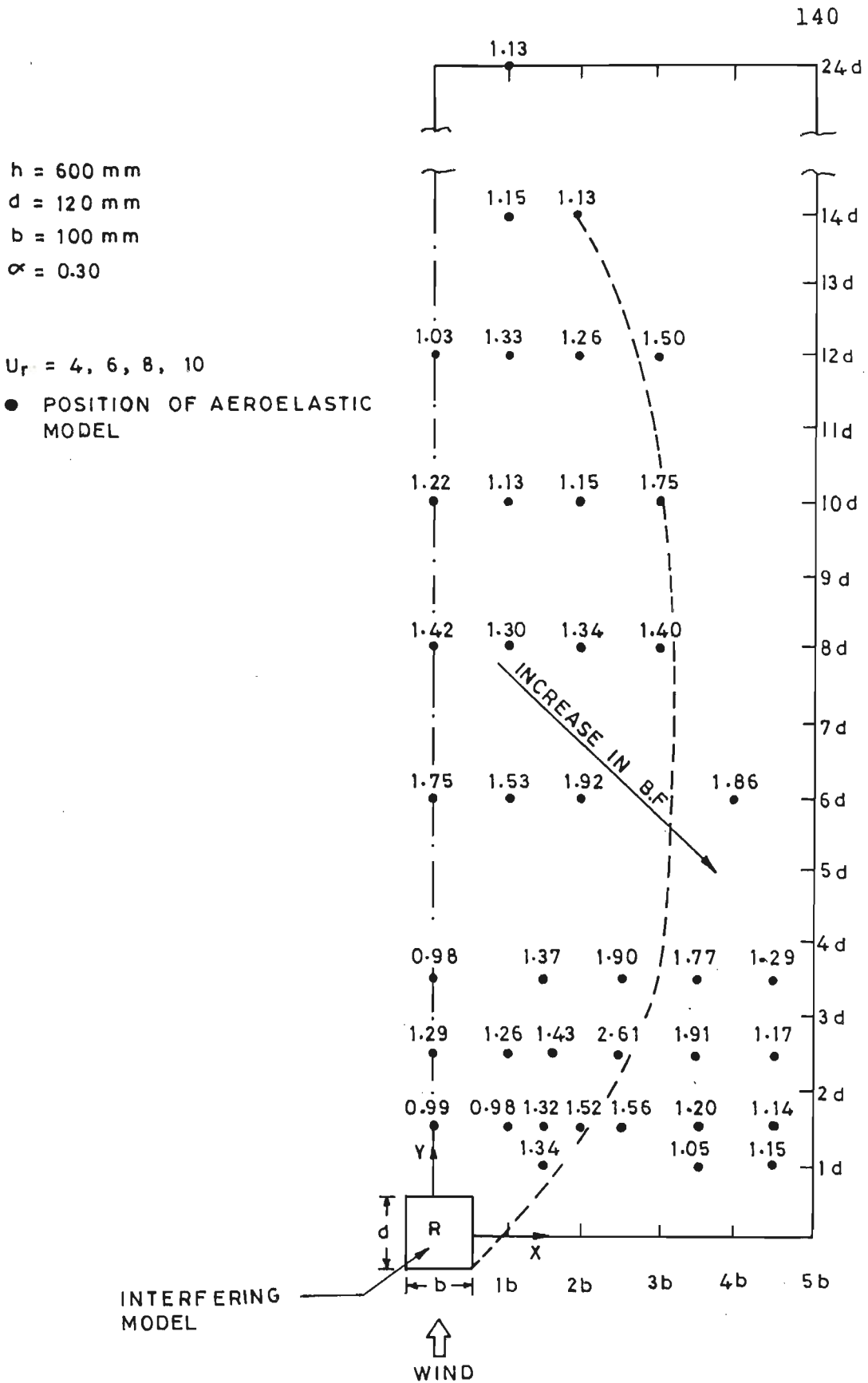


Fig.6.6 Maximum Buffeting Factors for Across-Wind Peak Fluctuating Component of Displacement

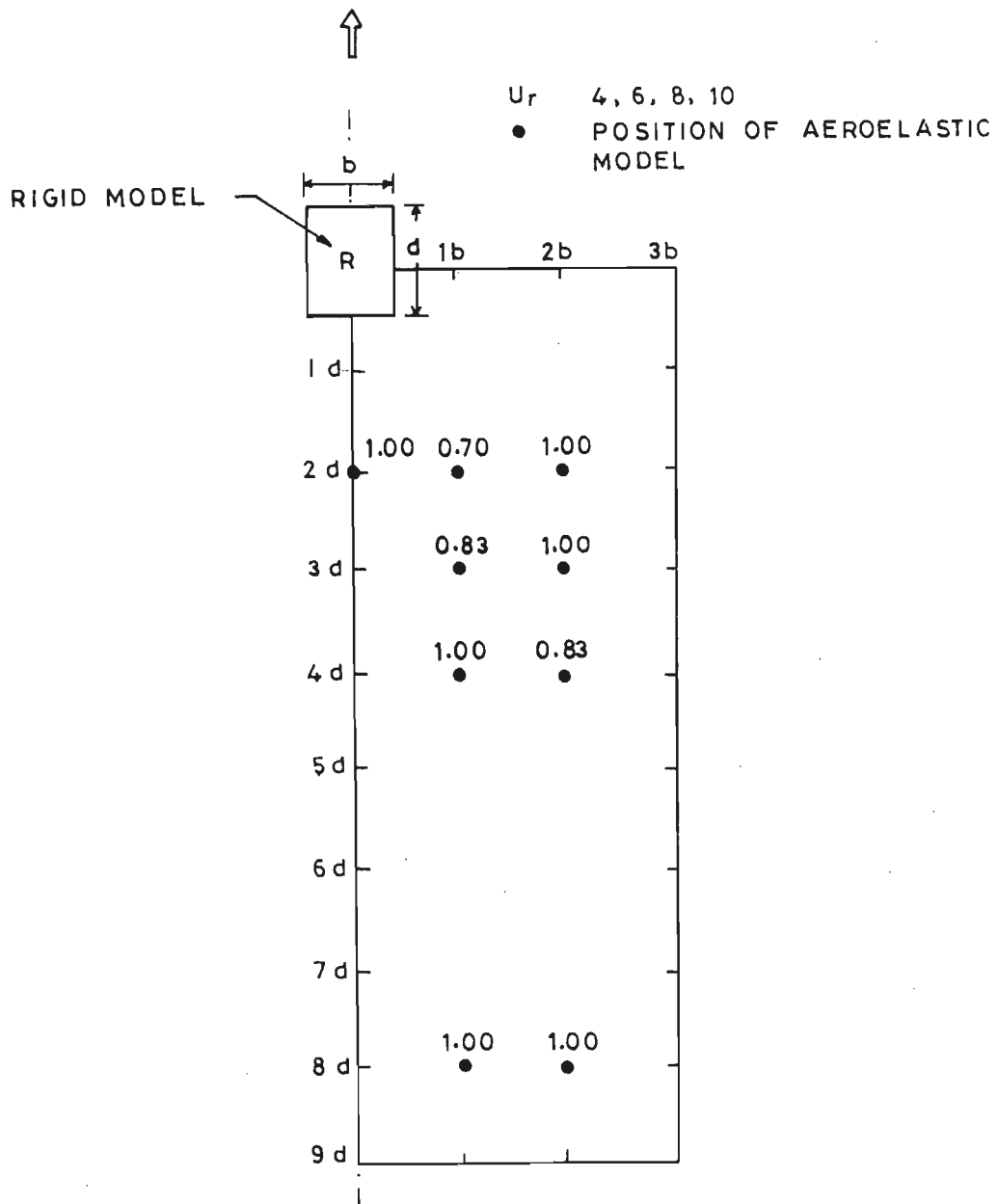


Fig.6.7 Maximum Buffeting Factors for Along-Wind Mean Response (Interfering Building Downstream)

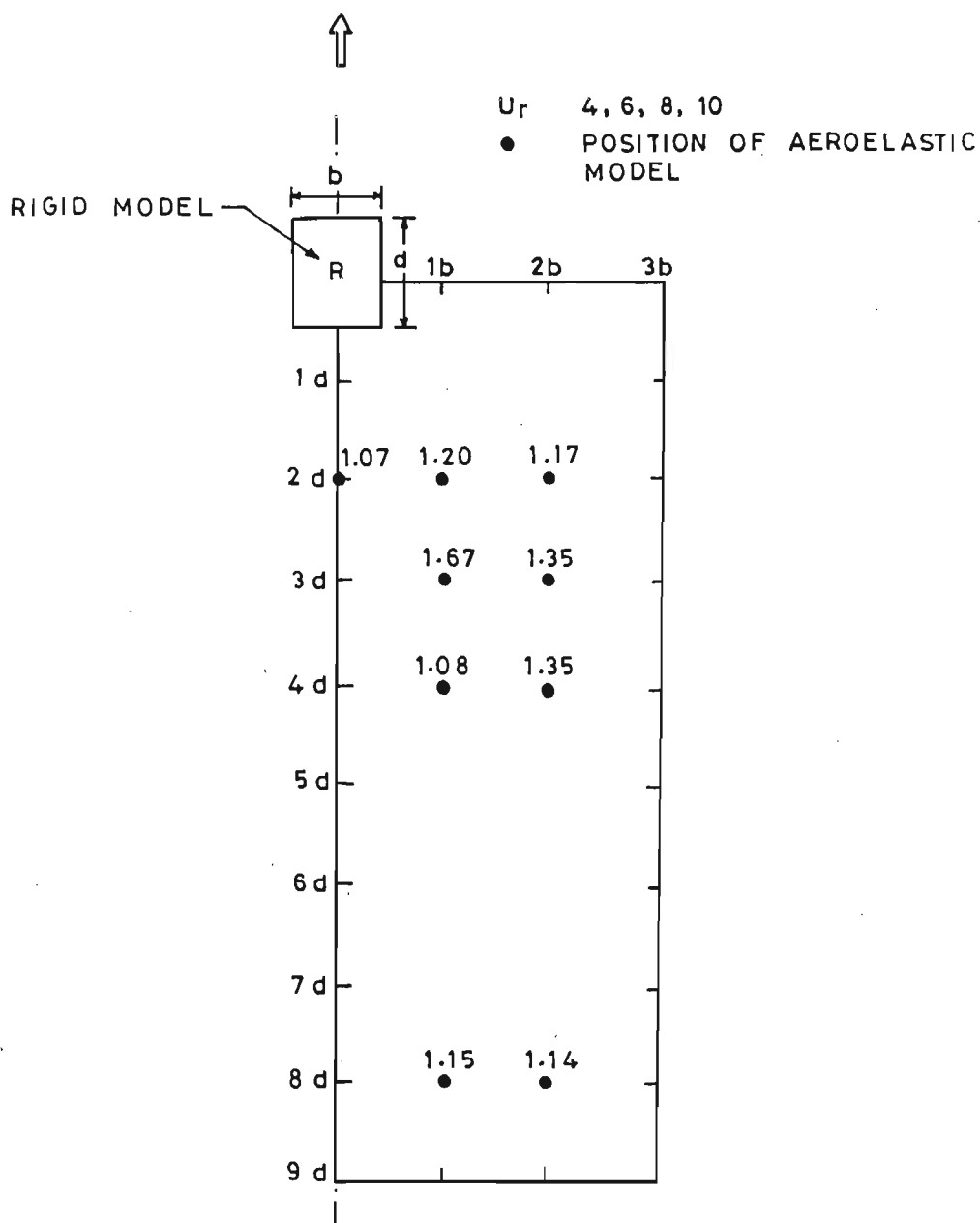


Fig. 6.8 Maximum Buffeting Factors for Along-Wind Peak Response (Interfering Building Downstream)

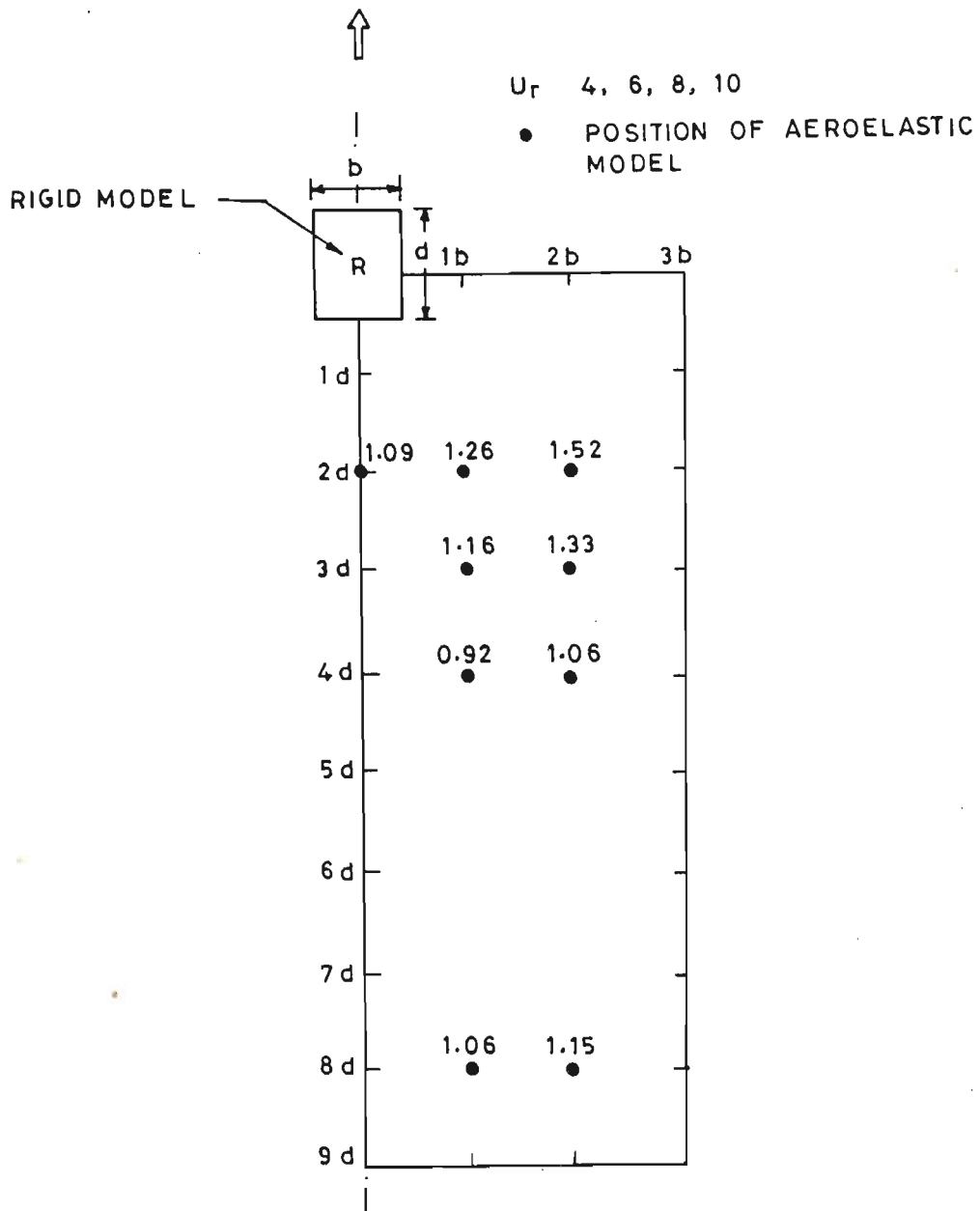


Fig.6.9 Maximum Buffeting Factors for Across-Wind Peak Response (Interfering Building Downstream)

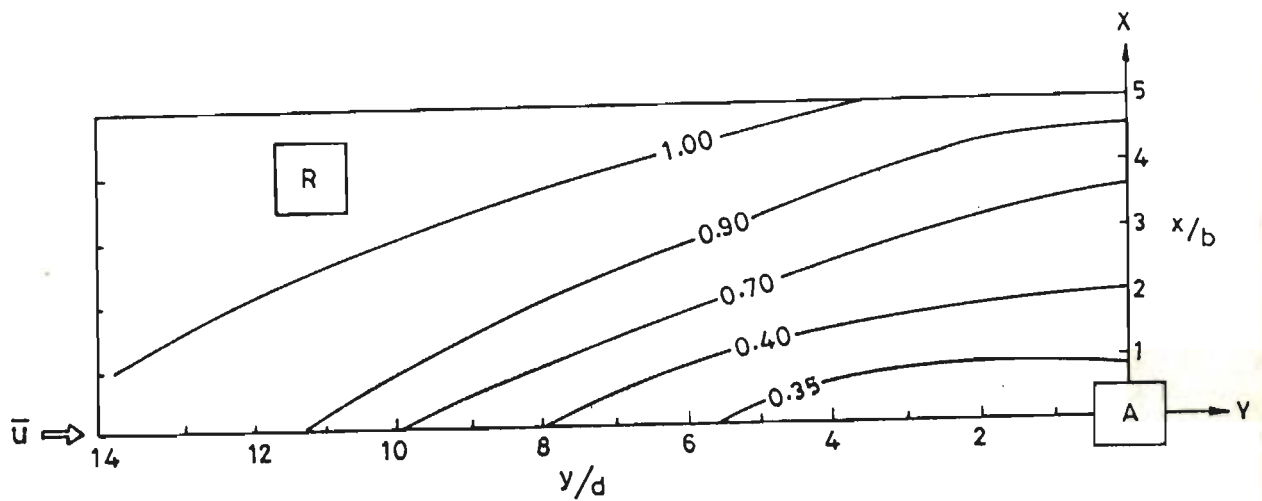


Fig.6.10 Buffeting Factor Contours (Mean Response)  
at  $U_r = 4$

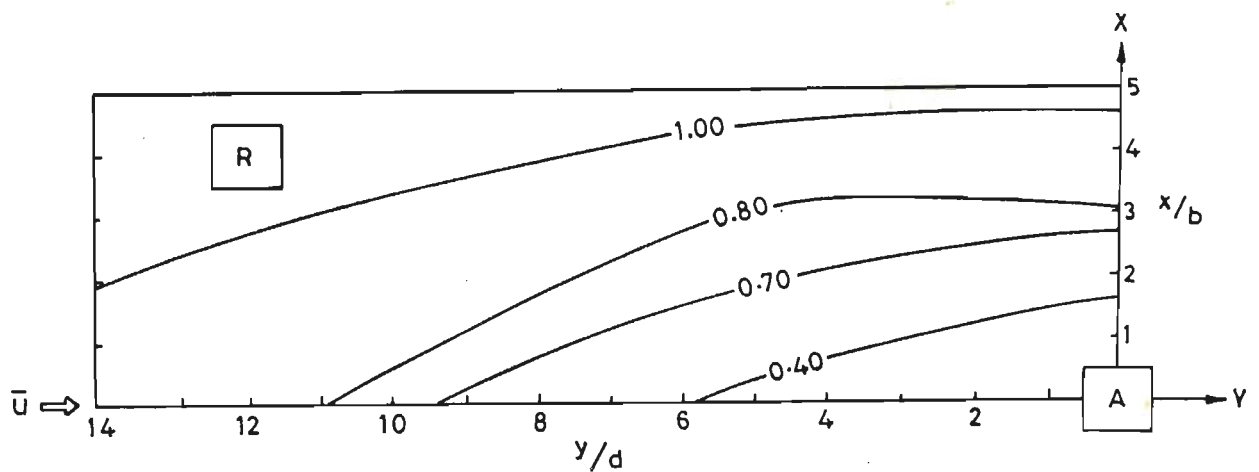


Fig.6.11 Buffeting Factor Contours (Mean Response)  
at  $U_r = 6$

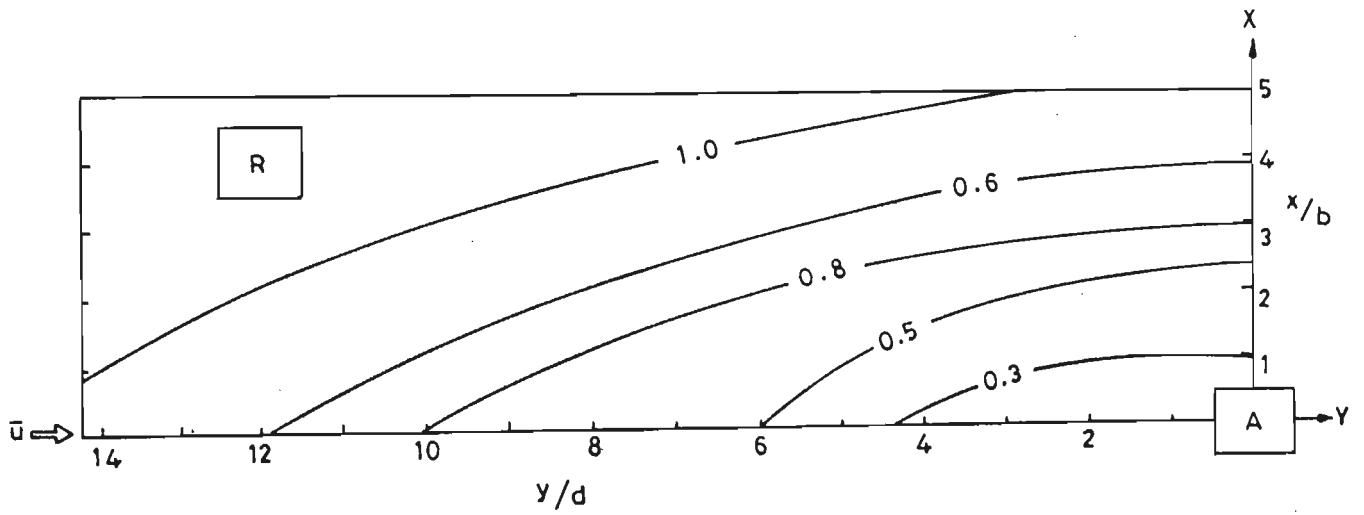


Fig. 6.12 Buffeting Factor Contours (Mean Response)  
at  $U_r = 8$

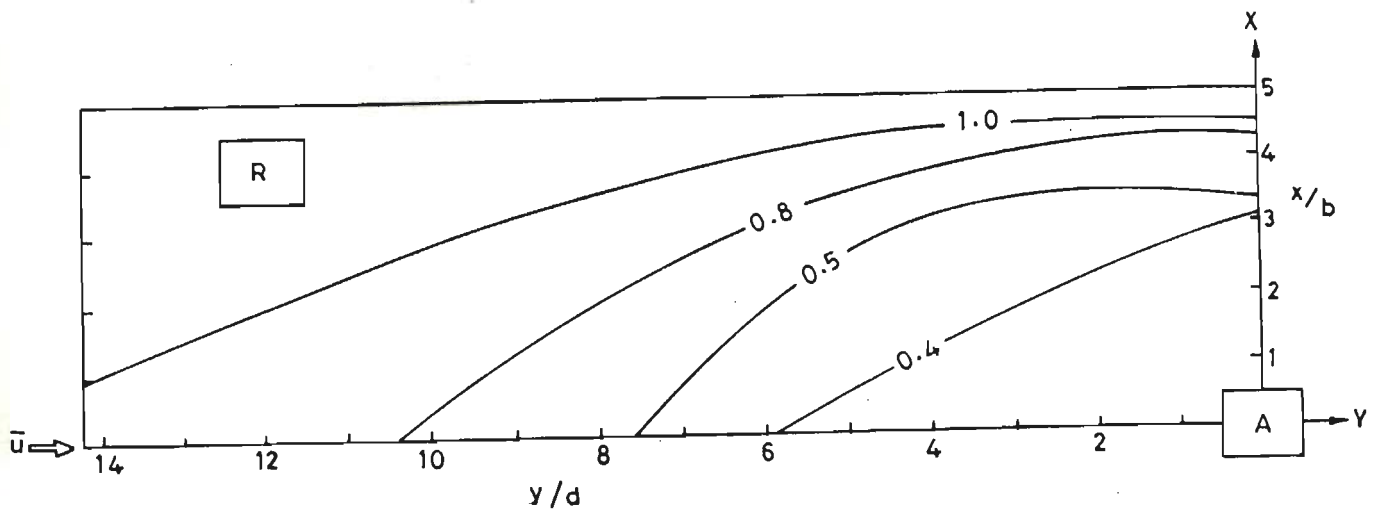
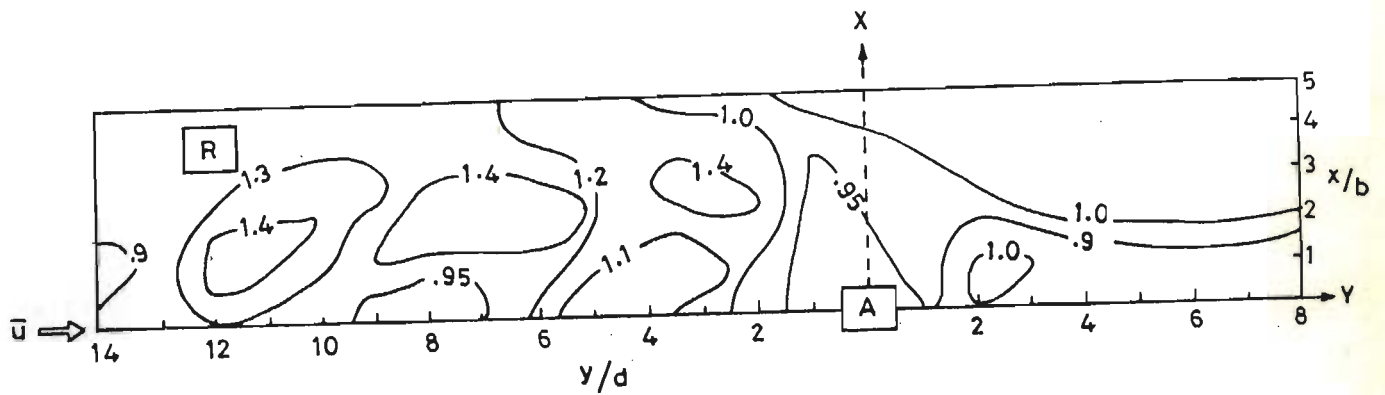
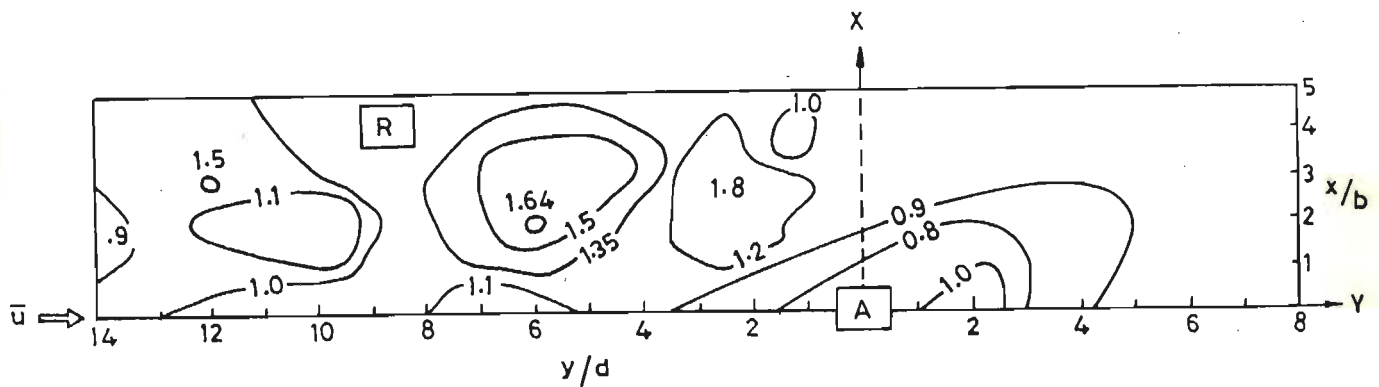


Fig. 6.13 Buffeting Factor Contours (Mean Response)  
at  $U_r = 10$



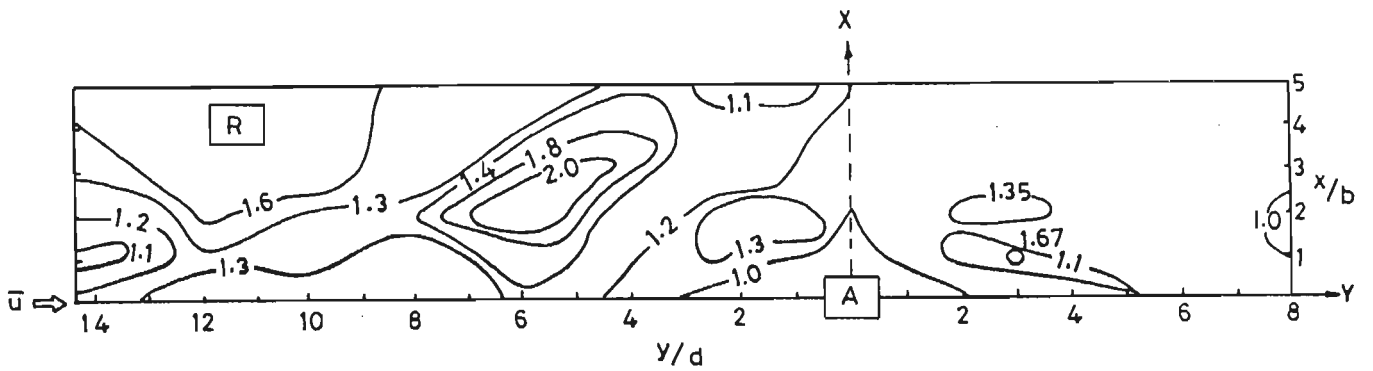


(a) ALONG-WIND

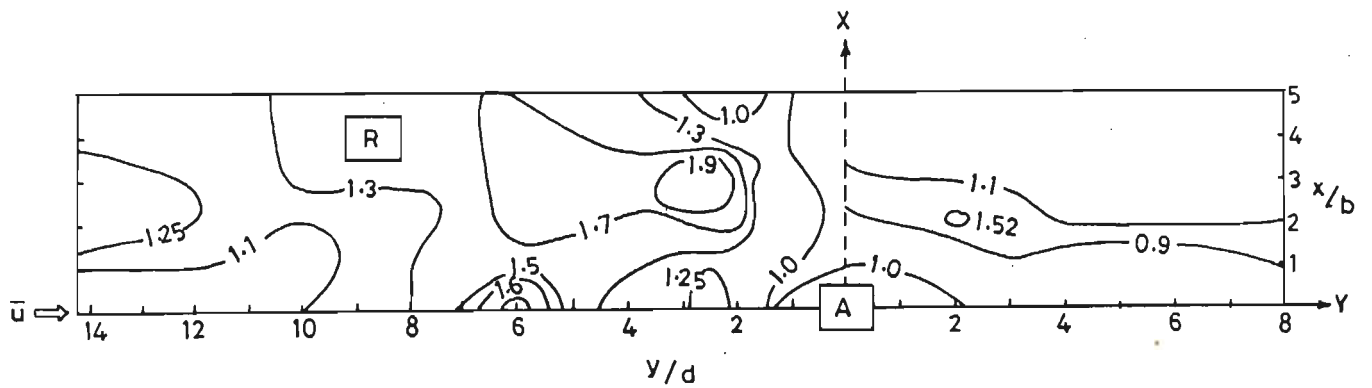


(b) ACROSS-WIND

Fig.6.14 Buffeting Factor Contours (Peak Response)  
at  $U_r = 4$

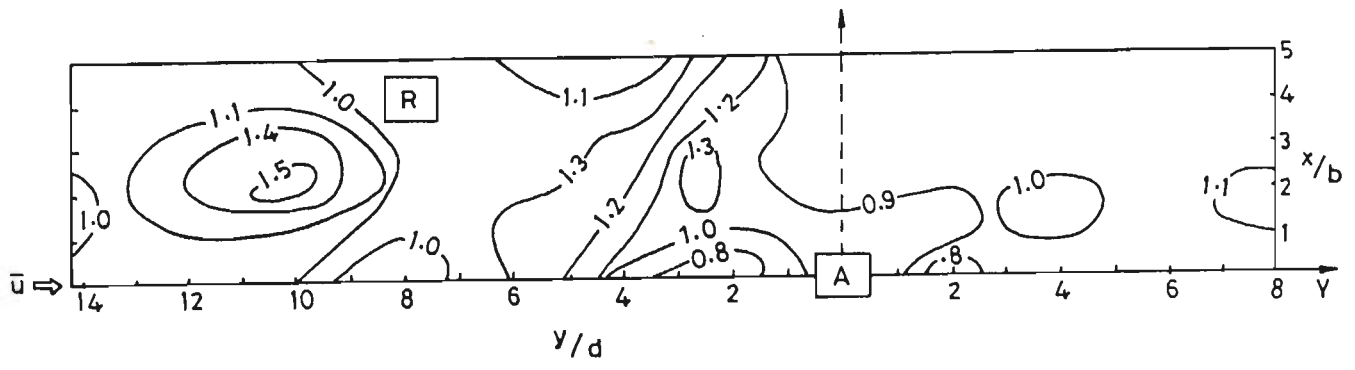


(a) ALONG-WING

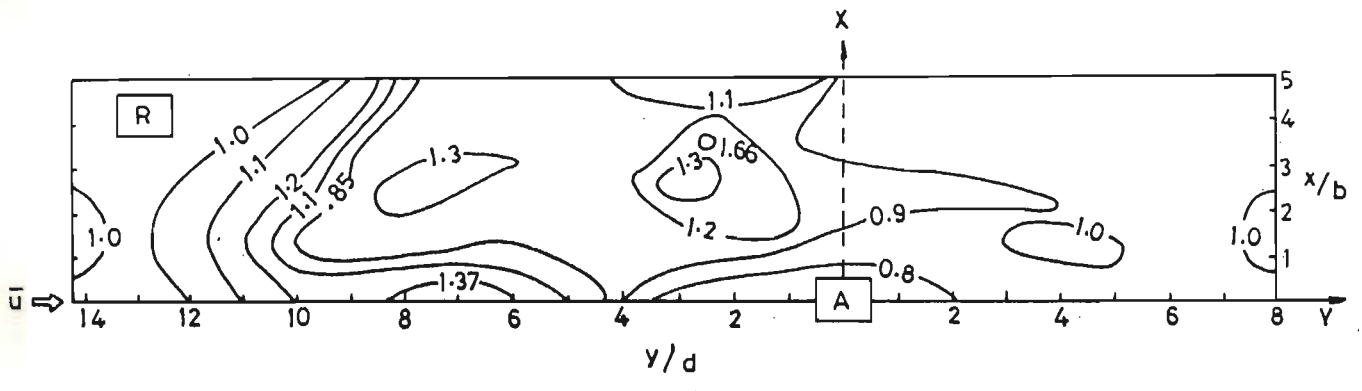


(b) ACROSS-WIND

Fig. 6.15 Buffeting Factor Contours (Peak Response) at  $U_r = 6$

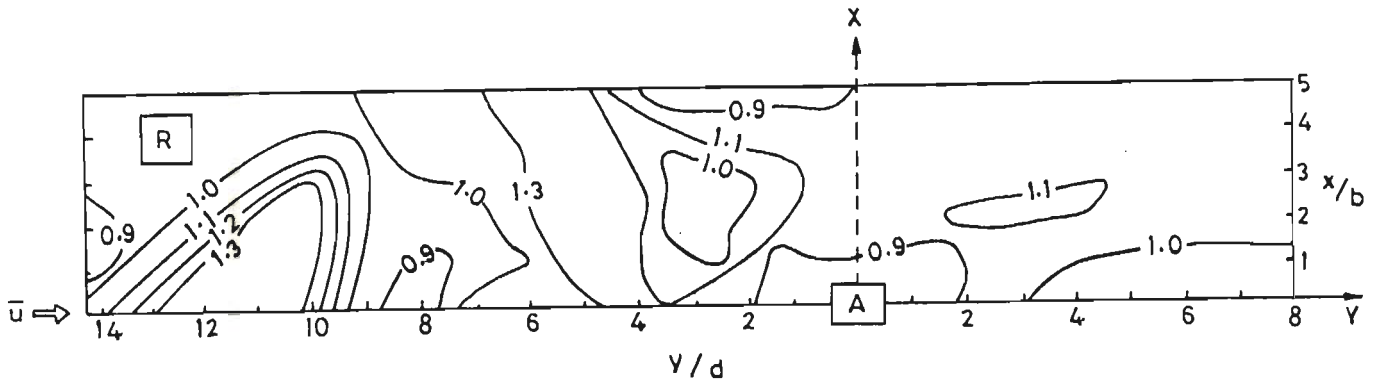


(a) ALONG-WIND

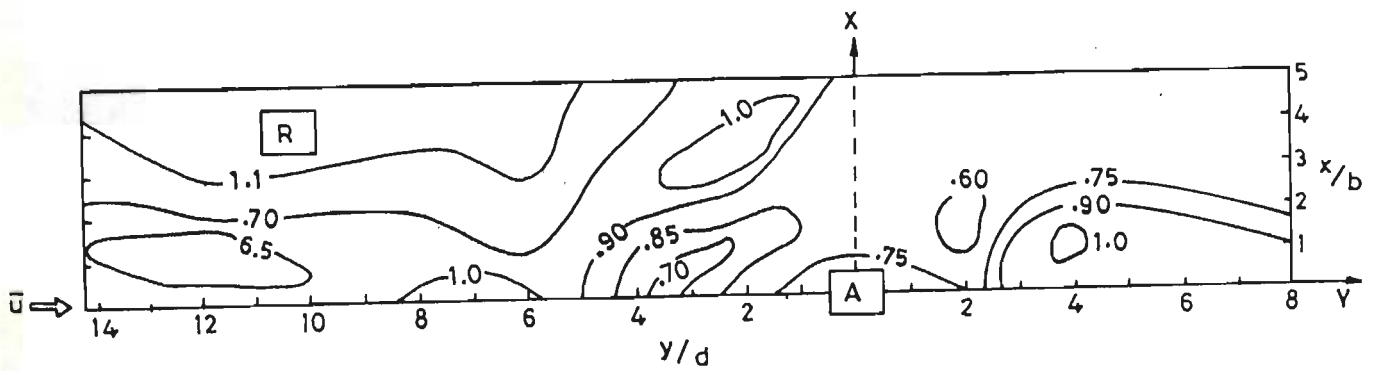


(b) ACROSS-WIND

Fig.6.16 Buffeting Factor Contours (Peak Response) at  $U_r = 8$



(a) ALONG-WIND



(b) ACROSS-WIND

Fig.6.17 Buffeting Factor Contours ( Peak Response )  
at  $U_r=10$

- △ ALONG-WIND (ISOLATED)
- ACROSS-WIND (ISOLATED)
- ▲ ALONG-WIND (INTERFERENCE)
- ACROSS-WIND (INTERFERENCE)

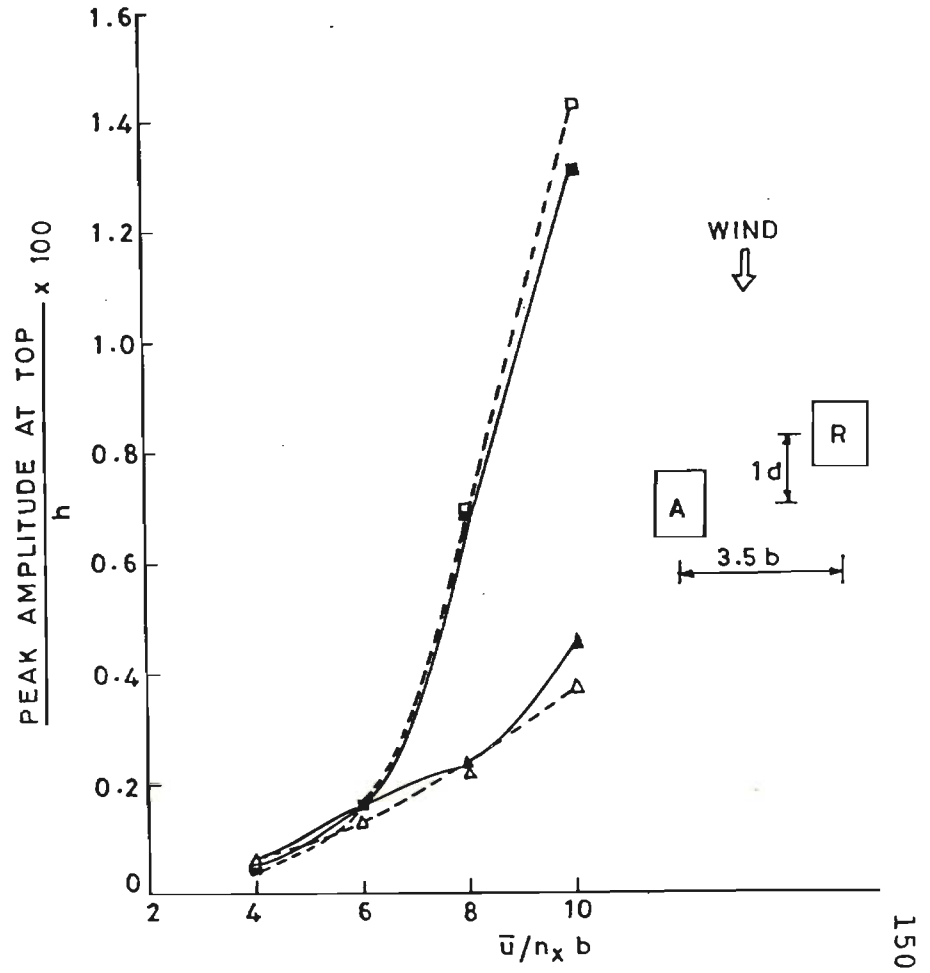
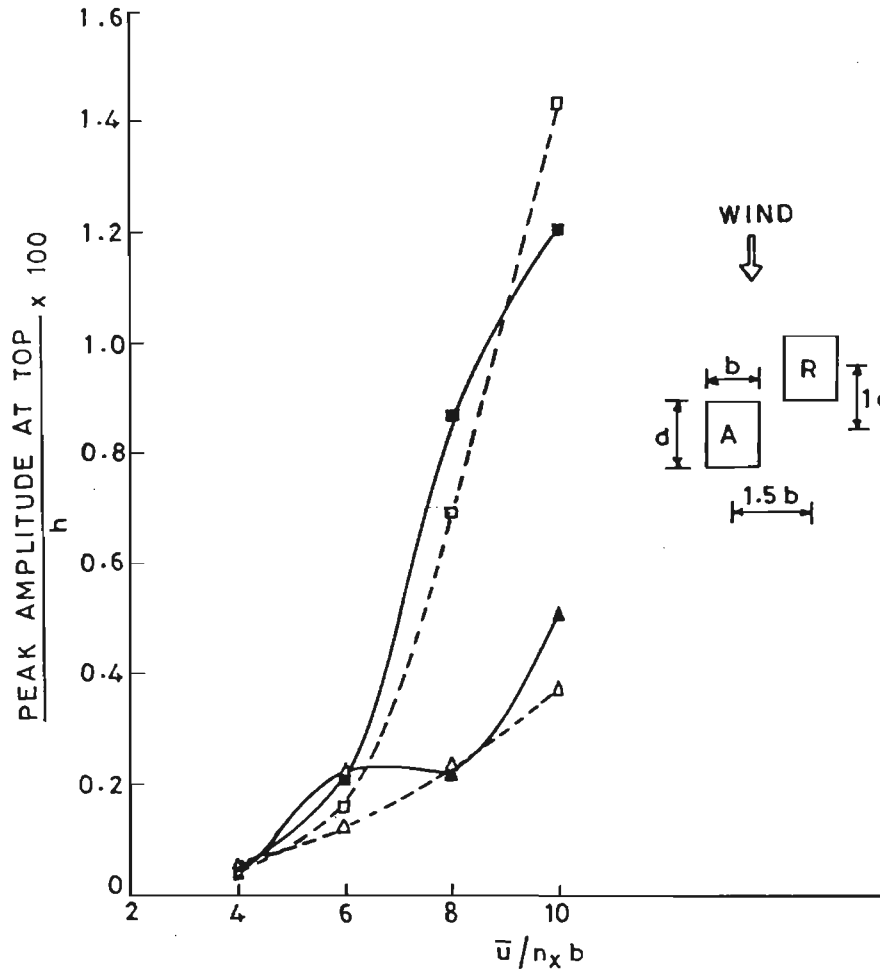


Fig. 6.18 Response of Aeroelastic Model , A

- △ ALONG-WIND (ISOLATED)
- ACROSS-WIND (ISOLATED)
- ▲ ALONG-WIND (INTERFERENCE)
- ACROSS-WIND (INTERFERENCE)

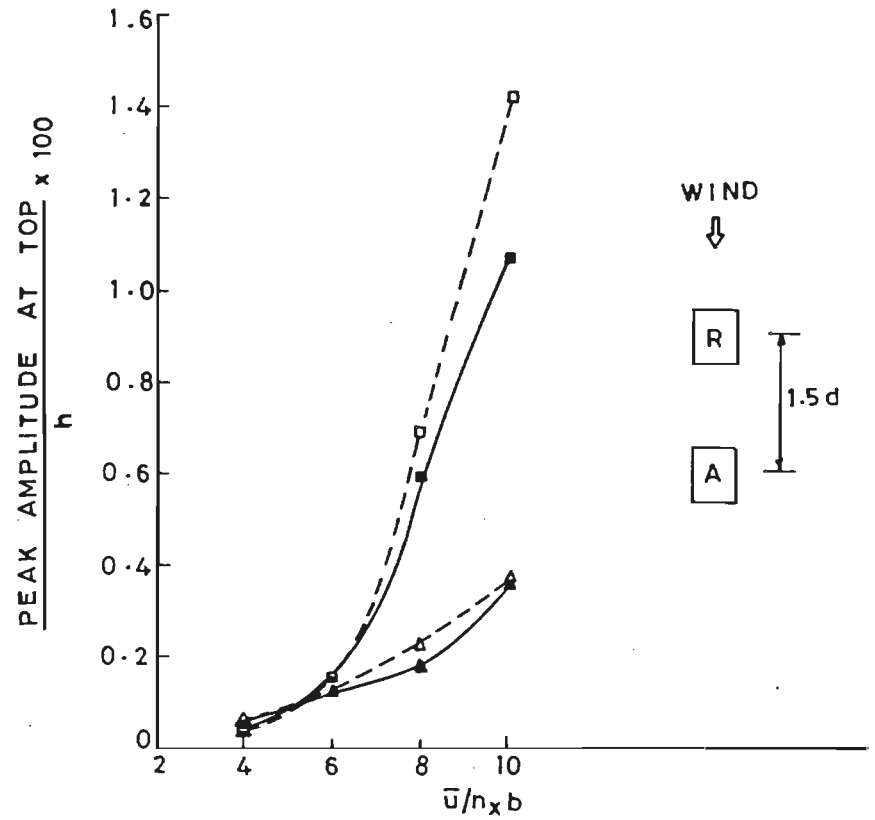
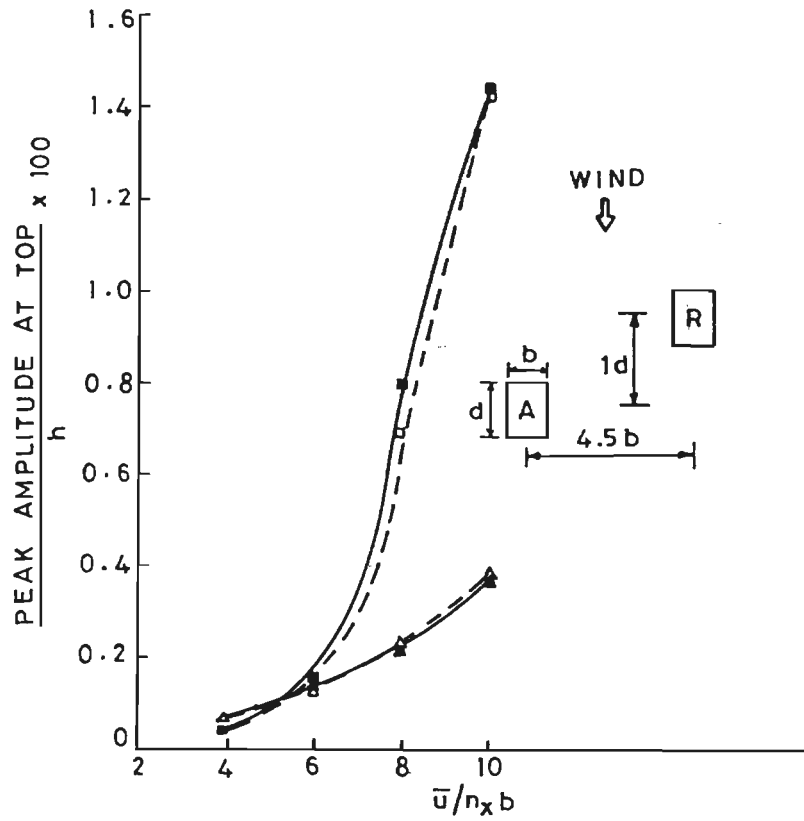


Fig. 6.19 Response of Aeroelastic Model , A

- △ ALONG-WIND (ISOLATED)
- ACROSS-WIND (ISOLATED)
- ▲ ALONG-WIND (INTERFERENCE)
- ACROSS-WIND (INTERFERENCE)

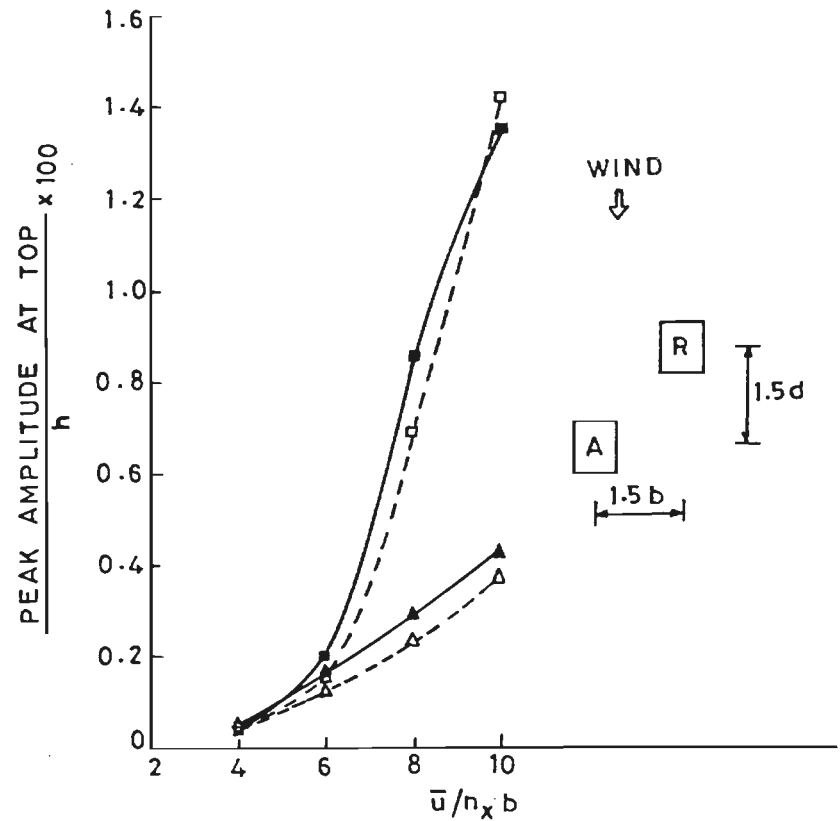
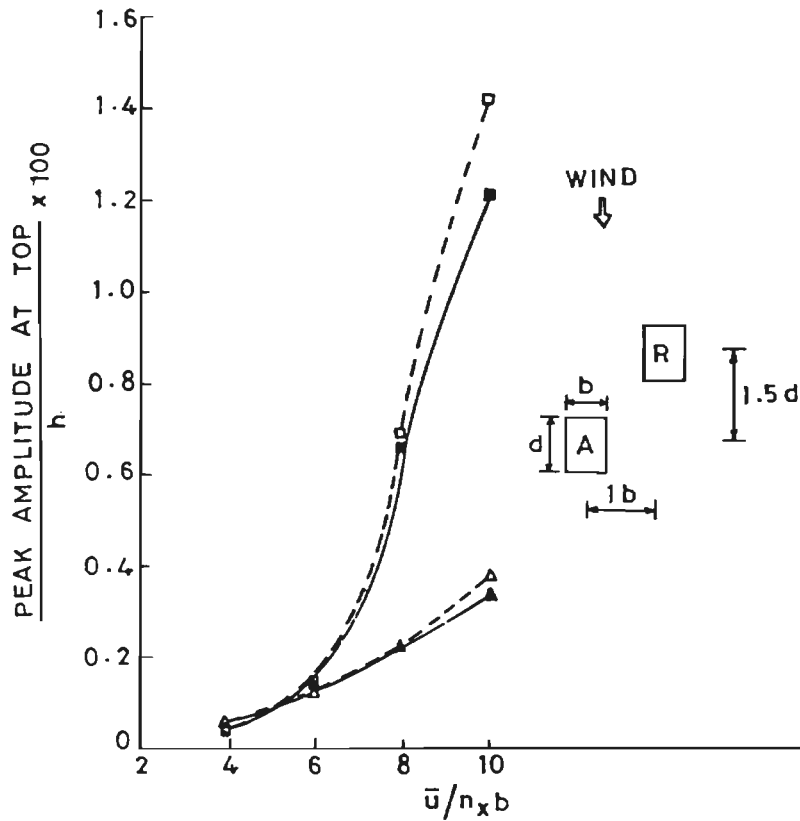


Fig. 6.20 Response of Aeroelastic Model, A

- △ ALONG-WIND (ISOLATED)
- ACROSS-WIND (ISOLATED)
- ▲ ALONG-WIND (INTERFERENCE)
- ACROSS-WIND (INTERFERENCE)

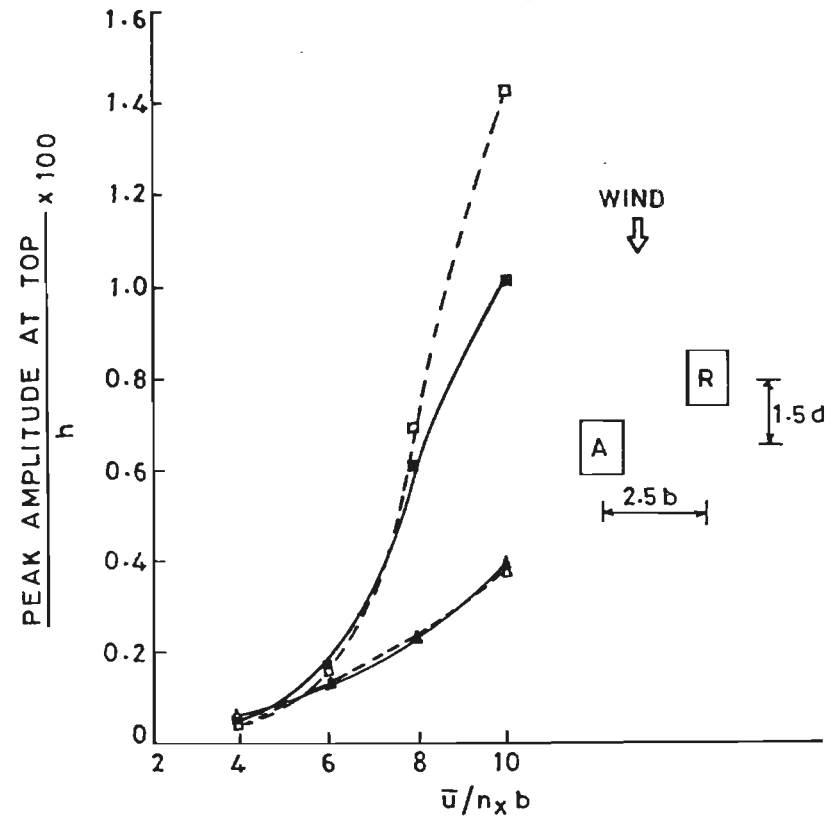
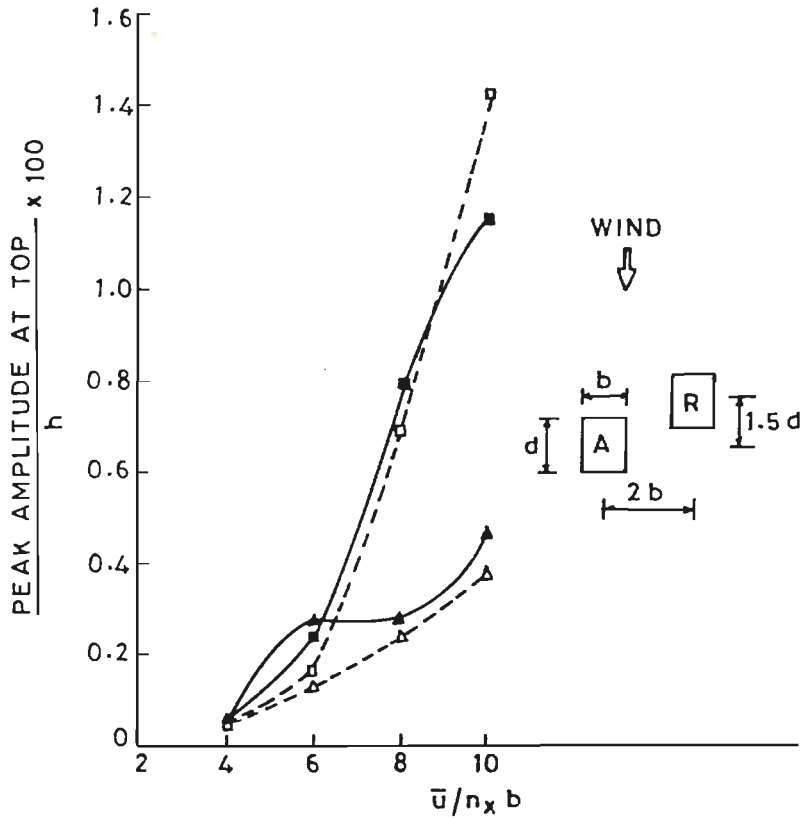


Fig. 6-21 Response of Aeroelastic Model, A



- △ ALONG-WIND (ISOLATED)
- ACROSS-WIND (ISOLATED)
- ▲ ALONG-WIND (INTERFERENCE)
- ACROSS-WIND (INTERFERENCE)

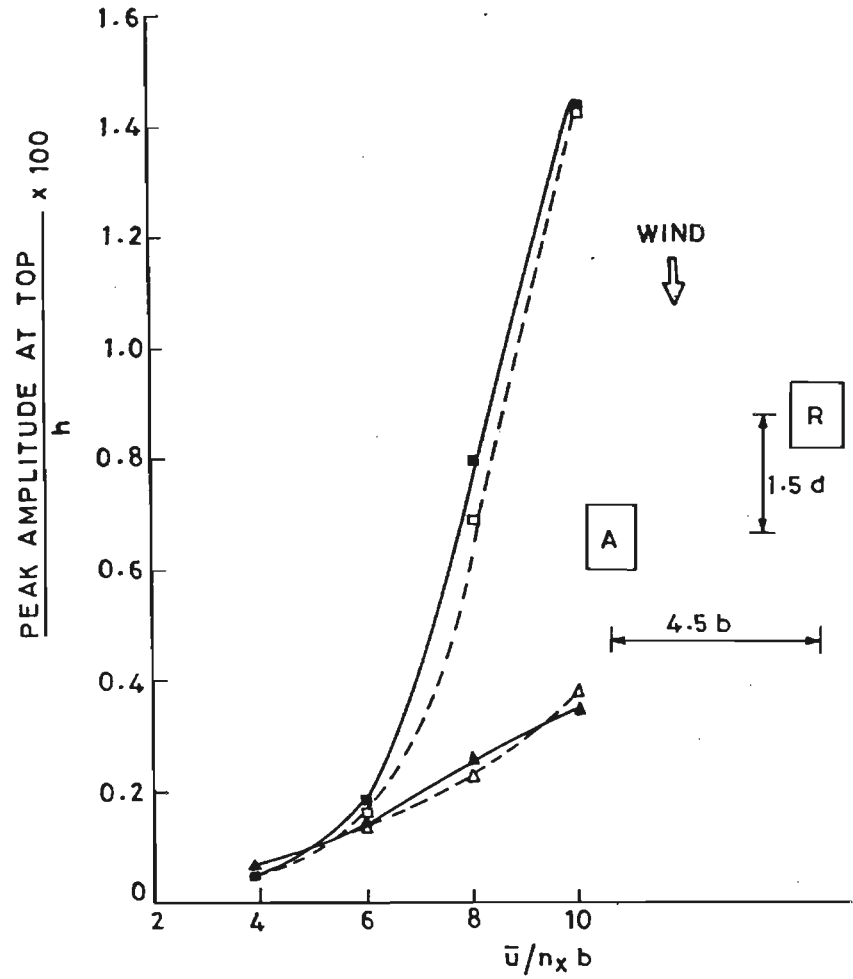
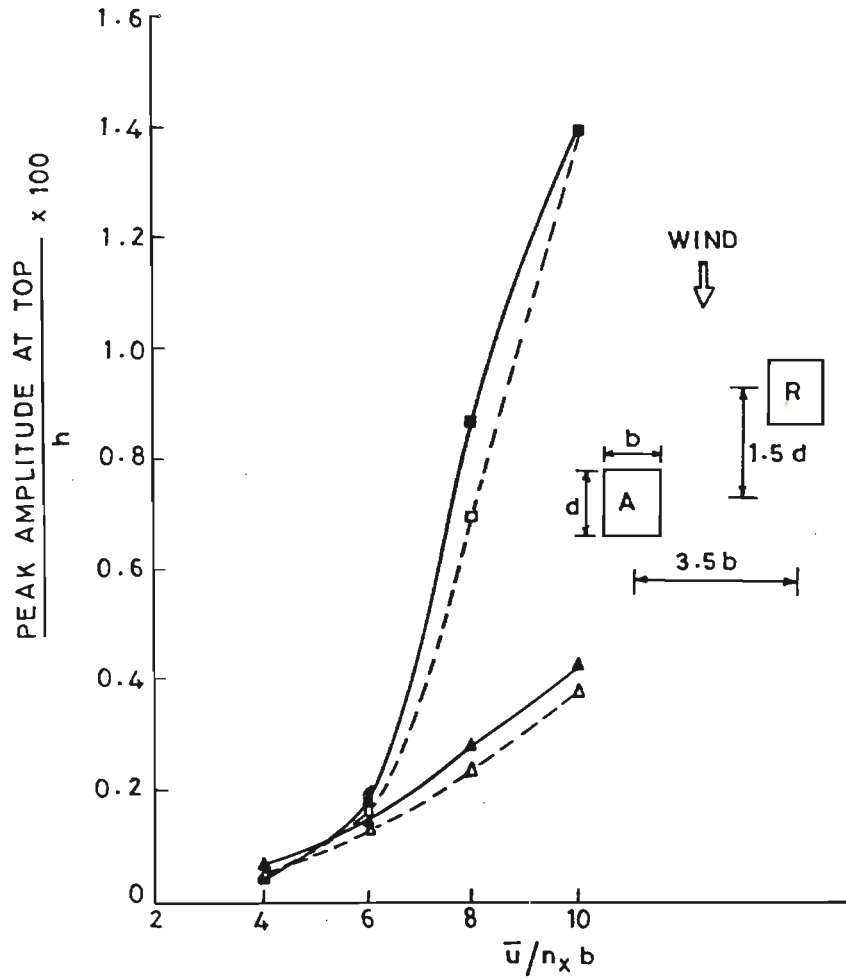


Fig. 6.22 Response of Aeroelastic Model, A

- △ ALONG-WIND (ISOLATED)
- ACROSS-WIND (ISOLATED)
- ▲ ALONG-WIND (INTERFERENCE)
- ACROSS-WIND (INTERFERENCE)

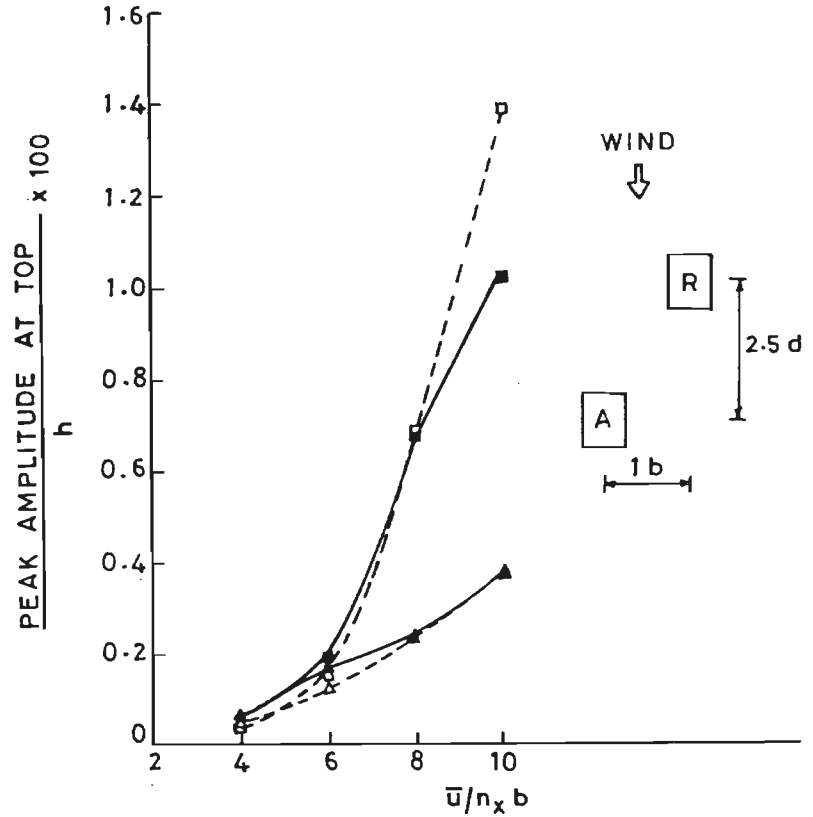
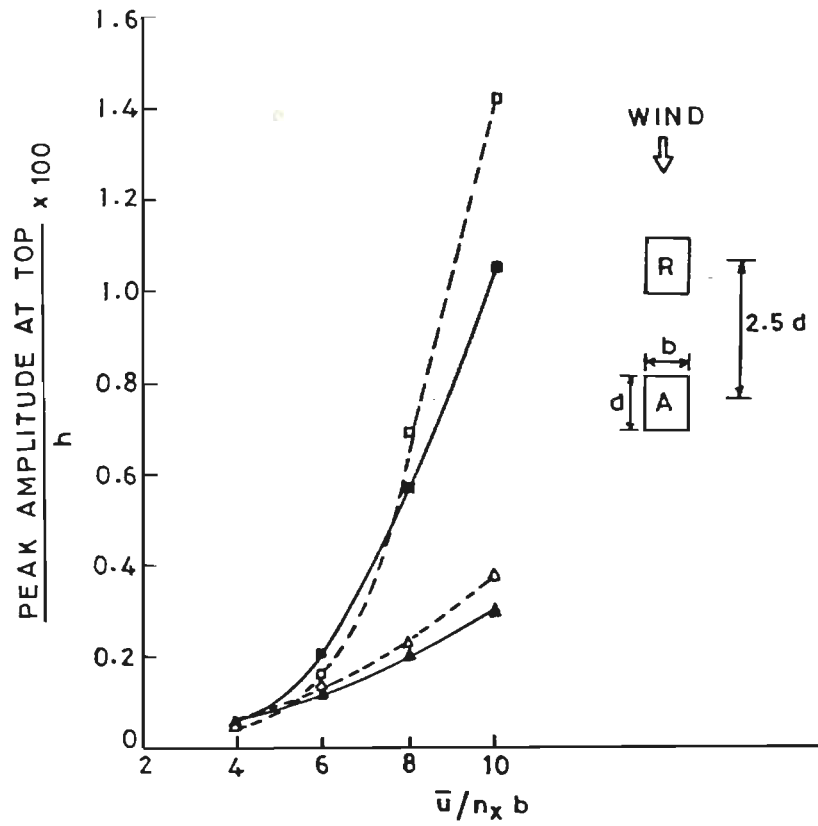


Fig. 6.23

Response of Aeroelastic Model, A

- △ ALONG-WIND (ISOLATED)
- ACROSS-WIND (ISOLATED)
- ▲ ALONG-WIND (INTERFERENCE)
- ACROSS-WIND (INTERFERENCE)

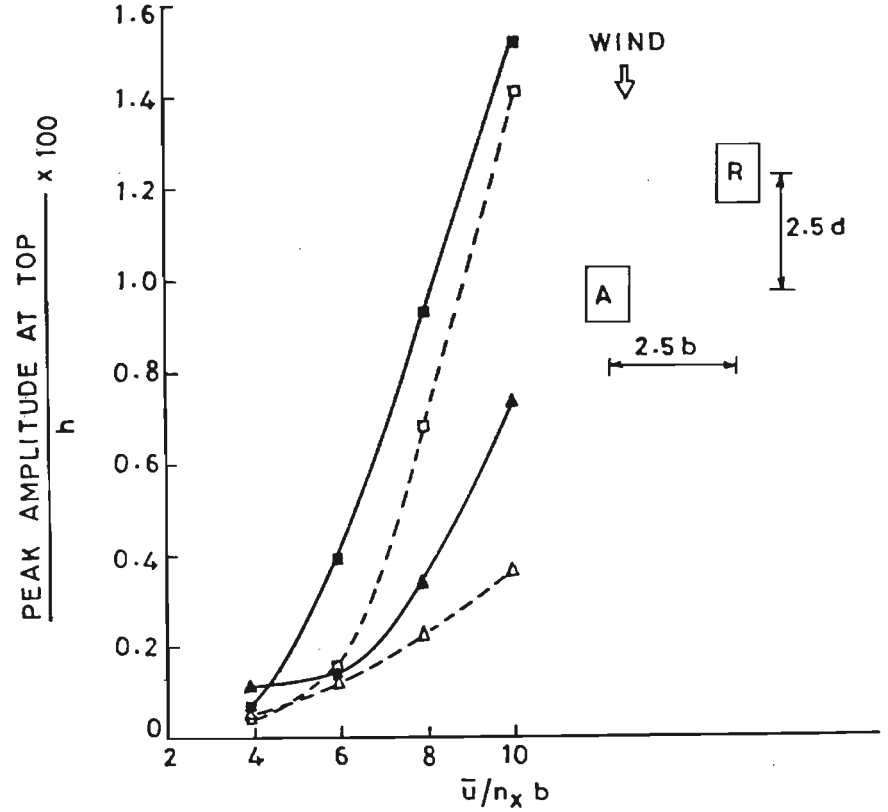
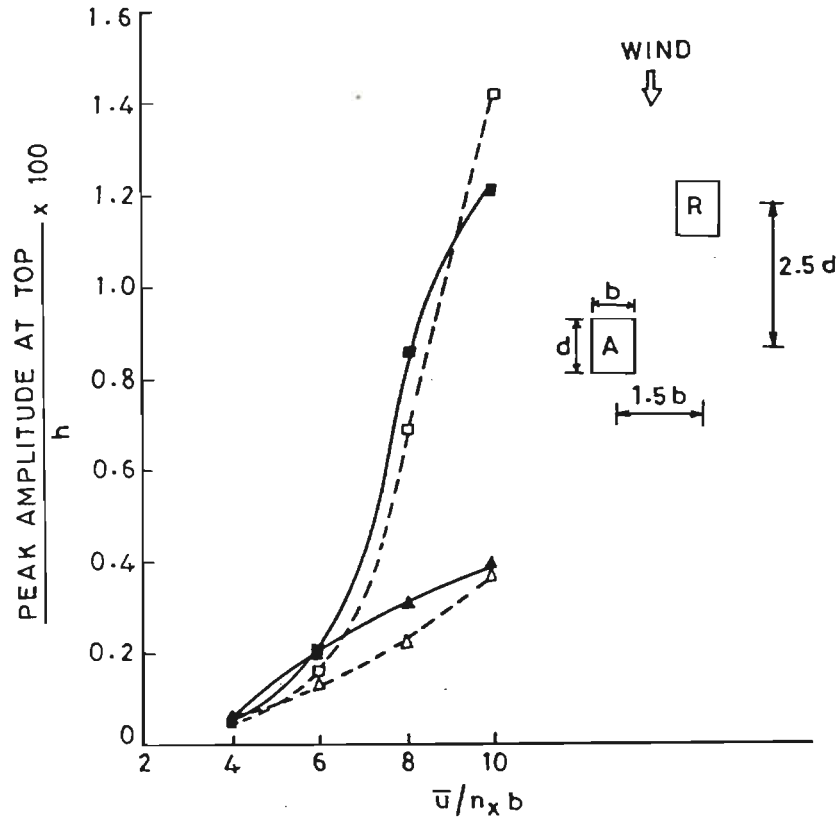


Fig. 6.24 Response of Aeroelastic Model, A

- △ ALONG-WIND (ISOLATED)
- ACROSS-WIND (ISOLATED)
- ▲ ALONG-WIND (INTERFERENCE)
- ACROSS-WIND (INTERFERENCE)

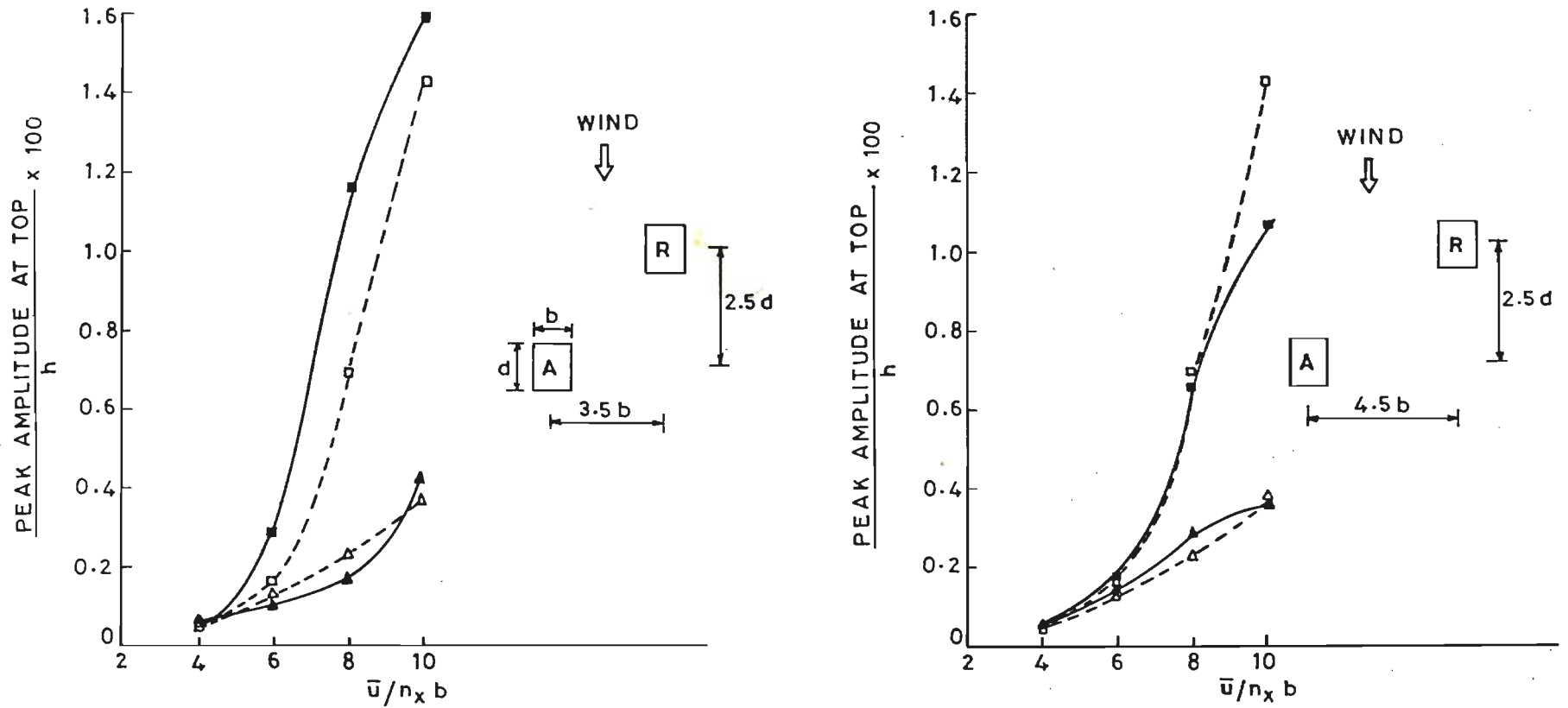


Fig. 6.25 Response of Aeroelastic Model, A

- △ ALONG-WIND (ISOLATED)
- ACROSS-WIND (ISOLATED)
- ▲ ALONG-WIND (INTERFERENCE)
- ACROSS-WIND (INTERFERENCE)

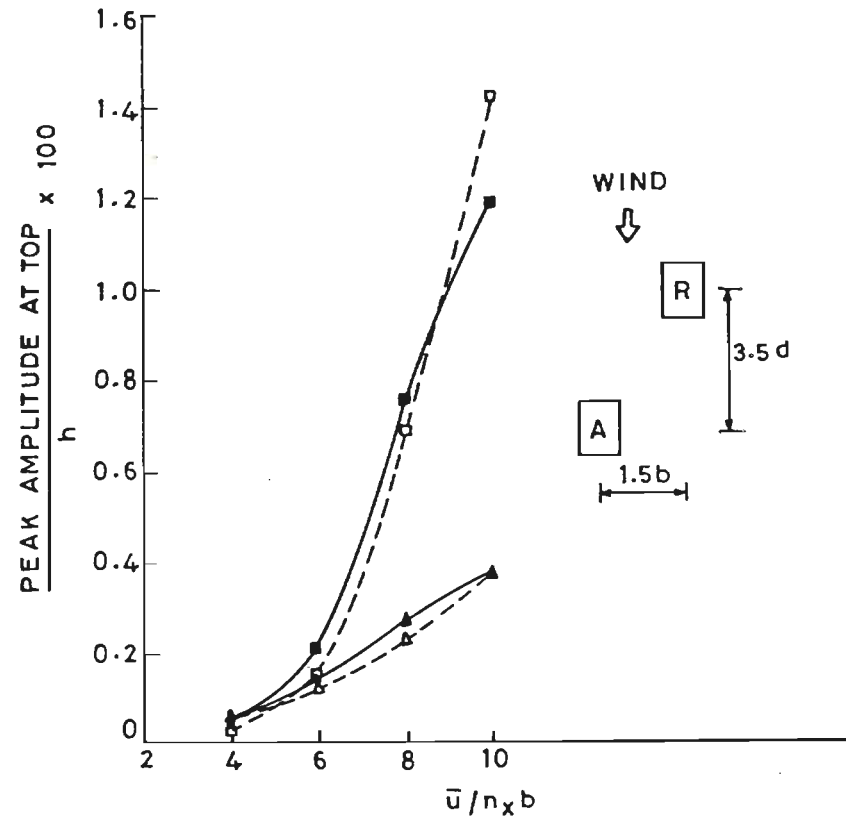
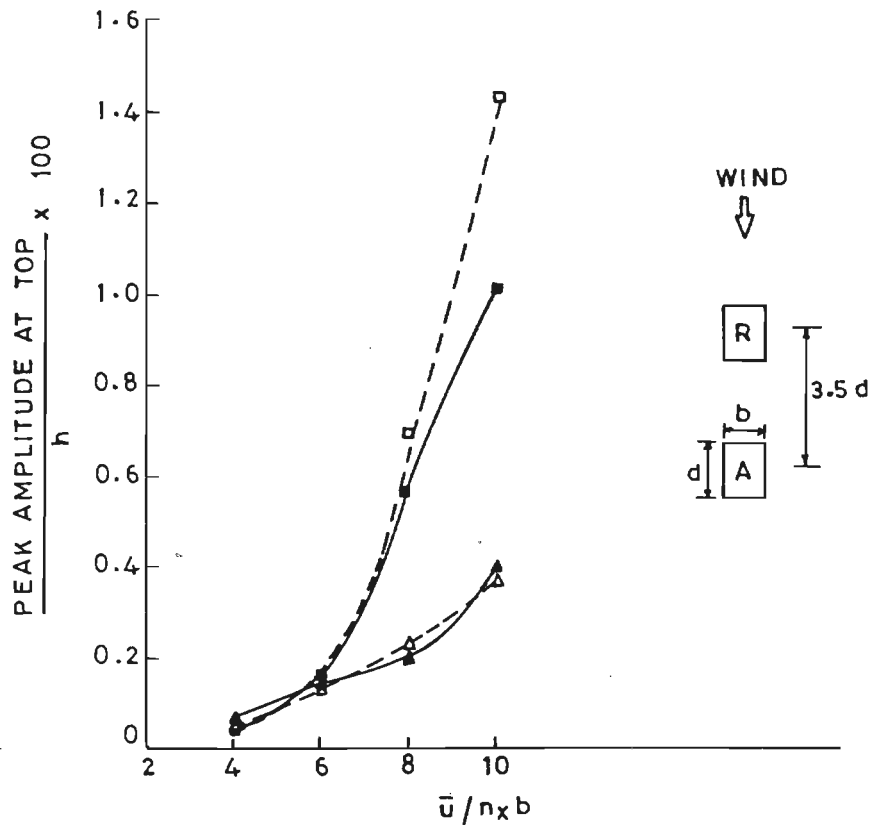


Fig.6.26 Response of Aeroelastic Model, A

- △ ALONG-WIND (ISOLATED)
- ACROSS-WIND (ISOLATED)
- ▲ ALONG-WIND (INTERFERENCE)
- ACROSS-WIND (INTERFERENCE)

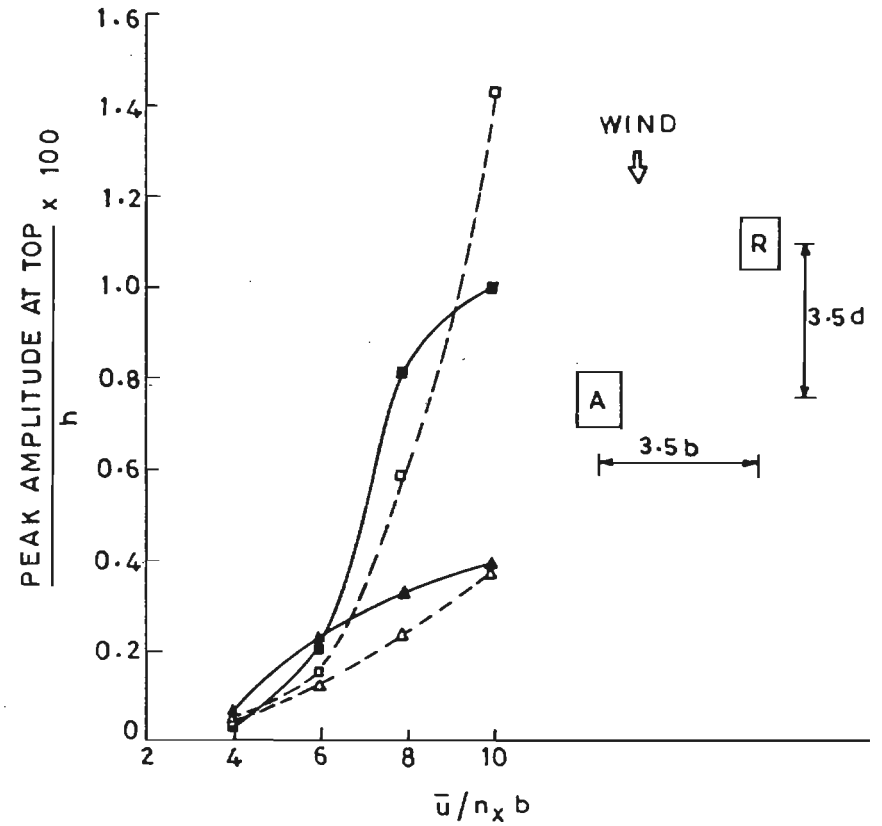
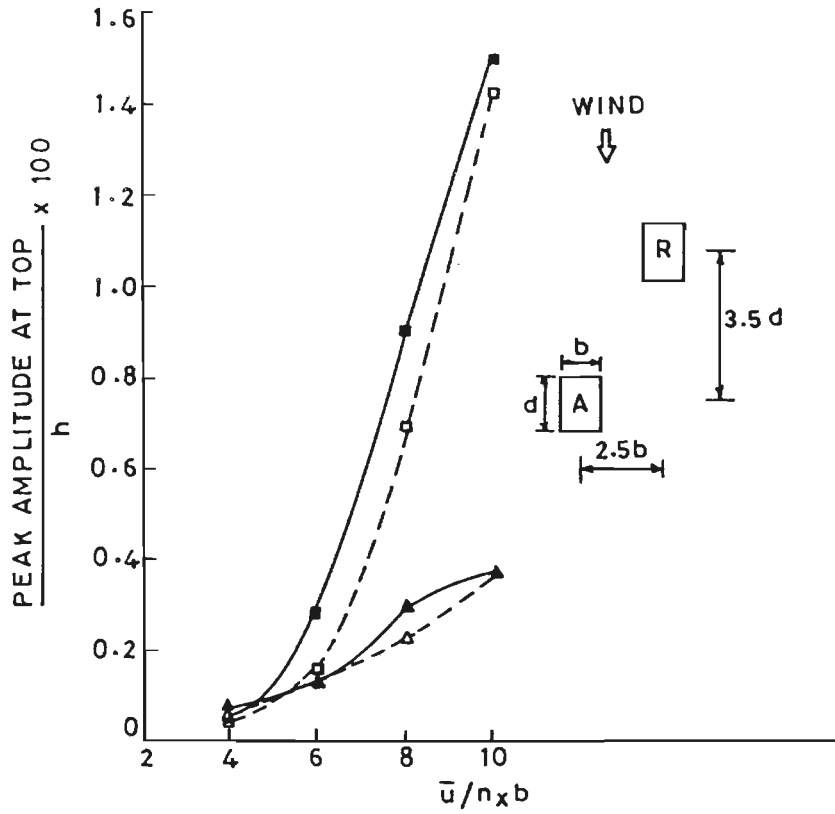


Fig.6.27 Response of Aeroelastic Model, A

- △ ALONG-WIND (ISOLATED)
- ACROSS-WIND (ISOLATED)
- ▲ ALONG-WIND (INTERFERENCE)
- ACROSS-WIND (INTERFERENCE)

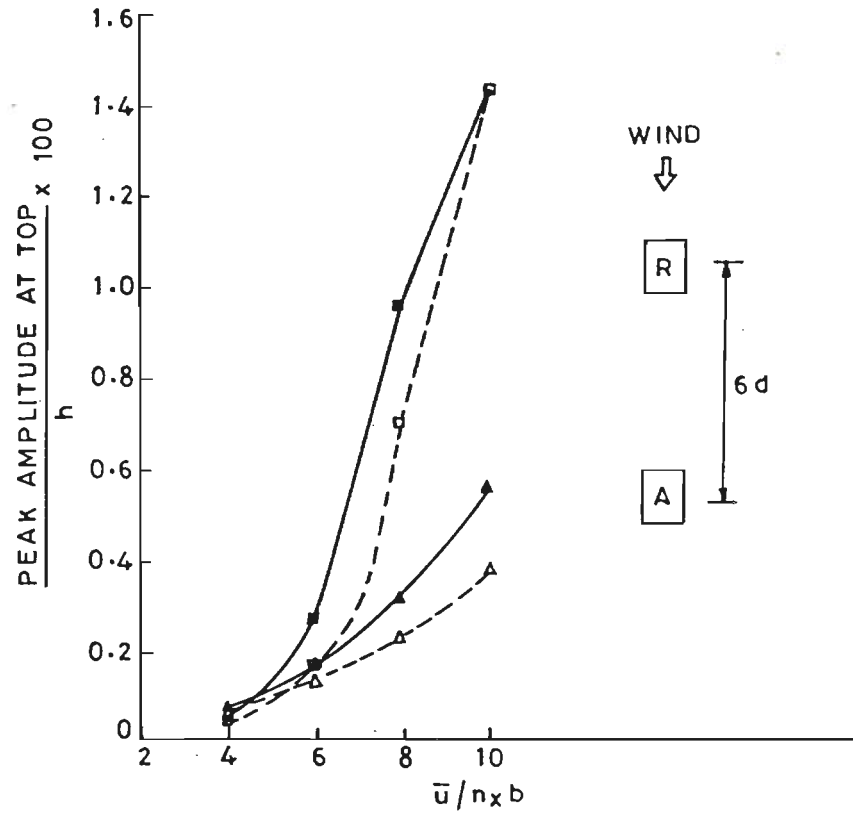
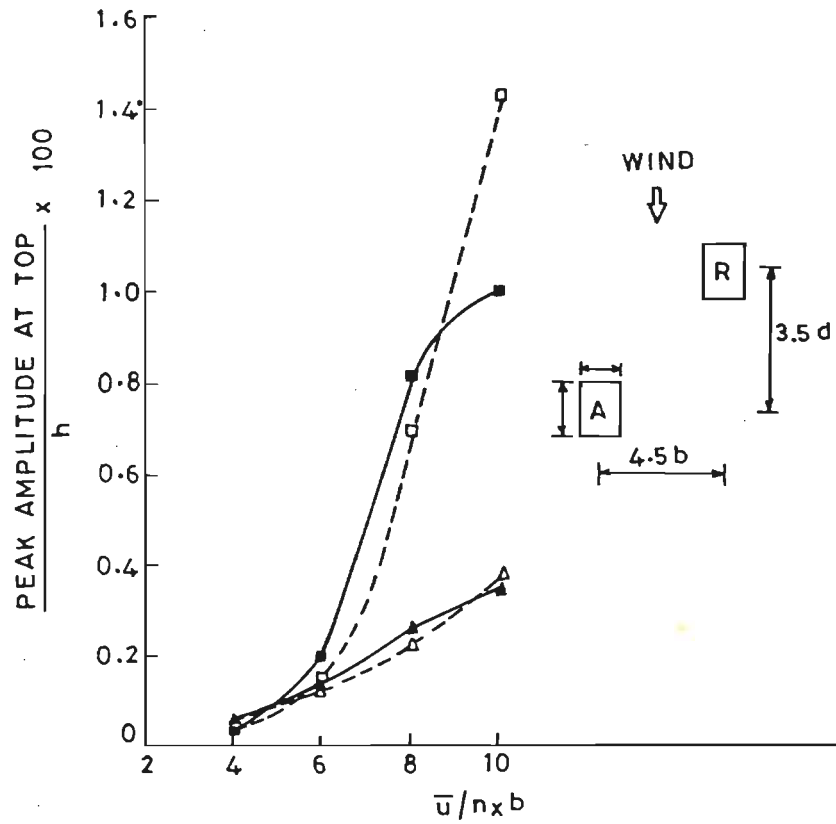


Fig.6.28 Response of Aeroelastic Model, A

- △ ALONG-WIND (ISOLATED)
- ACROSS-WIND (ISOLATED)
- ▲ ALONG-WIND (INTERFERENCE)
- ACROSS-WIND (INTERFERENCE)

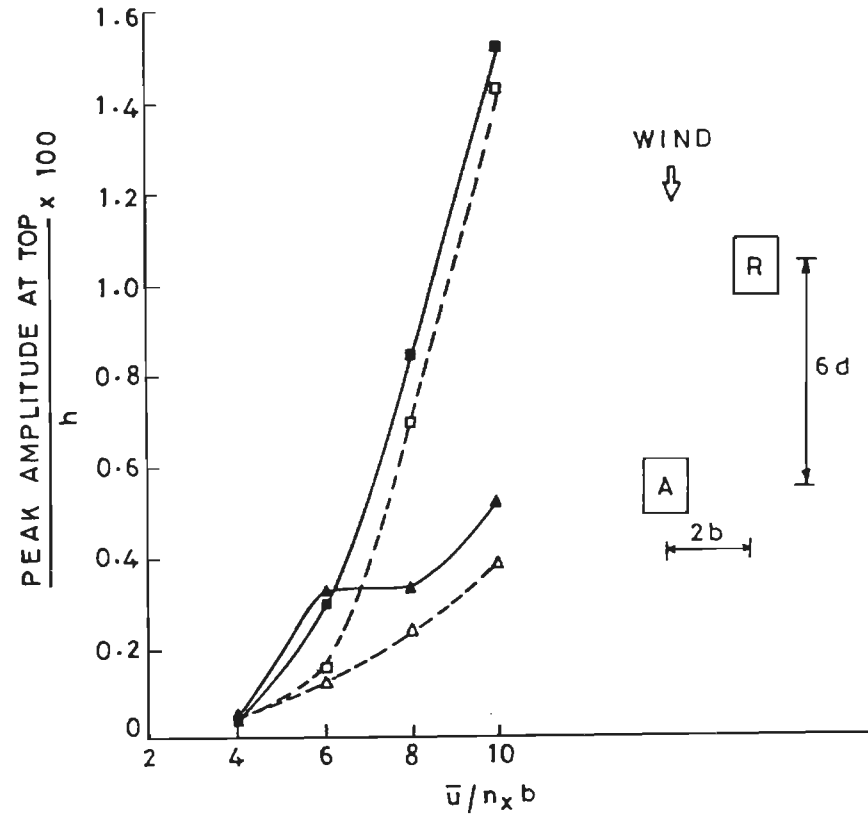
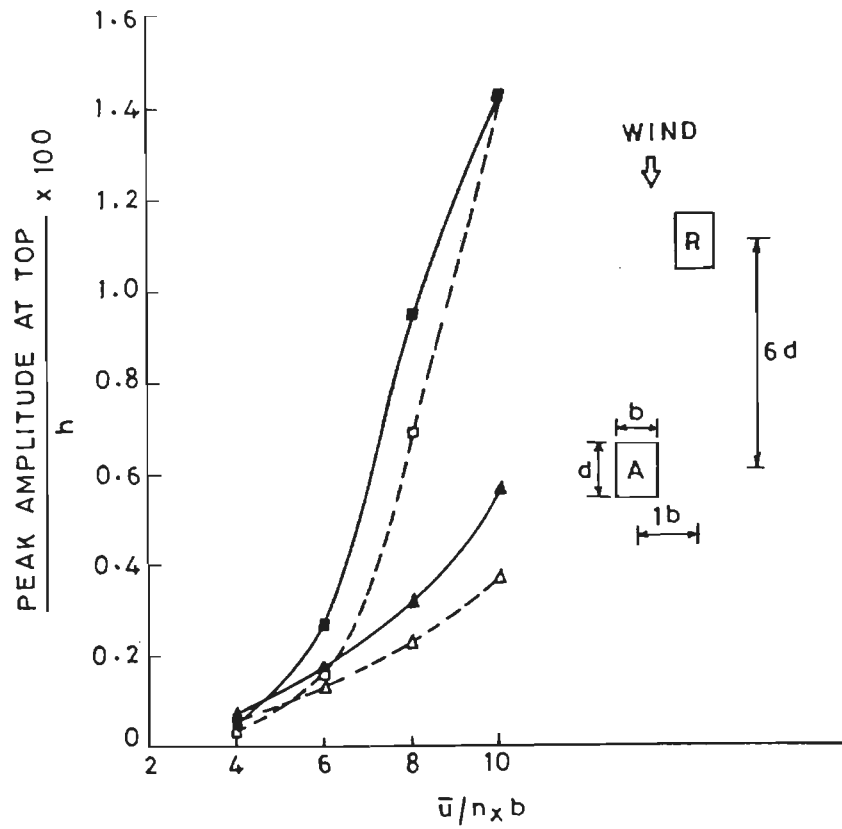


Fig. 6.29 Response of Aeroelastic Model, A



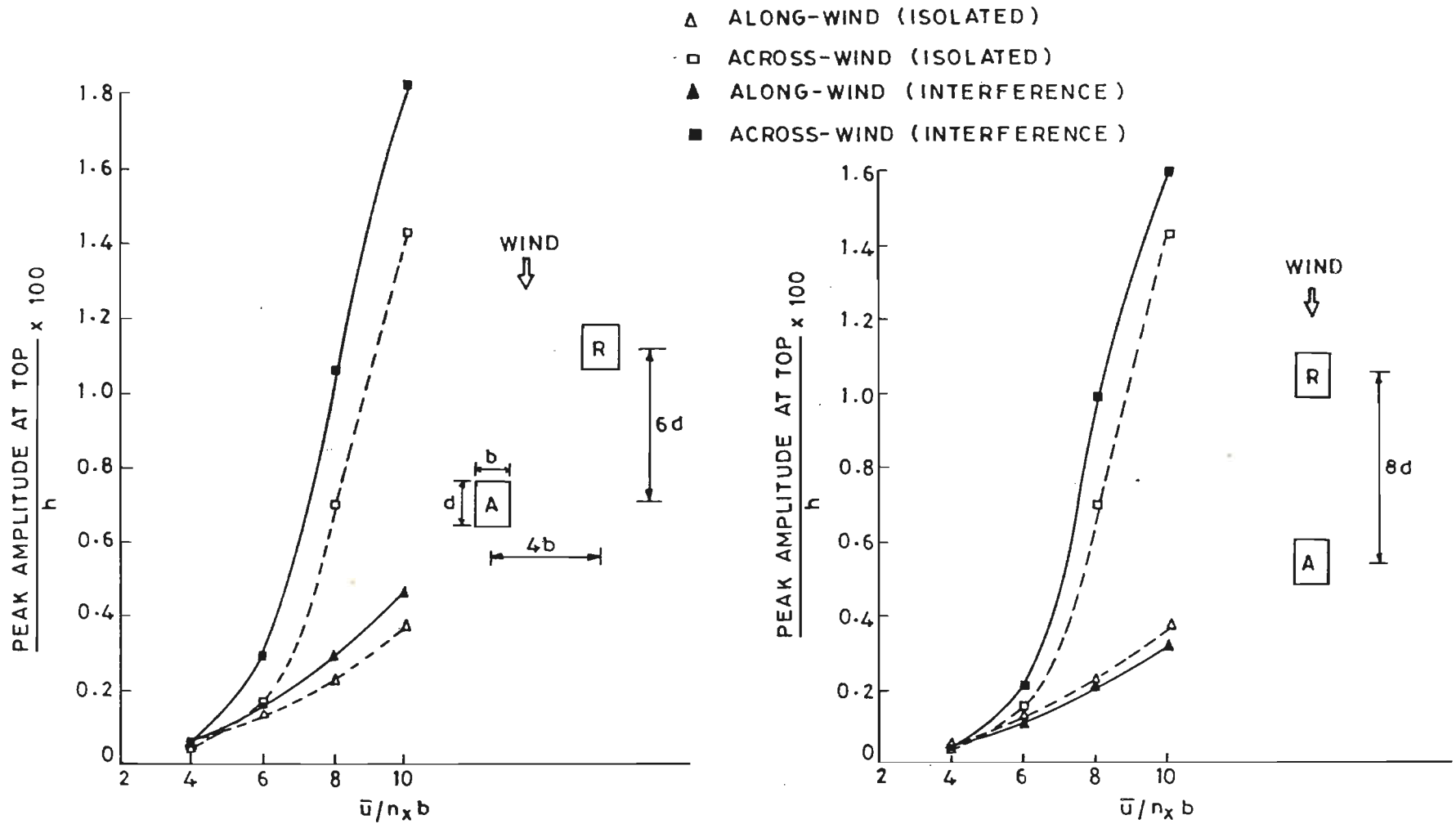


Fig. 6-30 Response of Aeroelastic Model, A

- △ ALONG-WIND (ISOLATED)
- ACROSS-WIND (ISOLATED)
- ▲ ALONG-WIND (INTERFERENCE)
- ACROSS-WIND (INTERFERENCE)

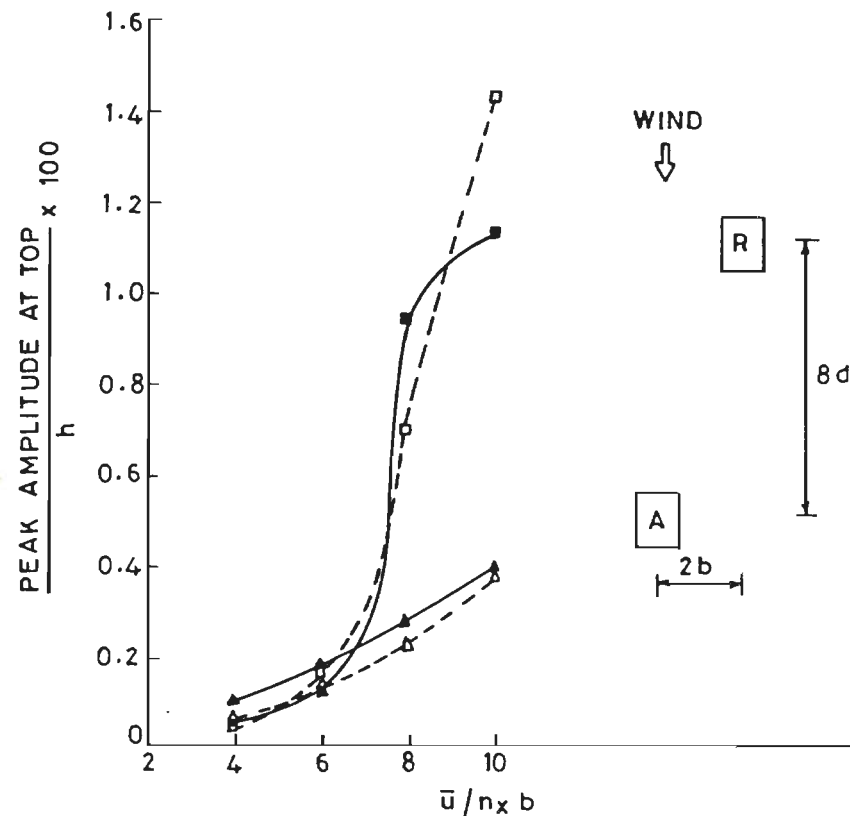
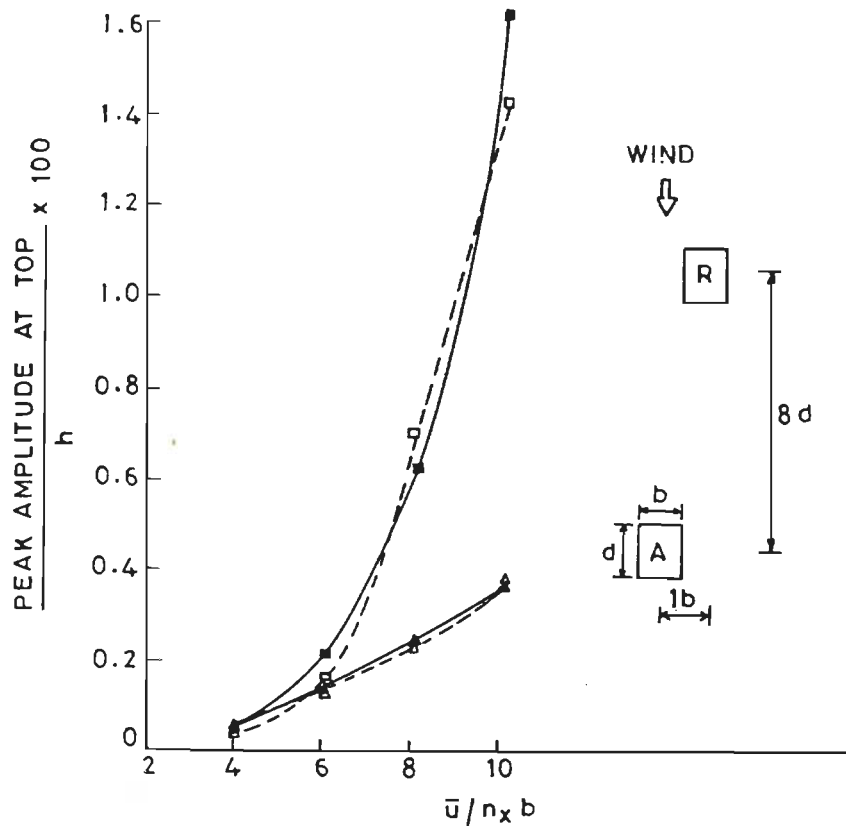


Fig. 6.31 Response of Aeroelastic Model, A

- △ ALONG-WIND (ISOLATED)
- ACROSS-WIND (ISOLATED)
- ▲ ALONG-WIND (INTERFERENCE)
- ACROSS-WIND (INTERFERENCE)

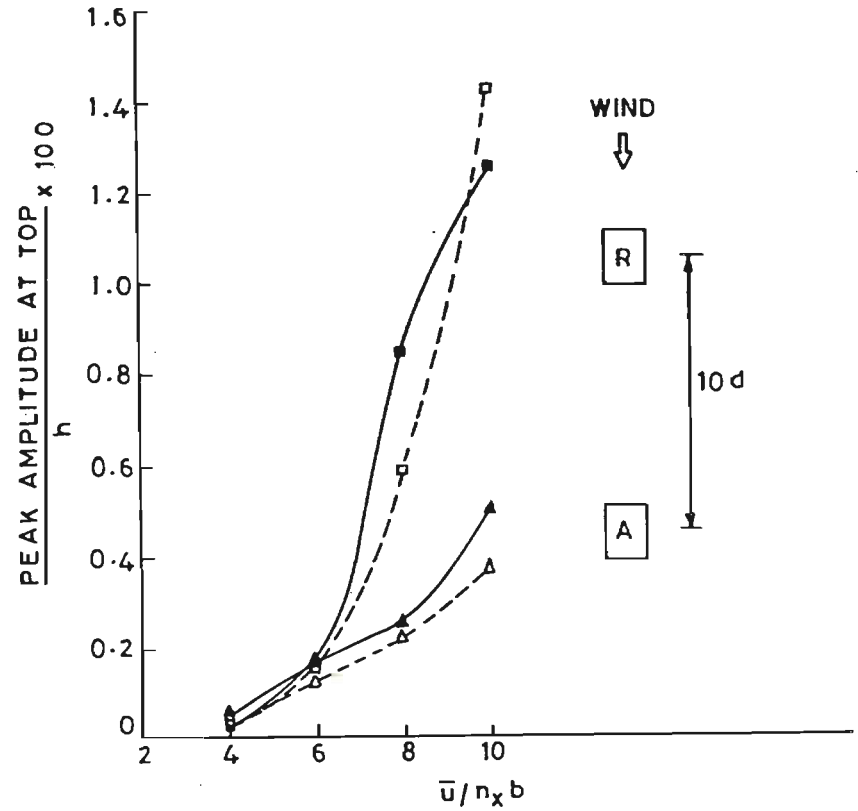
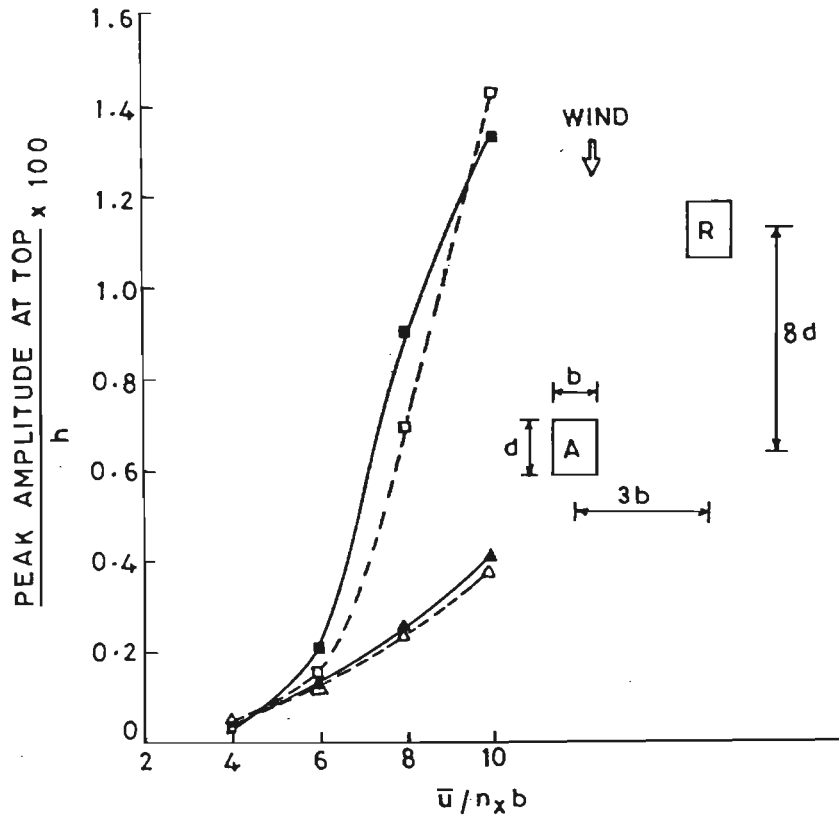


Fig. 6.32 Response of Aeroelastic Model, A

- △ ALONG-WING (ISOLATED)
- ACROSS-WING (ISOLATED)
- ▲ ALONG-WIND (INTERFERENCE)
- ACROSS-WIND (INTERFERENCE)

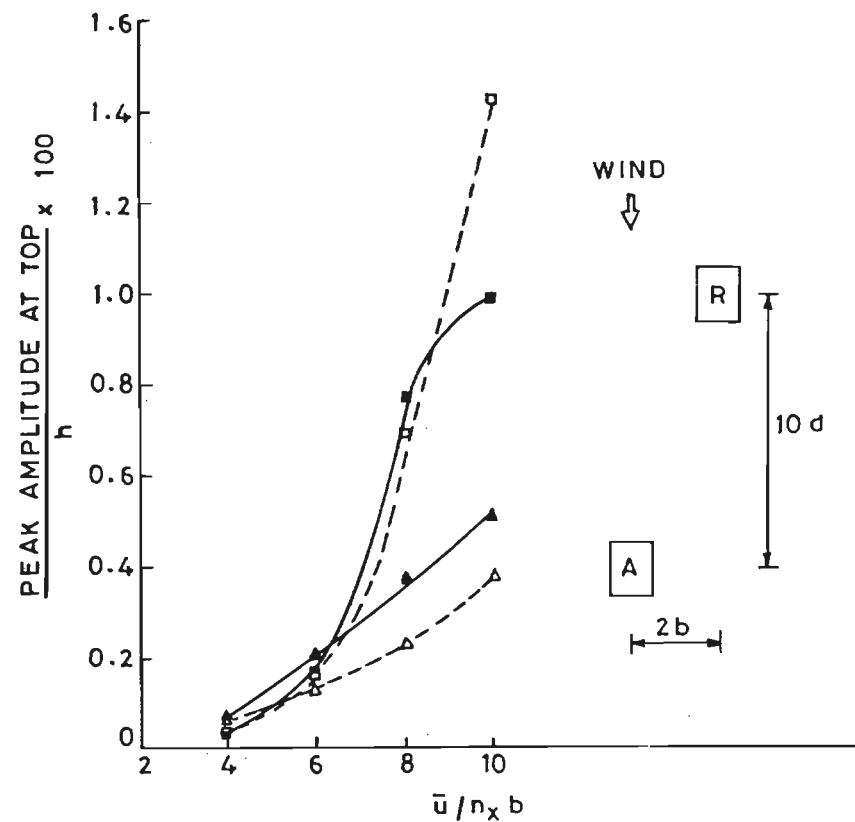
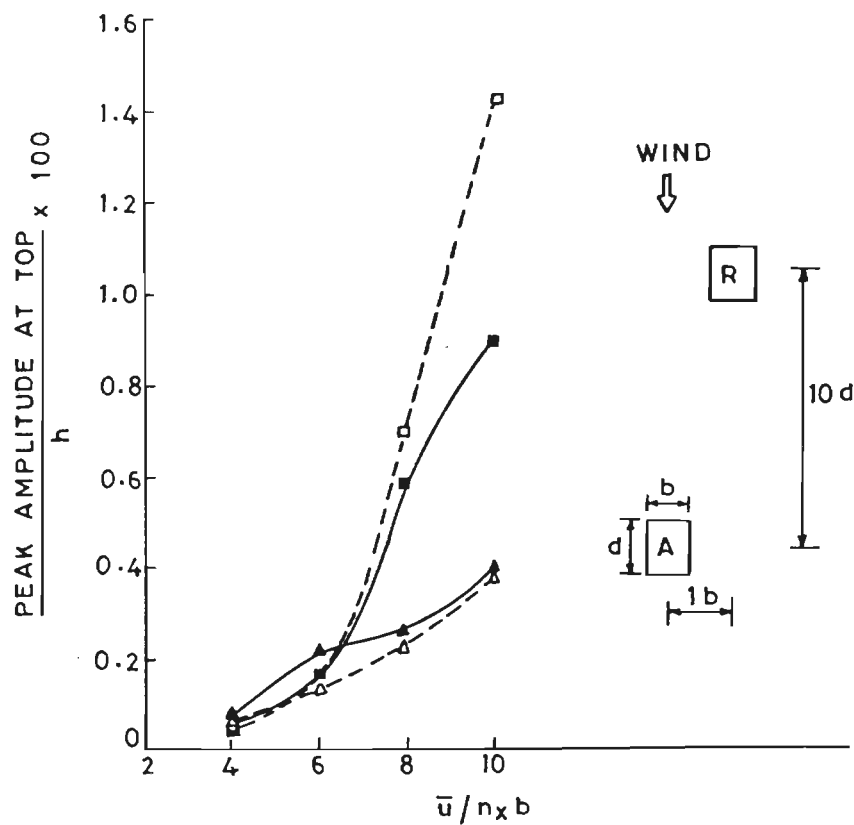


Fig. 6.33 Response of Aeroelastic Model, A

- △ ALONG-WIND (ISOLATED)
- ACROSS-WIND (ISOLATED)
- ▲ ALONG-WIND (INTERFERENCE)
- ACROSS-WIND (INTERFERENCE)

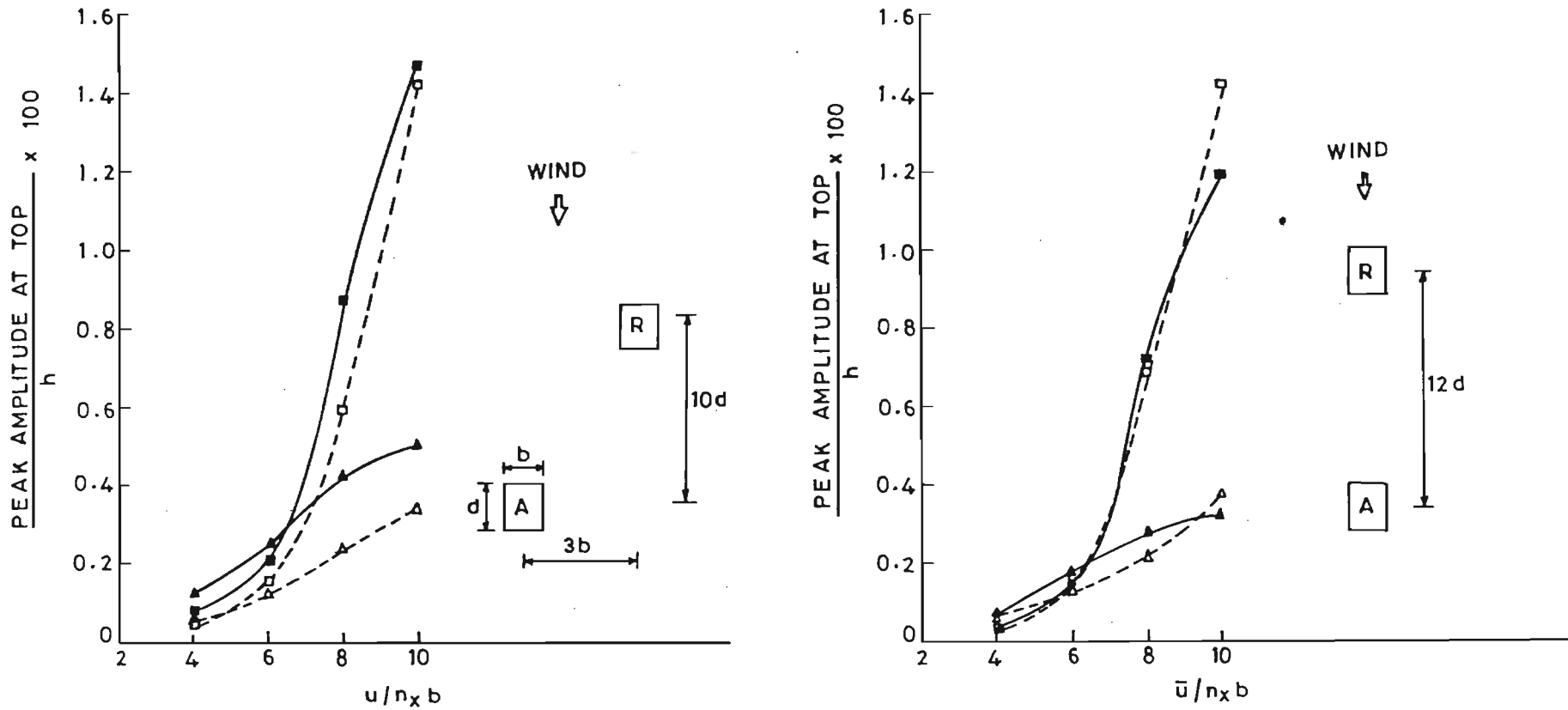


Fig.6.34 Response of Aeroelastic Model, A

- △ ALONG-WIND (ISOLATED)
- ACROSS-WIND (ISOLATED)
- ▲ ALONG-WIND (INTERFERENCE)
- ACROSS-WIND (INTERFERENCE)

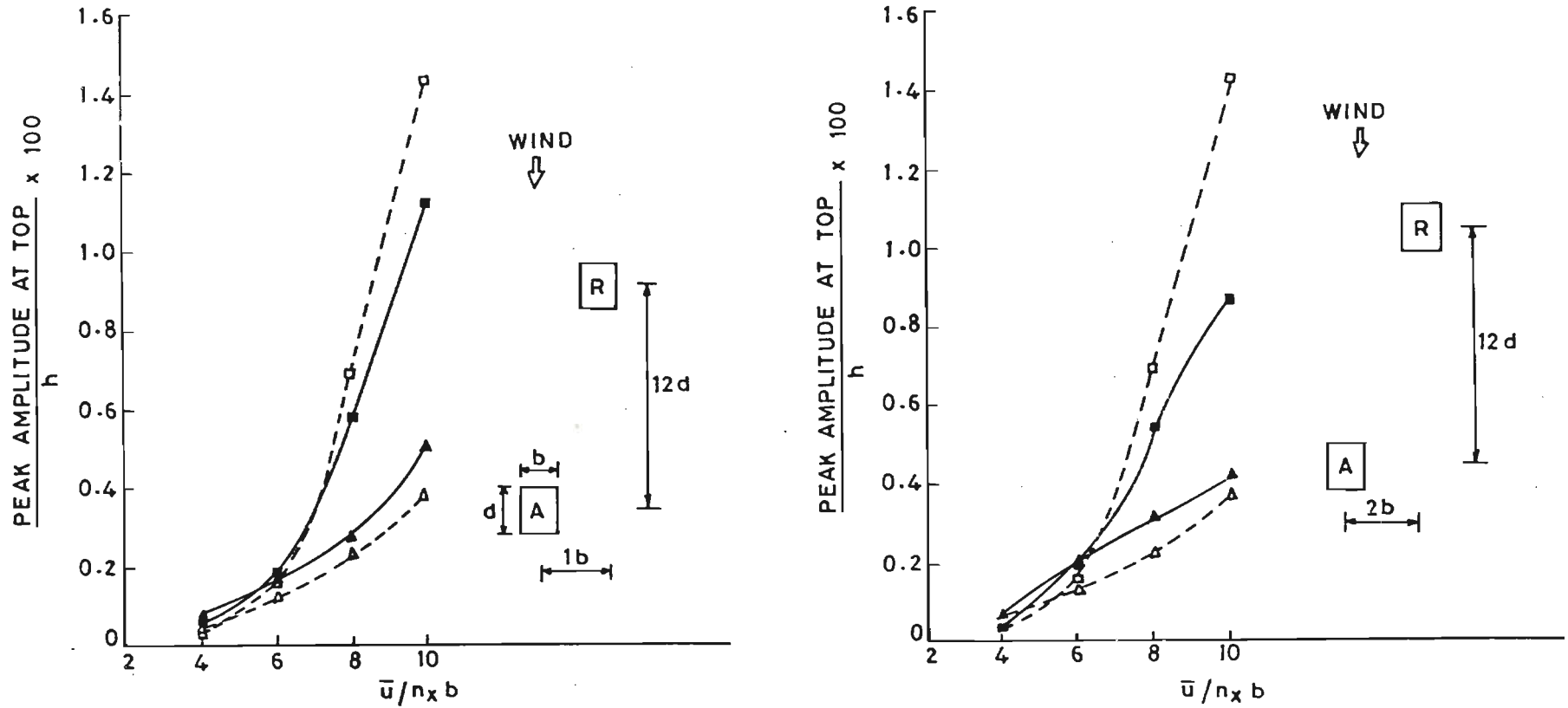


Fig. 6.35 Response of Aeroelastic Model, A

- △ ALONG-WIND (ISOLATED)
- ACROSS-WIND (ISOLATED)
- ▲ ALONG-WIND (INTERFERENCE)
- ACROSS-WIND (INTERFERENCE)

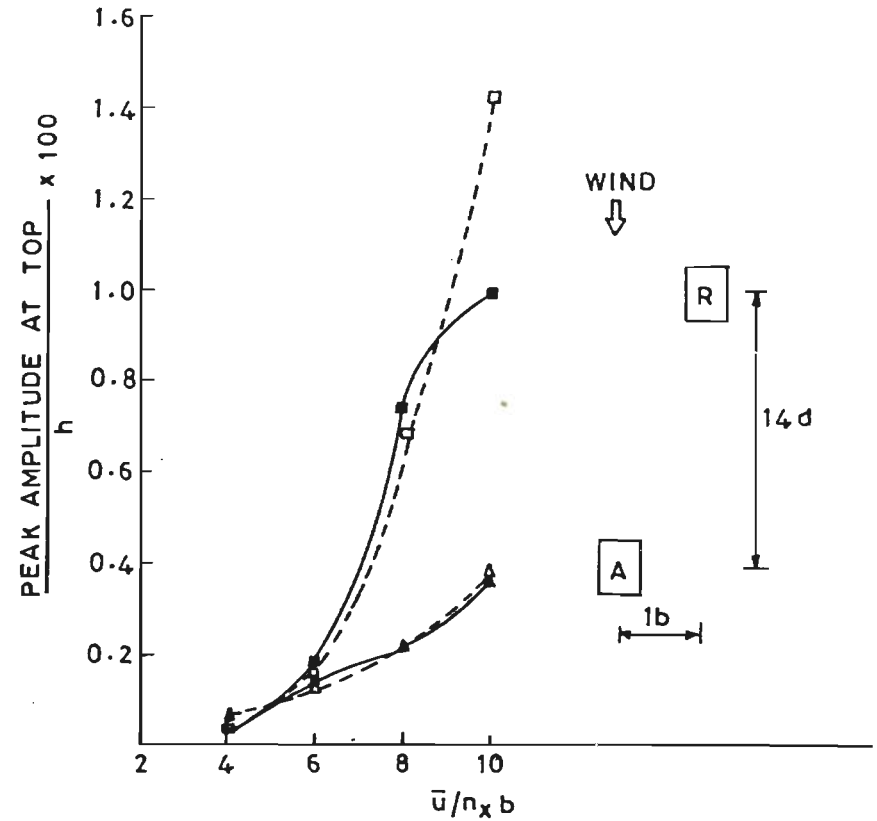
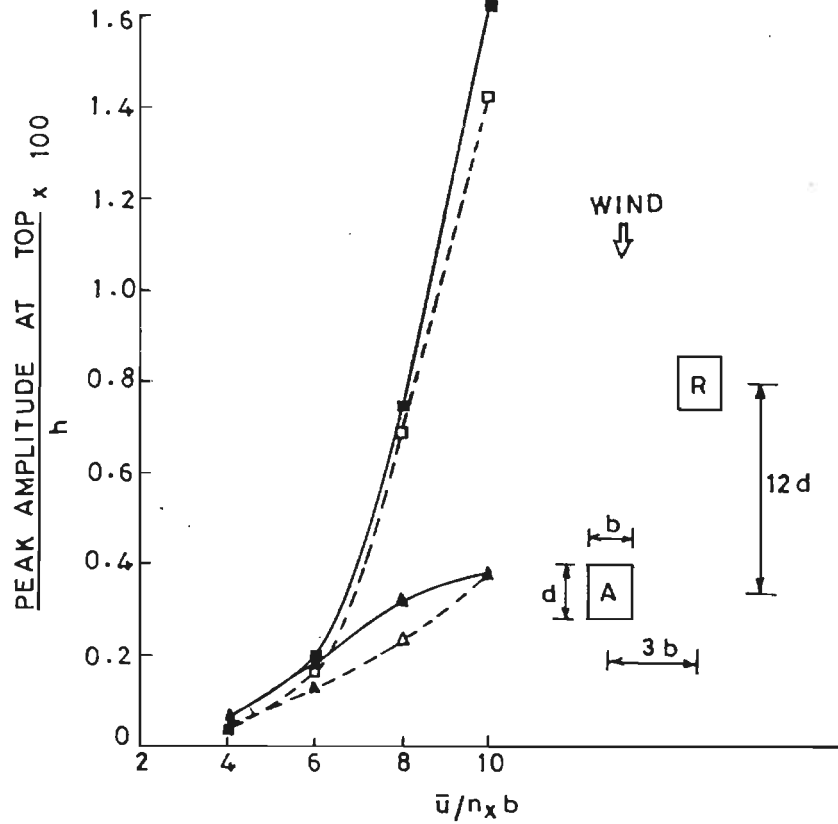


Fig. 6.36 Response of Aeroelastic Model, A

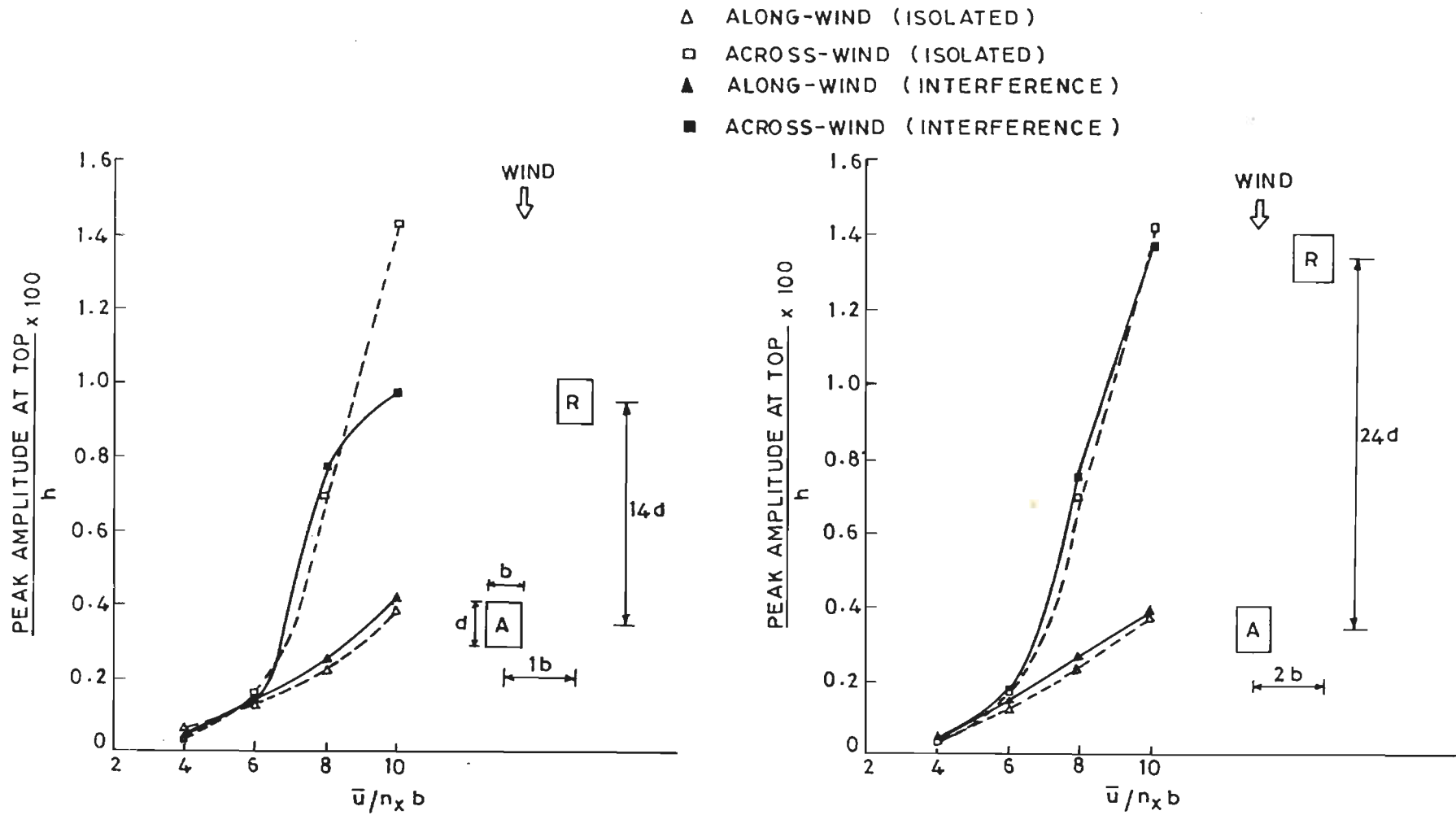


Fig.6.37 Response of Aeroelastic Model, A



- △ ALONG-WIND (ISOLATED)
- ACROSS-WIND (ISOLATED)
- ▲ ALONG-WIND (INTERFERENCE)
- ACROSS-WIND (INTERFERENCE)

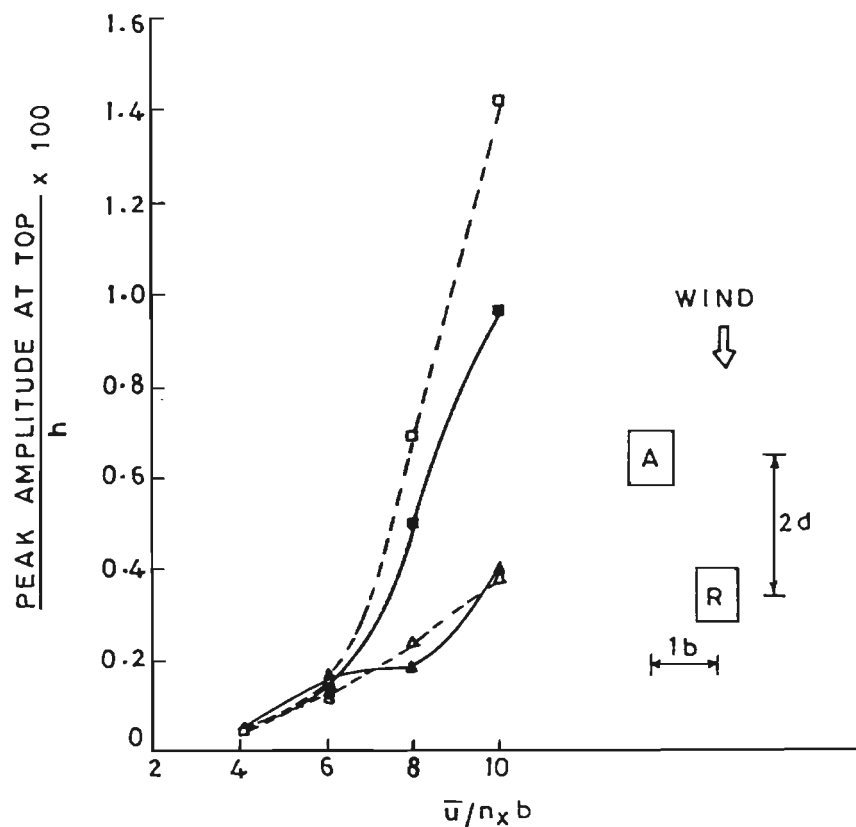
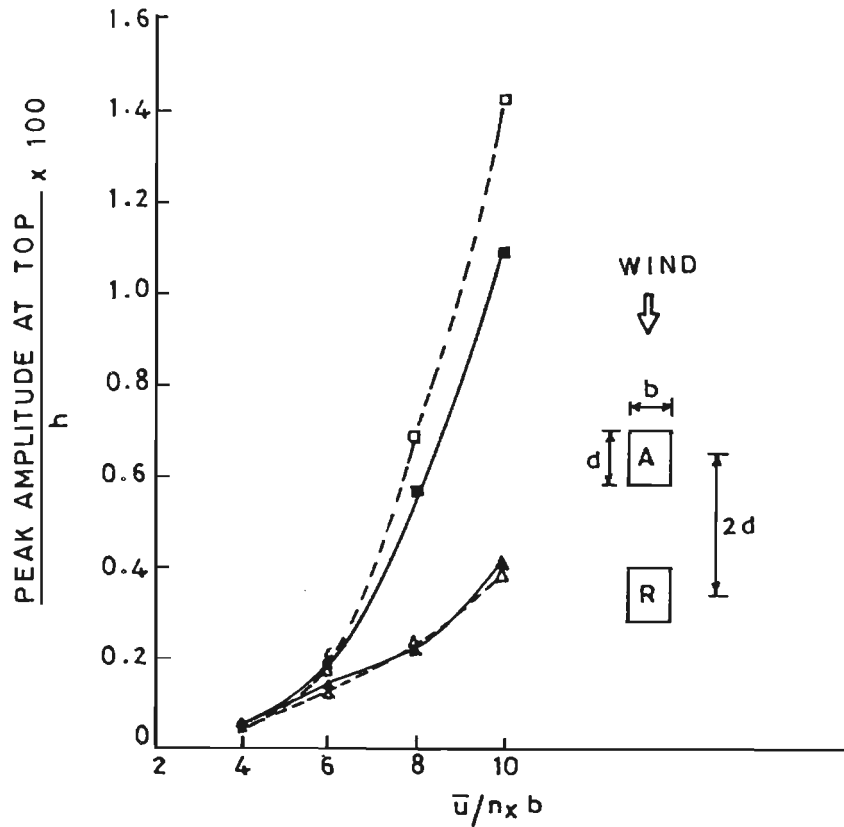


Fig. 6.38 Response of Aeroelastic Model, A

- △ ALONG-WIND (ISOLATED)
- ACROSS-WIND (ISOLATED)
- ▲ ALONG-WIND (INTERFERENCE)
- ACROSS-WIND (INTERFERENCE)

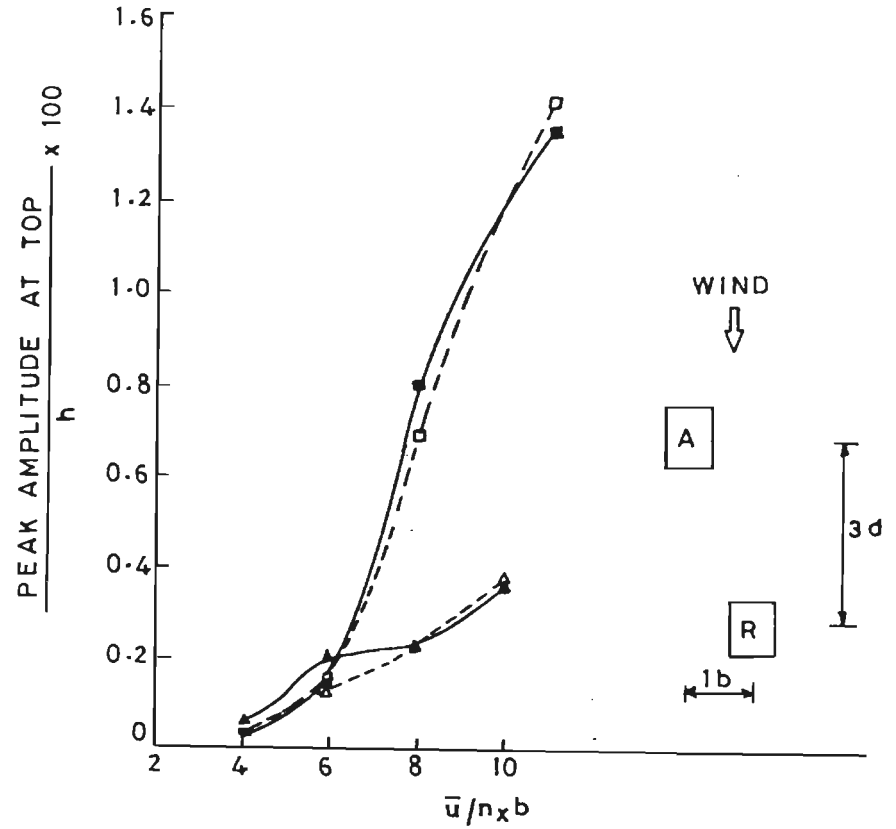
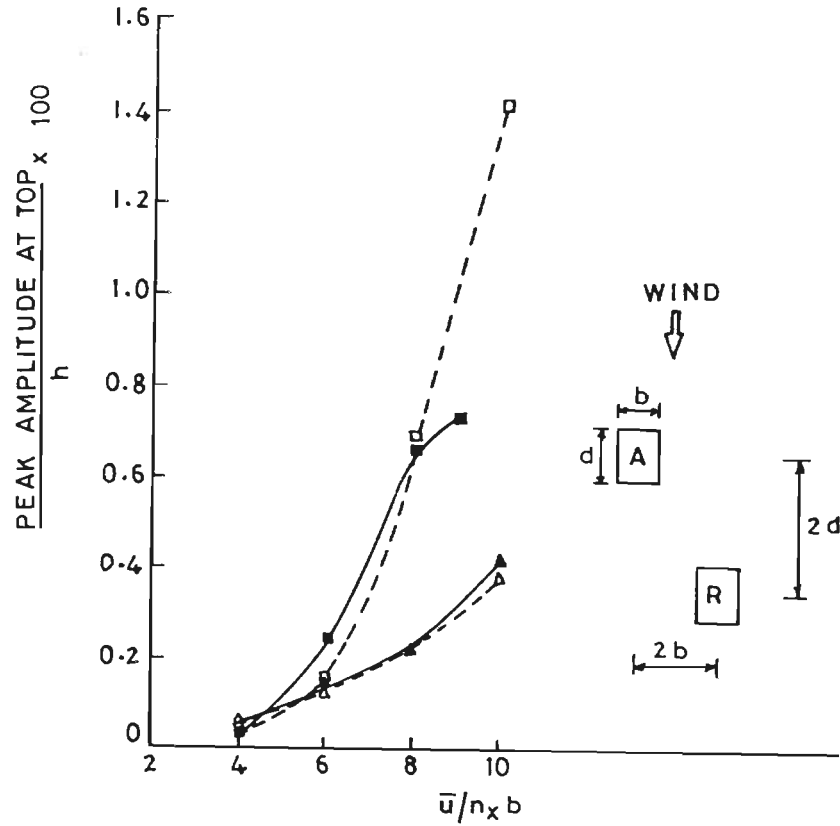


Fig. 6.39 Response of Aeroelastic Model, A

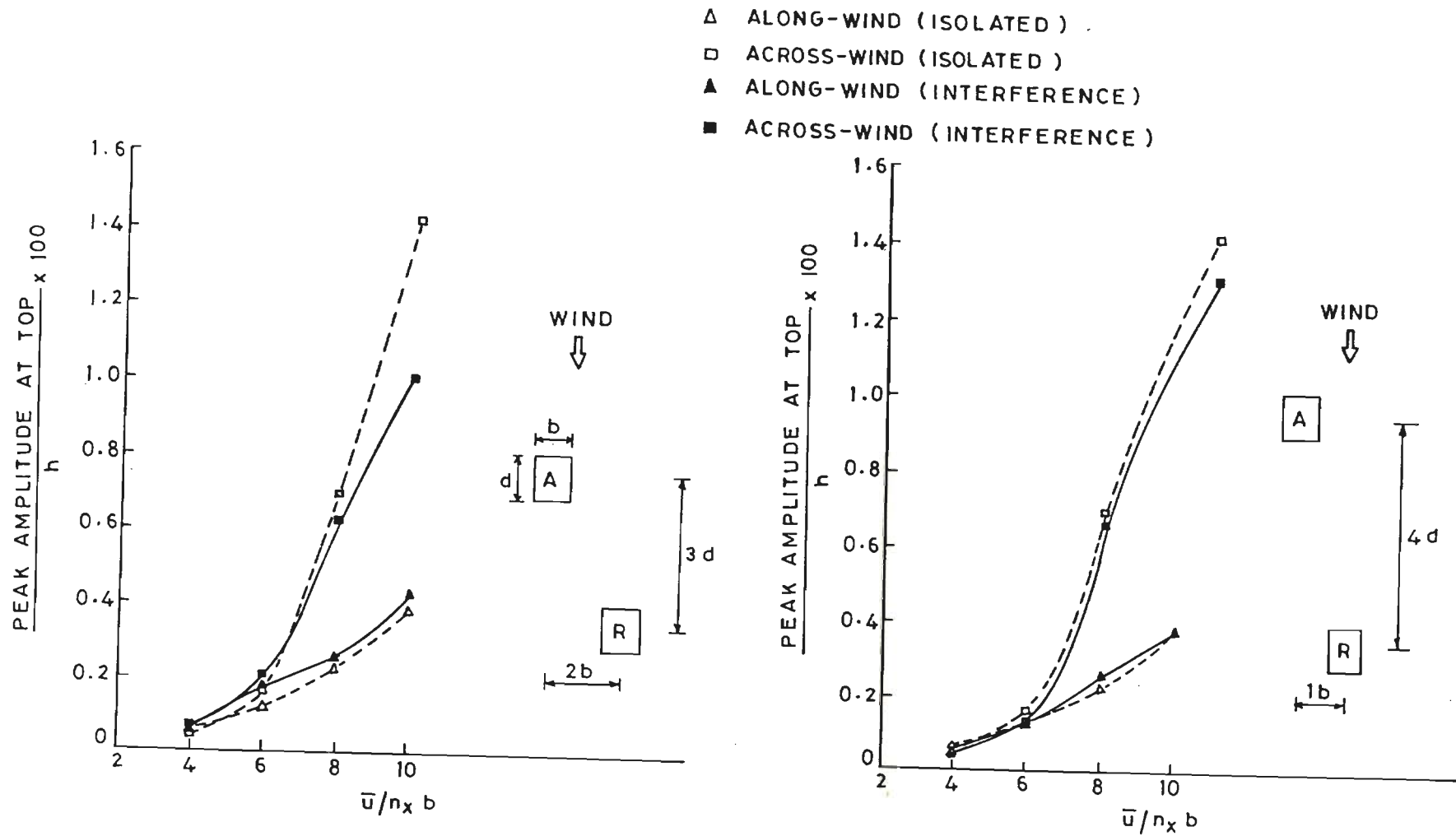


Fig.6.40 Response of Aeroelastic Model, A

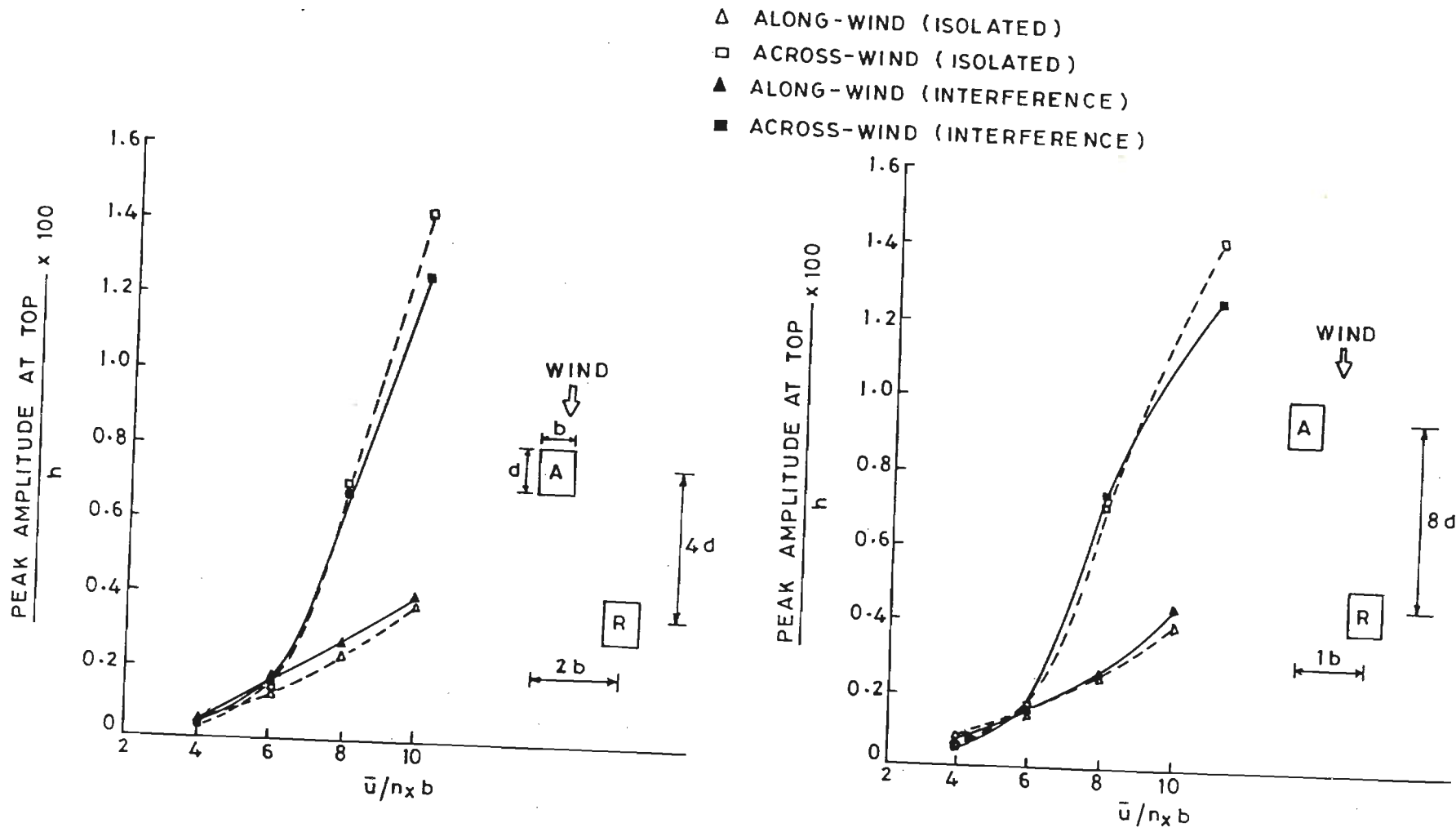


Fig.6.41 Response of Aeroelastic Model, A

- △ ALONG-WIND (ISOLATED)
- ACROSS-WIND (ISOLATED)
- ▲ ALONG-WIND (INTERFERENCE)
- ACROSS-WIND (INTERFERENCE)

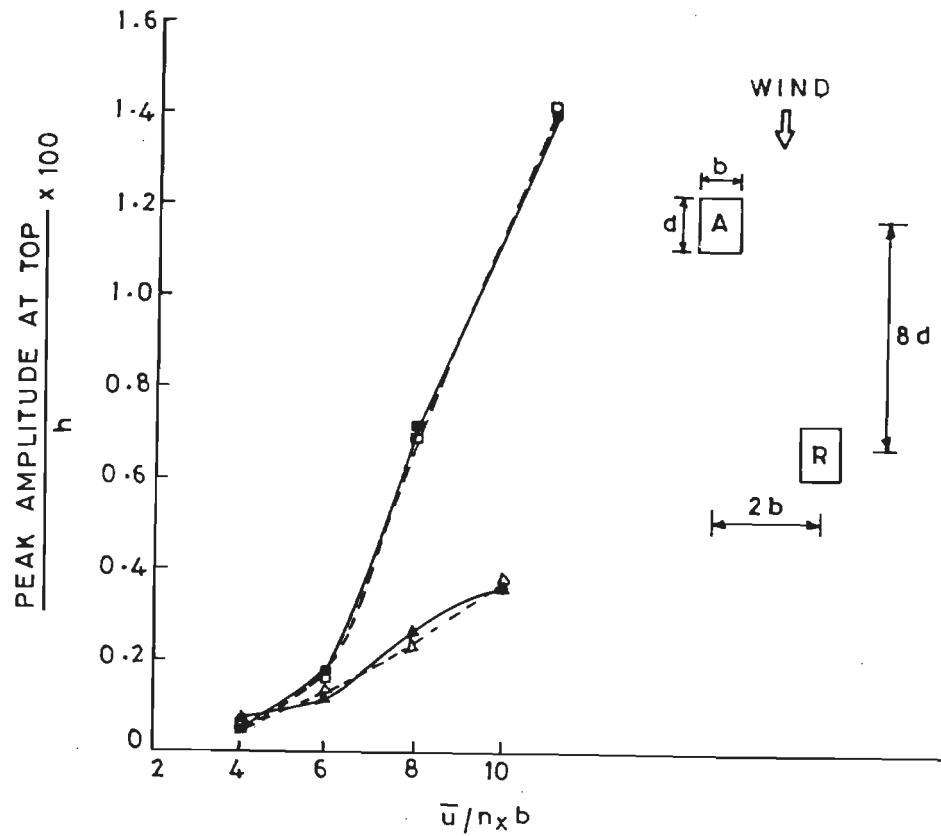


Fig.6.42 Response of Aeroelastic Model, A

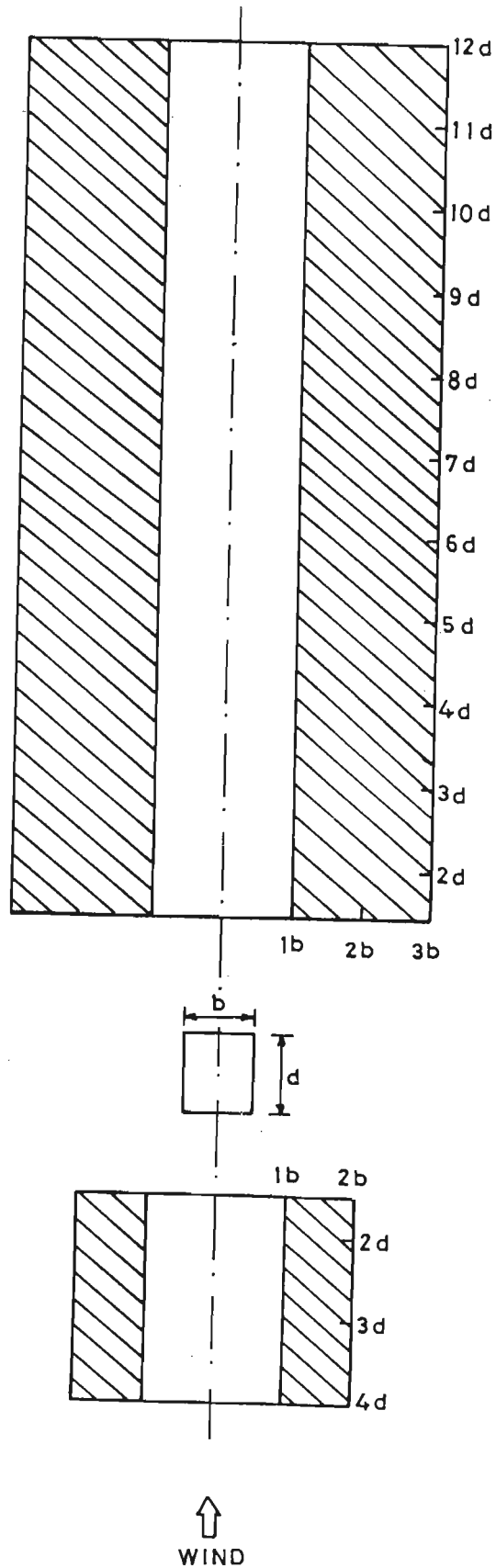


Fig.6.43 Critical Interference Zone for the Building Model

## APPENDIX-A

### DAMPING

Damping is known to affect significantly the dynamic response of structures. It is therefore an important parameter in the determination of aero-dynamic response. Since it is a complex physical phenomenon, it is generally difficult to estimate it accurately. The damping capacity of a structure may be defined as the ratio of energy dissipated in one cycle of oscillation to the maximum amount of energy accumulated in the structure in that cycle [74]. Damping in a building structural system is primarily due to

1. Material damping, and
2. Interfacial damping
3. Aerodynamic damping

#### A.1 Material Damping

In materials, damping is due to complex molecular interactions, grain boundaries, dislocations etc., and so the damping capacity in a structure is influenced by the type and amount of materials present, the mode of manufacture, heat treatment, residual stresses from rolling, machining etc. [76]. This means that because the material damping arises from micro-motions, the fundamental structural parameter that will affect the material damping capacity will be the magnitude of strain in each element.

For materials under uniform stress, it has been shown that the energy dissipated per cycle  $\Delta E$  is given by the following relation [76].

$$\Delta E = J \sigma^n \quad \text{A.1}$$

where  $J$  and  $n$  are material constants and  $\sigma$  is the symbol for stress. The value of  $n$  varies from 0.5 to 2.5.

The basic macroscopic quantity to describe structural damping is the loss factor  $\eta$  defined by the following energy ration,

$$\eta = \frac{\Delta E}{E_{\max}} \quad \text{A.2}$$

where,  $\Delta E$  is the energy dissipated in one cycle of vibration, and  $E_{\max}$  is the maximum energy stored in the system during the cycle. When the material is subjected to non-uniform stress or random narrow band strain fluctuations, the structural damping factor can be predicted quite reliably using equation A.2 wherein the damping is obtained by dividing the total energy dissipated per cycle by the elastic strain energy over the volume of the body.

Wherever there are welds or geometric discontinuities that will lead to stress concentrations, the high stress will promote large dissipation of energy in these regions. As the surrounding areas of material will normally have substantially lower stress levels, these concentrations of multi-axial stress will often be the main source of material damping in a fabricated structure [76].

The approximate material damping in terms of critical damping for the most common building materials, mainly from Grootenhuis [46] and Lazan [76], are

- |               |  |
|---------------|--|
| a)Mild steel: | 0.25-0.5% (alloy and high-strength steels are often lower by a factor of 2 or more). |
| b)Concrete;   |  |
| Reinforced :  | 0.5 - 1%   |
| Prestressed:  | 0.15-0.5% and  |
| c)Masonry:    | 10-20%   |

Vickery [131] had suggested the following damping ratios:



## (i) Low stress levels

Steel frames	0.5-1%
Reinforced or prestress concrete	0.5-1%

## (ii) Working stress

Steel frame	1-2%
Reinforced concrete	1.5-3%

## (iii) Near yield

Steel frame	4-6%
Reinforced concrete	5-10%

A study of literature shows that the internal (material) damping appears to contribute a significant amount to the total structural damping of most buildings, perhaps approaching 50% of the total [107].

**A.2 Interfacial Damping**

The theoretical treatment of interfacial damping, which constitutes the major component of structural damping of a tall building, is not nearly as well developed as the treatment of material damping [76]. Interfacial damping mechanisms in a structure are normally categorized as [107].

1. Coulomb damping in the form of dry interfaces for example, bolted joint, steel to concrete interfaces, loosely connected interfaces such as concrete infill, considerable number of interfaces throughout the frame and the infill walls;
2. Adhesively bonded surfaces- welded (and brazed) joints;
3. Foundation interfaces- building to base, base to soil or rock.

For most of the tall buildings it is the Coulomb friction developed from the relative motion within the wide variety of joints which forms the major part of interfacial damping.

The effect of the foundation on the overall structural damping appears to be complex and not clear but it could be argued, that if the stiffness and mass of the foundations are substantially higher than those of the building, then the effect of the foundation damping can be neglected [106].

### A.3 Methods of Increasing Structural Damping in Buildings

Some of the possible procedures for increasing the structural damping are given below:

1. Selection of material to be used- reinforced concrete has a damping capacity of 2-3 times that of mild steel and masonry has a damping capacity of 10-20%.
2. Use of viscoelastic dampers- about 20,000 viscoelastic sandwich layers were used successfully in the World Trade Tower. A factor of 10 fold increase in the damping capacity of viscoelastic sandwich layer beams has been achieved in higher frequency applications [46].
3. Optimization of damping in bolted joints- high damping could be possible. The theories mentioned in references [43], [126] and [134] may be used even though these theories have not reached the stage of simple design implementation, but with this device there will be problem of fretting corrosion and the interface seizing up [107]
4. The use of foundation damping- if foundations are designed to produce significant movements, they can be a major source of damping. Lazan [76] has obtained the damping in various soils and has found that many soils have a high damping value of about 5% of the critical damping.
5. Use of tuned mass damper- in this system a second mass is used to reduce the resonant amplification by inertial coupling [39]. The energy is dissipated by ancillary damping material or devices such as commercial shock-absorbers. This technique is effectively used in a

very high restaurant supported on a cable-stayed tube. The fire water in the ceiling of the restaurant would be used as the damper mass.

#### A.4 Aerodynamic Damping

When a building is immersed in an air flow, it starts vibrating. Due to the air viscosity the building is subjected to a frictional force which dampens the building oscillations. This type of damping is called "aerodynamic damping". This mechanism is initiated due to the resulting reduction in the relative velocity with respect to the structure. When the velocity of the vibrating structure and the wind velocity equals, the excitation energy diminishes and there will be no further increase in amplitude. If the wind velocity is lower than this limiting condition, an instability occurs at which the net mechanical and aerodynamic damping in a structural system approaches zero. In this case the aerodynamic damping is called "negative aerodynamic damping". As a result of this instability the amplitude of vibration keeps on increasing, unless nonlinearities rescue the system. The negative aerodynamic damping may result in considerable increase in the response of the structure leading to structural damage or at least discomfort to the occupants.

The aerodynamic damping is usually small as compared to that of mechanical damping, especially if the structural velocity is low.

Assuming that there will be no coupling force between the motion in various fundamental modes of vibration, i.e., along-wind, across-wind and torsional; linear mode shape (considering only the first mode) and uniform mass distribution, Saunders [107] has suggested the following empirical expressions for aerodynamic damping for a rectangular tall building at nearly zero angle of attack:

$$\begin{aligned}
 \text{i) Along-wind:} \quad \xi_y &= \frac{3 C_D \rho \bar{u}_h}{4\pi(3+\alpha)\rho_b N_y D} \\
 \text{ii) Cross-wind:} \quad \xi_x &= - \frac{3 \rho \bar{u}_h}{8\pi(3+\alpha)\rho_b N_x D} \frac{\partial C_x}{\partial \alpha} \\
 \text{iii) Torsional:} \quad \xi_z &= \frac{3 \rho \bar{u}_h^2}{8\pi^2(3+2\alpha)\rho_b N_z^2 D r_g} \frac{\partial C_z}{\partial \alpha}
 \end{aligned}$$

where  $\frac{\partial C_x}{\partial \alpha}$ ,  $\frac{\partial C_z}{\partial \alpha}$  = gradient of the transverse and torsional force coefficient curve at the angle  $\alpha$ ,

$\alpha$  = velocity profile exponent,

$\rho, \rho_b$  = air density and average density of building,

$\bar{u}_h$  = mean velocity at top of the building,

$D$  = building depth,

$C_D$  = drag coefficient,

$N_y, N_x, N_z$  = fundamental frequencies in along-wind, across-wind and torsional modes,

$r_g$  = building radius of gyration.

#### A.5 Damping in buildings

Damping in tall buildings in fundamental mode is very low which indicates that very little energy is dissipated by structural connections and the entire building is deformed as a rigid body. In higher modes of vibration where the flexural and shear deformations of the building are much greater, the damping will be more. Yakoo and Akiyama [140] have suggested an expression based on damping measurements of a number of buildings expressed

in terms of ratio of frequencies of the higher mode to the fundamental natural frequency as follows:

$$\frac{\xi_i}{\xi_1} = 1 + 0.38 \left( \frac{n_i}{n_1} - 1 \right)$$

where  $\xi_i$  and  $n_i$  represent the critical damping ratio and natural frequency of vibration in the  $i$ th mode.

Trifunac [125] obtained a good agreement between damping values measured from ambient tests with corresponding values derived from forced vibration tests of two buildings. Hart [51] reported that the influence of the soil-building response upon damping estimates is unclear. Korten [71] reported that the foundation of a tall building has hardly any influence on the total damping of the building subjected to wind excitations.

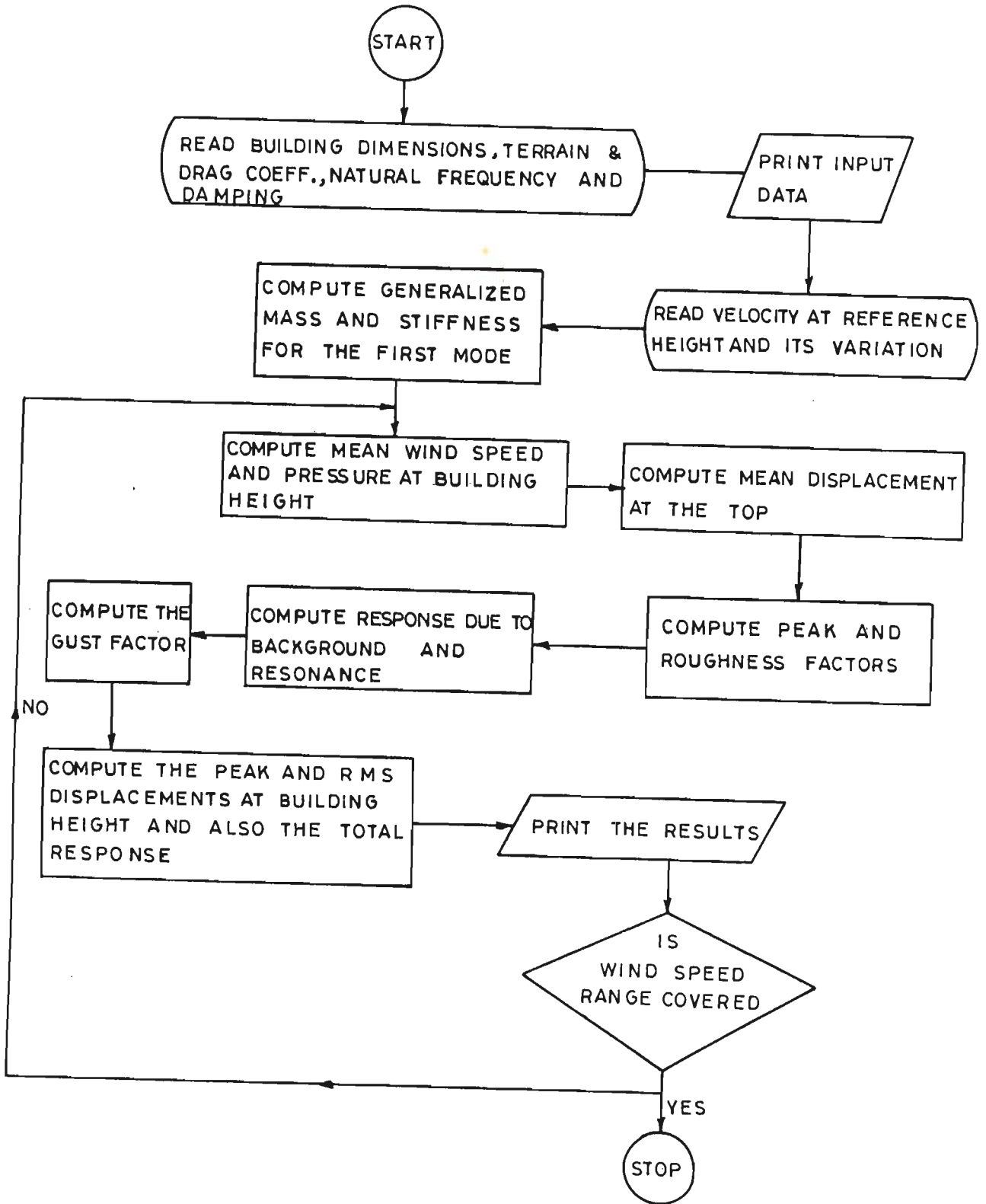


Fig.B-1 Flow Diagram for Along-wind Response of Tall Buildings

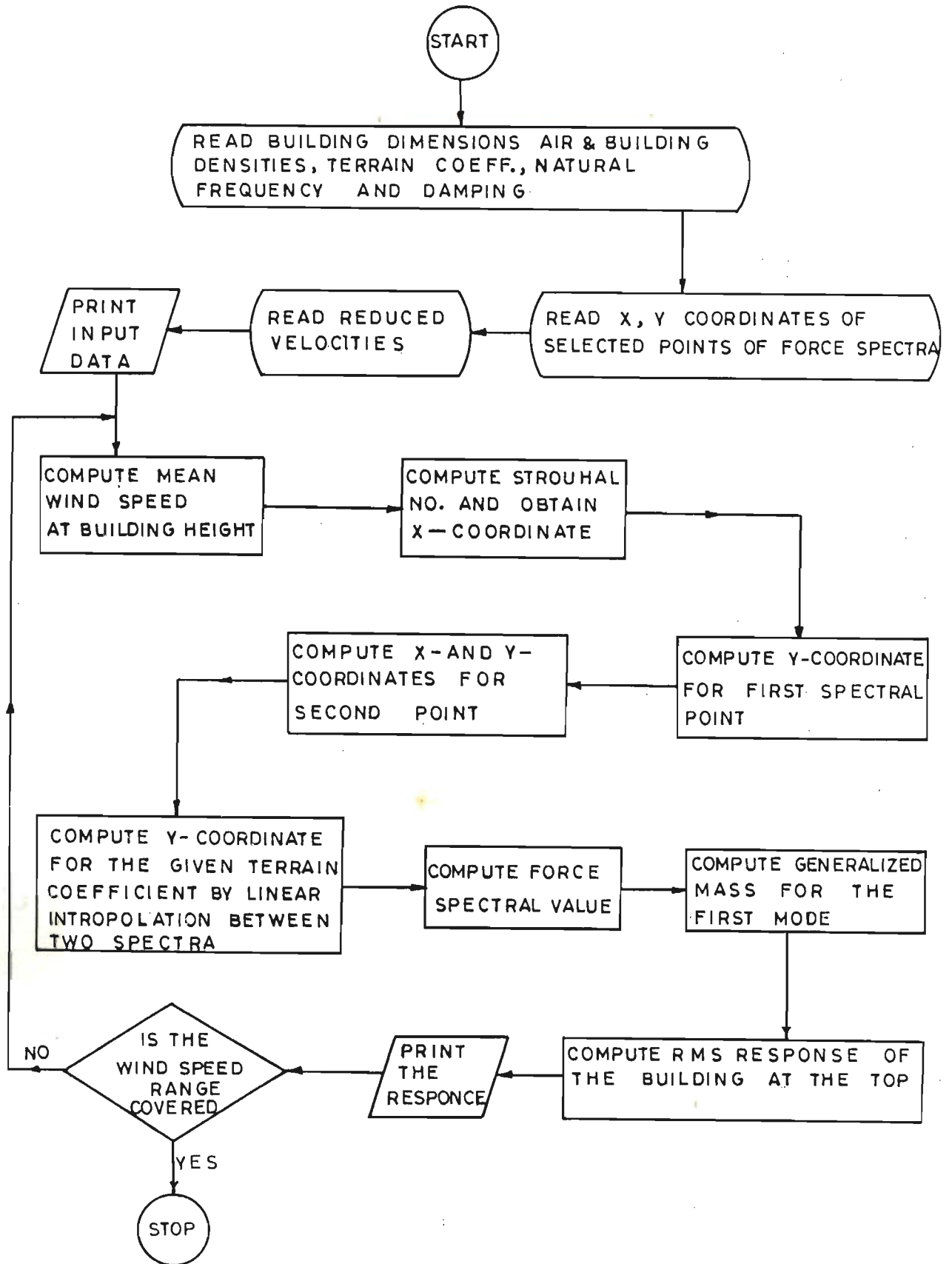


Fig.B-2 Flow Diagram for Across-wind Response of Tall Buildings





Photo 1. Aeroelastic Model in the Wind Tunnel

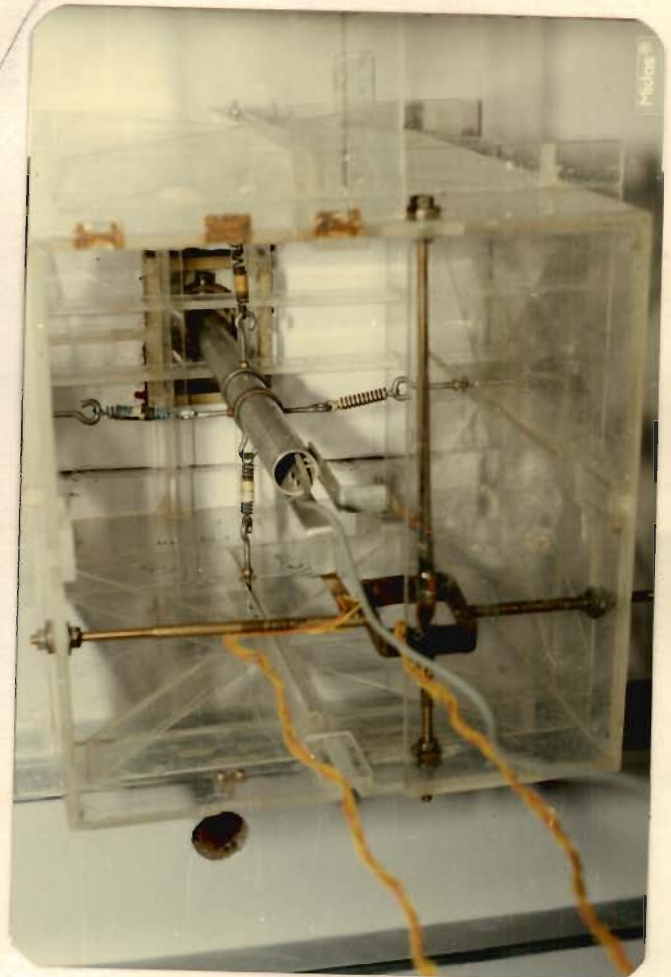
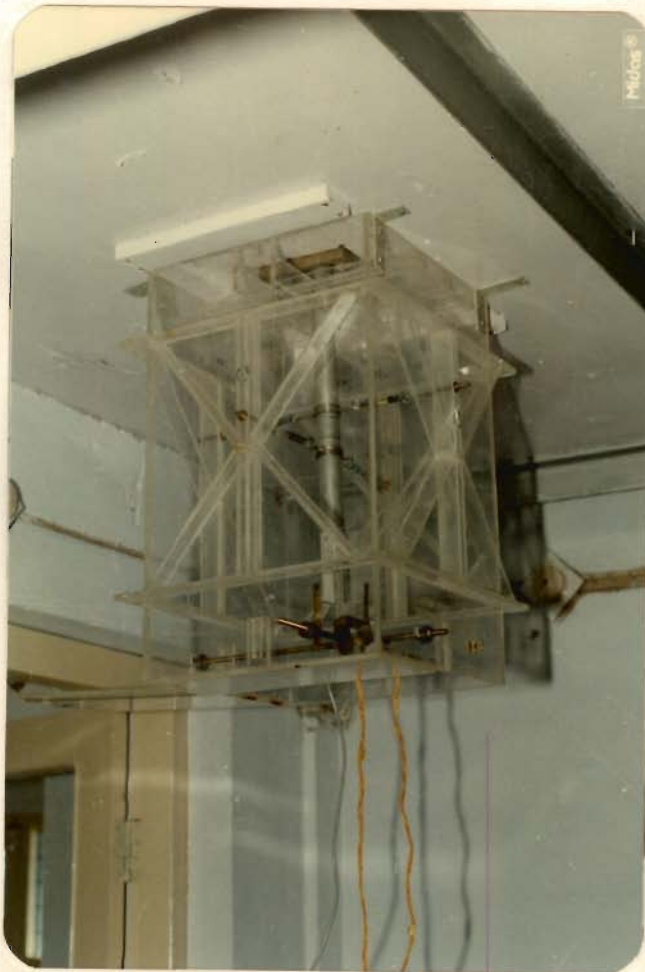


Photo 2. Details of Extended Portion of the Model Below Wind Tunnel Floor





Photo 3. Interference Study (Rigid Model Case)

Photo 4. Interference Study (Aeroelastic Model Case)

